Large-scale evolution of Holocene tidal basins in the Netherlands

Ad van der Spek

LARGE-SCALE EVOLUTION OF HOLOCENE TIDAL BASINS IN THE NETHERLANDS

Cover: Tidal flats south-east of the island of Ameland

CIP-DATA KONINKLIJKE BIBLIOTHEEK, DEN HAAG

Spek, Adam Jacobus Franciscus van der
Large-scale evolution of Holocene tidal basins in the Netherlands / Adam Jacobus Franciscus van der Spek. - Utrecht : Universiteit Utrecht, Faculteit Aardwetenschappen
Thesis Universiteit Utrecht. - With ref. - With summary in Dutch.
ISBN 90-393-0664-8
Subject headings: coastal evolution ; the Netherlands / sedimentary geology.

Large-scale evolution of Holocene tidal basins in the Netherlands

Grootschalige ontwikkeling van Holocene getijdebekkens in Nederland

(met een samenvatting in het Nederlands)

PROEFSCHRIFT

ter verkrijging van de graad van doctor
aan de Universiteit Utrecht
op gezag van de Rector Magnificus, Prof. Dr. J.A. van Ginkel,
ingevolge het besluit van het College van Decanen
in het openbaar te verdedigen
op 4 oktober 1994 des ochtends te 10.30 uur

door

Adam Jacobus Franciscus van der Spek

geboren op 19 januari 1961, te 's Gravenhage

promotor: Prof. Dr. D. Eisma
Instituut voor Aardwetenschappen

co-promotoren: Dr. D.J. Beets
voorheen Rijks Geologische Dienst

Dr. J.H. van den Berg
Instituut voor Ruimtelijke Wetenschappen

dit proefschrift werd mede mogelijk gemaakt met financiële steun van Nederlands Wetenschappelijk Onderzoek en Rijkswaterstaat-Rijks Instituut voor Kust en Zee/RIKZ

" .... dan was het nog een eindje lopen naar de dijk en als ik die had beklommen, stond ik weer voor de oneindigheid, een moddervlakte waar de zee zich slurpend en gorgelend uit terugtrok, wat het werd eb."

H.J.A. Hofland, Boven en Onder de Grond op Schiermonnikoog, Baarn, 1979

Contents

3. Holocene depositional sequences in the Dutch Wadden Sea south of the island of Ameland

accepted for publication in Mededelingen Rijks Geologische Dienst, vol. 53; to be published at the end of 1994

4. Mid-Holocene evolution of a tidal basin in the western Netherlands: a model for future changes in the northern Netherlands under conditions of accelerated sea-level rise?

co-author: D.J. Beets

Published in: J.F. Donoghue, R.A. Davis, C.H. Fletcher and J.R. Suter (Editors). Quaternary Coastal Evolution. Sedimentary Geology, 80: 185-197. Reproduced with permission of Elsevier Science Publishers

5. Reconstruction of tidal inlet and tidal channel dimensions in the Friesian Middelzee, a former tidal basin in the Dutch Wadden Sea

accepted for publication in: B.W. Flemming and A. Bartholomä (Editors), Tidal Signatures in Modern and Ancient Sediments, Spec. Publs. int. Ass. Sediment.; scheduled to appear befor mid-1995

6. Tidal asymmetry and long-term evolution of Holocene tidal-basins in the Netherlands: simulation of palaeo-tides in the Schelde estuary.

to be submitted

Dankwoord

Bij de totstandkoming van dit proefschrift en het werk dat eraan voorafging heb ik niet tevergeefs een beroep gedaan op een groot aantal mensen. Hierbij wil ik al die collega's van de RGD en RWS die mij met raad en daad hebben bijgestaan tijdens het boren, lakken, beschrijven, fotograveren, modelleren, plotten, tekenen, rekenen, etc. van harte bedanken. Zonder hen zou het allemaal een stuk langer geduurd hebben. Met name wil ik hier André Koers noemen die vrolijk bleef, al wijzigde ik de tekeningen steeds opnieuw, en Engelbert Vennix die met grote voortvarendheid de tekeningen voor de hoofdstukken 6 en 7 vorm gaf. Thea van de Graaff voorzag de meeste teksten niet alleen van correcties op het engels, maar gaf en passant een hoop bruikbare tips op het gebied van teksten redigeren. Ook wil ik hier mijn voormalige kamergenoten Martijn van der Zijp, James Baker en Peter Vos noemen, die met sloten koffie, mooie verhalen, slimme computer-trucjes en soms uit de hand lopende discussies het leven een stuk aangenamer maakten.

Het hier weergegeven onderzoek werd begeleid door een groot aantal mensen. Doeke Eisma, uiteindelijk mijn promotor, volgde mijn verrichtingen met enthousiasme en leverde vele nuttige aanwijzingen. De frequentie van ons telefonisch contact vertoonde de laatste tijd een sterk exponentieel verloop. Na de "Voordelta-tijd" bleef Janrik van den Berg mijn pad kruisen. Nooit gedacht dat je nog eens mijn co-promotor zou zijn. Het lag voor de hand dat onze samenwerking een "Terug naar Zeeland" zou worden. Kiek Jelgersma slingerde het onderzoek aan en effende via haar wijdvertakte relatie netwerk mijn weg. Poppe de Boer bleek altijd bereid manuscripten van commentaar te voorzien en lastige vragen te beantwoorden.

Mijn "eerste baas" Jan Mulder van RIKZ wil ik bedanken voor zijn luisterend oor en bereidwillige ondersteuning van het onderzoek. Kustgenese-projectleider Eric Bouwmeester verleende uit enthousiasme voor het geologisch kustonderzoek onmisbare steun aan mijn onderzoek en de productie van dit proefschrift, waarvoor mijn dank. Op deze plaats wil ik mijn waardering uiten voor Ad langerak van RIKZ-Middelburg voor alle tijd die hij vrij heeft gemaakt om me in getijmodellering en het wel en wee van de Westerschelde in te wijden. Daarnaast was hij bereid om te midden van de gepakte vakantiekoffers nog een manuscript van commentaar te voorzien.

Ondanks een scala aan contracten en dienstverbanden heb ik de afgelopen 6 jaar steeds gebruik mogen maken van de faciliteiten van de RGD. Hiervoor wil ik de directie van de RGD en hoofden van de hoofdafdeling Ondiepe Ondergrond Erne Oele en Ruud Schüttenhelm hartelijk bedanken. Er bleef steeds een werkruimte beschikbaar en extra wensen ("een nog snellere PC met een nog grotere harde schijf") werden steeds ruimhartig ingewilligd.

Mijn familie en vrienden ben ik dankbaar voor het begrip en geduld als ik het weer eens liet afweten omdat ik moest werken.

Tenslotte en "lest best" wil ik nog twee mensen bedanken. Dirk Beets, die mij met het juiste oog naar lakfilms leerde kijken, die mij inpeperde hoe kleine details grote gevolgen kunnen hebben en die mij iedere dag weer demonstreerde dat geologie nog altijd een "alleraardigst vak" is, en Marja die door structureel over te werken mij alle ruimte gaf om rustig door te blijven werken en die daarnaast nog tijd vond om de afronding van dit proefschrift met raad en daad, koffie en broodjes en eindeloos veel kopieer-, print- en typewerk te ondersteunen. Zonder jullie was het me nooit gelukt.

Samenvatting

Dit proefschrift beschrijft de ontwikkeling van de getijde- of waddengebieden langs de Nederlandse kust gedurende de afgelopen 8000 jaar. Aan het eind van de laatste ijstijd, het Weichselien, stond de zeespiegel aanzienlijk lager dan nu, waardoor de Noordzee droog lag. Door een toename van de gemiddelde temperatuur smolt het landijs af. Het daarbij vrijkomende water vond zijn weg terug naar zee, waardoor het gemiddeld zeeniveau snel steeg, met wel 0.75 m per eeuw of meer. Hierdoor breidde de Noordzee zich sterk uit en bereikte rond 7000 jaar voor heden de huidige Nederlandse kust. De Noordzee drong eerst de lage delen van het toenmalige landschap binnen, waardoor een grillige kustlijn ontstond. In zee stekende landhoofden en landinwaarts uitstrekkende waddengebieden wisselden elkaar af (vergelijk Fig. 1.1). Met het verder stijgen van de zeespiegel drong de zee verder landinwaarts en werden de waddengebieden dieper. Dit leidde tot een grote toevoer van zand en slib naar deze gebieden. Een deel van dit zand werd van de kust geërodeerd, waardoor de kustlijn zich terugtrok. Na 7000 jaar voor heden nam de stijging van de zeespiegel sterk af, tot ongeveer 0.15 m per eeuw na 5500 jaar voor heden. Hierna breidden de wadden- of getijdegebieden zich niet meer zo sterk uit en werden zij langzaam opgevuld met zand en slib en ten dele ook met veen. Uiteindelijk verlandden de meeste getijdegebieden en werden de bijbehorende zeegaten opgevuld met zand en slib. Het laatste zeegat in west Nederland, tussen Alkmaar en Bergen, sloot rond 3300 jaar voor heden, waardoor de kustlijn in West Nederland een min of meer vloeiend verloop kreeg. De voorloper van het huidige Waddengebied, ten oosten van Terschelling, werd echter nooit geheel opgevuld met sediment.

Nadat de kustvlakte grotendeels opgevuld was met sediment en veen, vertoonde de daaropvolgende ontwikkeling van de Nederlandse kust regionale verschillen. De kust van Noord- en Zuid-Holland werd nog slechts door de riviermonden van de Oude Rijn bij Katwijk en het Oer-Y tussen Castricum en Egmond aan Zee onderbroken. De zandaanvoer naar dit deel van de kust was voldoende groot om de kust uit te bouwen. Hierbij werd, grofweg tussen Den Haag en Alkmaar, een serie strandwallen van maximaal 8 km breedte gevormd.

Ten zuiden van de huidige Rijn-Maas monding daalde vanaf 2200 jaar voor heden het oppervlak van het veenlandschap door ontwatering als gevolg van zowel natuurlijke als menselijke oorzaken. Hierdoor verdween het veenlandschap geleidelijk onder water, waarna de zee het gebied opnieuw kon binnendringen. Dit leidde uiteindelijk tot grootschalige afbraak van het veenlandschap en het ontstaan van een aantal grote zeearmen zoals de Grevelingen en het Haringvliet in de Middeleeuwen.

Zoals gezegd is het Waddengebied nooit geheel verland. Na 3500 jaar voor heden breidde de Waddenzee zich weer naar het zuiden uit. De westelijke Waddenzee, tussen Texel en Terschelling, is pas na het begin van onze jaartelling ontstaan. Dit gebied lag relatief hoog en bleef daardoor lang buiten het bereik van de Noordzee. Aanvankelijk bevond zich hier nog een uitgestrekt drassig gebied, maar ook hier verdween het veen en kon de zee binnendringen. Uiteindelijk ontstonden hier onder andere het Marsdiep en het Zeegat van het Vlie, de grootste zeegaten van de huidige Waddenzee.

Het eerste deel van dit proefschrift behandelt de sediment opeenvolgingen welke afgezet zijn in enkele, zowel voormalig als recente, getijdegebieden in het Noorden en Westen van Nederland. In de Waddenzee ten zuiden van Ameland (Hoofdstuk 3) wordt een opeenvolging, van onder naar boven, van veen, lagunaire klei- en slikafzettingen aangetroffen, welke daar tussen ca. 7200 en 5500 jaar voor heden afgezet is. Hierop ligt een pakket wadzanden dat afgezet is in geulen en zeegaten, sinds ongeveer 3000 jaar voor heden. Deze geulen hebben de ondergrond omgewerkt, waardoor afzettingen uit de tussenliggende periode van 5500 tot 3000 jaar voor heden vrijwel ontbreken. Afzettingen uit deze periode worden wel aangetroffen op het huidige vasteland van Friesland, waar de omwerking door geulen veel minder intensief is geweest.

De sedimentopeenvolging in de Waddenzee laat zien dat het Waddengebied zich tijdens de periode met snelle zeespiegelstijging naar het zuiden heeft verplaatst. De verplaatsing stopte ongeveer 5000 jaar voor heden. Het meest zuidelijke deel van de toenmalige Waddenzee verlandde, waarbij uiteindelijk kwelders, welke vergelijkbaar zijn met de huidige, gevormd werden.

In Hoofdstuk 4 wordt de ontwikkeling van het voormalige getijdegebied in Noord- en Zuid-Holland beschreven. Tijdens de periode van snelle zeespiegelrijzing (tot ca. 5500 jaar voor heden) kwamen wadplaten in het gebied alleen langs de geulen voor. Echter, op enige afstand van de geulen werd nauwelijks zand afgezet en kwam vrijwel uitsluitend slib tot bezinking in lagunes. De sedimentaanvoer via het zeegat was in de periode met snelle zeespiegelrijzing te klein om het snel groter wordende bekken op te vullen. Hierdoor bleef de afzetting van zand beperkt tot de directe omgeving van de geulen en veranderden de gebieden die verstoken bleven van zandaanvoer in lagunes. Nadat de snelheid van zeespiegelrijzing aanzienlijk was teruggelopen, breidden de getijdegebieden in West Nederland niet meer uit en werden zij uiteindelijk opgevuld met zand en klei.

Uit de bovenstaande ontwikkeling van het getijdegebied in Holland onder invloed van een afnemende snelheid van zeespiegelstijging is een algemeen model voor het gedrag van getijdegebieden tijdens verschillende snelheden van zeespiegelstijging opgesteld. Hiermee kunnen de gevolgen van een eventuele versnelling van de huidige zeespiegelstijging in de Waddenzee van ongeveer 0.15 m per eeuw, als gevolg van een mogelijke opwarming van de aarde en het daarmee samenhangende afsmelten van het poolijs, zichtbaar gemaakt worden. Als de toename van de gemiddelde diepte door het stijgen van het zeeniveau niet meer gecompenseerd kan worden door sedimentaanvoer, zal het Waddengebied gaan lijken op het getijdegebied in west Nederland tijdens de snelle zeespiegelstijging in het verleden: wadplaten zullen alleen nog langs de geulen voorkomen, tussen de geulsystemen zullen lagunes ontstaan en de kwelders zullen verdwijnen.

Het belangrijkste verschil tussen het voormalige getijdegebied in Holland en de Waddenzee is dat het eerste gebied geheel verlandde, terwijl het laatste continu een getijdegebied bleef. De sedimentaanvoer in Holland was voldoende groot om na de verlanding van het getijdegebied en de opslibbing van de zeegaten een strandwallengordel uit te bouwen. De Waddeneilanden, echter, zijn steeds landwaarts verplaatst door erosie van hun onderwateroever, waarbij het geërodeerde zand naar het achterliggende bekken gevoerd werd. Eén duidelijke oorzaak voor dit verschil in sedimentaanvoer is niet aan te wijzen. De Noordzee is ten noorden van de Waddeneilanden dieper dan ten westen van Holland, waardoor er hier minder sediment binnen het bereik lag van de transportmechanismen welke sediment dwars op de kust omhoog brengen. Daarnaast is het Noordzee-getij ter hoogte van de Waddeneilanden meer symmetrisch, waardoor de netto verplaatsing van zand naar de kust door de getijstroming minder kan zijn. De overheersende wind uit westelijke richtingen versterkt driftstroming en golven op de wantijen achter de Waddeneilanden, waardoor de wantijen niet tot boven hoogwaterniveau kunnen opslibben om vervolgens te verlanden. De westelijke Waddenzee tenslotte, is verhoudingsgewijs zeer recent ontstaan, waardoor het tijdsverloop sindsdien te kort is geweest om voldoende sediment bekkeninwaarts te transporteren.

Het tweede deel van dit proefschrift (Hoofdstuk 5 tot en met 7) behandelt de ontwikkeling en toepassing van kwantitatieve benaderingen in de reconstructie van voormalige getijdegebieden. Uit de afzettingen van getijdegeulen is de breedte en diepte van de vormende geulen moeilijk af te leiden. Deze geulen verplaatsen zich in de tijd vaak zijwaarts, waardoor zij een gordel van afzettingen achterlaten, terwijl hun doorsnede eveneens kan variëren. Echter, de grootte van de doorsnede van een getijgeul staat in een min of meer vaste verhouding tot de afvoer door die geul. Als nu deze afvoer berekend kan worden door de oppervlakte van het gebied dat door die geul bediend wordt te vermenigvuldigen met het getijverschil, staat ook de doorsnede van de geul vast. Op deze manier kan de grootte van een geul die bij een bepaald gebied hoort geschat worden (Hoofdstuk 5). Voor grote getijdegebieden kan het getijdebiet beter berekend worden met een getijmodel (Hoofdstuk 6 en 7).

Daarnaast worden in Hoofdstuk 5 relaties afgeleid tussen debieten en maximale geuldieptes, omdat de maximale diepte vaak eenvoudig uit de dikte van een pakket geulafzettingen afgeleid kan worden. Toepassing van de genoemde relaties op afzettingen in de Middelzee, een middeleeuwse tak van de Waddenzee welke tot aan Sneek in Friesland doordrong, laat onder andere zien dat het debiet in het bijbehorende zeegat zo groot was dat het niet door één enkele geul afgevoerd kan zijn. De maximale geuldiepte van 30 m onder NAP was bekend uit boringen op Terschelling. Het debiet in het zeegat moet daarom verdeeld zijn geweest over twee geulen, hetgeen overeenkomt met de oudste zeekaarten van dit zeegat. Daarnaast blijkt uit de sedimentbalans, opgesteld voor de verlanding van de Middelzee, dat hier jaarlijks gemiddeld $1{,}9 \times 10^6$ m^3 sediment afgezet werd. Deze waarde is goed vergelijkbaar met de huidige zandimporten in de zeegaten van de Waddenzee.

Het getij langs de Nederlandse kust stijgt sneller dan het daalt, waardoor de landwaarts gerichte vloedstroming sterker is dan de ebstroming. Hierdoor vindt er een resulterend zandtransport plaats via de zeegaten naar de getijdegebieden. Dit zal in het verleden niet wezenlijk anders geweest zijn. Echter, het onderlopen en leegstromen van eventuele wadplaten in het getijdegebied vertraagt de stroming in het zeegat. Hierdoor vindt de maximale vloedstroming in het zeegat bij een hogere waterstand plaats, waardoor de maximale stroomsnelheid afneemt. De maximale ebstroming vindt bij een lagere waterstand plaats, waardoor de maximale ebsnelheid toeneemt. Hierdoor neemt de verhouding tussen maximale vloed- en ebstroming, en daarmee de resulterende zandtransportcapaciteit in de vloedrichting, af. Met andere woorden, de aanwezigheid van wadplaten in een getijdegebied leidt uiteindelijk tot tegenwerking van de asymmetrie in de getijstroming, en dus de zandimport in het zeegat. Een uitbreiding van de wadplaten ten gevolge van afzetting van het aangevoerde zand zal dus leiden tot een afname van de zandimport.

Deze hypothese is getoetst aan de ontwikkeling van de Westerschelde tussen 1650 en nu. De Westerschelde veranderde van een groot, wijdvertakt en betrekkelijk ondiep getijdegebied in 1650 in het relatief smalle en diepe estuarium van vandaag. Hierbij nam het oppervlak aan actieve wadplaten sterk af door opslibbing en bedijking. Dientengevolge werd een afname van de tegenwerking van de getijasymmetrie in de monding van het estuarium verwacht. Simulatie van de getijbeweging in de Westerschelde voor 1650, 1800 en 1968 met behulp van een eenvoudig getijmodel (Hoofdstuk 6) laat zien dat tussen 1650 en nu de tegenwerking van de getijasymmetrie in de monding toeneemt. Dit blijkt een gevolg te zijn van de toename van de snelheid van de getijgolf in de Westerschelde, als gevolg van de toegenomen diepte. Hierdoor lopen de resterende platen in het estuarium in korte tijd onder, waardoor het getij in de monding duidelijk beïnvloed wordt. In de vroegere situatie besloeg het onderlopen van de uitgestrekte plaatgebieden een lange periode, waardoor een duidelijk effect op het getij in de monding uitbleef. De zandimport in de Westerscheldemonding zal hierdoor in de loop van de tijd afgenomen zijn.

Simulaties van het getij voor een aantal stadia in de ontwikkeling van het voormalige getijdegebied in Noord-Holland laten zien dat ook hier de getijasymmetrie in het zeegat afnam met het opvullen van het achterliggende getijdebekken. Daarnaast kunnen de reconstructies van dit gebied, gebaseerd op geologische gegevens, getoetst worden. Geologische informatie laat vaak ruimte voor meerdere interpretaties, waardoor reconstructies tegenstrijdigheden kunnen bevatten. Daar echter het zand- en slibtransport binnen een getijdegebied, waar de geologische situatie het eindprodukt van is, nauw samenhangen met de waterbeweging, kan een simulatie van de waterbeweging veel nieuwe informatie opleveren. Zo liet een van de simulaties zien dat Noord-Holland rond 7200 jaar voor heden niet uit één, grote lagune bestaan kan hebben. Simulaties voor 5500 jaar voor heden laten zien dat de grootte van het zeegat in die tijd, zoals afgeleid uit de omvang van het kleilichaam dat later hierin afgezet is, niet in overeenstemming te brengen valt met de grootte van het achterliggende getijdegebied. De doorsnede van dit kleilichaam suggereert een veel te groot zeegat. Dientengevolge moet in een deel van deze doorsnede reeds slib afgezet zijn, terwijl het zeegat nog in een ander deel van de doorsnede actief was.

1. Introduction

Tidal basins in the Holocene coastal plain of the Netherlands

The formation and subsequent evolution of tidal basins largely determined the Holocene evolution of the Dutch coast. Tidal basins are defined as semi-enclosed embayments, connected to the open sea by a (narrow) entrance and subject to daily tidal action. They are bounded by land and/or tidal watersheds at the landward side and by islands or some kind of barrier at the seaward side. Fluvial discharge in these basins is negligible.

As a result of the Holocene rise in sea level the North Sea expanded and invaded the low-lying parts of the coastal landscape changing these areas into tidal basins. No influx of fluvial sediments nor influence of fluvial currents has been demonstrated for the Dutch tidal basins. However, fresh water, supplied by either small rivers and brooklets or by surface run-off, did affect sedimentation on the most landward side of the basins. The basins deepened and expanded landward as sea level rose. The growth of the basin volume was counteracted by the influx of sediments eroded from the adjacent coast and from the North Sea. The amount of sediment deposited in the basins was not sufficient to compensate the increase in basin volume, and consequently the coastline retreated continuously. This landward shift of the tidal basins in the western Netherlands (Fig. 1.1: Holland tidal basin) stopped between 5000 BP and 4400 BP (Beets et al., 1992; Van der Valk, 1992; Vos and Van Heeringen, 1993), after the rate of sea-level rise had dropped from more than 0.75 m per century prior to 7000 BP to about 0.15 m per century after 5500 BP. The tidal basins were slowly filled with sediment and accreted to above mean water level, after which they changed into marshes with fresh-water vegetation and peat accumulation. The northern part of the Holland tidal basin did not fill up until 3300 BP. In contrast, the tidal basins in the northern Netherlands (Boorne and Hunze valleys, Fig. 1.1) did not fill up completely with sediment (Griede 1978; Griede and Roeleveld, 1982; Roeleveld, 1974).

The evolution of the Dutch coast started to diverge after the basins had been filled with marine sediments and peat. The tidal basins in the western Netherlands (Fig. 1.1: Holland tidal basin) and their inlets were filled in. The sediments, supplied by both the North Sea and by local sources, such as the eroding Rhine-Meuse alluvial plain and the Texel High (Fig. 1.1), then caused seaward progradation of the coast, as revealed by series of beach barriers (Beets et al., 1992; Van der Valk, 1992). Once the inlet near Alkmaar and Bergen had silted up around 3300 BP, the coast of the western Netherlands consisted of a continuous barrier which was only interrupted by the outlets of

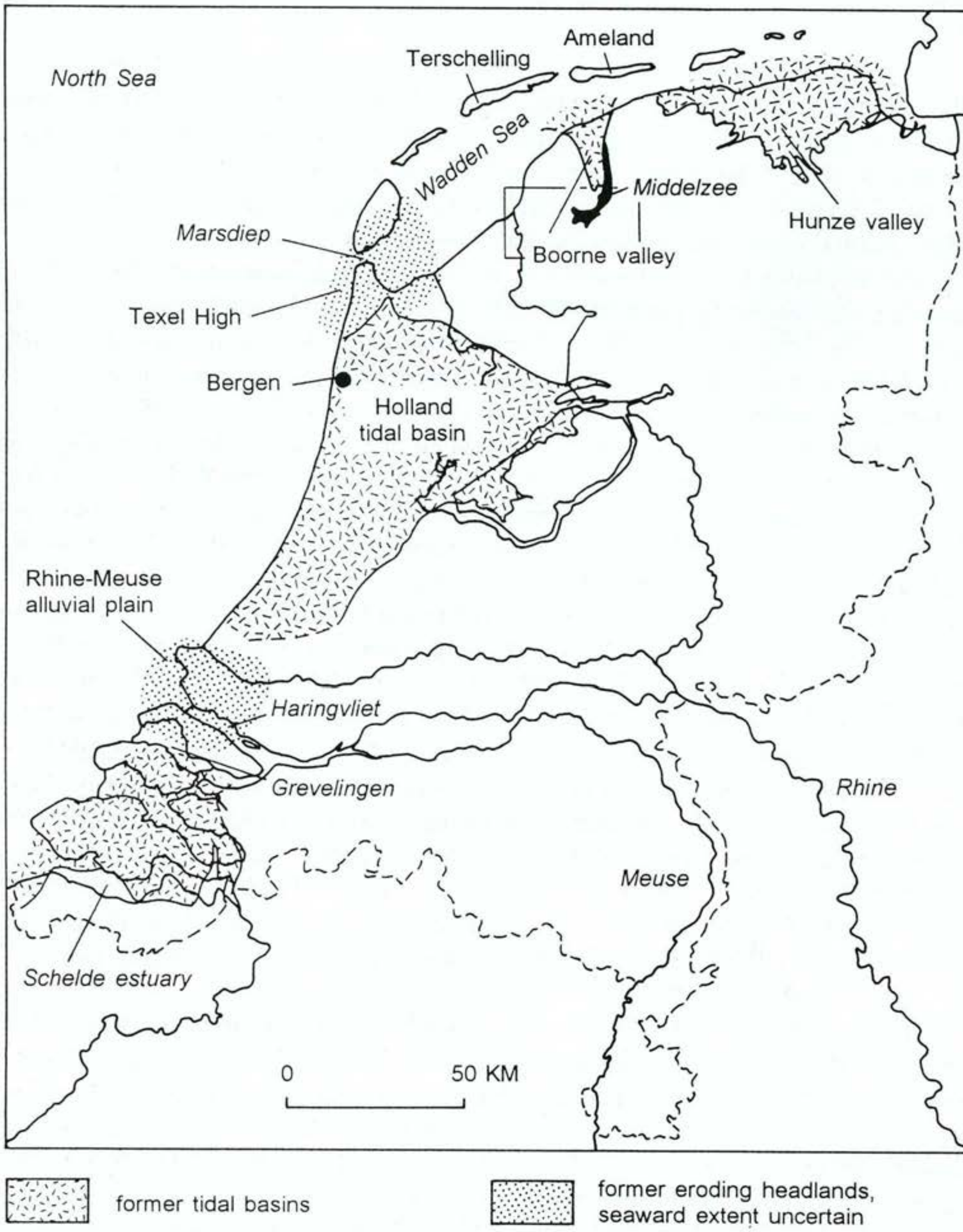

Figure 1.1 Location of former and recent tidal basins and former eroding headlands in the Netherlands. Inset is shown in Fig. 1.2

the rivers Oer-Y and Oude Rijn.

The tidal basins south of the alluvial plain of the rivers Rhine and Meuse had silted around 5000 BP and were changed completely into a peat landscape around 4000 BP (Vos and Van Heeringen, 1993). Increasing drainage, by both natural and human factors, caused lowering of the land from about 2200 BP onwards. Tidal action penetrated inland again and sediment was deposited in the peat landscape. This caused rapid compaction and erosion of the peat, further landward expansion of the tidal flow and, finally, the creation of large estuaries such as the Haringvliet and the Grevelingen (Fig. 1.1) around 1200 AD

The tidal basins in the eastern part of the present-day Wadden Sea never filled up completely. New ingressions into low-lying areas led to several cycles of expansion followed by partial siltation of the tidal basins after 3500 BP.

Important changes occurred in the most northern part of Holland and the western part of the Wadden Sea, between Bergen and the island of Terschelling (Fig. 1.1), in historical time. Deterioration of the peat landscape resulted in lowering of the surface and eventual drowning. Finally, large tidal channels like the Marsdiep (Fig. 1.1) developed once a connection with the inland lake Almere was established.

The evolution of the Dutch coast shows that the presence of storage potential in the coastal plain (caused by an absolute rise in sea level or by subsidence of the land surface) will eventually lead to ingression by the sea. The thus created accommodation space will cause basinward sediment transport and coastal erosion, since part of the sediment supply is derived from erosion of the adjacent coastline. Consequently, a sandy coast with tidal basins cannot be stable, since sand from the coast will always be imported into the basins. The resulting infilling of the tidal basins will lead to retrogradation of the coastline. Moreover, the evolution of the tidal inlets that connect the basin to open sea is determined by the evolution of the basin morphology and the basin hydraulics (Van den Berg, 1986).

Ingressions often followed the paths of existing drainage systems. During silting up of a tidal basin the sandy deposits in the former channels usually accreted to relatively high levels. The distal parts of the basin often received less, predominantly fine-grained sediment. In time, compaction of these deposits resulted in low areas, which often attracted the drainage systems of the hinterland. These low areas were prone to flooding once the relative sea level rose which caused renewed expansion of the tidal basin. Erosion of the surrounding peat landscape accelerated the basin expansion in these low areas. This cycle of ingression and subsequent sedimentation finally led to infilling of almost the entire coastal plain. The filling history of most tidal basins shows a

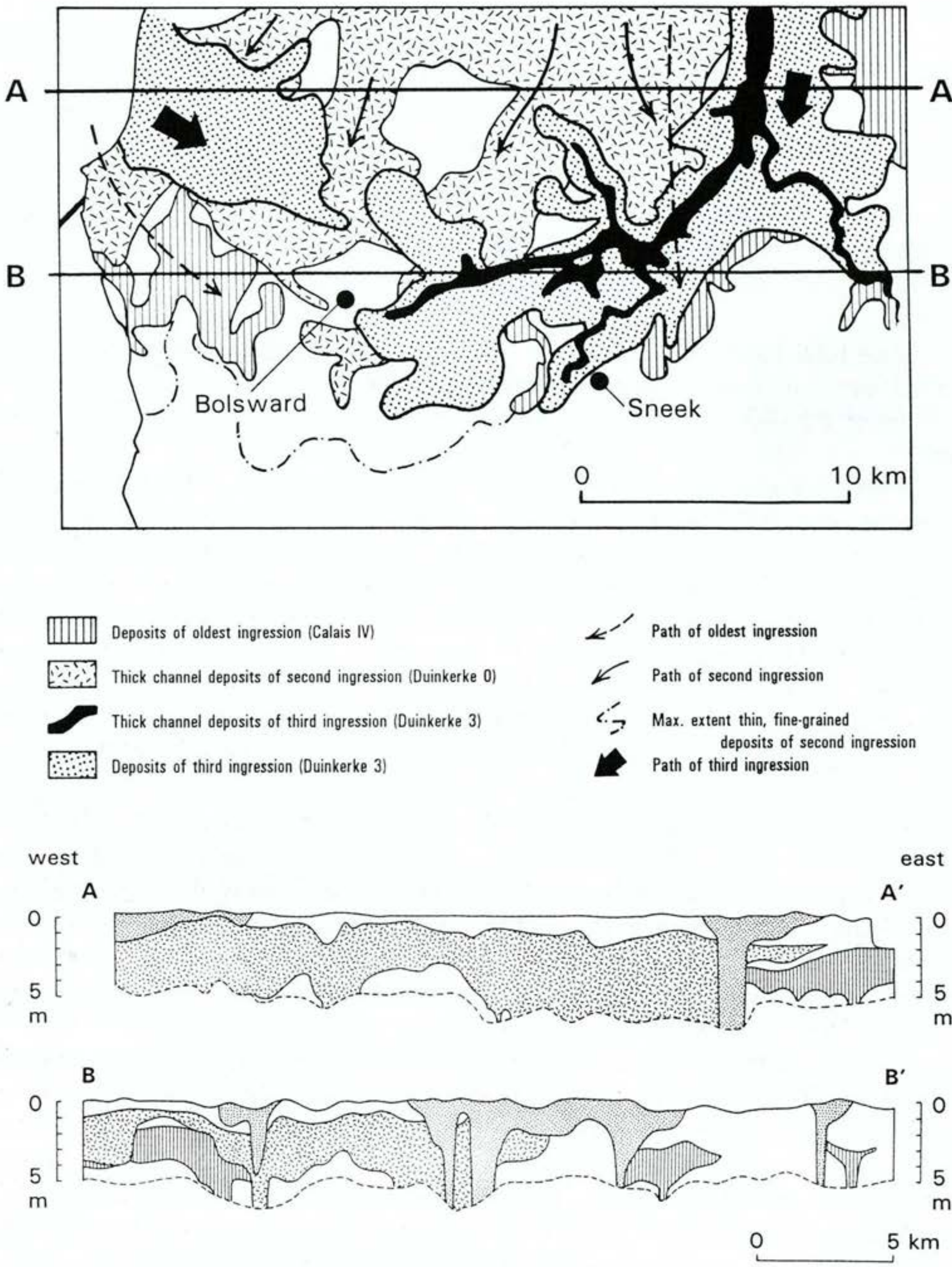

Figure 1.2 Stacking of sediment lobes deposited during successive ingressions in the Boorne valley and the area west of it, since the Subboreal. The Middelzee was formed during the third ingression. See Fig. 1.1 for location. (Modified after Ter Wee, 1976; De Groot et al., 1987.)

continuous shifting of depocentres resulting in only partly overlapping sediment lobes (Fig. 1.2). This mechanism is typical for the evolution of the Dutch coast during the slow sea-level rise (less than 0.15 m/century) of the Subboreal and the Subatlantic. Clear examples of this mechanism are found in the North-Holland tidal basin (see De Mulder and Bosch, 1982: figs. 18 to 22) and the former Boorne valley (Fig. 1.2).

Outline of this thesis

This thesis consists of five papers which treat several aspects of the evolution of the Holocene Dutch tidal basins in detail. Reconstructions of the tidal basins are based on the interpretation of geological and sedimentological information. Chapter 2 presents the general conclusions of this thesis. Chapter 3 describes the Holocene sedimentary sequence of the Wadden Sea south of the island of Ameland (Fig. 1.1). Here, a succession of Atlantic peats and fine-grained deposits was saved from reworking by younger laterally migrating tidal channels. Chapter 4 presents a description of the evolution of the palaeo-morphology of the Holland tidal basin (Fig. 1.1) at varying rates of sea-level rise. A model based on this information may predict the consequences of a possible future increase in the rate of sea-level rise for the Dutch Wadden Sea. The basic concept of this model is the balance between sediment accommodation space and sediment supply. The preliminary outline of this concept was mentioned by Van Straaten (1957, 1961, 1963) and other authors (e.g., Roy et al., 1980).

Chapters 5 to 7 illustrate a more quantitative approach to tidal-basin reconstruction. Chapter 5 discusses the formation and subsequent reclamation of the Middelzee, a medieval expansion of the Wadden Sea south of Terschelling (Fig. 1.1). The reconstruction of the basin evolution has been refined by approximating the dimensions of tidal channels and inlets from the extent of the basin, using relationships between the cross-sectional area and the discharge of a channel. Chapter 6 describes the development of a method for simulating tidal conditions in reconstructed basins and the application of that simulation method to several evolutionary stages of the Schelde estuary (Fig. 1.1). The simulations show the effects of morphological changes on the tidal flow and sand transport in the estuary. The preliminary results of the simulation of the tidal motion for reconstructions of the northern part of the Holland tidal basin (Fig. 1.1) has provided new insights into the environmental conditions in, and the siltation history of this basin (Chap. 7).

2. Synthesis: general discussion and conclusions

The first part of this thesis describes the sedimentary sequences of some Holocene tidal basins in the northern and western part of the Netherlands. Chapter 3 discusses the sedimentary sequence found in the Wadden Sea south of Ameland, on the eastern flank of the former Boorne valley. Here, an Atlantic peat/lagoonal clay/mud-flat sequence is found, which is overlain by a series of Subatlantic tidal channel deposits. Subboreal deposits are missing owing to channel erosion. A complete sequence of Subboreal deposits occurs in the formerly most landward parts of the Wadden Sea, below the present Frisian mainland. The sedimentary sequence indicates southward migration of the precursor of the Wadden Sea, which ended in the Subboreal period. The landward part of the basin accreted to about high-water level and tidal salt marshes similar to the ones we know today developed. The thus formed regressive facies sequence (from bottom to top: tidal channel/sand-flat/mud-flat/salt marsh) differs from the transgressive Atlantic facies sequence (peat/lake or lagoon/mud-flat/sand-flat/tidal channel). The Atlantic facies sequence in and near the main channels in the Holland tidal basin (Chap. 4) resembles that of the Atlantic Wadden Sea. However, the facies sequence found in the interchannel areas is different. It shows a continuous succession of lagoonal clays, which is overlain by Subboreal peats or lake deposits. The sediment supply was, as a consequence of the fast-rising sea level during the Atlantic, too small to fill the lagoons between the channel belts. Sand settled just in and close to the channels, leading to vertical aggradation of tidal flats along the channels with 0.6 to over 0.8 m per century. In the present-day Wadden Sea vertical sedimentation is very slow (about 0.15 m/century). After a drop in the rate of sea-level rise, sediment supply started to fill up the interchannel areas with sand and mud.

The Atlantic mud-flat deposits found in the Wadden Sea (Chap. 3) are relatively thick when compared with other fossil tidal-flat sequences from the Netherlands. Whether this is also resulting from a position close to a tidal channel cannot be determined because too few data are available.

The evolution of the Holland tidal basin under different rates of sea-level rise may be applicable to forecast the consequences of a possible future accelerated sea-level rise for the Wadden Sea: Tidal flats would be restricted to the direct vicinity of the (larger) tidal channels, lagoons would form in between and salt marshes will be eroded and finally disappear.

An important difference between the Holland tidal basin and the Wadden Sea is the fact that the seaward part of the former filled up resulting in closing of the inlet, whereas the latter still forms a tidal basin. The coast of Holland received enough sediment for the coastline to prograde after the inlets of the basin had been closed. Conversely, the Wadden-Sea barrier islands, have been migrating landward owing to shoreface erosion ever since they formed. Obvious reasons for this difference in sediment supply cannot be pointed out. The relatively deep North Sea, north of the Wadden Sea, probably limited the rate of cross-shore sediment transport. Moreover, in the Central North Sea the asymmetry of the tide, and thus the sediment transport capacity, is less than that in the southern North Sea. This may cause a difference in shoreward tidal sediment transport. The orientation of the Wadden Sea perpendicular to the prevailing westerly winds reinforces drift currents and wave action in the tidal watersheds. This precludes accretion of the watersheds to high-tide level and stabilization by vegetation (Van Veen, 1950). Finally, the western part of the Wadden Sea formed relatively recently. Time has been too short to enable a substantial infilling of the area.

The second part of this thesis (Chap. 5 to 7) describes the use of quantitative methods in geological basin reconstruction. Tidal-channel deposits usually do not represent a single channel, since tidal channels tend to migrate laterally and while their cross-section varies with time. This hampers reconstruction of the dimensions of a single tidal channel. Nevertheless, the relationship between the channel cross-sectional area and the discharge through this cross-section enables the determination of the dimensions of a channel that floods and drains a certain surface area (Chap. 5). Discharges can be estimated from the surface area of the basin in combination with the tidal range, or, for larger tidal basins, can be calculated using a numerical flow model (Chap. 6 and 7). Calculations show that the flood volume of the Middelzee, the medieval ingression into the Boorne valley, was too large for the maximum depth of the inlet that could be inferred from the Holocene erosion below the island of Terschelling. This led to the conclusion that the inlet must have consisted of two major channels, which is confirmed by historical data.

The North Sea tide along the Dutch coast rises faster than it falls, resulting in higher landward current velocities. As a consequence sand is transported into the tidal basins. This influx mechanism is counteracted by distortion of the tide inside the basin caused by interaction with the basin morphology. The flooding and draining of the tidal flats in the basin cause a reduction in the flood flow velocity and reinforce the ebb flow velocity at the inlet (e.g., Boon and Byrne, 1981; Friedrichs et al., 1990). Consequently, an increase in total tidal-flat surface area in the basin will cause a decrease in the net sediment-transport capacity in the flood direction at the inlet. The Schelde estuary evolved from a relatively shallow estuary with several branches and large tidal-flat areas in 1650 to the deep, funnel-shaped estuary with only a small intertidal surface area of today. A decrease in distortion of the basin tide and thus a decrease in counteraction of the North Sea tide at the entrance of the estuary was to be expected since the total tidal-flat area decreased. However, simulation of the tides in the estuary using a numerical flow model (Chap. 6) showed the opposite: The counteraction of the North Sea tide increased. The more synchronous flooding of the remaining tidal-flat area in the present-day Schelde, caused by an increase in celerity of the tidal wave, had a similar effect as an increase in tidal-flat surface area. This means that the amount of sediment transported into the Schelde estuary due to the dominance of the flood currents at the entrance of the basin has diminished since 1650 AD.

Tidal simulations for the North-Holland tidal basin (Chap. 7) show that infilling of the basin and expansion of the tidal-flat area led to a decrease in the flood-dominant tidal asymmetry at the mouth of the basin, and a reversal of the direction of net sediment transport within the basin from a flood to an ebb direction. Silting up of the Westerschelde and the North-Holland tidal basin both apparently resulted in a decrease in active tidal-flat surface area caused by accretion of the tidal flats to high-tide level, whereas the opposing effect of the flats on the tidal asymmetry at the basin entrance was not diminished. The tidal flow and the variations in water level became more in phase as a result of the reduction in active tidal-flat area.

The results of the tidal simulations for the North-Holland tidal basin indicated several inaccuracies in the basin reconstructions. The calculation showed that around 7200 BP the basin was not predominantly lagoonal, as had been inferred from core data. The basin morphology in 7200 BP probably was simular to that in 5500 BP. Moreover, the cross-sectional area of the Bergen inlet, indicated by the size of the Bergen Clay that was deposited in it, proved to be too large for the flood volume calculated for the maximum basin extension around 5500 BP. This means that the cross-sectional area suggested by the Bergen Clay does not represent the inlet dimensions at any particular moment and that part of the Bergen Clay was deposited while the inlet was still active.

3. Holocene depositional sequences in the Dutch Wadden Sea south of the island of Ameland

Abstract

Over a hundred cored boreholes form the basis for a reconstruction of the Holocene depositional history of the Dutch Wadden Sea south of the island of Ameland.

The general stratigraphic sequence shows basal peat grading into reed clays and mud-flat deposits of Atlantic age, erosively overlain by Subatlantic, sandy channel-point-bar deposits. Radiocarbon dating of the peat shows that the area has been below mean sea level since 7100 BP. Subboreal deposits were completely eroded by shifting Subatlantic channels. However, an almost complete sequence of mud and peat, deposited in the distal part of this tidal basin, ranging in age from Late Atlantic to Late Subatlantic, has been preserved onshore, in the present-day province of Friesland.

An idealized channel-point-bar sequence was constructed from 14 box cores. It shows cross-bedded to parallel-laminated sands that grade upwards into ripple-bedded sands with intercalated flaser bedding. Comparison of this reference sequence with the channel deposits in the cores from the boreholes shows that the sequences found in the latter are incomplete.

A gradual lateral transition from marine sandy deposits to brackish muddy deposits existed in the Atlantic. In the present-day Wadden Sea this gradient no longer exists. The parts of the basin at the landward side have been reclaimed and the dikes form abrupt boundaries between land and sea. Net deposition of fine-grained sediments is limited to a small part of the area.

Introduction

This paper describes the Holocene sedimentary sequences found in cores from boreholes in the Dutch Wadden Sea south of the island of Ameland (Fig. 3.1). Previous studies in the present Dutch Wadden Sea concentrated mainly on the present-day tidal flats and barrier islands. Important sedimentological studies of the Dutch Wadden Sea have been published by Van Straaten (e.g. 1950, 1954, 1961), Van Straaten and Kuenen (1957, 1958) and Postma (1954, 1961, 1981). Most sedimentological papers on the German Wadden Sea are not entirely applicable to the situation in the Dutch Wadden Sea. According to Reineck (1972), the average mud content of the sediments in the German part of the Wadden Sea is higher than in the Dutch part. Sha (1989a,b,c,d; 1990), Sha and De Boer (1991) and Sha and Van den Berg (1993) give detailed analyses of the sedimentology and morphodynamics of the major tidal inlets and associated ebb-tidal deltas of the Dutch part of the Wadden Sea. Dune formation on the barrier islands is discussed by De Jong (1984). For an overview of the geology of the Dutch barrier islands, the Dutch Wadden Sea and the neighbouring onshore sediments the reader is referred to Van Staalduinen (1977). A general overview of the development of the coastal plain of the Netherlands during the Holocene is given by Zagwijn (1986).

The present knowledge of the Holocene evolution of the Dutch Wadden Sea is mainly based on the study of marine deposits in the northern parts of Groningen and Friesland, the most landward parts of the former Wadden Sea. These deposits consist predominantly of clay and intercalated peat layers. The time frame for the evolution of this area is established based on pollen analysis and on radiocarbon dating of the peat layers. For stratigraphic studies on this area the reader is referred to e.g. Wensink and Bakker (1951), Bakker (1954), Wensink (1958), Jelgersma (1961), Roeleveld (1974), Ter Wee (1976), Griede (1978), Griede and Roeleveld (1982) and De Groot et al. (1987).

The sediments described in this paper were deposited in the mouth of the Boorne valley and east of it on the northward-trending spur of the Drenthe till plateau (Fig. 3.2). The sedimentary cover of this spur was locally not reworked by migrating tidal channels and therefore provides the most complete record of the Holocene depositional history.

Late-Weichselian relief

The Pleistocene landscape determined for an important part the Holocene evolution of the Dutch Wadden Sea. At the end of the Weichselian the northern Netherlands and the adjacent North Sea formed a slightly northward-dipping, periglacial landscape (Fig. 3.2). The relief was dominated by two glacial-till outcrops dating from the Saalian glaciation. An ice-pushed ridge with a maximum elevation of 15 m above NAP (NAP= Amsterdam Ordnance Datum, which corresponds approximately with the present-day mean sea level) forms the core of the island of Texel and extends into the western part of the Wadden Sea (Fig. 3.2: Texel High). A northward-sloping extension of the Drenthe glacial-till plateau is found in the central part of the Wadden Sea near Ameland (Fig. 3.2). The plateau is an almost flat, gently westward-dipping area bordered in the east by a northward-trending glacio-fluvial valley (Ter Wee, 1962; Van den Berg and Beets, 1987). This depression has been filled in since the Late Saalian (Van Staalduinen, 1977; Bosch, 1990). In the Holocene, remnants of it still existed which are known as the Hunze valley (Fig. 3.2). A northward-flowing river, draining the western part of the platform, developed in the Saalian and Late Pleistocene (De Groot et al., 1987; De Gans and Van Gijssel, this volume). This river was the precursor of the Holocene Boorne and its medieval successor the Middelzee (Figs. 3.1 and 3.2). These valleys were the first parts of the Wadden Sea to become inundated during the Holocene sea-level rise. The area west of the line Vlie inlet - Harlingen (Fig. 3.2) was not subjected to tidal sedimentation until the early Subatlantic (Jelgersma and Ente, 1977), because locally, the Pleistocene surface was situated at a relatively high elevation.

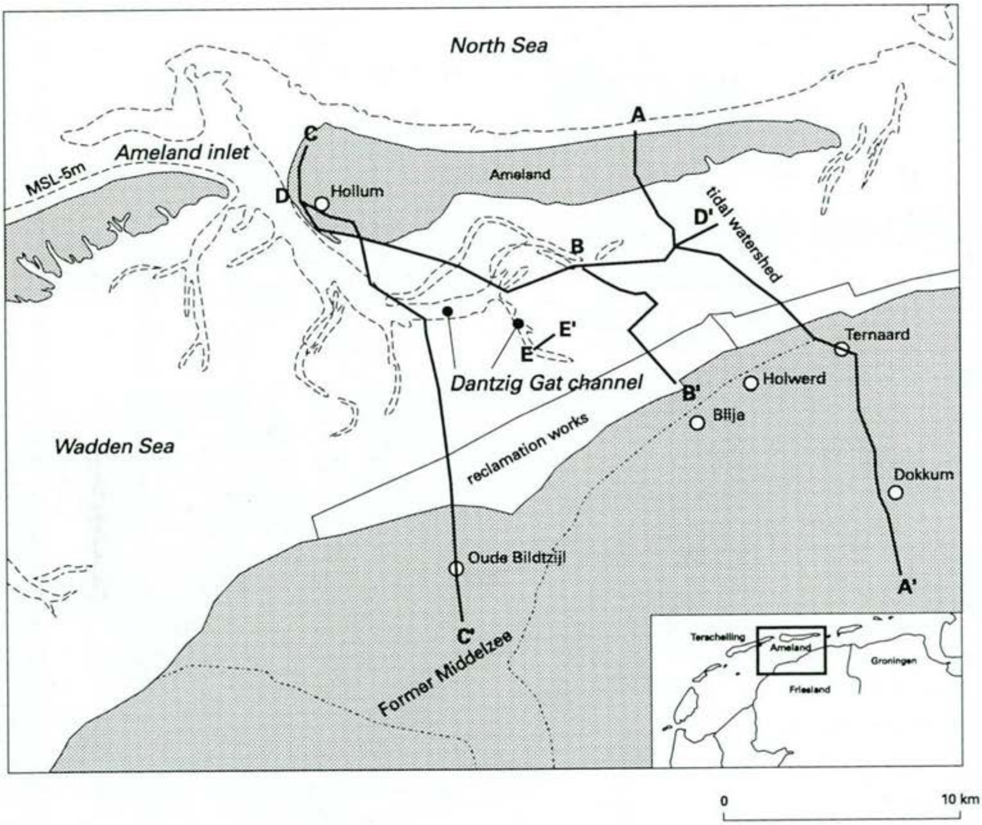

Figure 3.1 Location map of the study area in the Dutch Wadden Sea near the island of Ameland. The cross-sections indicated: AA' etc. are given in Figs. 3.5, 3.7 to 3.9 and 3.15. The MSL-5 m contour represents the 1978 situation.

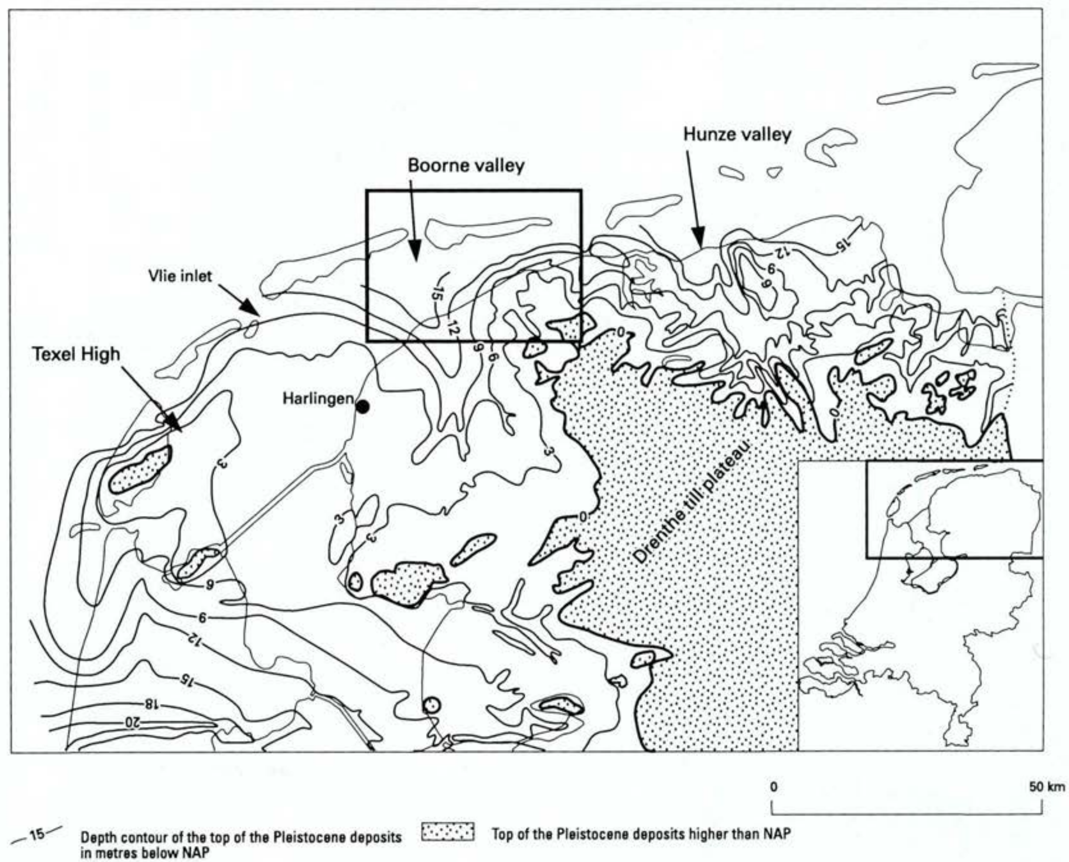

Figure 3.2 Map of the early Holocene relief in the Northern Netherlands. The inset shows the study area. N.B. the depth contours are schematic, they correspond only roughly with Figure 3.4. (After Zagwijn, 1986.)

Holocene sea-level rise

Overall trend curves for the Holocene relative sea-level rise in the Netherlands, mainly based on the start of peat formation in the back-barrier areas, are given by Jelgersma (1961, 1977, 1979) and Van de Plassche (1982). These curves represent the rise in ground-water level in the coastal plain of the Netherlands. Contrary to Jelgersma (1979), Van de Plassche (1982) assumes small variations in rate and direction of sea-level movement after 5000 BP. These variations, however, have not been confirmed as yet. Roep and Beets (1988) published a trend curve for the rise of the mean sea level at the coast of the western Netherlands since 5600 BP on the basis of sedimentary structures in the barrier sequence. Van de Plassche and Roep (1989) combined the peat and barrier curves into a more general framework encompassing possible variations in the rate of sea-level rise.

The rate of sea-level rise amounted to more than 0.75 m per century until about 7000 BP, 0.40 to 0.30 m per century between 7000 BP and 5500 BP and 0.15 m per century between 5500 BP and 3500 BP (Chap. 3; based on Jelgersma, 1979). Subsequently it started to decrease to an average rate of 0.05 m for the last 2000 years (Fig. 3.3).

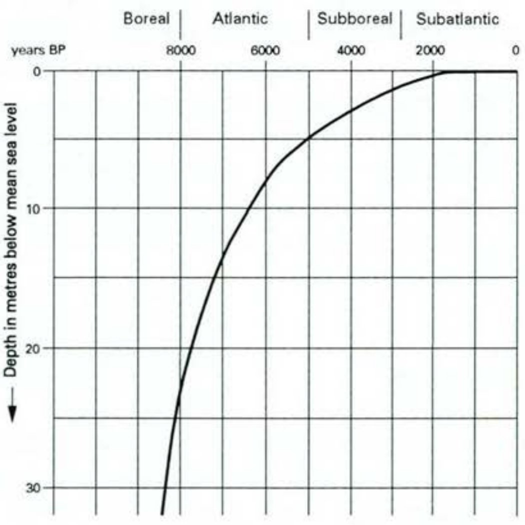

Figure 3.3 Trend curve for the relative sea-level rise in the coastal plain of the Netherlands. The curve shows a strong decrease in the rate of sea-level rise between 6000 BP and 5500 BP. After Jelgersma (1979).

Methods

This investigation is based on 108 continuously cored boreholes, most of which had a diameter of 0.07 m. The cores were taken by the Friesland Directorate of Rijkswaterstaat and the Geological Survey of The Netherlands (RGD). Further lithological data on the barrier islands, the Wadden Sea and the Frisian mainland were derived from RGD's database. These were collected during the past decades as part of a regional inventory study. Lithological data obtained from the area of land-reclamation works (Fig. 3.1) were provided by the Flevoland Directorate of Rijkswaterstaat.

The lithology of 15 cores was described in detail and median grain sizes of the sandy deposits were estimated using a grain-size comparator. Grain size is not shown in the lithological logs of Figs. 3.11 to 3.14, 3.19 and 3.20, since the estimated median grain sizes show little varation. Sedimentary structures were studied using lacquer peels. An idealized vertical sequence for the sub- and intertidal point-bar deposits of the Dutch Wadden Sea was compiled from a series of Reineck box cores. Clayey intervals were examined for pollen and diatom content by the RGD Palaeobotanical Department. Depositional ages were established by analysis of pollen assemblages and by radiocarbon dating of shell material. Fifteen carefully selected shell samples were radiocarbon-dated by Accelerator Mass Spectrometry (AMS, see Van der Borg et al., 1987, for a description of the method) at Utrecht University. Juvenile specimens that had an unabraded habitus and a complete periostracum were selected. These specimens are assumed to have been transported for a short period only and over a short distance before deposition, since transportation over longer distances would have worn the shell. These shells are therefore likely to provide an accurate indication of the age of the deposits that contain them. Moreover, the radiocarbon datings have been cross-checked against pollen information to preclude errors introduced by selecting shell material that is older than the host sediment.

The Wadden-Sea sequence

The Holocene sediments in the Wadden Sea form part of the Westland Formation, a unit that consists mainly of Holocene coastal, marine, lagoonal and tidal deposits (Zagwijn and Van Staalduinen, 1975). The Holocene sequence consists of a basal peat which grades into humic and root-bearing clay, overlain by bioturbated, muddy silts and fine-grained sands. A thick sequence of predominantly sandy point-bar and intertidal deposits forms the top of the Holocene sequence in the study area.

The base of the Holocene sequence in the study area is found at depths ranging from about NAP on the Frisian mainland to more than 30 m below NAP beneath the island of Ameland (Fig. 3.4). A Pleistocene 'core', which could be the continuation of the Drenthe plateau, has not been found below the island of Ameland (Fig. 3.5).

The time boundaries of the Holocene substages on the basis of pollen datings used in this paper are: Atlantic, 8000 BP to 5000 BP; Subboreal, 5000 BP to 2900 BP and Subatlantic, 2900 BP to present (Zagwijn, 1986).

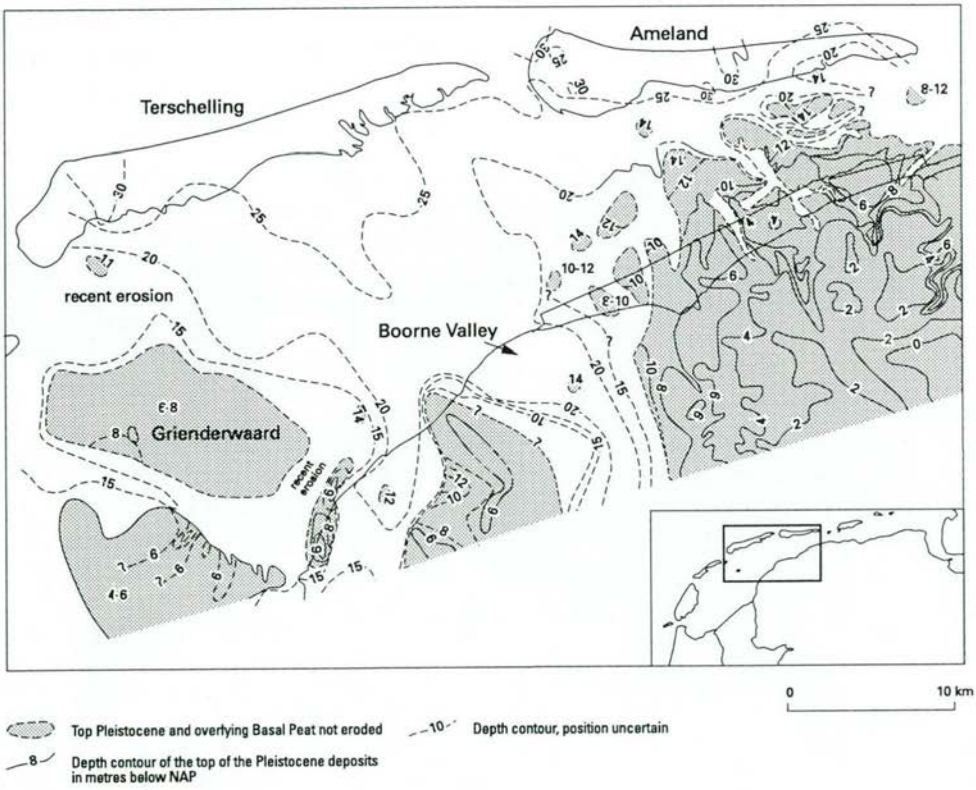

Figure 3.4 Detailed map of the depth of the base of the Holocene deposits south of Terschelling and Ameland. The Basal Peat and overlying fine-grained Atlantic deposits are missing where younger channels scoured into the Pleistocene subsurface, e.g. in the mouths of the former Boorne Valley and the Middelzee (Fig. 3.1). The map is based on unpublished information of the Geological Survey of The Netherlands and the Friesland and Flevoland Directorates of Rijkswaterstaat and on data collected by Griede (1978).

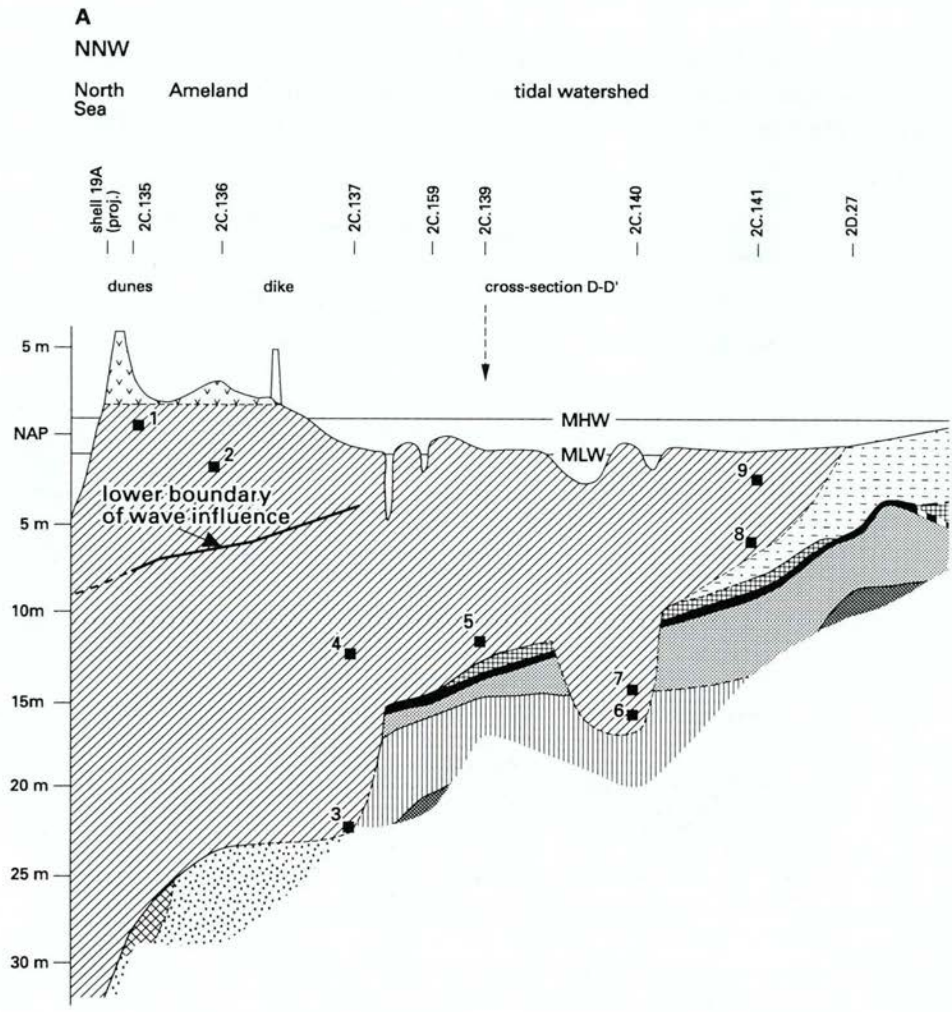

Figure 3.5 Cross-section AA′ through the Holocene and Pleistocene deposits from central Ameland to the Frisian mainland. Location of the cross-section is shown in Fig. 3.1. The Holocene succession consists of Atlantic peat and clay that is overlain by a thick wedge of Subatlantic cross-bedded sands in the Wadden Sea. Subboreal deposits are missing here due to erosion by migrating tidal channels. On the mainland of Friesland a more complete sequence of

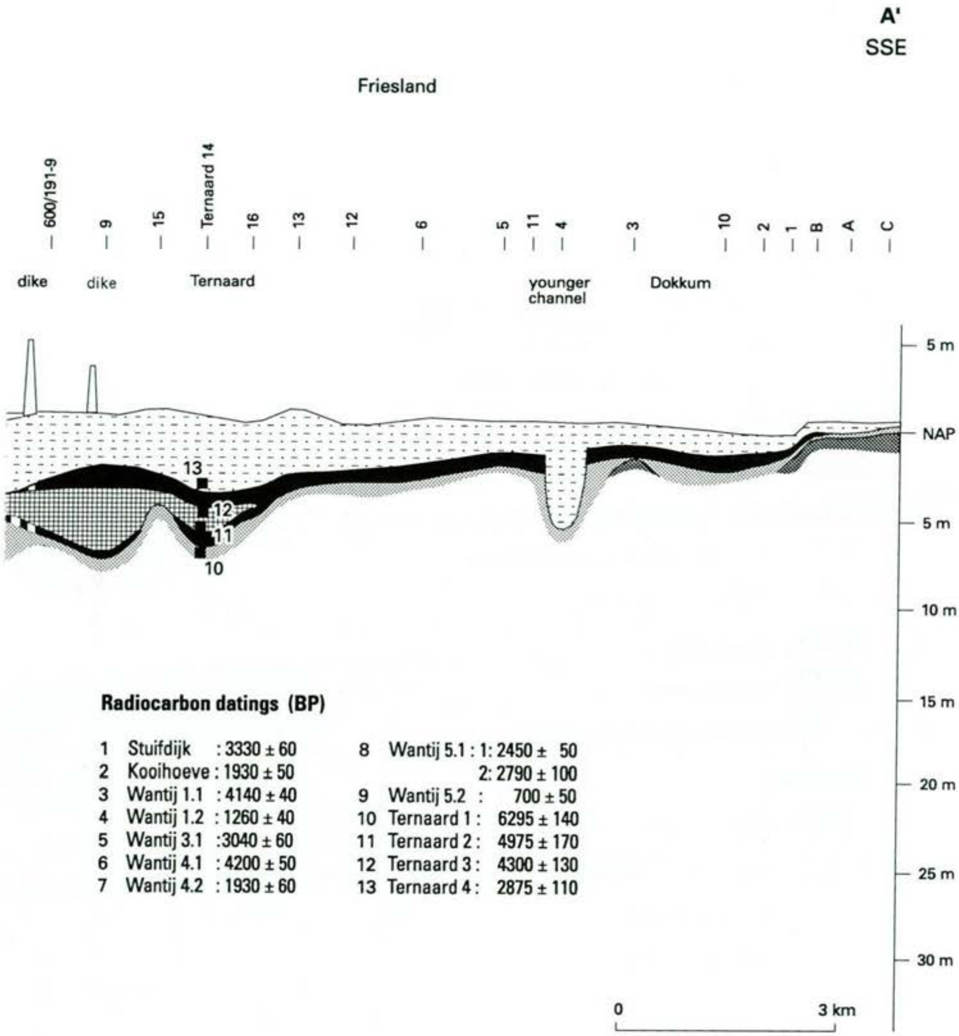

clays and peats is found. See overleaf for legend. The cores 2C.137, 2C.141 and Ternaard 14 are shown in detail in the Figs. 3.14, 3.11 and 3.20 respectively. See Tables 3.1 and 3.2 and Fig. 3.10 for more information on the radiocarbon-dated shells and peats. The mainland part of this cross-section was published by Jelgersma (1961).

Legend to Figures 5,7,8 and 9

Holocene

- Dune and salt-marsh deposits
- Clayey sand / sandy clay
- Cross-bedded sands (channel-point-bar deposits , overlain by sandy to muddy intertidal deposits) and, on the northern side of Ameland, a thin layer of beach deposits
- Bioturbated silts and fine-grained sands
- Humic and / or root clay
- Peat

Pleistocene

- Weichselian, (predominantly) cover sand
- Eemian marine sands and clay
- Saalian glacial till
- Elsterian Potclay
- Undifferentiated Pleistocene sand

Miscellaneous

- Washed-out gravel and stones
- Early-Holocene or Eemian marine sands and clay
- Boundary uncertain
- Radiocarbon dating

Figure 3.5, continued

Pleistocene

Outcrops of Pleistocene sediments occur on the Frisian mainland, see Fig. 3.2. Where the top of the Pleistocene sediments has not been eroded in the study area, it consists of Late-Weichselian deposits. These Weichselian deposits include eolian cover sands and fluvial loamy sands of the Twente Formation (Zagwijn and Van Staalduinen, 1975; Fig. 3.6). They overlie the Saalian glacial till of the Drenthe Formation (Fig. 3.6) in part of the area. Eemian marine sands and clays are found between the Weichselian and Saalian deposits in the central part of the study area (Figs. 3.5 to 3.7).

In the Boorne valley, south of the inlet between the islands of Terschelling and Ameland, and in the Wadden Sea south of Terschelling, the top of the Pleistocene sequence has been eroded (Figs. 3.4 and 3.8). Below Ameland, erosion has cut down into the stiff glacio-lacustrine Potclay and associated fine-grained sands of the Peelo Formation which were laid down during the Elsterian glaciation (Zagwijn, 1973; Ruegg, 1975; Figs. 3.5, 3.6 and 3.9). In the Boorne Valley the top of the Pleistocene is formed by a thin layer of washed-out gravel and stones and remnants of cover sand, overlying Saalian glacial till (cross-section CC', Fig. 3.8).

Basal Peat

Where not eroded by Holocene channels, a podzolic soil with vertical root traces is found at the top of the Pleistocene deposits. It is overlain by a thin, dark-brown to black, strongly compacted peat, sometimes with thin, intercalated clay layers and frequently containing wood remains. The lower part of this Basal Peat is often sandy. Towards the top the peat becomes clayey and usually grades into organic-rich clay (see below). Locally, the Basal Peat is directly overlain by sandy point-bar deposits. The peat consists of *Alnus* fen wood peat grading into *Phragmites* peat. The maximum total thickness of the peat layer is 0.45 m. In the Wadden Sea south of Ameland the Basal Peat occurs at depths ranging from 4.5 to 16 m below NAP. Figure 3.4 shows the distribution of the Basal Peat.

Peat formation in the coastal plain of the Netherlands was mainly due to a rising ground-water table caused by poor drainage as a consequence of the rising sea level (Jelgersma, 1961; Van Straaten, 1963). The resulting evolution of the vegetation is illustrated clearly by the composition of the Basal Peat in core 1H.108 (cross-section DD', Fig. 3.9). It consists of woody fen peat, which overlies 0.1 m of humic sand, and grades upwards into slightly clayey *Phragmites-Carex* peat. This succession indicates the replacement of a temperate forest vegetation by a swampy forest vegetation

geochronology		stratigraphy of the Wadden-Sea area, south of Ameland lithostratigraphic units	 lithological descriptions
	Holocene	Westland Formation	marine to brackish sands and clay, peat
Late Pleistocene	Weichselian	Twente Formation	eolian sands, locally fine-grained fluvial sands, loams and peat
Late Pleistocene	Eemian	Eem Formation	marine sands and clay
Middle Pleistocene	Saalian	Drenthe Formation	glacial till and coarse-grained sands
Middle Pleistocene	Holsteinian	?	?
Middle Pleistocene	Elsterian	Peelo Formation	glacio-lacustrine fine-grained sands and clay (Potclay)
Middle Pleistocene	Elsterian	?	?

Figure 3.6 Simplified stratigraphic table of the Mid and Late Pleistocene and Holocene deposits in the study area.

Table 3.1 Radiocarbon datings of peats from the central part of the Dutch Wadden Sea. The dated peats were either Basal Peat or peat layers intercalated in the humic and root clays. Sample locations are given in Fig. 3.10. Refs.: a. Jelgersma (1961); b. Ente (1977).

sample location and name	depth below NAP (m)	material	stratigraphic position	age BP	analysis nr.	reference
cross-section AA′, Fig. 3.5; borehole Ternaard 14 (Fig. 3.20)						
Ternaard 4	3.58- 3.61	*Sphagnum* peat	- top intercalated peat layer	2875 ± 110	GrN-602	a
Ternaard 3	4.29- 4.33	*Phragmites* peat	- base intercalated peat layer	4300 ± 130	GrN-499	a
Ternaard 2	5.91- 5.96	gyttja	- top Basal Peat	4975 ± 170	GrN-601	a
Ternaard 1	6.62- 6.65	*Eriophorum* peat	- base Basal Peat	6295 ± 140	GrN-606	a
cross-section BB′, Fig. 3.7; borehole RYP 18						
Blija 1	7.77- 7.80	*Phragmites/Carex* peat	- base intercalated	5540 ± 40	GrN-7748	b
Blija 2	idem	idem	peat layer	5440 ± 60	GrN-8107	b
cross-section DD′, Fig. 3.9; borehole 1H.108						
Molengat 2	13.53-13.56	wood peat	- base of Basal Peat	7095 ± 50	GrN-18285	
Molengat 1	13.56-13.62	humic sand	- base of soil below Basal Peat	7025 ± 50	GrN-18286	
location Grienderwaard: Fig. 3.10						
Grienderwaard 2	1.80- 1.90	*Phragmites* peat	- top intercalated peat layer	3015 ± 35	GrN-7291	b
Grienderwaard 1	6.50- 6.55	*Phragmites* peat	- top Basal Peat	5290 ± 70	GrN-7747	b

and eventually by a reed vegetation as the rising ground-water table reaches the surface level. The increase in clay content in the peat, and the associated increase in Chenopodiaceae pollen indicate an increasing marine influence.

The base of the Basal Peat in core 1H.108 (cross-section DD', Fig. 3.9; Fig. 3.10) was radiocarbon dated at 7095 $\pm$ 50 BP to 7025 $\pm$ 50 BP (Table 3.1: datings Molengat). The top of the Basal Peat at the Grienderwaard, south of the island of Terschelling (Fig. 3.10), was dated by Ente (1977) at 5290 $\pm$ 70 BP (Table 3.1). Both radiocarbon datings agree with the Atlantic pollen assemblages found in the Basal Peat from this part of the Wadden Sea.

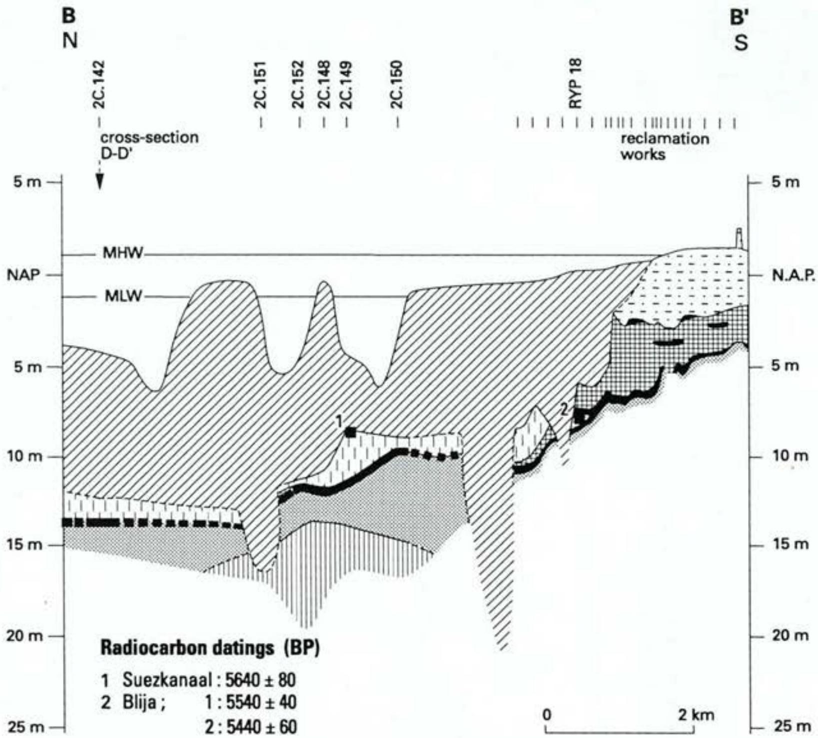

Figure 3.7 Cross-section BB', below the tidal flats north of Blija. Location of the cross-section is shown in Fig. 3.1. The section shows Atlantic Basal Peat overlain by Atlantic mud-flat deposits (bioturbated silts and fine-grained sands). In the southern part a continuous sequence of clays and intercalated peats is found. A thick layer of Subatlantic cross-bedded sands overlies the Atlantic deposits in the Wadden Sea erosively. Core 2C.148 is given in detail in the Figs. 3.13 and 3.14. See Fig. 3.5 for lithological legend. The base of the Holocene sequence follows the contours of Fig. 3.4 where its position is not directly known from boreholes. See Tables 3.1 and 3.2 and Fig. 3.10 for more information on the radiocarbon-dated shells and peats. The landward part of the cross-section is based on information of the Flevoland Directorate of Rijkswaterstaat and Ente (1977, fig. 3.2.3).

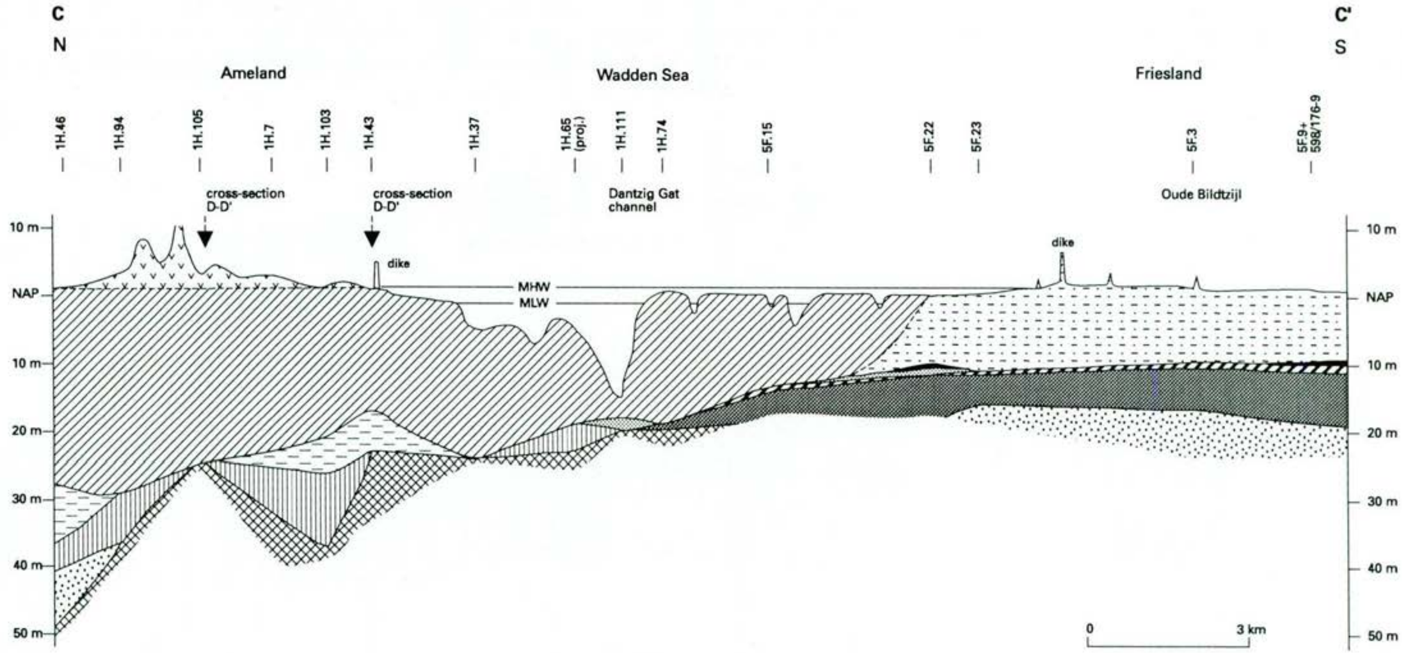

Figure 3.8 Cross-section CC′ trends south through the Holocene and Pleistocene deposits from the western end of Ameland into the former Middelzee. Location of the cross-section is shown in Fig. 3.1. The section shows a thick sequence of sandy channel deposits that becomes clayey towards the south. No distinction can be made between Eemian and early Holocene marine deposits below Ameland. See Fig. 3.5 for lithological legend. The section is based on unpublished information of the Geological Survey of The Netherlands. N.B. uncertain boundaries have not been indicated by dashed lines considering the vertical scale of this section.

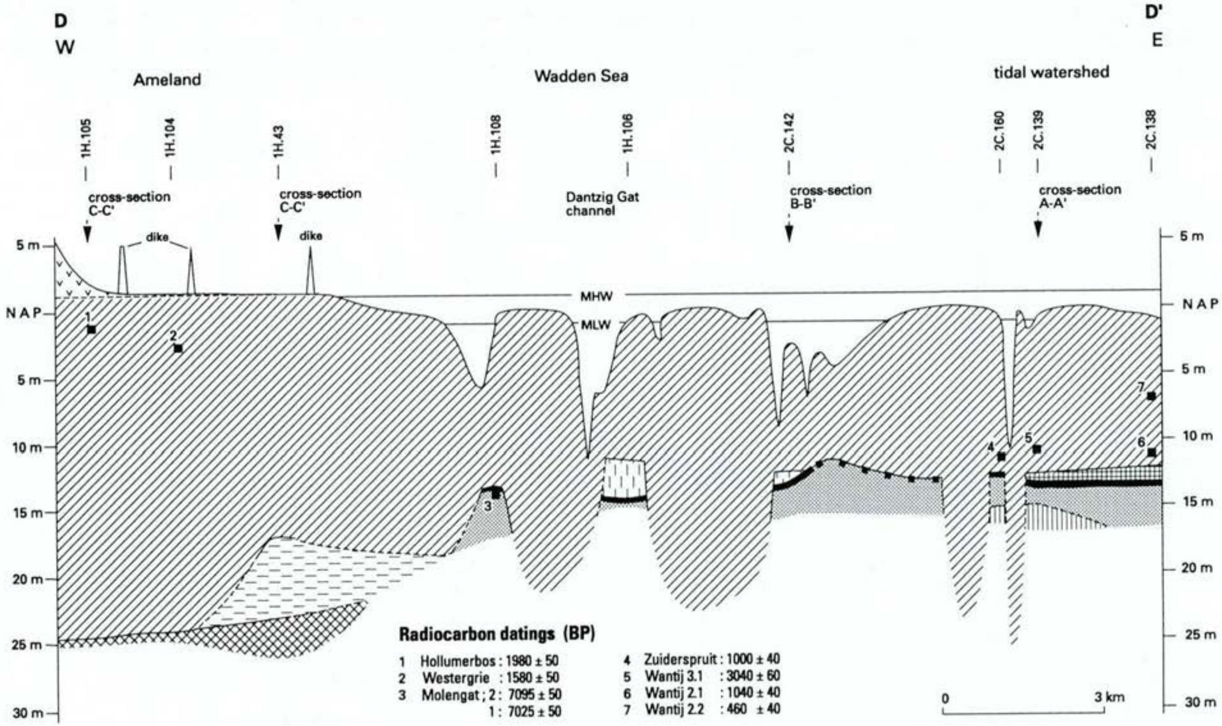

Figure 3.9 Cross-section DD′ through the Holocene and Pleistocene deposits in the Wadden Sea. It trends parallel to the island of Ameland; the location is shown in Fig. 3.1. The cross-section shows a thick sequence of sandy channel deposits overlying and cutting into Atlantic peats, clays and mud-flat deposits (bioturbated silts and fine-grained sands). See Fig. 3.5 for lithological legend. No distinction can be made between Eemian and early Holocene marine deposits below Ameland. The base of the Holocene sequence follows the contours of Fig. 3.4 where its position is not directly known from boreholes. See Tables 3.1 and 3.2 and Figure 3.10 for more information on the radiocarbon-dated shells and peats.

Humic and root-bearing clay

A parallel-laminated, dark to blue-grey, organic-rich clay frequently overlies the Basal Peat. It contains very thin layers (less than 1 mm) of silt and also thin layers of (peat) detritus and/or plant remains. The organic content decreases towards the top. However, humic intervals that sometimes grade into peaty clays are found locally (e.g. core 2C.141, Fig. 3.11, between 7.93 m and 8.10 m). Penetration by *Phragmites* roots occurs, although not directly above the Basal Peat. Occasionally, thick, woody roots are found (e.g. core 2C.141, Fig. 3.11, between 8.63 m and 8.69 m). The clay has a maximum thickness of 0.8 m and is erosively overlain by silts and sands.

A root-bearing, grey clay layer that is less rich in organic material and contains intervals of mm-thick layers of very fine-grained sand overlies the humic clay in cores 2C.138 and 139 (cross-sections AA' and DD', Figs. 3.5 and 3.9). The roots are very thin (not more than 2 mm in cross-section) and can be traced vertically over short intervals only. A similar root pattern is known from *Salicornia*, a short-living upper-intertidal to supratidal plant. *Salicornia* roots can be preserved during rapid clay sedimentation (D. de Jong, Rijkswaterstaat-RIKZ, pers. comm.). The probable occurrence of *Salicornia* in this clay is supported by the high percentages of Chenopodiaceae pollen (Cleveringa, pers. comm.).

The humic clays were deposited in a fresh to brackish environment dominated by reed vegetation. The upward decrease in organic constituents reflects the decline of the vegetation in the area and the further rise of the (ground-)water table that eventually resulted in drowning of the Basal Peat. The clay must have been derived from the North Sea since no major fluvial sediment source existed in this part of the Wadden Sea. Intercalated reed peat (e.g. core 2C.141, Fig. 3.11) indicate a lateral alternation of pond-like water bodies where clay deposition prevailed, and vegetated zones where reed peat was formed. Diatom assemblages show elements of stagnant, shallow, fresh to brackish water bodies, salt marshes and (upper-intertidal) mud flats (RGD, unpublished data). This indicates deposition of the clays in an open environment comprising ponds and pools, alternating with zones where reed vegetation prevailed. Although there is no evidence of tidal influence, importation of marine clay is certain. Marine diatoms were introduced together with the clay. The facies can be characterized as a (temperate) coastal swamp.

The clays containing *Salicornia* roots in cores 2C.138 and 139 were, in contrast with the clays described above, laid down in a more open mud-flat environment. This is suggested by the (extremely) high percentages of

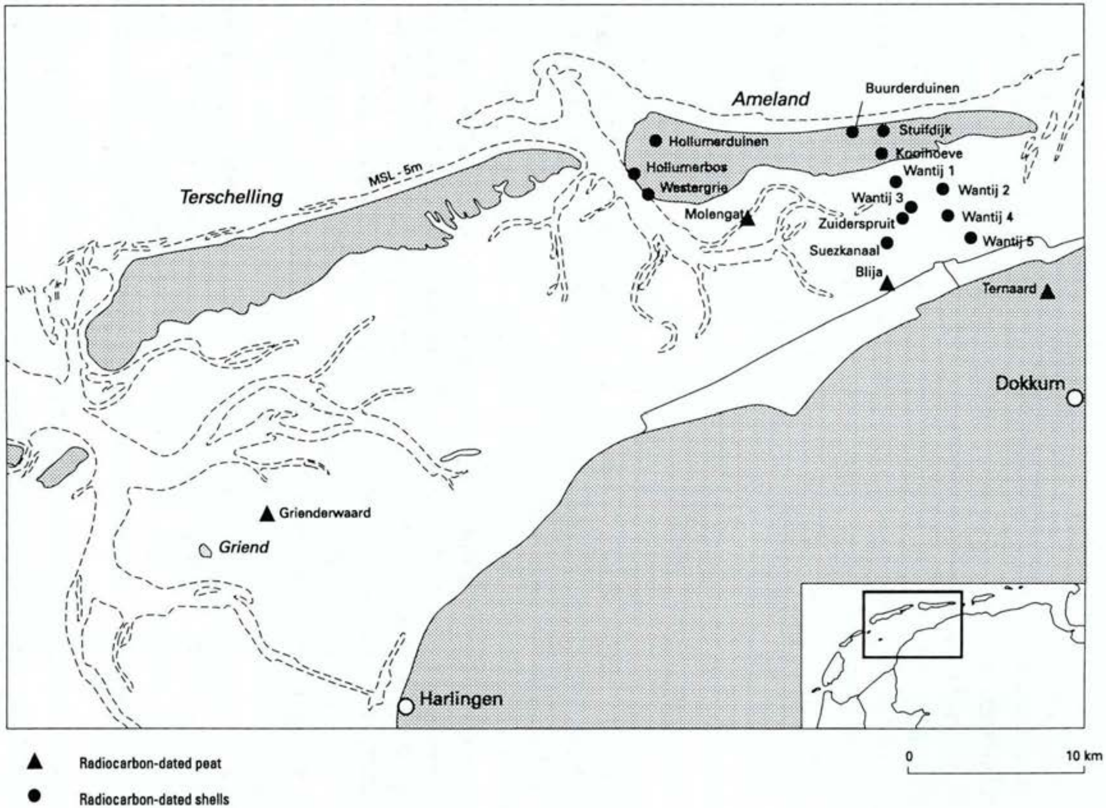

Figure 3.10 Location map of radiocarbon datings given in text, cross-sections and Tables 3.1 and 3.2.

Chenopodiaceae pollen and relatively low percentages of Gramineae pollen. The absence of bioturbation and the occurrence of pollen of *Ruppia*, a plant that thrives in low-energetic, shallow pools and can survive large fluctuations in salinity, point to a supratidal facies. The diatom assemblages indicate that clay deposition started in a mainly fresh-water, supratidal environment which became flooded gradually and evolved into an upper-intertidal one (H. de Wolf, RGD, pers. comm.). This facies is probably the seaward continuation of the reed clay facies.

The clays are Atlantic in age. Radiocarbon dates of intercalated peat layers were published by Ente (1977). The base of a peat layer below the reclamation works near Blija (cross-section BB', Fig. 3.7; Fig. 3.10) was dated at 5540 $\pm$ 40 BP to 5440 $\pm$ 60 BP (Table 3.1). Clay deposition continued during the Subboreal below the present-day tidal watershed south of Ameland (cores 2C.139 and 2C.141; cross-section AA', Fig. 3.5) and the Grienderwaard (Figs. 3.4 and 3.10). The base of a reed peat that overlies 4.6 m of (sandy) clay in the Grienderwaard was dated at 3015 $\pm$ 35 BP (Table 3.1).

Bioturbated muddy silts and very fine-grained sands

A strongly bioturbated muddy silt to very fine-grained sand (median grain size d_{50}: 125 to 180 μ) erosively overlies the humic clay in some of the cores from the area south of the island of Ameland (Fig. 3.1: CC'). The sediment is dark to very dark (brown-)grey and alternates with intervals of mud-free, very fine-grained sand. In-situ shells and fragments of *Scrobicularia plana* and *Cerastoderma sp.* are abundant. Burrows which contain mud mixed with peat detritus and shells of *Peringia ulvae* (formerly *Hydrobia ulvae*) are common. Occasionally, the sandy sequence has been bioturbated only partly and shows small-scale (cross-)bedding with mud-draping and escape structures. These intervals are up to 1 m thick and grade upwards into strongly bioturbated muddy silts and sands. The maximum thickness of the strongly-bioturbated intervals is 0.5 m. The total thickness of this deposit ranges from a few decimeters up to 3 m. In one case (core 1H.106; cross-section DD', Fig. 3.9), the sediment grades into a heavy clay with humic spots. The unit is in all cases erosively overlain by cross-bedded sandy deposits. The interval between 11.3 m and 10.8 m below NAP in core 2C.148 (Figs. 3.12, 3.13) is a good example of this deposit. It shows an upward transition from cross-bedded and mud-draped sand to an alternation of parallel laminae of sand and mud. The top is truncated by a shell lag.

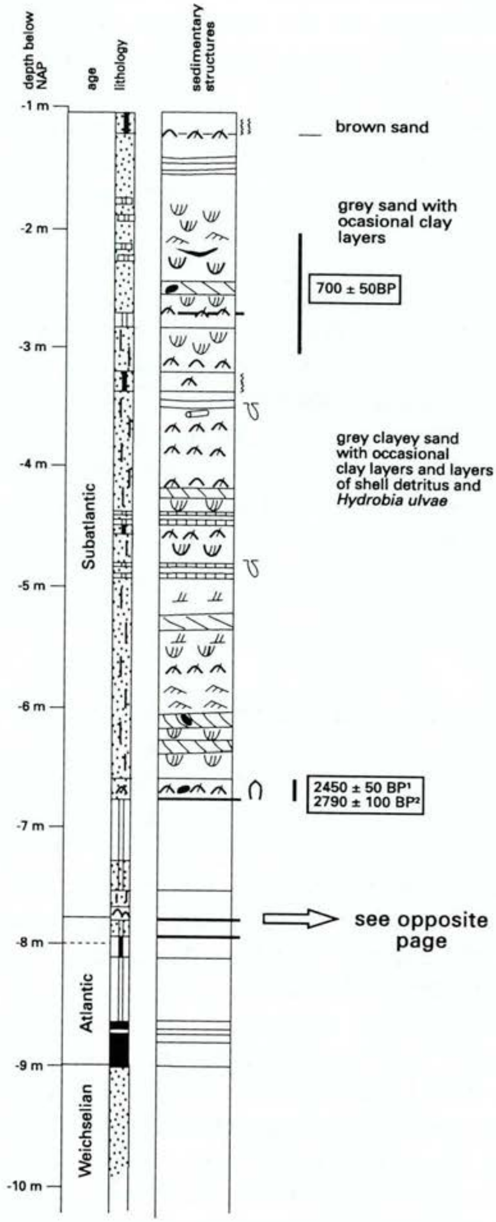

Figure 3.11 Detailed log of core 2C.141 from the tidal watershed south of Ameland (cross-section AA', Fig. 3.5). It shows Atlantic peats and root clays that are overlain by a very short interval of Subboreal sandy clays with an overall coarsening-up sequence of clayey and sandy Subatlantic channel deposits on top. See overleaf for legend. Ages mentioned in the log are

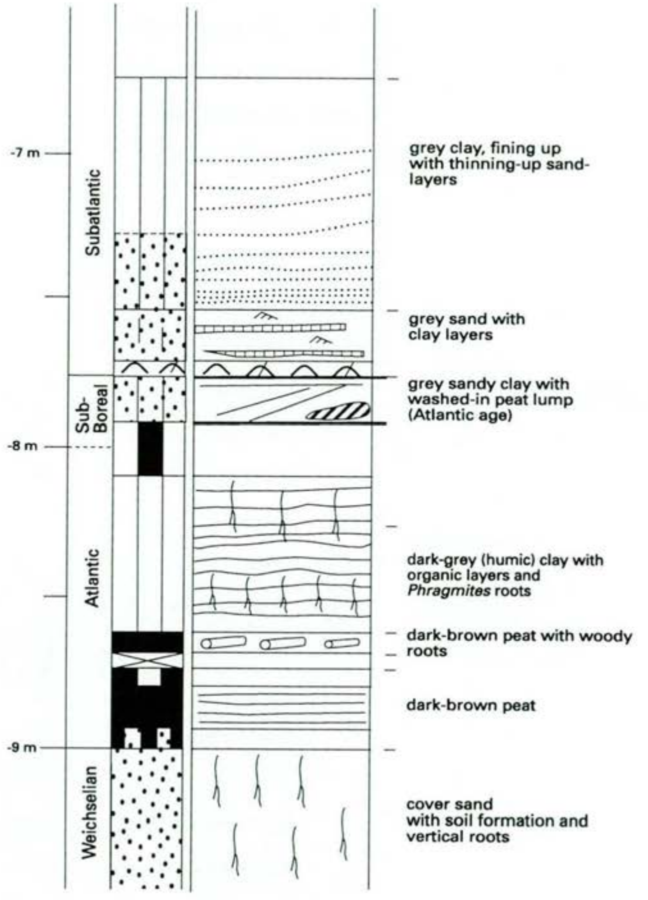

based on pollen assemblages. Both calcium carbonate (1) and organic carbon (2) from a shell pair found at a depth of 6.62 to 6.69 m have been radiocarbon dated. The radiocarbon ages are given in the log. See Table 3.2 and Fig. 3.10 for more information on the radiocarbon-dated shells.

Legend to Figures 11,12,14,19 and 20

Lithology

- Clay
- Sandy clay
- Humic to peaty clay
- Peat
- Clayey peat
- Sandy peat
- Sand
- Clayey sand
- Muddy sand
- Muddy silt
- Mud
- Gyttja
- Over 50% shells
- No recovery

Sedimentary Structures

- Trough cross lamination
- Ripple lamination
- Distinct ripples
- (Low-angle) parallel lamination
- Mega cross-bedding
- Erosional boundary
- 1961±32 BP Radiocarbon-dated interval
- Flasers
- Mud-draped ripples
- Sand lenses
- Mud balls
- Clay layers
- Sand layers
- Detritus layers
- Peat lump
- Shells
- Shell fragments
- Bivalves in living position
- Wood
- Plant remains
- Roots
- Burrow/escape structure
- Bioturbation/disturbed sediment

Figure 3.11, continued

Table 3.2 Radiocarbon datings of shells collected from channel-point-bar deposits below the island of Ameland and the Wadden Sea south of it. See Fig. 3.10 for sample locations. The age of sample Stuifdijk does not agree with its stratigraphic position. The samples numbered GrN-.. were dated conventionally. The samples numbered UtC-.. were dated using AMS (see Van der Borg et al., 1987, for more information). Ages are normalized to a delta-13 value of -25 per mil. The datings were corrected for the reservoir age of the North Sea (which is 400 radiocarbon years).

sample location and name	depth below NAP (m)	analysed species	stratigraphic position	age BP	Del-13 (per mil)	analysis nr.
cross-section AA′: Fig. 3.5						
Stuifdijk (2C.135)	+0.34-+0.84	various	dispersed	3330 ± 60		GrN-16267
Kooihoeve (2C.136)	1.32- 1.82	various	shell layer	1930 ± 50		GrN-16268
Wantij 1.2 (2C.137)	12.80-13.02	*Cerastoderma edule*	shell layer	1260 ± 40	-.5	UtC-1817
Wantij 1.1 (2C.137)	22.38-22.59	*Cerastoderma edule*	base channel lag	4140 ± 40	-.7	UtC-1816
Wantij 3.1 (2C.139)	10.62-10.85	*Cerastoderma edule*	top shell layer	3040 ± 60	-.2	UtC-1820
Wantij 4.2 (2C.140)	14.34-14.56	*Cerastoderma edule*	shell layer	1930 ± 60	-.6	UtC-1822
Wantij 4.1 (2C.140)	15.55-15.71	*Cerastoderma edule*	shell layer	4200 ± 50	-1.3	UtC-1821
Wantij 5.2 (2C.141)	2.05- 3.05	*Cerastoderma edule*	dispersed	700 ± 50	-.6	UtC-1825
Wantij 5.1 (2C.141)	6.62- 6.69	*Cerastoderma edule*	channel base	2450 ± 50	.1	UtC-1823
		organic carbon	idem	2790 ±100	-18.5	UtC-1824
cross-section BB′: Fig. 3.7						
Suezkanaal (2C.149)	8.98- 9.01	*Scrobicularia plana*	top silt layer	5640 ± 80	-3.2	UtC-1827
cross-section DD′: Fig. 3.9						
Hollumerbos (1H.105)	0.67- 1.67	*Cerastoderma edule*	dispersed	1980 ± 50		GrN-16266
Westergrie (1H.104)	2.50- 3.50	*Cerastoderma edule*	dispersed	1580 ± 50		GrN-16265
Zuiderspruit (2C.160)	11.14-11.36	*Cerastoderma edule*	shell layer	1000 ± 40	.2	UtC-1815
Wantij 3.1 (2C.139) see cross-section AA′						
Wantij 2.2 (2C.138)	6.56- 6.81	*Cerastoderma edule*	shell layer	460 ± 40	-.1	UtC-1819
Wantij 2.1 (2C.138)	11.39-11.85	*Cerastoderma edule*	channel lag	1040 ± 40	.4	UtC-1818
Central Ameland: Fig. 3.10						
Buurderduinen 3 (2C.157)	0.5 - 5.0	*Spisula subtruncata*	dispersed	1290 ± 50	.2	UtC-1814
Buurderduinen 2 (2C.157)	15.0 -17.0	*Spisula subtruncata*	shell layer	2110 ± 60	.9	UtC-1813
Buurderduinen 1 (2C.157)	24.0 -26.0	*Spisula subtruncata*	channel lag	2490 ± 40	.2	UtC-1812
West Ameland: Fig. 3.10						
Hollumerduinen (1H.109)	19.00-19.75	*Spisula subtruncata*	channel lag	2870 ± 50	-.4	UtC-1826

These mud-flat deposits formed during the Atlantic. This is supported by the radiocarbon age of a *Scrobicularia plana* shell pair, found in living-position in core 2C.149 (cross-section BB', Fig. 3.7) that was dated at 5640 $\pm$ 80 BP (Table 3.2: dating Suezkanaal).

The bioturbated muddy silts and very fine-grained sands are the earliest Holocene lower-intertidal to subtidal deposits found near Ameland. The thin, cross-bedded sandy sequences are inferred to have been deposited by laterally migrating tidal gullies. They grade upwards into an alternation of sand and mud laminae overlain by strongly bioturbated to completely homogenized muddy tidal-flat deposits.

The large amount of preserved mud, the small-scale cross-bedding in the gullies and the preservation of a thick, strongly bioturbated tidal-flat sequence (up to 0.5 m) indicate a quiet environment. These mud-flat deposits were formed in the sheltered, most-landward parts of the Atlantic precursor of the Wadden Sea. This type of quiet environment is not found in the present-day Dutch Wadden Sea since such parts have been reclaimed by diking. Consequently, the present-day Wadden Sea is more turbulent and most mud deposited on the tidal flats is sooner or later removed by waves and currents. Moreover, preservation of intertidal deposits in the present-day Wadden Sea was reported to be rare because of reworking by laterally migrating tidal channels (Van Straaten, 1954, 1961).

Summing up: the earliest Holocene deposits in the Wadden Sea south of Ameland consist of a series of fine-grained sediments and peat of Atlantic age. These sediments were formed in the most landward parts of the Atlantic Wadden Sea after 7100 BP. They show an upward transition from a fresh-water, mostly landward facies into a muddy tidal-flat facies.

Cross-bedded sands

A package of mainly cross-bedded sands erosively overlies the Atlantic sediments described above. This sediment body wedges out towards the south. The Holocene sequence below the island of Ameland and in a large part of the Wadden Sea south of it consists entirely of these cross-bedded sands.

This deposit includes fine-grained sands (d_{50}: 150 to 210 μ) with intercalated clay- and shell layers. Basal lag deposits of medium- to coarse-grained sand, shells and gravel are common. Mega cross-bedding (expressed as foresets dipping at low to high angles in planar sections of the cores) alternates with ripple bedding. Occasionally, clay pebbles and peat detritus are found incorporated in the foresets. Bioturbation and mud-drapes are rare. In the upper part of the sequence large-scale cross-bedding is absent. Instead, small-scale cross-bedding and, in the cores from Ameland, (low-angle) parallel lamination occurs. The bioturbation rate increases upwards.

This sequence is basically composed of point-bar deposits of migrating tidal channels. In the Wadden Sea, the sequence has a maximum thickness of about 16 m. It grades upwards into a thin veneer of intertidal-flat deposits. The sequences near and below Ameland, which were formed by migrating inlet channels, are up to about 30 m thick. On the barrier islands the inlet point-bar sequences and intertidal deposits are overlain by salt-marsh deposits and/or eolian dunes.

Point-bar deposits of migrating tidal channels

In the cores, the sequence consists from bottom to top of basal shell lags, megaripple bedding and low-angle cross- to parallel lamination alternating with small-scale cross-bedding and flasers, grading upward into predominantly small-scale cross-bedding. Shell lags at the base of the sequence may reach thicknesses of more than 1 m. *Cerastoderma edule*, *Macoma balthica*, *Mytilus edulis* and *Peringia (Hydrobia) ulvae*, shells representing a typical tidal-flat assemblage are found in layers or scattered throughout the sediment.

The sand was mainly transported by strong to medium tidal currents (depth-averaged, maximum current velocities over 0.45 ms^{-1}), as can be deduced from the sedimentary structures (cf. Terwindt, 1981). Wave influence is only evident in the top part of the sequence near the inlets. Occasionally, in the present-day intertidal reach, the top consists of small-scale cross-bedding and flaser bedding, sometimes overlain by a completely homogenized layer of brown, muddy sand. Deposits laid down on the upper-intertidal flat as described by Van Straaten (1954, 1961), Reineck (1972) and Reineck and Singh (1980) are not found in the cores; drilling boreholes was only possible in the channels and on the lower intertidal flats (up to 0.6 m below NAP), because of operational limitations of the drilling vessel that was used for coring.

The clay content of the sandy deposits increases with distance from the inlets (see core 2C.141, Fig. 3.11, and cross-sections AA' and CC', Figs. 3.5 and 3.8). Locally, clayey channel-fills are found intercalated in the sandy point-bar deposits. The top of the second-generation channel in core 2C.137 (Fig. 3.14: 7.6 m to 4.9 m - NAP) consists of 2.7 m of low-angle cross-laminated clay with thin intercalations of sand and detritus. This clay was deposited after a sharp decline in current velocity, probably due to abandonment of the channel. Clay-rich intertidal deposits are found mostly in places where wave and current energy are low, viz. in the most landward parts of the Wadden Sea and along the tidal watersheds.

Pollen assemblages in the intercalated mud and clay layers indicate that the sandy channel deposits in the Wadden Sea were laid down during the Subatlantic (RGD, unpublished data). Locally, at the tidal watershed south of Ameland (cross-section AA', Fig. 3.5), the base of the point-bar deposit has a Subboreal age (core 2C.139; core 2C.141: Fig. 3.11). Juvenile shells, collected from cores 2C.137, 139, 140 and 141 (cross-section AA', Fig. 3.5) and 2C.138 and 160 (cross-section DD', Fig. 3.9) were dated (see Fig. 3.10 for locations). The results range from 4200 $\pm$ 50 BP to 460 $\pm$ 40 BP (Table 3.2: datings Wantij and Zuiderspruit). Cores which were dated at more than one level, were all found to become younger upwards. However, some of the radiocarbon dates are not in accordance with those on the basis of pollen. Datings Wantij 1.1 and 4.1 (Table 3.2) are considered too old. Apparently, the specimens that were selected for dating were too old, despite their 'fresh' appearance. Both samples were taken from thick basal shell layers and are apparently not representative for the overlying channel deposits.

Datings Wantij 2.1, Wantij 5.2 and Zuiderspruit (Table 3.2, Fig. 3.10) show that channels that had depths almost identical to the current ones have existed at these locations since 1000 BP.

Core 2C.137 (Fig. 3.14; cross-section AA', Fig. 3.5), collected directly south of the island of Ameland, nicely illustrates the stacking of three 'generations' of channel deposits. It starts with a 1-m-thick basal shell lag with peat lumps and gravel, overlain by 10 m of cross-bedded sand. The next interval starts at 13.05 m below NAP with a sandy shell lag followed by 5 m of cross-bedded sand and 2.75 m of sandy clay. The third channel sequence starts on top of the clay interval, at 4.9 m below NAP. The upper metre of the core consists of mud with many in-situ mussel shells, overlain by 0.1 m of bioturbated brown-grey sand. Pollen analyses of intercalated mud and clay layers show that the whole sequence upwards from 21.6 m below NAP was formed after 700 AD Apparently, the sediments deposited by a 22-m-deep channel was very soon after its formation eroded by a second channel of 10 m depth, since the age of 1260 $\pm$ 40 BP of dating Wantij 1.2 (Table 3.2) corresponds with 700 AD. The second channel was partly filled in with mud. This deposit was subsequently eroded by a tidal gully. The radiocarbon date of the base of the core (Fig. 3.14) yields an age of 4140 $\pm$ 40 BP (Table 3.2: dating Wantij 1.1). This does not agree with the age of the overlying cross-bedded sequence. Either the basal part of the shell lag is part of an older channel system or, unfortunately, reworked older material was sampled for dating.

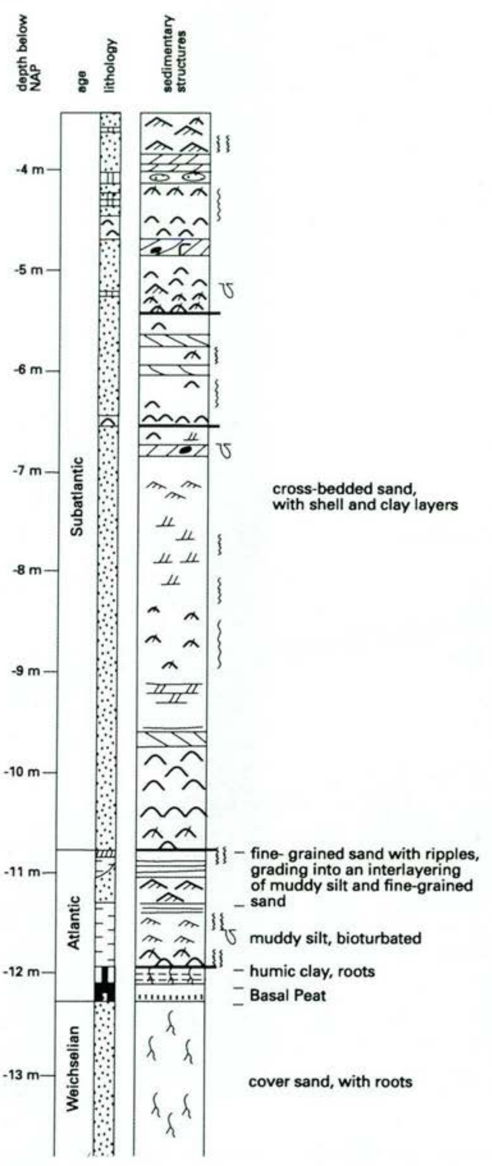

Figure 3.12 Detailed log of core 2C.148 from a channel south of Ameland (cross-section BB', Fig. 3.7). It shows thin Atlantic peat and root-bearing clay layers that are erosively overlain by Atlantic mud-flat deposits. The upper 11 m consists of Subatlantic sandy channel-point-bar deposits. See Fig. 3.11 for legend. Ages mentioned in the log are based on pollen assemblages. Figure 3.13 shows a lacquer peel of part of this core, from 10.50 m to 12.45 m below NAP.

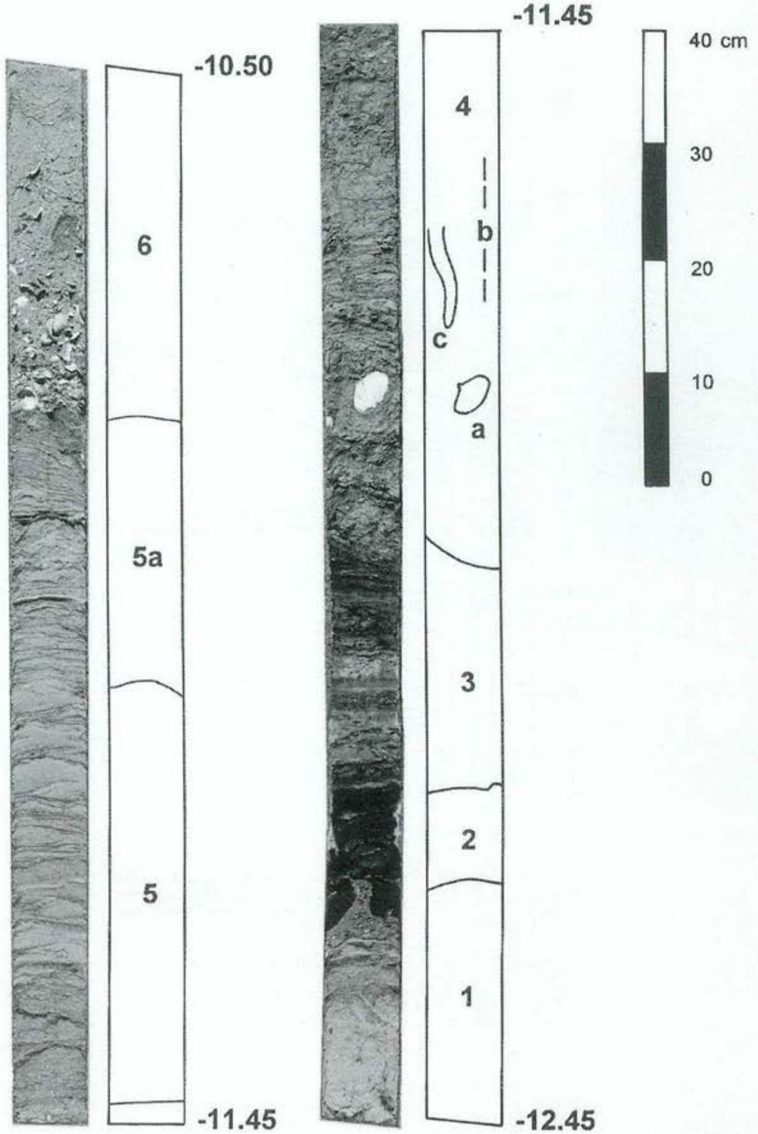

Figure 3.13 Lacquer peel of core 2C.148 (cross-section BB', Fig. 3.7), from 10.50 to 12.45 m below NAP. The peels show, from bottom to top: Weichselian cover sand (1), Basal Peat (2) and laminated humic clay with roots (3), erosively overlain by bioturbated muddy silts with shell fragments at the base (4). Locally, a complete *Scrobicularia plana* shell (a), partly disturbed (bioturbated?) small ripple bedding (b) and a burrow (c) can be seen. The bioturbated interval is overlain by ripple-bedded mud and very fine-grained sand with flasers (5) which grade into an alternation of muddy silts and very fine-grained sand and finally bioturbated mud (5a). This sequence of Atlantic age is erosively overlain by a shell lag and fine-grained sandy point-bar deposits of Subatlantic age (6). Compare with the detailed core log in Fig. 3.12.

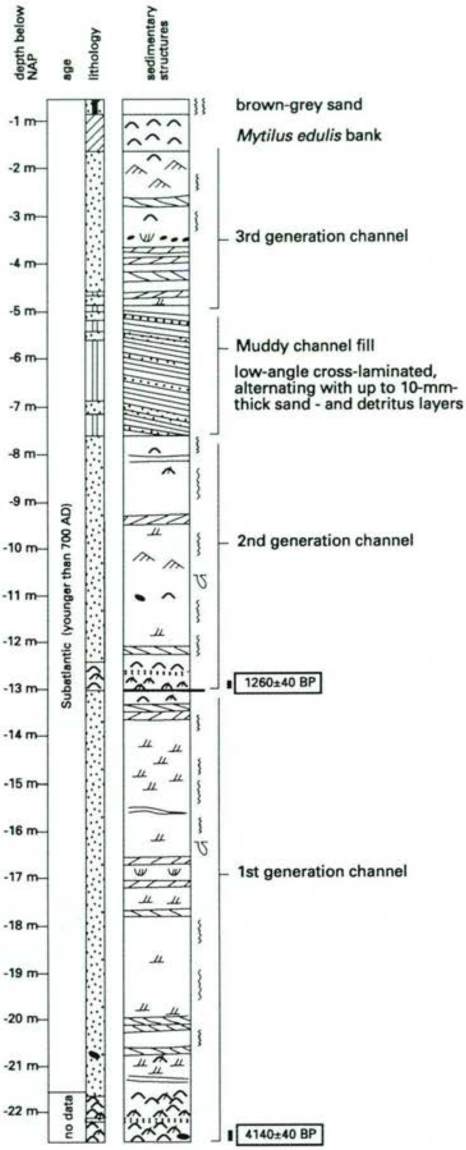

Figure 3.14 Detailed log of core 2C.137 from the tidal watershed south of Ameland (cross section AA', Fig. 3.5). See Fig. 3.11 for legend. The log shows stacking of three generations of channel deposits. The lower two generations start with a basal shell lag. The second channel deposit ends in a clayey interval, that probably represents infilling after channel abandonment. This clay fill is cut by the deposit of a third channel. Ages mentioned in the log are based on pollen assemblages. Radiocarbon ages are based on dated juvenile *Cerastoderma edule* shells. The date of 4140 $\pm$ 40 BP does not agree with the pollen ages of the overlying channel sands. Further discussion is given in text. See Table 3.2 and Fig. 3.10 for more information on the radiocarbon-dated shells.

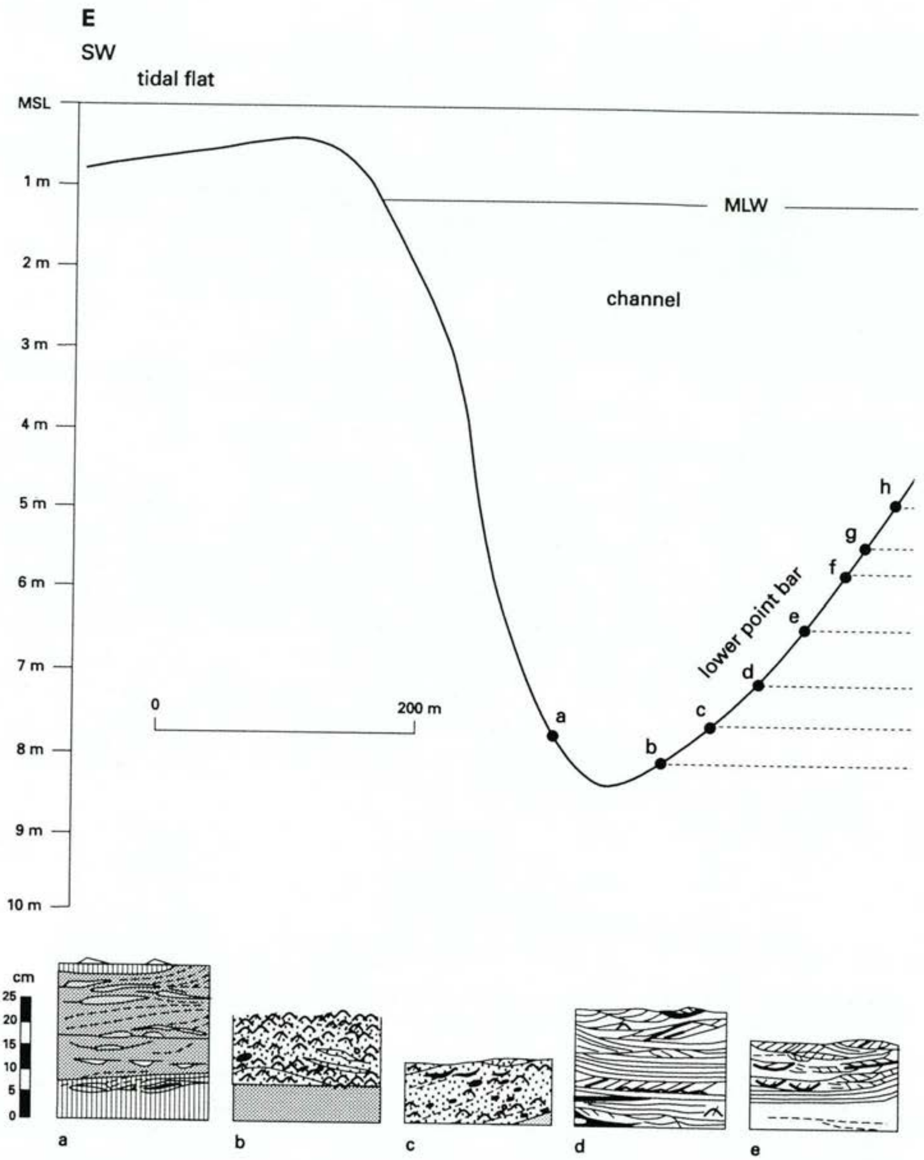

Figure 3.15 Series of box cores along a transect crossing a channel and adjacent point bar and

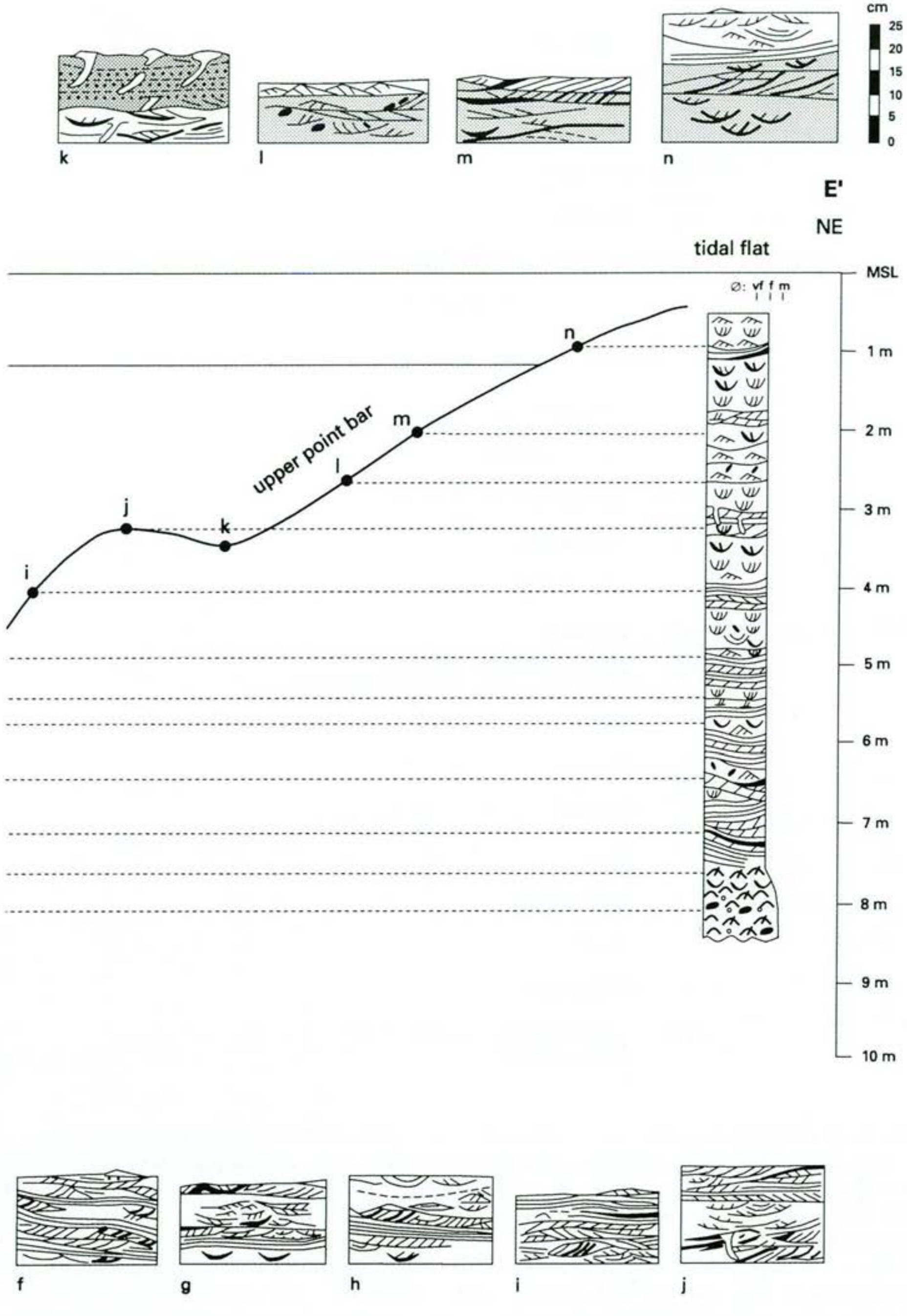

tidal flat in the Wadden Sea south of Ameland. *(continued overleaf)*

Legend to Figure 15

Lithology

- Mud
- Sandy mud
- Muddy sand
- Fine-grained sand (150-210μm)
- Medium-grained sand (210-300μm)

Structures

- Trough cross-lamination
- Ripple cross-lamination
- (Low-angle) parallel lamination
- Cross-bedding
- Structure vague
- Mud drapes
- Mud flasers
- Mud balls (sometimes armoured)
- Mud flakes
- Burrows
- Shells
- Shell fragments
- Gravel
- Detritus layer

N.B. Larger structures are drawn after lacquer peels

Figure 3.15 continued Location is shown in Fig. 3.1, cross-section EE'. From the box cores an idealized vertical point-bar sequence has been composed (N.B. sedimentary structures in this idealized sequence are not to scale). The variation of lithology and sedimentary structures with depth shows up clearly. See overleaf for legend. Interpretation of sedimentary structures is discussed in the text. The box cores were collected 3 days after neap tide, under very calm conditions. Mud deposits that are found in the channel floor and in local depressions are probably due to reduced tidal flow and prolonged conditions of fair weather prior to collection. The outer bank of the channel was too steep to collect box cores. Orientation of the box cores relative to the north was not recorded.

Recent point-bar sequence compiled from box cores

Although the analyzed cores consist mainly of point-bar deposits, the sedimentary structures were often incomplete, poorly preserved or disturbed during sampling and are therefore difficult to recognize. Moreover, the presence of several shell beds in the cores suggests that several point-bar sequences cut into previous ones. A series of box cores was collected from a recent point bar south of Ameland (Fig. 3.1: EE') to establish a complete reference sedimentary sequence that is representative for the Dutch Wadden Sea. This recent succession can be compared with the fossil point-bar deposits.

Literature on channel deposits from the Wadden Sea is limited. Van Straaten (1954, 1961) and Wunderlich (1978) give brief descriptions of the sedimentary structures and compositions of the sediments deposited on channel point bars and their transition to the adjacent tidal flats. The latter author also shows, on the basis of photographs, a short sequence of sedimentary structures from shallow-subtidal and intertidal flats (also in Reineck and Singh, 1980: fig. 595). This information does not give much detail on the various sedimentary structures in the subenvironments of the point bar. Channel deposits described from the estuaries and tidal basins in the SW Netherlands (e.g. Terwindt, 1971, 1981; Nio et al., 1980; Van den Berg, 1982) formed in a different hydrodynamical setting. There, channels are usually much deeper, are occasionally invaded by North Sea waves and have a different orientation with respect to the direction of propagation of the tidal wave. Consequently, these point-bar deposits differ from those in the Wadden Sea.

Fourteen box cores were collected on a transect across the channel axis, point bar and adjacent shallow-subtidal and intertidal flat (Fig. 3.15). Sampling took place around neap tide, under fair weather conditions.

The core from the outer bend of the channel (Fig. 3.15: core a) shows an alternation of sandy mud and mud with sand lenses, formed by migrating ripples, and cut-and-fill structures with sand at the base, that mimic megaripple foresets. This muddy channel-fill is likely to be eroded by strong currents during high spring tides or winter storms. It is not a part of the point-bar deposits. The base of the point-bar sequence (Fig. 3.15: cores b and c; Fig. 3.16) is formed by large-scale cross-bedded sets of shells and shell fragments and medium-grained sand, with very coarse quartz and chert grains and (armoured) mud balls, erosively overlying muddy sand or mud. Sets of low-angle, parallel-laminated fine-grained sand, interbedded with planar and trough-shaped cross-lamination, occur higher up on the point bar (Fig. 3.15: core d; Fig. 3.17). Occasionally, mud drapes are intercalated in the sand.

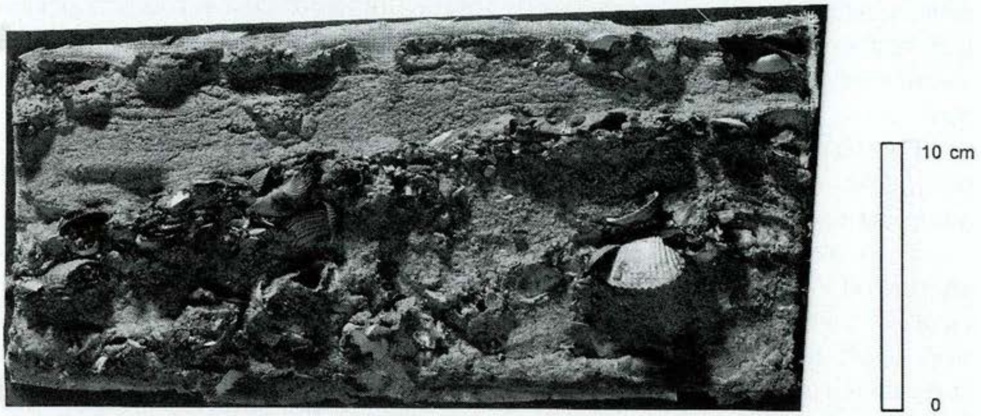

Figure 3.16 Lacquer peel of box core c (Fig. 3.15) showing large-scale cross-bedded medium-grained sand with intercalated shells and shell fragments of predominantly *Cerastoderma edule* and mud balls (missing on the peel). The top of the sequence consists of ripple-bedded sand with mud flasers. The core was collected at the toe of a channel point bar in the Wadden Sea south of Ameland, at a depth of about 7.5 m below NAP. See Fig. 3.14 for detailed log.

Upwards, the parallel-laminated sets become thinner and finally disappear. The ripple lamination becomes more diverse in orientation and structure (Fig. 3.15: cores e to j; Fig. 3.18). A local depression is filled with mud with thin intercalated laminae of sand and peat detritus (Fig. 3.15: core k). Abundant sand-filled burrows are found in the mud. The shallow-subtidal and lower intertidal flat is characterised by ripple bedding with thin intercalated mud layers and flasers (Fig. 3.15: cores l to n).

The low-angle parallel-laminated sets, with thin mud layers intercalated in the mud-free sets (Fig. 3.15: core d; Fig. 3.17) are interpreted as the toe sets and bottom sets of megaripples and/or cross-sections of megaripple foresets (see Terwindt, 1971, fig. 4, for a clear illustration). Reineck (1978, fig. 31) also presented lacquer peels from cross-sections through a megaripple that show a similar parallel lamination. Other modes of formation of the parallel-laminated sets were considered but eliminated. Formation by wave oscillation is unlikely at a depth of 7 m below MSL since the average significant wave height and period in the areas sheltered by the barrier islands range from 0.2 m to 0.45 m and 1.8 s to 2.6 s respectively (Wemelsfelder, 1957-1962, in Eysink, 1979; Koning and Kreuk, 1974). The corresponding maximum depth of wave influence would be only 3 m below the surface of the sea. The maximum depth of sediment movement would be even shallower. Moreover, the occurrence of parallel-laminated sets increases with depth, whereas the occurrence of wave-generated structures would decrease with depth. Formation of parallel lamination in the upper flow regime is unlikely given the depth of occurrence, the low-angle inclination of the lamination and the intercalated thin mud layers. Moreover, local maximum current velocities in the channel, averaged over the upper 5 m of the water column, vary from 0.98 ms^{-1} during flood tide to 1.08 ms^{-1} during ebb tide during spring tides (Hydrografische Dienst, 1987). The maximum current velocities near the channel bottom will be smaller. Finally, settling of sand from suspension after it had been stirred up by wave action on shoals (cf. Terwindt, 1971, and Van den Berg, 1981) is unlikely since thin mud layers are intercalated in the parallel-laminated sets.

Summarizing it can be stated that a channel with a depth of about 8 m and a width of about 800 m in the Wadden Sea produces a point-bar sequence that consists of (large-scale) cross-bedded sets of (fragmented) shells and medium-grained sand, overlain by alternations of megaripple cross-bedding and planar and trough-shaped cross-laminated fine-grained sand. Megaripple cross-bedding dies out upward and ripple lamination becomes dominant. The top of the sequence becomes more muddy. This sequence is summarized in the depositional point-bar model of Fig. 3.15.

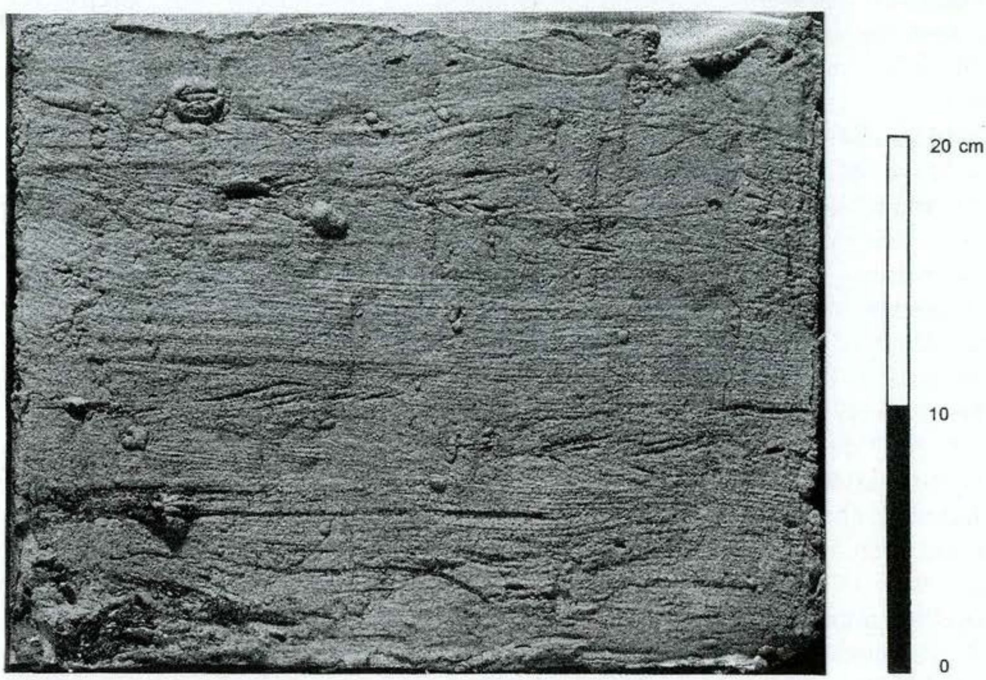

Figure 3.17 Lacquer peel of box core d (Fig. 3.15) showing sets of low-angle, parallel-laminated fine-grained sand, alternating with sets of ripple cross-lamination. Thin mud layers occur in the lower parallel-laminated set. The parallel-laminated sets are interpreted as toe sets and bottom sets of megaripples. See text for further discussion. Box core from a lower point bar of a tidal channel, water depth about 7 m below NAP. See also Fig. 3.15.

Comparison of this model with the point-bar deposits in the cores shows that complete point-bar sequences have not been preserved in the cores. The muddy upper point-bar to lower intertidal-flat deposits (the top part of the model) have usually been reworked and replaced by deposits of migrating tidal gullies. The obvious trend in the sedimentary structures as found in the box cores is frequently disturbed or missing in the cores from the boreholes. Apparently, the cross-bedded sequences in the cores from the boreholes are the products of several cycles of erosion and deposition by migrating channels of different depth.

Deposits of migrating inlet channels

The sandy sequences found underneath the barrier island of Ameland reach thicknesses of about 30 m. These sands have been deposited by migrating inlet channels. The sequence generally starts with intervals of coarse-grained sand (d_{50}: 300 μ and coarser) and shell fragments and shells that have a maximum thickness of 3.5 m. The fine-grained sand (d_{50}: 145 to 165 μ) that overlies the shell-rich lags at the base shows megaripple cross-bedding with thin intervals of planar small-ripple bedding. At a depth of 8 to 10 m below NAP the megaripple cross-bedding is gradually replaced by low-angle cross-bedding and parallel bedding formed by wave-oscillations, alternating with planar and trough-shaped small-scale cross-bedding. Wave-generated parallel bedding, with intercalations of ripple bedding prevails above 6 to 8 m below NAP. Shells that occur in this interval are usually orientated with the convex side up. Shells, in layers and dispersed throughout the sediment, are abundant but they disappear towards the top of the sequence. Shells of littoral North-Sea molluscs such as *Spisula spec.* and *Donax vittatus* are present in the sediment. Basal lags consist mainly of shells of *Cerastoderma edule* and *Spisula*, mixed with shells of *Macoma baltica* and *Mytilus edulis* and reworked Pleistocene shells and sparse gravel (quartz, chert). The compositions of the shell layers change upwards, and *Macoma*, *Cerastoderma* and *Donax* become the dominant species. The bioturbation rate is low; burrows are mostly found above 10 m below NAP. On Ameland the inlet sequence is overlain by root-bearing, (very) fine-grained sand, with small-scale cross-bedding and parallel lamination, alternating with clay layers, on top of which soils and eolian deposits occur.

Distinct differences can be observed between sequences from the central part and the western part of Ameland. Cores from central Ameland (Fig. 3.1) show predominantly large-scale cross-bedding. Mud deposition and small-ripple bedding are rare, indicating strong current action. Wave-generated low-angle parallel bedding becomes dominant upwards from 10 m below MSL.

Figure 3.18 Lacquer peel of box core j (Fig. 3.15) showing small-scale cross-bedding of various orientations and intercalated mud flasers. A parallel-laminated set occurs almost at the top of the sequence. The presence and thickness of parallel-laminated sets is considerably less than in core d (Fig. 3.17). Box core from the upper point bar of a tidal channel, water depth about 3 m below NAP. See also Fig. 3.15.

This strongly suggests deposition in a deep tidal inlet, open to high waves. The lower limit of the parallel-laminated interval is found at progressively shallower levels towards the south (Fig. 3.5). This reflects the breaking of penetrating North-Sea waves on shoals in or close to the tidal inlet. This is an important difference with the point-bar sequences from the sheltered Wadden Sea where the small, locally generated waves can at best produce combined-flow ripples.

Small-ripple bedding and mud intercalations are common in cores from western Ameland (e.g. core 1H.104, Fig. 3.19). Parallel lamination occurs only in the most seaward cores, from 4.5 m below NAP upwards. These deposits must have formed under less energetic conditions, sheltered from strong wave action. Together with the comparatively shallow channel depths, 17 m below palaeo-MSL in core 1H.104 (Fig. 3.19: 2nd generation channel), this points to formation in a channel directly landward of a tidal inlet (e.g. comparable with the location of borehole 1H.104 on the SW coast of Ameland, Fig. 3.10: Westergrie).

The inlet sequence described above roughly resembles the model of Kumar and Sanders (1974), although the Wadden Sea sequence was formed in channels twice as deep and is overlain by an eolian dune sequence. The fossil inlet sequences found below central Ameland are comparable to the hypothetical sequences produced by inlet migration which were described by Sha (1989b, 1990) for Texel Inlet, about 60 km west of Ameland. However, the deposits of migrating marginal channels and wave-dominated shoals which were expected by Sha do not occur in the sequences from Ameland.

Pollen samples taken from core 1H.104 were analyzed. Late-Subboreal deposits (Fig. 3.19: 1st channel generation) are overlain at 18 m below NAP by Subatlantic deposits, formed after 0 AD (Fig. 3.19: 2nd channel generation). This is in accordance with radiocarbon-dated shells from this interval (Table 3.2: sample Westergrie). The upper 1.6 m formed after 700 AD.

Radiocarbon-dated shells from other boreholes drilled on the island of Ameland set the time frame for the inlet and tidal-channel deposits. The radiocarbon ages of the samples Buurderduinen (Table 3.2; Fig. 3.10) indicate the presence of a 25-m-deep tidal inlet in central Ameland around 2500 BP (NB Depth relative to palaeo-MSL). A 16-m-deep inlet channel eroded this sequence around 2100 BP. Sample Hollumerduin (Fig. 3.10, Table 3.2) suggests a 18-m-deep inlet channel in west Ameland around 2900 BP (Table 3.2).

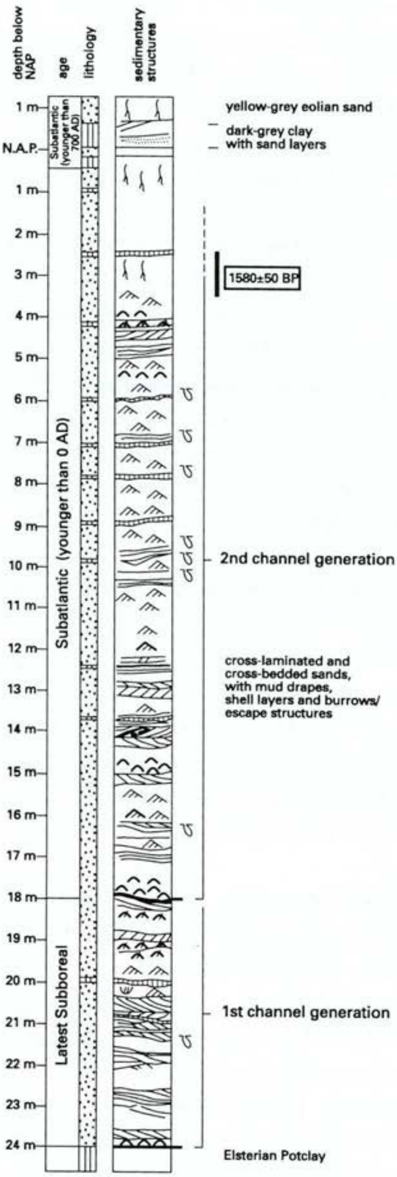

Figure 3.19 Detailed log of core 1H.104 from the western part of the island of Ameland (cross section DD', Fig. 3.9). For legend see Fig. 3.11. The log shows stacking of Late Subboreal and Subatlantic channel deposits. The latter shows a significant influence of wave action and must have been formed close to a tidal inlet. The channel sequence is capped with sandy shoal and salt-marsh deposits, with eolian dune sand on top. Ages mentioned in the log are based on pollen assemblages. See Table 3.2 and Fig. 3.10 for more information on the radiocarbon-dated shells.

The Mainland sequence

The sand-rich facies sequence found in the Wadden Sea south of Ameland differs considerably from the predominantly clayey sequences that are known from the mainland of Groningen and Friesland.

The mainland sequence starts with Basal Peat (generally *Phragmites* and *Carex* peat) overlain by humic and heavy clays, peaty clays and sandy clays, grading into or erosively overlying each other. The sandy clays, in which the sand is sometimes arranged in thin layers, were generally deposited in and near channels and creeks (Griede, 1978). The sequence becomes more clayey in a landward direction and away from the channels. Thin intercalations of *Phragmites* and *Carex* peat and roots are common. The sequence reaches a maximum thickness of up to 20 m in the large palaeo-channels (e.g. in the Boorne valley) and pinches out against the Pleistocene deposits of the Drenthe till plateau in the south (cross-section AA', Fig. 3.5). The average thickness of the sequence on the present mainland is about 6 m.

The southern part of cross-section AA' (Fig. 3.5, south of the former dike) was published by Jelgersma (1961). It shows a succession of oligotrophic peat, overlain by humic and heavy clay (borehole Ternaard 14, Fig. 3.20). The clay is overlain by a peat layer that can be followed to the south where it joins the Basal Peat (Fig. 3.5). This peat layer is erosively overlain by a sandy clay with shell fragments that grades laterally into heavy clay and humic clay. Jelgersma (1961) dated the Basal Peat in core Ternaard 14 (Fig. 3.20) between 6295 $\pm$ 140 BP and 4975 $\pm$ 170 BP and the upper peat between 4300 $\pm$ 130 BP and 2875 $\pm$ 110 BP (Table 3.1).

The Late-Weichselian depression of the Boorne valley is filled with predominantly sandy Holocene channel deposits, erosively overlying the Pleistocene (cross-section CC', Fig. 3.8). Towards the south the sand becomes more muddy and is predominantly very fine-grained.

The Basal Peat started to form during the late Atlantic and early Subboreal, reflecting the rising Holocene sea level. The overlying clay deposits can be dated from early Subboreal to late Subatlantic (medieval period) onwards.

The Basal Peat and the overlying clay deposits are equivalent to those found in the Wadden Sea. The Atlantic mud-flat deposits, which occur in the Wadden Sea, extend below the land reclamation works (cross-section BB', Fig. 3.7). Further correlations with the sediments described by Griede (1978) were not possible. The sandy deposits along the mainland channels and creeks can be considered the landward continuation of the channel sands in the Wadden Sea.

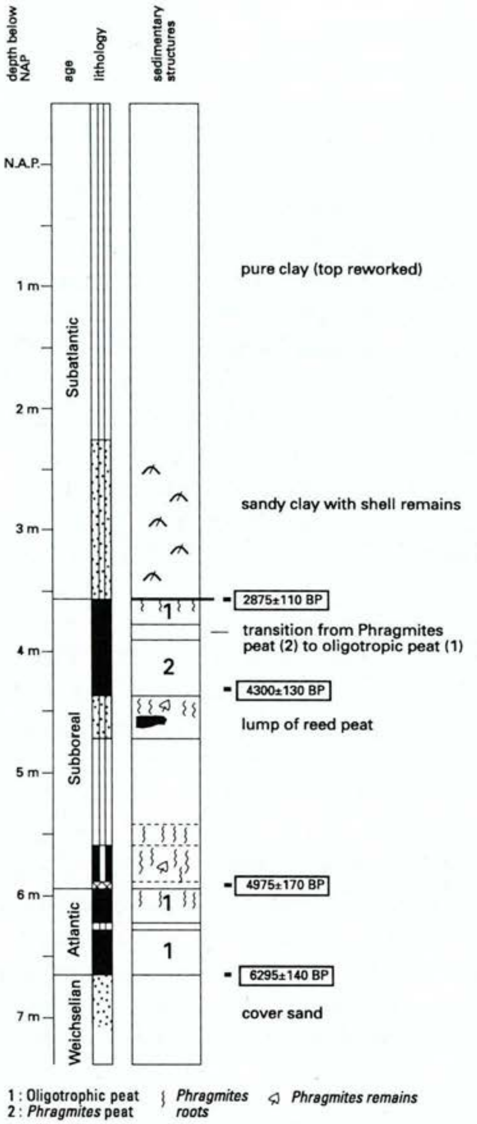

Figure 3.20 Detailed log of core from borehole Ternaard 14 (after Jelgersma, 1961). For legend see Fig. 3.11. A peat layer that grades into root-bearing, humic clay overlies the Weichselian cover sand. Heavy and sandy clay in turn overlies this clay. The second peat layer indicates silting of the area to supratidal level. A sequence of 4 m of (sandy) clay overlies this peat erosively. *Phragmites* roots in the upper part of the oligotrophic peat (at NAP-3.5 m) show that the top of the peat is missing. See Table 3.1 and Fig. 3.10 for more information on the radiocarbon-dated peats.

It is clear that sediment reworking by migrating channels in the distal part of the Wadden Sea, which is now situated on the present mainland, was not very intense. The Holocene sequence is more complete here than that in the Wadden Sea.

Concluding remarks

Holocene stratigraphy of the Wadden Sea south of Ameland

In summary, an Atlantic sequence that consists of Basal Peat grading into humic clay, which is locally penetrated by rootlets, overlain by subtidal to lower intertidal mud flats, is found in the Wadden Sea south of Ameland at a depth varying between 4 m and 16 m below NAP. It is overlain by a thick, predominantly sandy sequence of mainly Subatlantic channel point-bar deposits (Fig. 3.21). These Atlantic deposits are found south of the central part of Ameland (Fig. 3.4), on the northward-sloping extension of the Drenthe till plateau. They are almost completely absent south of the Ameland inlet (Fig. 3.4), because there they were eroded by migrating channels in the former Boorne valley and its successor the Middelzee (Fig. 3.8). Atlantic-age mud-flat deposits with thin rootlets, occur only below the present-day tidal watershed south of Ameland. Strongly bioturbated, sandy subtidal to intertidal mud flats are found at the same level, more westerly in the study area (cross-section DD', Fig. 3.9).

The Subatlantic channel deposits form the top layer in the Wadden Sea near Ameland. Subboreal deposits are scarce, probably because these were eroded by younger channels. Shells of Subboreal age, selected from thick basal shell lags (Table 3.2: datings Wantij 1.1 and 4.1), confirm this. However, Subboreal deposits are common in the Grienderwaard, at the western boundary of the Boorne Valley (Fig. 3.10). Here, the top of the Pleistocene deposits lies at about NAP-7 m (Fig. 3.4). Ente (1977) published the description of a core from this area. It consists of 4.5 m of (sandy) clay that is intercalated between a Late-Atlantic and Late-Subboreal peat. This clay must have been deposited mainly during the Subboreal. The sequence is capped with 0.5 m marine sand, which indicates that this area was not reworked by tidal channels.

The Atlantic Wadden Sea

During the Atlantic, the lateral facies sequence in the Wadden Sea consisted, from land to sea, of peat swamps grading into a more open area with clay deposition and reed growth. Sand was deposited along the channels

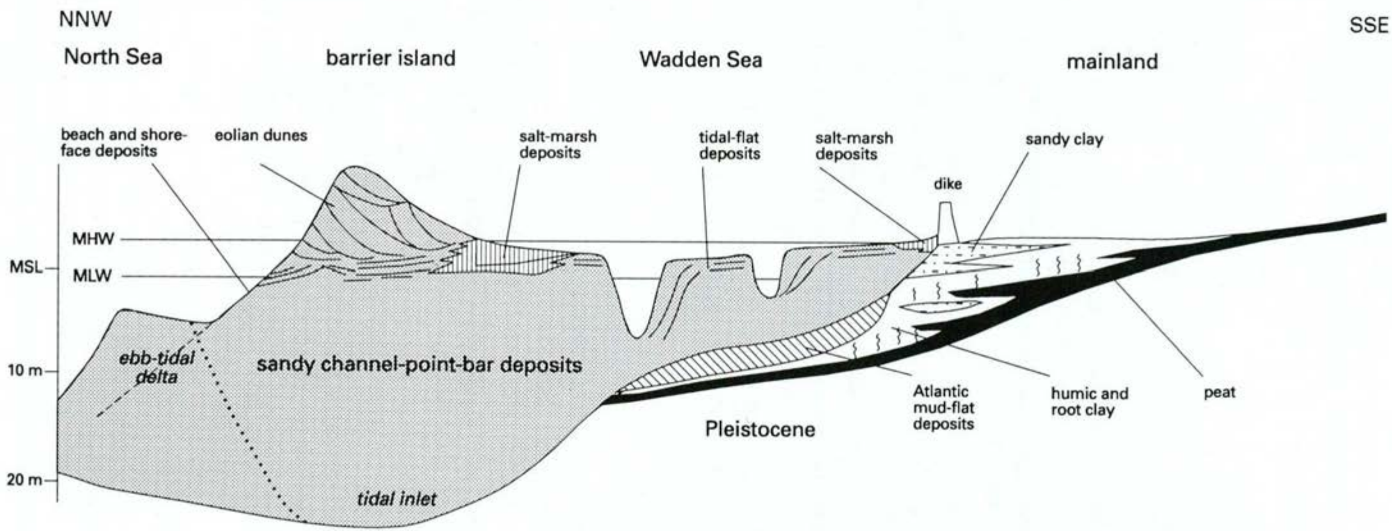

Figure 3.21 Hypothetical cross-section through the central part of the Dutch Wadden Sea and the Frisian mainland showing a sequence of Atlantic peats, clays and muds that grade into younger peats and clays below the mainland. This sequence is erosively overlain by a landward-thinning prism of Subatlantic channel-point-bar deposits. The recent Wadden Sea deposits are predominantly sandy. Clay settles in salt marshes sheltered by the barrier islands and in front of the dikes along the mainland. N.B. the tidal range has been exaggerated.

that connected this area with the tidally dominated mud flats. The mud flats graded into sand flats and the Wadden Sea was most likely bounded by barrier islands with tidal inlets in between. Sediment composition varied from almost completely sandy near the inlets to almost completely clayey at the landward boundary of clastic deposition. This is due to the active inward accumulation of suspended particles and the decrease in tidal energy with distance from the inlet which favours clay deposition (Postma, 1954, 1961; Van Straaten and Kuenen, 1957; De Glopper, 1967). Water salinity in these environments ranged from almost full-marine in the tidal inlets to completely fresh in the marshy zones at the landward boundary.

As sea level rose, the lateral facies sequence shifted landward and also upward along the Late-Pleistocene relief (Van Straaten, 1975, his fig. 3). This almost continuous landward shift stopped at the beginning of the Subboreal period in the Ameland area. The rate of relative sea-level rise had dropped to 0.15 m per century by that time and the accommodation space for sediment created by the rising level must have been filled with sediment (Chap. 3). Subsequent expansion of the Wadden Sea was no longer determined by the Pleistocene relief. The sea penetrated into local depressions formed e.g., by sediment compaction, surface subsidence resulting from draining or peat digging. Most of these inundated areas were filled with sediment within a relatively short period. The Wadden Sea no longer expanded southwards. The most landward facies belts aggraded on the spot and eventually developed into almost permanently dry land. The overall facies sequence in the Wadden Sea changed from transgressive to regressive.

The present-day Wadden Sea

The gradual transitions in both sediment composition and salinity no longer exist in the present-day Wadden Sea. Since about 1000 AD dike have been protecting the predominantly clayey deposits which resulted from siltation to above high-tide level from renewed tidal action. Consequently, the transition from a marine, mainly sandy sedimentary environment into a brackish to fresh environment in which clay deposition prevailed, nowadays takes place over a short distance, in front of the dikes. Moreover, the area in which suspended sediments settle permanently, was strongly reduced. Mud is now deposited in the reclamation works in front of the dikes and on the tidal watersheds (Fig. 3.1). Extensive quiet environments in which deposition of fine-grained sediment prevails, comparable with the Atlantic mud flats, do not exist any more.

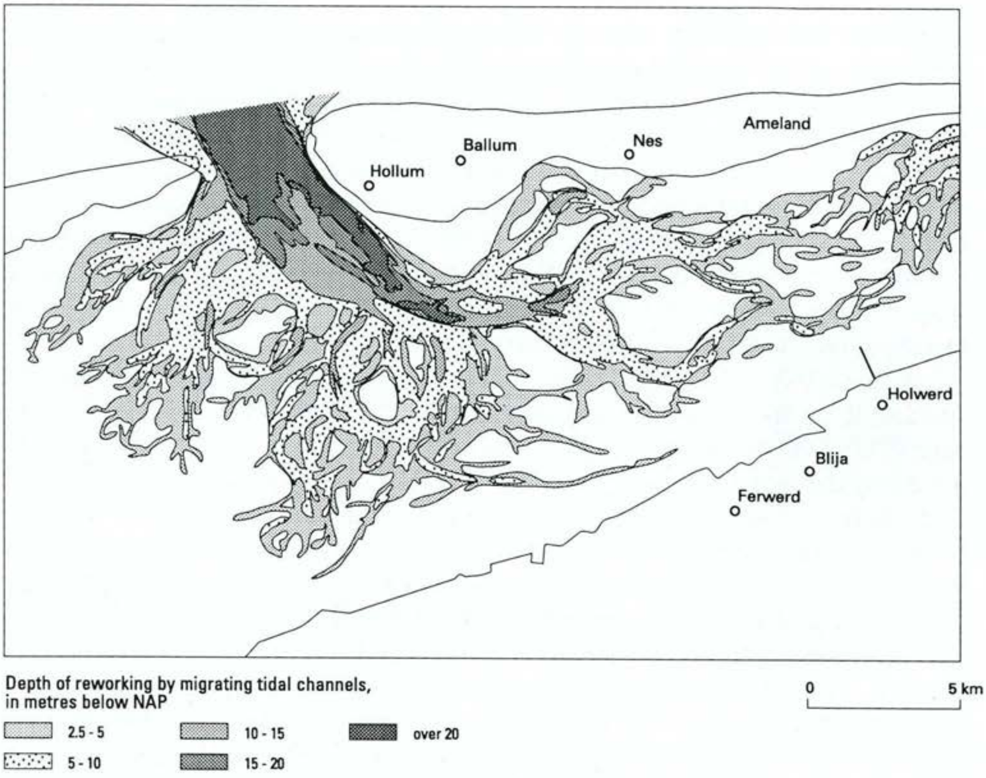

Figure 3.22 Map of depth and areal extent of sediment reworking by migrating tidal channels deeper than NAP-2.5 m in the Wadden Sea south of Ameland between 1831 and 1984, compiled from a series of sounding charts. The migrating channels reworked 47% of the surface area of 325 km^3 of the flood basin during this period.

Migration of tidal channels and tidal inlets in the Wadden Sea and, consequently, reworking of Holocene deposits, continued on the seaward side of the dikes. Reineck (1958, in Reineck, 1978, and Reineck and Singh, 1980) states that 58 % of the backbarrier of the German Wadden island of Wangerooge was reworked in 68 years by laterally migrating tidal channels. In the flood basin of the Ameland inlet, between the tidal watersheds south of Terschelling and Ameland (Fig. 3.22), laterally migrating channels, deeper than 2.5 m below NAP, have reworked 47 % of the surface area in the period between 1831 and 1984. The reworked surface area decreases with increasing channel depth. The sediment volume (below NAP-2.5 m) reworked over this period amounts to 670 million m^3, which is 4.4 million m^3 annually. The Holocene deposits are reworked to a depth of more than 20 m in and near the tidal inlet (Fig. 3.22). The depth of sediment reworking decreases with distance from the inlet (Fig. 3.22). Tidal gullies and tidal channels that dissect mixed sand-mud flats migrate 25 m to 30 m a year (Trusheim, 1929, in Reineck, 1978; Van Straaten, 1951). Tidal channels that erode sand flats can shift laterally up to about 100 m per year (Lüders, 1934, in Reineck, 1978). The Holocene depositional sequences in the Wadden Sea are prone to reworking by migrating tidal channels and will eventually be replaced by fine-grained sandy point-bar sequences.

Acknowledgements

This investigation was financed by the Netherlands Organisation for Scientific Research (NWO), grant CO_2-77.125. The project was supported by the Geological Survey of The Netherlands, the Sedimentology Department of the Earth Sciences Institute of Utrecht University, the Friesland and Flevoland Directorates and the National Institute for Coastal and Marine Management/RIKZ (formerly Tidal Waters Division) of Rijkswaterstaat, and the Netherlands Institute for Sea Research (NIOZ).

First of all I would like to thank Dirk Beets for his enthusiasm and advice and his constructive criticism during the 'growth' of this paper. I am indebted to Saskia Jelgersma for sharing her extensive knowledge of the geology of the Netherlands and sea-level movements. The paper benefitted from comments on an earlier draft by Janrik van den Berg, Poppe de Boer, Piet Cleveringa, Wim Dubelaar, Doeke Eisma, Evert van de Graaff, Bert van der Valk en Peter Vos. The box cores were collected by the NIOZ research vessel *Navicula*. Thanks to skipper Cor Wisse of NIOZ and Albert Oost of Utrecht University for a successful cruise.

Mr. Y. Zijlstra and Jaap Nijdam of the Friesland Department of Rijkswaterstaat are thanked for putting cores at my disposal. Skipper Theo Bosch and the crew of the drilling vessel *Heffesant* are thanked for their pleasant cooperation. Mr. R. Koopstra of the Flevoland Directorate of Rijkswaterstaat provided access to the results of the surveys of the former Rijksdienst IJsselmeer Polders in the Wadden Sea.

Thanks to dr. K. van der Borg and dr. A. de Jong of the Van de Graaff laboratory of Utrecht University for the swift execution of the radiocarbon datings.

I appreciated the discussions with Piet Cleveringa and Hein de Wolf on pollen and diatom matters and facies reconstructions. John van Delft took the photographs of the lacquer peels and André Koers prepared the drawings. All other colleagues at the Geological Survey are also thanked for their pleasant cooperation and helpfulness.

4. Mid-Holocene evolution of a tidal basin in the western Netherlands: a model for future changes in the northern Netherlands under conditions of accelerated sea-level rise?

Abstract

A scenario for the future development of the Dutch Wadden Sea is derived from an evolutionary model for tidal basins during a rise in sea level. The model is based on the evolution of the Atlantic/Subboreal Holland tidal basin, between 7000 BP and 3500 BP. It emphasizes the balance between the storage capacity created by a sea-level rise and the amount of sediment available.

If the rate of relative sea-level rise exceeds the rate of sediment supply, the innermost (central) portions of the basin will not receive sufficient sediment for an intertidal morphology to be preserved. Eventually, sand will be deposited only in tidal channels and in the flood-tidal delta through which the sediment is supplied, mud deposition will occur in the interchannel areas and salt marshes will disappear.

Introduction

An accelerated rate of sea-level rise may have serious consequences for intertidal areas like the Dutch Wadden Sea (Fig. 4.1). A global warming of 2.5°C would result in a eustatic rise in sea level of 0.31 to 1.10 m, with a best estimate of 0.66 m in the year 2100 according to Warrick and Oerlemans (1990). The present rate of relative sea-level rise in the Dutch Wadden Sea is 0.13 m per century (De Ronde and Vogel, 1988). This means that the total rate of sea-level rise in the year 2100 may exceed 0.7 m per century, which is comparable to the Holocene rate of sea-level rise during the Atlantic.

Our present understanding of hydraulic processes and sediment transport in tidal environments does not permit accurate numerical simulation of these processes. Therefore, predictions of the future evolution of tidal basins at an accelerated rate of sea-level rise are based on budget calculations using extrapolations of recent observations on relative sea-level rise, sediment transport and sediment accretion. In addition, empirical equilibrium equations, relating morphological and hydraulic parameters, are used to estimate future morphologic development (Misdorp et al., 1990). The value of these predictions is limited, since consequences of a possible sediment deficit for the intertidal morphology remain unknown.

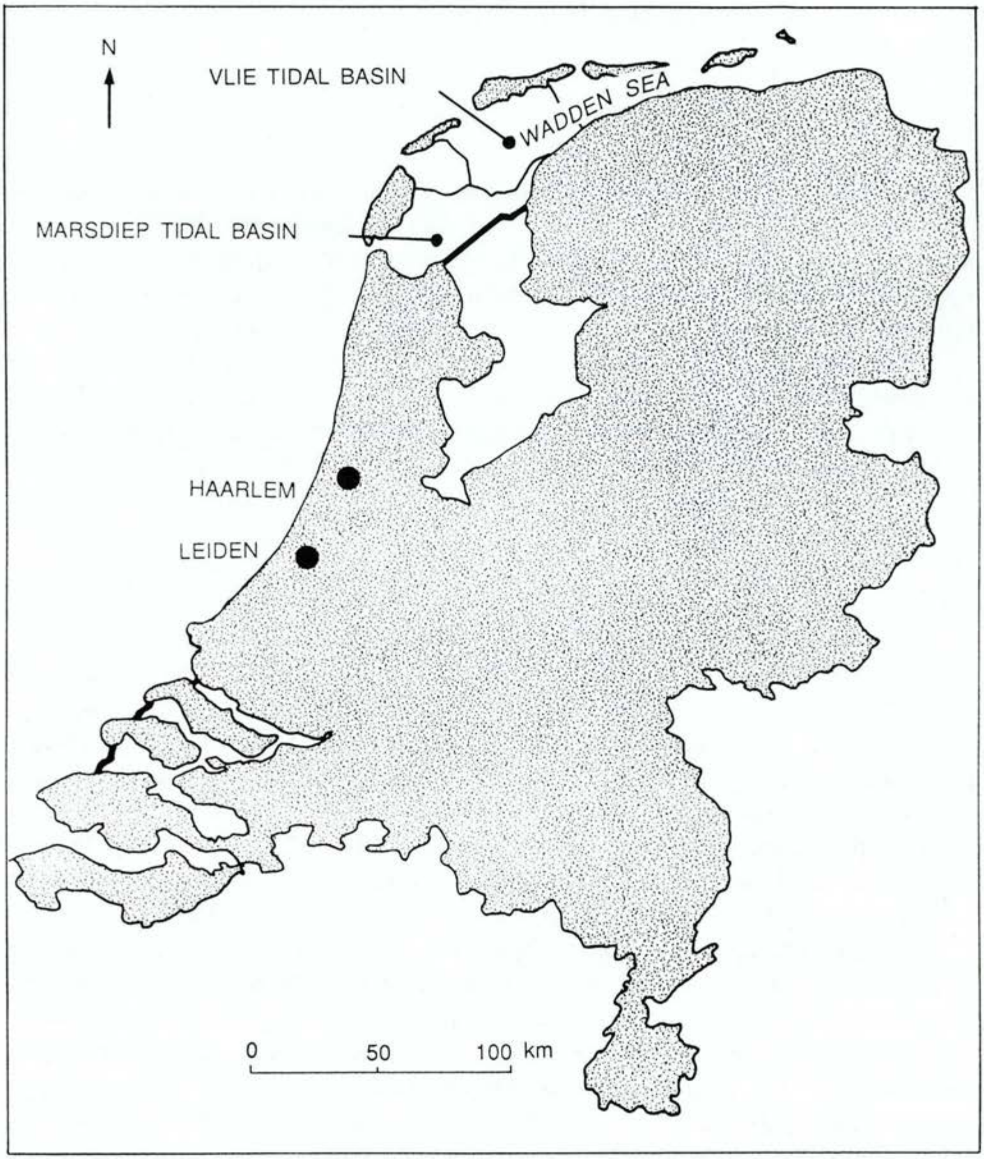

Figure 4.1 The location of the Wadden Sea in the Netherlands.

A conceptual model for predicting future development of the Dutch Wadden Sea can be derived by studying the evolution of sedimentary facies in Holocene back-barrier basins in the coastal plain of the Netherlands at different rates of sea-level rise. The Holocene coastal plain of the Netherlands (Fig. 4.2) evolved into three separate barrier/back-barrier systems during the Atlantic and Subboreal; one in the northern and two in the western part of the Netherlands. Unlike the northern back-barrier basin, which in time evolved into the present Wadden Sea, one of the tidal basins in the western Netherlands was filled by sediment and its inlets closed successively between about 5500 and 3300 BP. The Atlantic tidal deposits have therefore been well preserved in the shallow subsurface of the western Netherlands, whereas similar deposits in the north have largely been removed by the lateral migration of channels during the Subboreal and Subatlantic. For that reason, an analysis of the sedimentary succession deposited in the tidal basin of the western Netherlands can be used to develop a conceptual model for facies development at high rates of sea-level rise. This model is verified by comparing it with the remaining Atlantic and Subboreal deposits in the northern back-barrier basin. Finally, the applicability of the model to the present Wadden Sea is discussed.

Development of the Holocene coastal plain of the Netherlands

Sea-level history

The relative sea-level rise in the coastal plain of the Netherlands was studied by Jelgersma (1961, 1979) and Van de Plassche (1982). The rise in groundwater levels in the coastal plain, corresponding to the rise in mean sea level along the coast (Jelgersma, 1979), was established by radiocarbon dating of peat deposits overlying compacted sands (Jelgersma, 1961, 1979; Van de Plassche; 1982). Recently acquired additional data based on dating of shells in living position in barrier deposits (Roep and Beets, 1988; Van de Plassche and Roep, 1989) improved the curve for the period 5500 to 2000 BP. For the scale of this study, the trend curve shown in Fig. 4.3 is satisfactory. The curve shows a rapidly rising sea level until about 7000 BP. This rise was mainly resulting from the melting of the Scandinavian and Laurentide icecaps. Between 7000 and 5000 BP the rate of relative sea-level rise started to decline and after 5000 BP it declined markedly.

If the discrepancy between radiocarbon age and true age is taken into account, true age may be more than 800 years older than radiocarbon age. This means that the relative rate of sea-level rise between 5000 and 3000 BP is less than that indicated by the radiocarbon-age curve, and that the calibrated

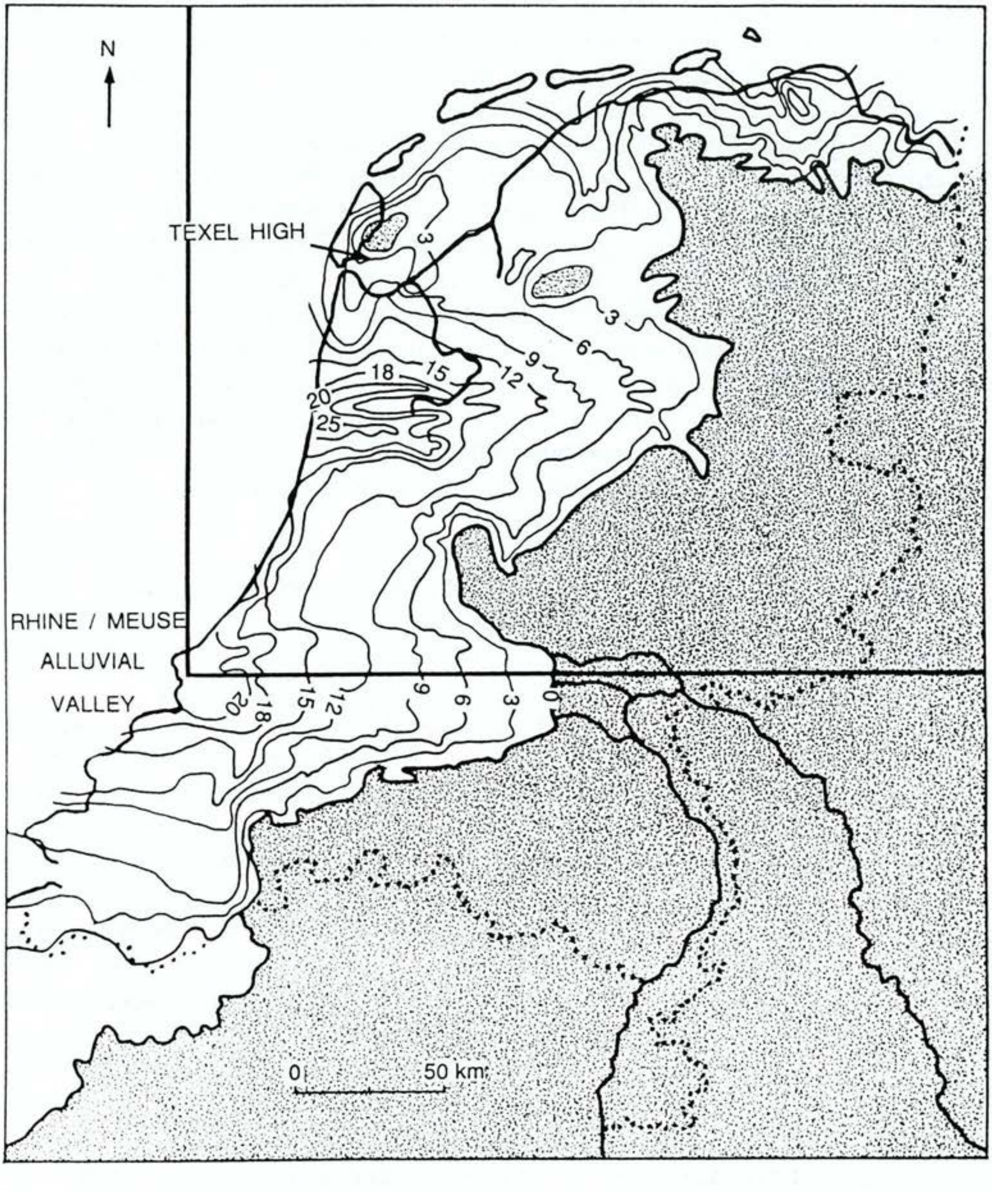

Figure 4.2 The top of the Late Weichselian surface of the Netherlands prior to flooding in the Holocene. The inset is shown in detail in Fig. 4.4. (After Zagwijn, 1986.)

curve shows a sharper rate of decline from 5000 to 3000 BP (Fig. 4.3).

In this paper the following rates of sea-level rise will be used: a rate of >75 cm/100 years for the period before 7000 BP, a rate of 40 to 30 cm/100 years for the period from 7000 to 5500 BP and a rate of 15 cm/100 years for the period from 5500 to 3500 BP.

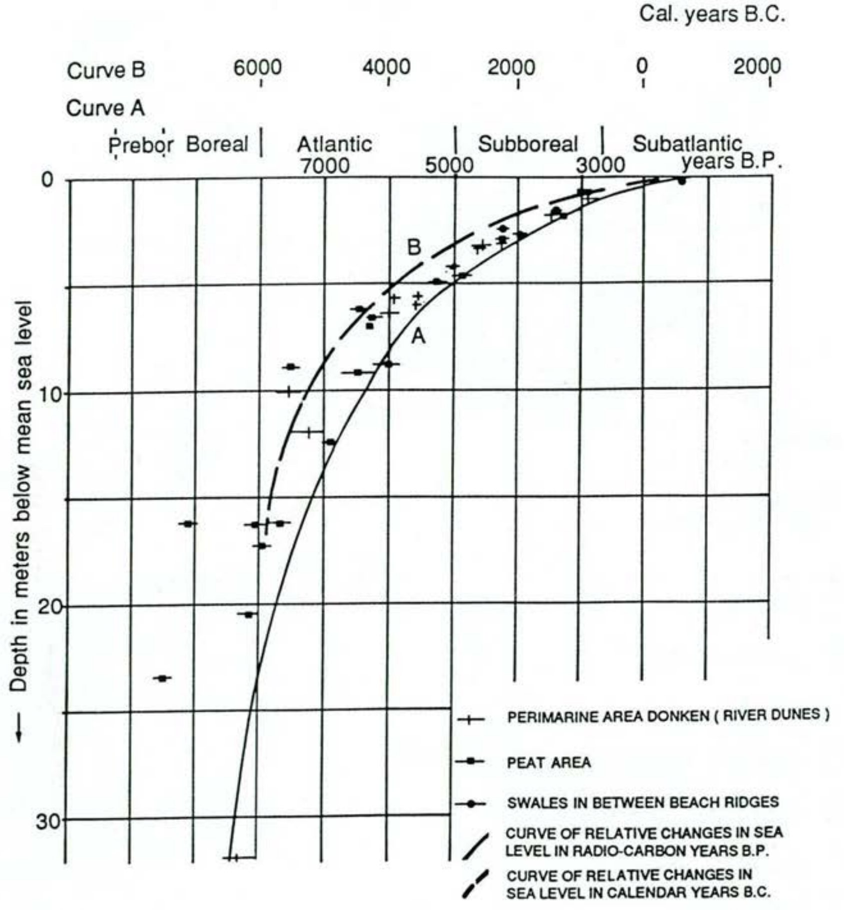

Figure 4.3 Time-depth diagram of relative sea-level rise in the coastal plain of the Netherlands. The solid line gives sea-level rise in radiocarbon age. The dashed line gives the calibrated curve. The calibrated curve shows a marked decline of the rate of relative sea-level rise between 3000 and 5000 BC. (Modified after Jelgersma, 1979).

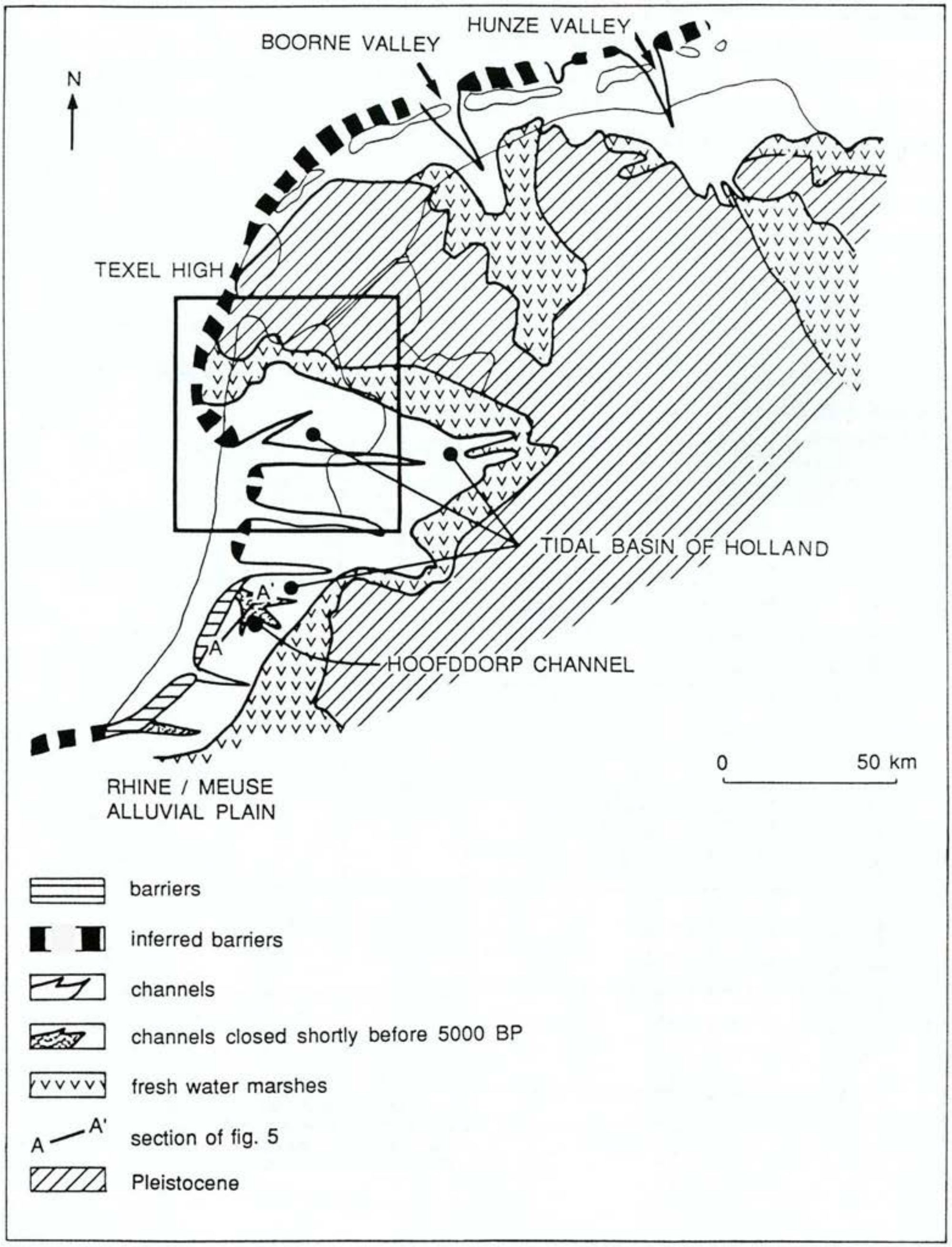

Figure 4.4 Simplified palaeogeographic map of the western and northern Netherlands at about 5000 BP. The inset is shown in detail in Figs. 4.7 and 4.8.

Coastal-plain development

This summary is based on the 1 : 50 000 mapping program of the Quaternary deposits of the Netherlands by the Geological Survey and additional academic research. Reviews are given by Pons and Wiggers (1959, 1960), Jelgersma (1961, 1979), Pons et al. (1963), Van Straaten (1965), Hageman (1969), Ente et al. (1975), De Mulder and Bosch (1982), Griede and Roeleveld (1982), Zagwijn (1986) and Beets et al. (1992), and for more details the reader is referred to these.

Rapid flooding of the southern North Sea basin started during the Boreal (Jelgersma, 1979). Around 7500 BP the sea invaded the valleys of the western Netherlands, and by 7000 BP those in the north (Fig. 4.2). Barriers and spits developed attached to topographic highs, changing the coastal plain into a barrier/lagoon system (Pons et al., 1963; Van Straaten, 1965; Zagwijn, 1986). Figure 4.2, which gives the morphology of the Late-Weichselian surface now covered by Holocene deposits, shows two E-W-running valleys in the western part of the Netherlands and two smaller N-S-running valleys in the north. Around 5000 BP, when mean sea level had risen to 5 m below its present level, the palaeogeography still reflected this original morphology (Fig. 4.4). The Boorne and Hunze valleys of the northern Netherlands (Fig. 4.2) had developed into the precursor of the present eastern Wadden Sea (Griede and Roeleveld, 1982; Zagwijn, 1986). The northern basin was separated from the back-barrier basin in the western Netherlands, the Holland tidal basin (Fig. 4.4), by the Texel High (Jelgersma, 1979). The Rhine/Meuse alluvial valley (Fig. 4.2) did not develop into a back-barrier basin. These rivers supplied sufficient sediment to fill their valley during the sea-level rise, and at 5000 BP the mouths of these rivers formed a promontory at the coast, as can be seen from the strike of the oldest preserved barrier (Fig. 4.4). Until the early Subboreal the Rhine and Meuse followed this E-W-course. They discharged directly into the North Sea and had no tributary leading to any of the back-barrier basins (Pons et al., 1963; Zagwijn, 1986). During the Holocene the smaller local streams, such as the Boorne and Hunze, were reduced to brooklets with little transport capacity (Beets et al., 1992). Consequently, all sediment was supplied by longshore and cross-shore transport by waves and tidal currents and was transported into the barrier/back-barrier system via the inlets by tidal currents. Sand and mud in the present Wadden Sea have the same provenance (Postma, 1961; 1981)

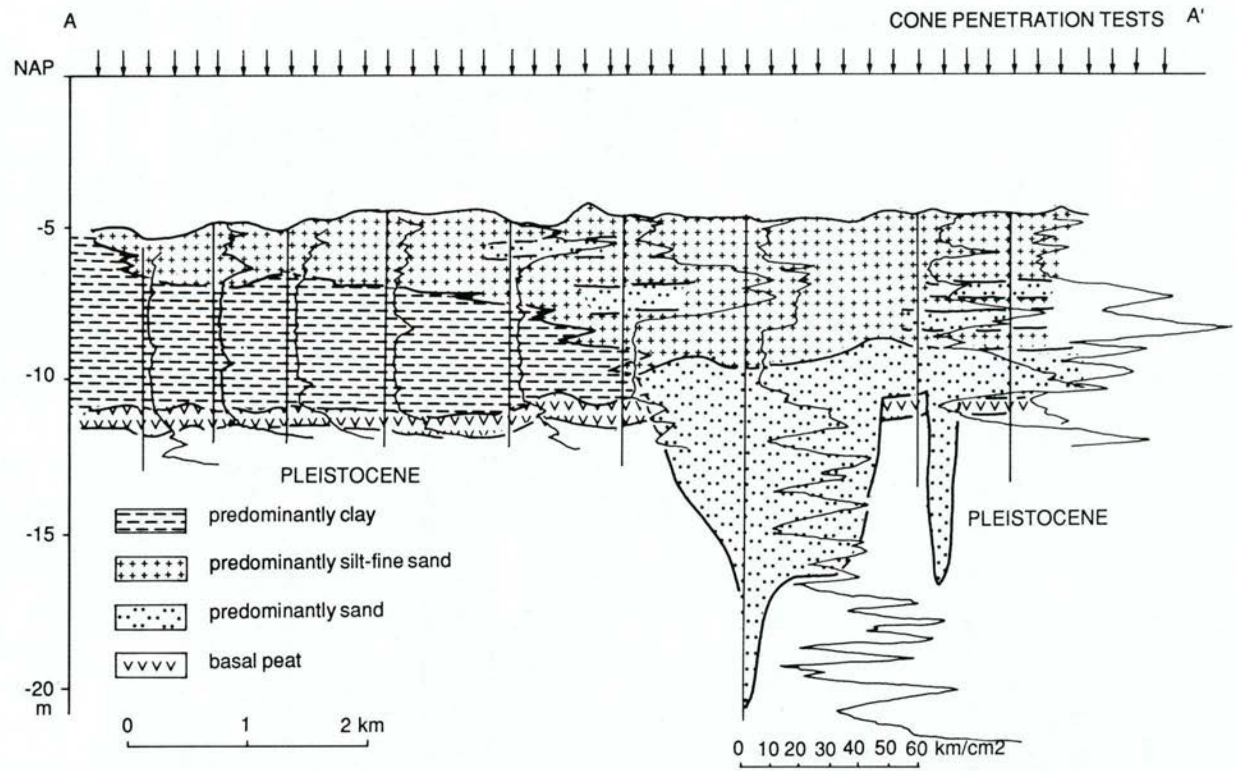

Figure 4.5 Section of the sedimentary sequence of the Atlantic/Subboreal Holland tidal basin, south of Haarlem, mainly based on cone penetration tests. Cone penetration tests have been developed for soil mechanical studies. They register continuously the resistance of soil layers to a steel rod with a cone-shaped end which is pushed into the sediment succession. Because a strong correlation exists between cone resistance and grainsize, these tests are valuable for facies analysis. For location see Fig. 4.4.

The Holland tidal basin

Between 6000 and 5000 BP the Holland tidal basin probably had its most extensive development (Fig. 4.4). At 6000 BP the barrier was still shifting eastward. Stabilization of the barrier started along the southern margin of the back-barrier area near the Rhine/Meuse alluvial plain around 5500 BP (Van der Valk et al., 1985). By 5000 BP the barrier of the relatively narrow southern half of the basin was stabilized and the inlets were closed (Fig. 4.4). Stabilization of the barrier of the wide northern part of the Holland tidal basin started around 4500 BP when large parts of the basin changed into fresh-water marshes. The size of the tidal basin decreased continuously and it was filled completely by 3300 BP when the last tidal inlet closed (De Mulder and Bosch, 1982; Roep and Van Regteren Altena, 1988).

The change from a transgressive to a regressive barrier was directly related to a lower rate of sea-level rise (Fig. 4.3). The balance between the supply of sediment to the tidal basin and the storage capacity created by sea-level rise changed in favour of the former. This resulted in infilling of the basin, decrease of the tidal prism of the inlets and, eventually, silting up of channels and inlets.

Sedimentary sequences of the Holland tidal basin

As described by Westerhoff et al. (1987) and Westerhoff and Cleveringa (1990) sedimentary sequences in the Atlantic/Subboreal Holland tidal basin differ considerably from those in the present Wadden Sea. The sedimentary succession of the latter is the well-known fining-upward tidal sequence of a channel/point-bar succession overlain by intertidal and supratidal deposits (Van Straaten, 1954; Dörjes et al., 1970; Reineck and Singh, 1980; Chap. 3), resulting from a relatively rapid lateral migration of channels. In contrast, the channels in the Atlantic/Subboreal Holland tidal basin showed a more restricted lateral migration. Consequently, different facies sequences developed in adjacent areas. This is illustrated in Fig. 4.5, a 9-km-long section south of the Hoofddorp Channel (see Fig. 4.4 for location), and in Figs. 4.6 and 4.7 showing cores and a schematic palaeogeographic reconstruction of the northern part of the Holland tidal basin around 5500 BP. The section in Fig. 4.5 shows a fixed, sand-rich channel system adjacent to clay-rich basin deposits; it represents at least 1500 years of deposition. Lateral migration of the channel occurred within a 2-km-wide zone. Figure 4.7 shows two main channel systems, representing flood-tidal deltas (the Uitgeest inlet and Alkmaar/Bergen inlet), separated by a large interchannel area.

The channel facies is represented by core 19D-273 (Fig. 4.6; see Fig. 4.7

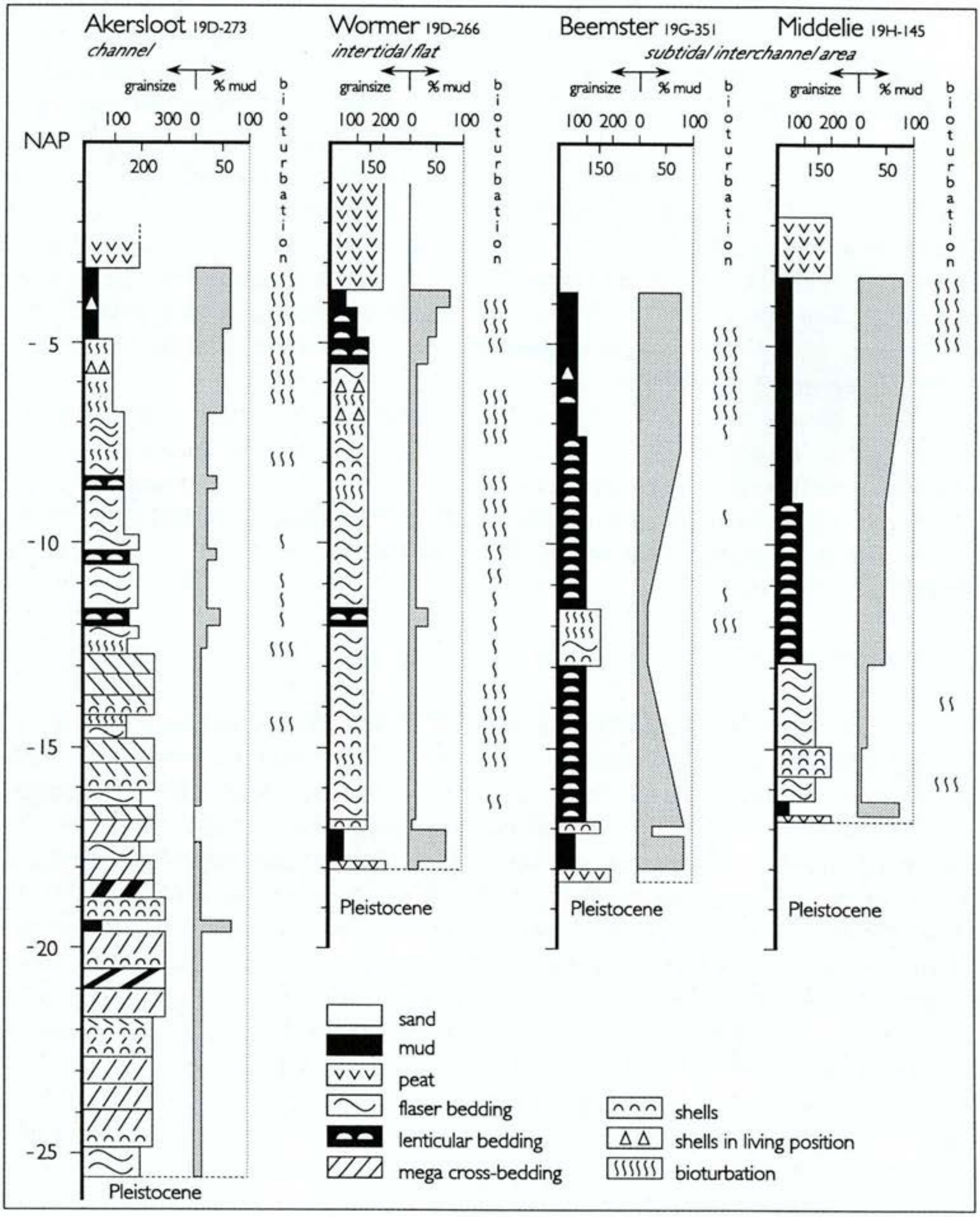

Figure 4.6 Sedimentary succession of undisturbed cores of the Atlantic/Subboreal Holland tidal basin. Core 19D-273 shows a channel facies, 19D-266 the intertidal-flat facies and 19G-351 and 19H-145 the mainly subtidal interchannel facies. For locations of cores see Fig. 4.7.

for location). It shows a fining-upward sequence with mega-crossbedding in the lower half passing into interbedded sand/mud lenticular and flaser bedding. Lag deposits of shells and mud pebbles are common in the lower part, as are clay drapes along the foresets. Burrowing is absent in the lower half of the core indicating high-energy conditions; in the upper part a few flaser-bedded units show some burrowing. The top of the core is strongly burrowed.

Black muds with a variable amount of fine sandy intercalations make up the bulk of the interchannel facies. Cores 19H-145 and 19G-351 (Figs. 4.6 and 4.7) represent this facies. In both cores the top of the Pleistocene sequence has not been eroded and the Holocene succession starts with a fresh-water peat. The tidal sequence overlying the peat in core 19H-145 is sand-rich in its lower 4-5 m, but from 13 m-NAP upward (NAP stands for Dutch Ordnance Datum, which is approximately present-day mean sea level) the amount of mud in the section increases rapidly and the upper half of the clastic section consists of more than 80% mud. The muds are overlain by peat, deposited in fresh-water marshes that were formed after roughly 4400 BP, when the sea had withdrawn from this part of the tidal basin. The sandy part near the base of the core contains a few shell lags and shows flaser bedding; upwards it grades into lenticular bedding with thin sand lenses and isolated ripples. Weak bioturbation occurs in the sands, but the clay-rich sequence above 13 m-NAP shows no burrowing, except for the upper 1.50 m, which is completely homogenized by bioturbation.

Core 19G-351 is slightly sandier than core 19H-145, but exhibits the same general characteristics: on top of the Pleistocene a thin layer of fresh-water peat occurs, overlain by a black, mud-rich tidal sequence with a variable amount of sand. The amount of sand increases from the base to about 8 m-NAP, above which it gradually decreases. Bioturbation is absent in most of the core, only the sandy central part and mud-rich top are considerably bioturbated. Considering the large amount of clay, the interchannel areas represent low-energy environments with weak tidal currents and little or no wave influence. The absence of bioturbation in the core, except for the very top, strongly suggests that the sequence was deposited subtidally with prolonged stagnant conditions. Diatom analysis (Vos and De Wolf, 1988) yields the same result. When the rate of sea-level rise slowed down after 5000 BP, and sediment supply consequently exceeded the created storage capacity, the interchannel areas were filled up to the intertidal level, which is represented by the strongly burrowed upper few metres of the cores.

Channels and interchannel areas were separated by intertidal sand flats forming flood-tidal deltas (Fig. 4.7). Core 19D-266 (Figs. 4.6 and 4.7) is an example of an intertidal sand-flat succession on the edge of the Uitgeest

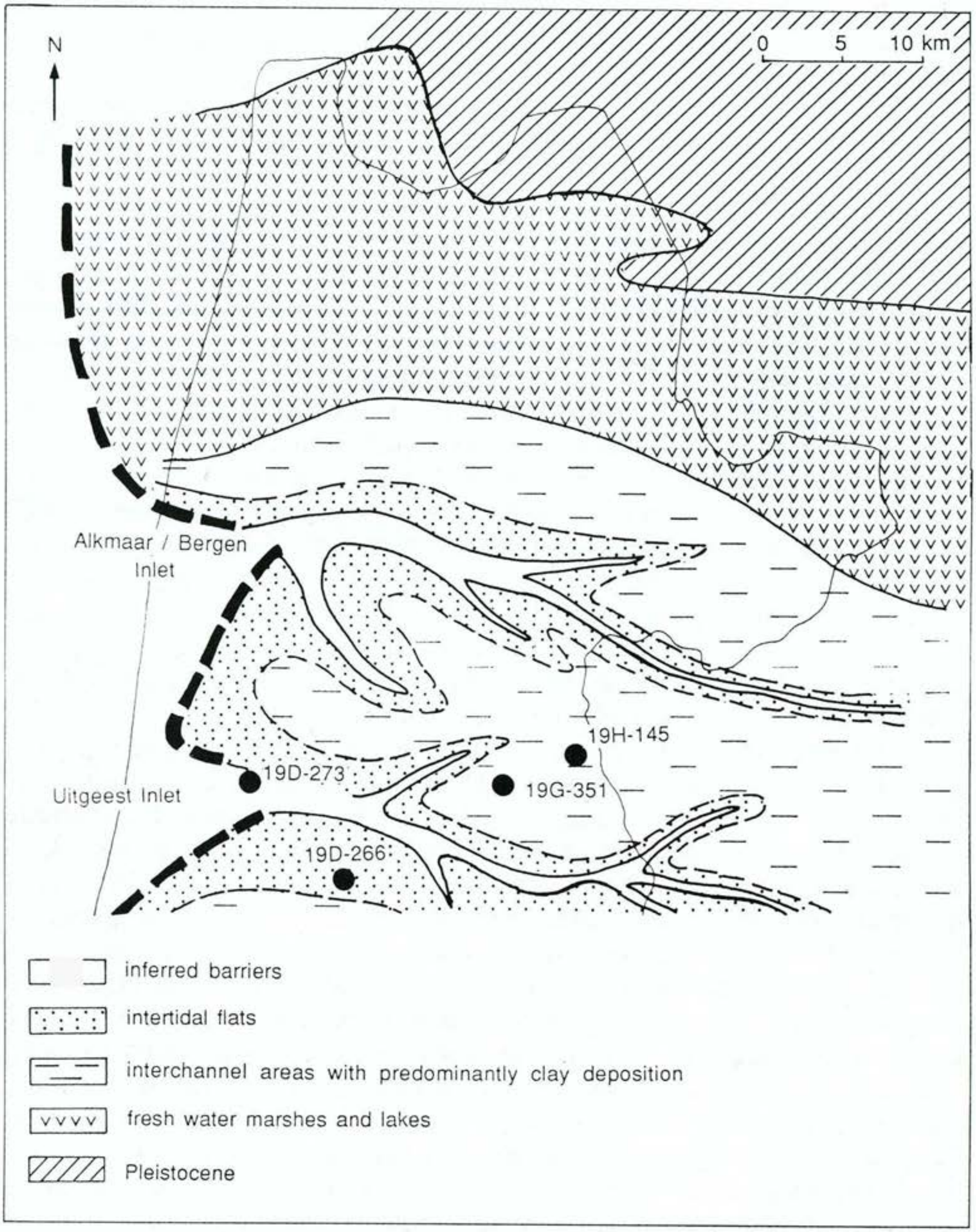

Figure 4.7 Simplified palaeogeographic map of the northwestern part of the Holland tidal basin at 5500 BP. The reconstruction is based on at least one borehole per km^2. For location see inset in Fig. 4.4. (Modified after Zagwijn, 1986; Westerhoff et al., 1987.)

channel. It represents an almost 18-m-thick Holocene section with fresh-water peat at its base overlain by a sand-rich tidal sequence. Flaser bedding predominates; mega-crossbedded sets are absent. Strong bioturbation occurs in distinct layers throughout the entire sequence. *Cerastoderma edule* was found in living position on top of some of the burrowed layers; near the base of the section a shell-rich interval with *Peringia (Hydrobia) ulvae* and *Cerastoderma edule* shells occurs at the base of a completely homogenized layer, which strongly suggests burrowing by *Arenicola marina*. Although strong bioturbation does not necessarily imply intertidal conditions, recent studies of the intertidal and subtidal macrozoobenthos of the western Wadden Sea (Beukema and De Vlas, 1979; Dekker, 1989) point to the relative absence of *Cerastoderma edule* and *Arenicola marina* in the subtidal environment. This, the position of the core at the edge of one of the main channels in the tidal basin, and the presence of a low-energy subtidal environment nearby, strengthen our view that the channels are surrounded by tidal flats, which protect the interchannel areas.

Interpretation

The morphology of the tidal basin before 5000 BP reflects the adjustment of a tidal system with a *moderate sediment supply* to a rapid rise in sea-level: sand introduced into the system by tidal currents via the inlets was deposited mainly in and along the channels. Sandy intercalations in the muds of the interchannel area suggest deposition as crevasse splays. Lateral channel migration was limited, possibly because storage capacity was created continuously. Once the mud-rich interchannel areas were formed, these provided additional stability to the channels since the clays are strongly resistant to erosion. The interchannel areas were efficient mud traps. In such a system no sediment and little space is available for salt marshes. Going from the inlets towards the margins of the tidal basin the amount of sand decreases, and the subtidal interchannel areas increase in size and merge into the fresh-water marshes with peat formation surrounding the basin. Thus, salt marshes fringing the tidal basin are absent but reed marshes occur instead. The only localities left for salt marshes to develop would be the flats along the channels and the area behind the barrier. However, neither cores nor exposures indicate the presence of salt marshes prior to 5000 BP in the Holland tidal basin. The strongly burrowed nature of the muds in the upper 2 to 3 m of the cores of the interchannel areas (Fig. 4.6) suggests that these sediments were deposited intertidally. This is probably due to the sea-level rise levelling off between 6000 and 5000 BP, and sediment supply exceeding the creation of storage capacity.

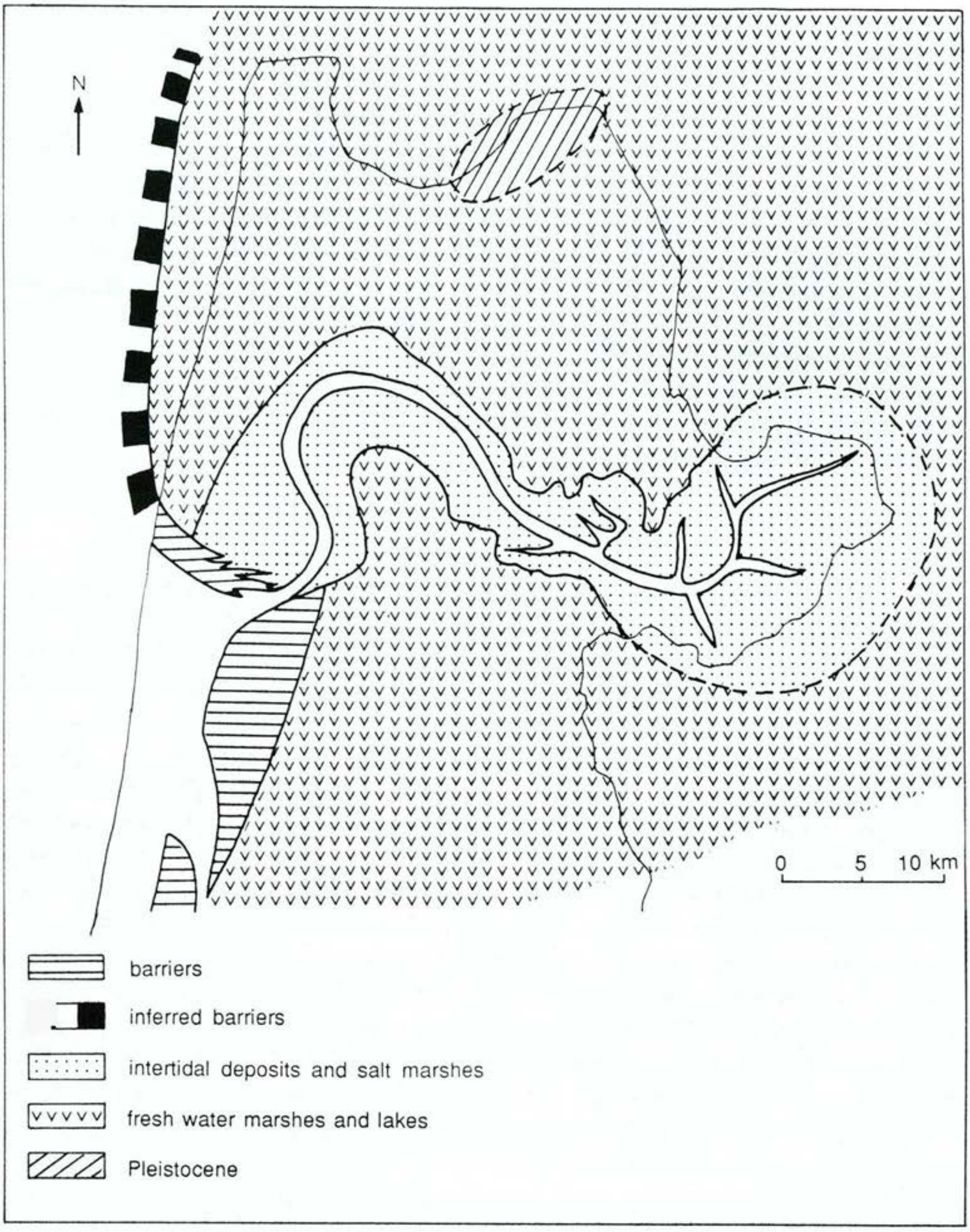

Figure 4.8 Simplified palaeogeographic map of the West-Friesland tidal basin at 3600 BP. Same location as Fig. 4.7. (Modified after Ente, 1963; De Mulder and Bosch, 1982.)

Final stage of the Holland tidal basin

While the Atlantic/Subboral Holland tidal basin was gradually filling up with sediment, the tidal inlets silted up and closed. Between 4500 and 3500 BP the Alkmaar/Bergen inlet was the only remaining tidal inlet. Figure 4.8, after Ente (1963), De Mulder and Bosch (1982) and Roep and Van Regteren Altena (1988), is a reconstruction for the period between 3800 and 3500 BP of the tidal basin flooded and drained by this inlet. The sea withdrew from the area before 3275 BP (Roep and Van Regteren Altena, 1988) and this land was colonized by Bronze-Age farmers. These farmers lived in a wide-spread area of salt marshes of this tidal system, indicating that at the rate of sea-level rise that is characteristic for the Late Subboreal in the Netherlands, salt marshes are a common morphologic feature.

Model for the evolution of the Holland tidal basin at different rates of sea-level rise

In the evolution of the Holland tidal basin three different stages can be distinguished.

(1) When the sea level rose relatively fast (more than 0.75 m per century), prior to 7000 BP (Fig. 4.3), intertidal flats occurred in flood-tidal deltas, which were restricted to the vicinity of tidal inlets and channels. Channels showed only a limited lateral migration. Sand was deposited on the tidal flats along the channels, probably by crevassing, separating the channels from subtidal interchannel areas, in which mud deposition prevailed. The mud-rich lagoons merged landward into fresh-water swamps. Salt marshes did not form.

(2) When the rate of sea-level rise declined to 0.40-0.30 m per century, between 7000 and 5500 BP, sediment supply started to balance the storage capacity of the relatively narrow southern part of the Holland tidal basin. This eventually led to the closure of the tidal inlets from 5500 BP onward. In the wide, northern part of the basin the flood-tidal delta grew at the expense of the interchannel area (Fig. 4.7). Salt marshes were still rare or absent.

(3) When the rate of sea-level rise slowed down further to 0.15 m per century, between 5500 BP and 3500 BP, the sediment supply was sufficient to fill the entire basin. The tidal flats expanded and the interchannel areas were filled up with sand and mud, and after 4000 BP salt marshes became common features (situation 3600 BP, Fig. 4.8).

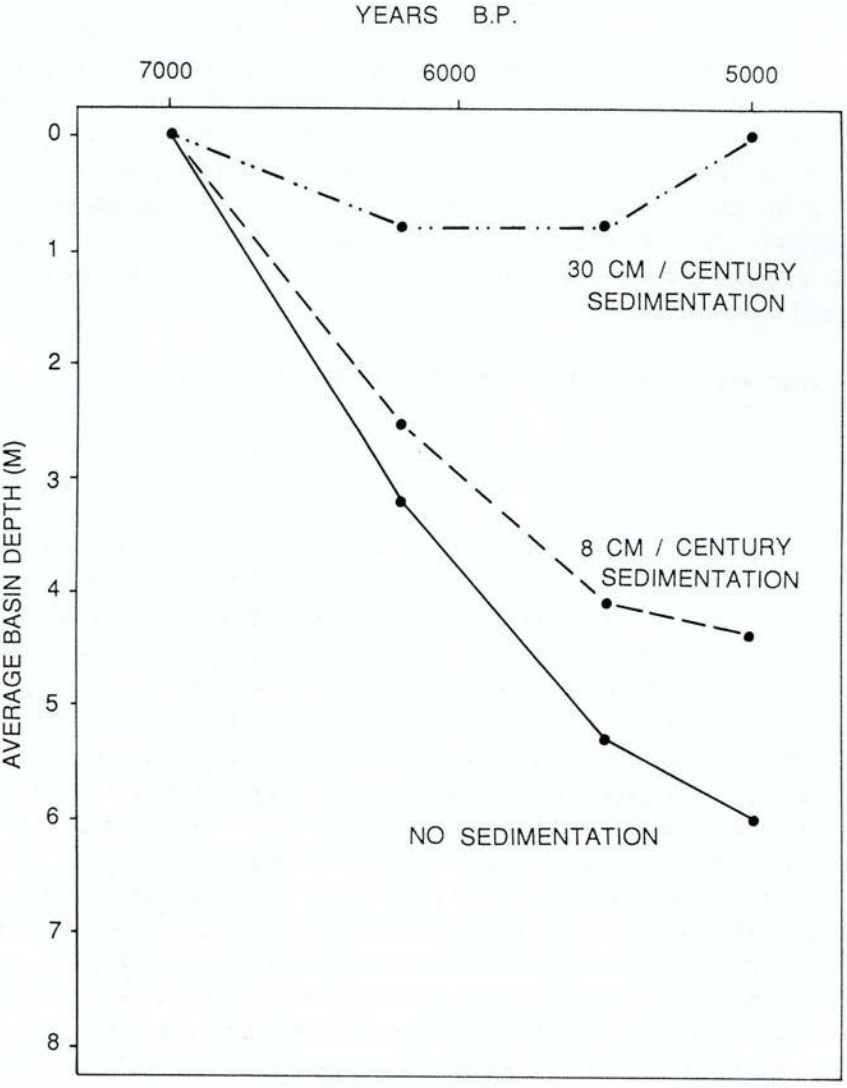

Figure 4.9 Diagram showing the change in average depth of the southern part of the Holland tidal basin between 7000 and 5000 BP at different rates of sediment supply.

Budget calculations

The estimates of Beets et al. (1992) of the sand volume stored in the barrier of the western Netherlands between 5000 and 2000 BP give an idea of the sand supply to the Holland tidal basin. Closure of the tidal inlets after 5000 BP resulted in progradation of the barrier. Between the eroding headlands at the site of the Texel High in the north and the estuary of Rhine/Meuse in the south (Fig. 4.2 and 4.4), and with predominantly westerly winds, the barrier became a sink for sand. Therefore we infer that the amount of sand supplied by cross-shore and longshore transport and stored in the barrier system per unit of time was roughly similar to that in the preceding period. The sediment supplied by longshore transport from the Rhine/Meuse estuary in the south and the Texel High in the north (Fig. 4.4), and that supplied by cross-shore transport are both estimated at 3 x 10^9 m^3 sand (Beets et al., 1992). If a total amount of 6 x 10^9 m^3 sand was deposited between 5000 and 2000 BP, a period of roughly 4000 calendar years, the mean annual sand supply was 1.5 x 10^6 m^3 by longshore and cross-shore transport. The shoreface erosion of the barrier islands prior to 5000 BP is an additional source of sand. Since palaeo positions of disappeared barriers are unknown, we assume that another 1.5 x 10^6 m^3 sand is derived from barrier erosion, which brings the total annual input of sand at 3.0 x 10^6 m^3. Averaged over the total surface area of the Holland tidal basin, some 3600 km^2 (Beets et al., 1992), this results in a vertical accretion of 0.08 m of sand per century. This build-up rate is by no means adequate to compensate for the sea-level rise during that period (Fig. 4.3).

The southern part of the Holland tidal basin, situated between the present city of Haarlem and the Rhine/Meuse alluvial plain (Fig. 4.1 and 4.4), was flooded around 7000 BP, subsequently silted up and was closed off from the North Sea around 5000 BP. During these 2000 years mean sea level rose 6 m (Figs. 4.3 and 4.9). This enables a calculation of the amount of sediment required to fill this part of the basin. For the basin to close it must at least have been filled up to mean sea level. This requires a vertical accretion of 0.30 m per century (Fig. 4.9).

The sedimentary sequence in the Holland tidal basin has an average mud content of 50 to 60%. This means that on average 0.12 to 0.15 m of sand and 0.15 to 0.18 m of mud had to be accumulated each century to fill the southern part of the basin. The volumes of sand and mud imported annually into the entire Holland tidal basin had to amount to 4 to 5 x 10^6 m^3 of sand and 5 to 7 x 10^6 m^3 of mud. If the estimates are correct, the amount of sand derived from barrier erosion must have been larger than assumed above: 3 to 4 x 10^6 m^3 per year.

The northern tidal basin

In the present Wadden Sea remnants of the Atlantic and Subboreal deposits are rare, because these have been eroded by lateral migration of tidal channels and tidal inlets (Chap. 3). However, the sedimentary succession of the more distal areas of the Atlantic/Subboreal basin have been preserved in the northern provinces of the Netherlands. Roeleveld (1974) and Griede (1978) have shown that the distribution of the sedimentary environments is basically similar to that in Holland: channels flanked by tidal flats, which, landward, merge into clay-rich lagoons passing into fresh-water marshes. Salt marshes occured from 4000 BP onwards and became widespread after 3000 BP.

Future evolution of the Wadden Sea

Warrick and Oerlemans (1990) expect an additional eustatic sea-level rise of between 0.31 and 1.1 m, with a best estimate of 0.66 m, in the next 100 years, if the present emission rates for greenhouse gases remain constant. Added to the present rate of 0.13 m per century in the Dutch Wadden Sea, this will result in a rate of sea-level rise of approximately 0.8 m per century in the year 2100.

If we apply the conceptual model outlined above without further considerations to the future development of the Wadden Sea, and accept the expected accelerated sea-level rise, we can conclude that, in the year 2100, the Wadden Sea might resemble the Holland tidal basin during the Atlantic. Tidal flats will be restricted to flood-tidal deltas in the vicinity of the inlets and along the channels, subtidal areas will have grown at the expense of the former flats, in particular in the interchannel areas and near the basin margins, and salt marshes will have disappeared.

However the present Wadden Sea differs in a number of important aspects from the Atlantic/Subboreal tidal basins. These are:

(1) *tidal regime*. Modelling of the tidal regime at lower sea levels in the southern North Sea by Franken (1987) indicates that the mean tidal range during the Atlantic and Subboreal was considerably less than the present range at the Wadden Sea coast which varies between 1.50 m in the west to about 2.25 m in the east. At a sea level of 5 m below the present one, the tidal range at sea was 10 to 30% less. When the basin size is the same, a larger tidal range implies a larger tidal volume and thus more sediment transport capacity and probably also a larger sand supply.

Recent studies show that most of the sand that is imported into the Dutch Wadden Sea is derived from shoreface erosion of the barrier. Stive et al.

(1991) calculate a net annual sand influx of about 9×10^6 m^3. This represents a vertical accretion of 0.44 m per century.

From the evolution of the Atlantic/Subboreal Holland tidal basin a long-term annual sand influx of 4 to 5×10^6 m^3 was concluded. If the same amount of sand is introduced into the present Wadden Sea, which has a surface area of only 56% of that of the Holland tidal basin by a comparable barrier length, this will lead to a vertical accretion of 0.21 to 0.27 m per century.

The annual sand influx calculated by Stive et al. (1991) could cope with an additional sea-level rise of approx. 0.30 m, which will be reached around 2050 according to the IPCC scenario. If the long-term average value for sand import derived from the Holland tidal basin is used, double the recent rate of sea-level rise could still be compensated.

(2) *Basin shape*. Flooding of the coastal plain of the Netherlands during the Atlantic resulted in basins penetrating far into the former alluvial valleys, and thus oriented perpendicular to the shoreline. The present Wadden Sea, on the contrary, is aligned parallel to the barrier and has only a few shore-normal embayments. The shape of the Atlantic/Subboreal tidal basins is probably an important factor controlling the stability of the tidal channels. As a result of the restricted lateral migration of the channels in these basins over 50% of the sedimentary fill consists of mud. Long-term net accumulation of mud in the Wadden Sea is low because of resuspension by storms (Postma, 1961) and reworking of the sediments by channel migration. Whether the stability of the Atlantic/Subboreal channels was also influenced by the rise in sea-level, which continuously created storage capacity, is not known. If so, the channels of the present Wadden Sea might show a similar stability in the future, resulting in more long-term mud deposition.

The present shape of the Wadden Sea is largely determined by constructions such as dikes. This adaptation of basin geometry is likely to influence the behaviour of the channels. Whether and how these will influence the future development is not known.

(3) *Basin fill*. The Holocene rate of sea-level rise decreased from more than 0.7 m to 0.15 m per century, which resulted in the Holland tidal basin being filled by sediment. In the future, the rate of sea-level rise may accelerate. This will cause a different behaviour of the Wadden Sea which is nearly filled with sediment at present. An increase in the rate of sea-level rise will cause an increase of the tidal prism, which will lead to scouring of the channels, since channel dimensions are directly related to the tidal prism (Gerritsen and De Jong, 1985). Sand scoured from the channels might be stored on the tidal flats and reduce the tidal prism. Similar developments were observed in an estuary in the southwest of the Netherlands (Van den Berg, 1986).

The differences between the Holland tidal basin at decreasing rates of sea-level rise and the present Wadden Sea at increasing rates of sea-level rise show that the model derived from the evolution of the former cannot be applied straight away in order to give a detailed impression of the future behaviour of the Wadden Sea. Considering the higher present influx of sand per unit of time, the Holland tidal-basin model represents a "worst-case".

Recent research on sedimentation in the present-day salt marshes in the Wadden Sea by Dijkema et al. (1990) supports one of the conclusions of our model. They show that if acceleration of the rate of sea-level rise leads to reduced deposition in the mud flats adjacent to the marshes, it is likely that the pioneer zone will no longer develop into salt marshes and lateral expansion of the salt marshes stops. Since new salt marshes will no longer be formed in the pioneer zone, the area covered by salt marsh will decrease as a result of wave erosion. Dijkema et al. (1990) conclude that the naturally formed salt marshes of the Wadden Sea are not likely to survive an acceleration of the rate of sea-level rise.

An important aspect of the Holland tidal-basin model is the channel behaviour, which strongly promoted mud deposition. It is not kwown whether this behaviour is controlled by the shape of the basin, the rate of sea-level rise, or both.

Simulation of paleotides in the Holland tidal basin (Chap. 7) will be the next step to a better understanding of the impact of rising sea level on back-barrier basins.

In our view, the most important aspect of the derived model is that it visualizes the consequences of sea-level rise for back-barrier basins.

Conclusion

The Atlantic and Subboreal evolution of the Holland tidal basin, governed by sea-level rise, is summarized in a conceptual model. This model can be used to visualize the future evolution of the Dutch Wadden Sea at higher rates of sea-level rise. However, the future development of the Wadden Sea will not be an exact image of the evolution of the Holland tidal basin, because of the higher tidal range, a different basin shape and an increase instead of a decrease of the rate of sea-level rise. The larger present sand import, probably caused by the higher tidal range, is sufficient to balance an addition sea-level rise of 0.30 m, which will be reached by the year 2050 according to the IPCC scenario (Warrick and Oerlemans, 1990). Nevertheless, from then on, a growing deficit will occur, which is not compensated by increasing tidal prisms as the size of the Wadden Sea basin is fixed by dikes. This will cause drowning of the tidal flats, eventually, after which the Dutch Wadden Sea will start to resemble the Holland tidal basin as it was during the Atlantic.

The Holocene tidal basins show that salt marshes will disappear when the rate of sea-level rise surpasses the present one. The study of Dijkema et al. (1990) seems to confirm this with regard to natural salt marshes.

Acknowledgements

We wish to thank Saskia Jelgersma, Janrik van den Berg, Poppe de Boer, Piet Cleveringa, Kees Dijkema and two anonymous reviewers for their critical remarks and valuable suggestions for improving an earlier draft of this paper. Research by the first author was supported by the Netherlands Organisation for Scientific Research (NWO), grant CO_2-77.125 and the National Institute for Coastal and Marine Management/RIKZ (formerly Tidal Waters Division) of Rijkswaterstaat.

The authors are grateful to their colleagues at the Geological Survey of The Netherlands for their cooperation and for putting their data at our disposal.

5. Reconstruction of tidal inlet and tidal channel dimensions in the Frisian Middelzee, a former tidal basin in the Dutch Wadden Sea.

Abstract

The Middelzee, a Late-Holocene tidal basin in the Dutch Wadden Sea, was created by marine flooding and erosion in the Boorne Valley. It reached its maximum extension around 1000 AD The basin was rapidly filled in and supratidal salt marshes were formed which were subsequently secured with dikes. By 1600 AD the landward part of the Middelzee had been reclaimed. This caused partial infilling of the remaining channels in the Wadden Sea and the Ameland tidal inlet.

The cross-sectional surface area and depth of the tidal channels and tidal inlet were calculated from the basin surface area and the tidal discharge, using empirical relationships derived in this paper as well as published in the literature. The calculations show that, given the maximum thickness of inlet channel deposits, the tidal prism was distributed over 2 inlet channels until 1700 AD This is in agreement with historical nautical charts.

The calculated maximum channel depths for tidal channels in the Middelzee are in agreement with the channel sediment thicknesses found in borings. Locally, these calculated maximum depths are significantly less than the maximum thickness of the channel deposits. This indicates that Middelzee channels have cut down into channel sediments deposited during earlier transgressions in the Boorne valley. This provides valuable information on the evolution of the tidal basin.

The minimum annual sediment import between 1000 AD and 1600 AD, estimated from the decrease in basin surface area and the infilling of the channels, is $1.9 * 10^6\ m^3$. This rate falls well within the range of the estimated present-day sediment input into the individual Wadden Sea tidal basins.

Introduction

The present-day Dutch Wadden Sea can be subdivided into several tidal basins, separated by tidal watersheds, and each of them being flooded and drained through their own inlet. This subdivision was even more explicit in the past, when the orientation of these basins was governed by north-south running Pleistocene valleys. The long-term development of these tidal basins is poorly understood.

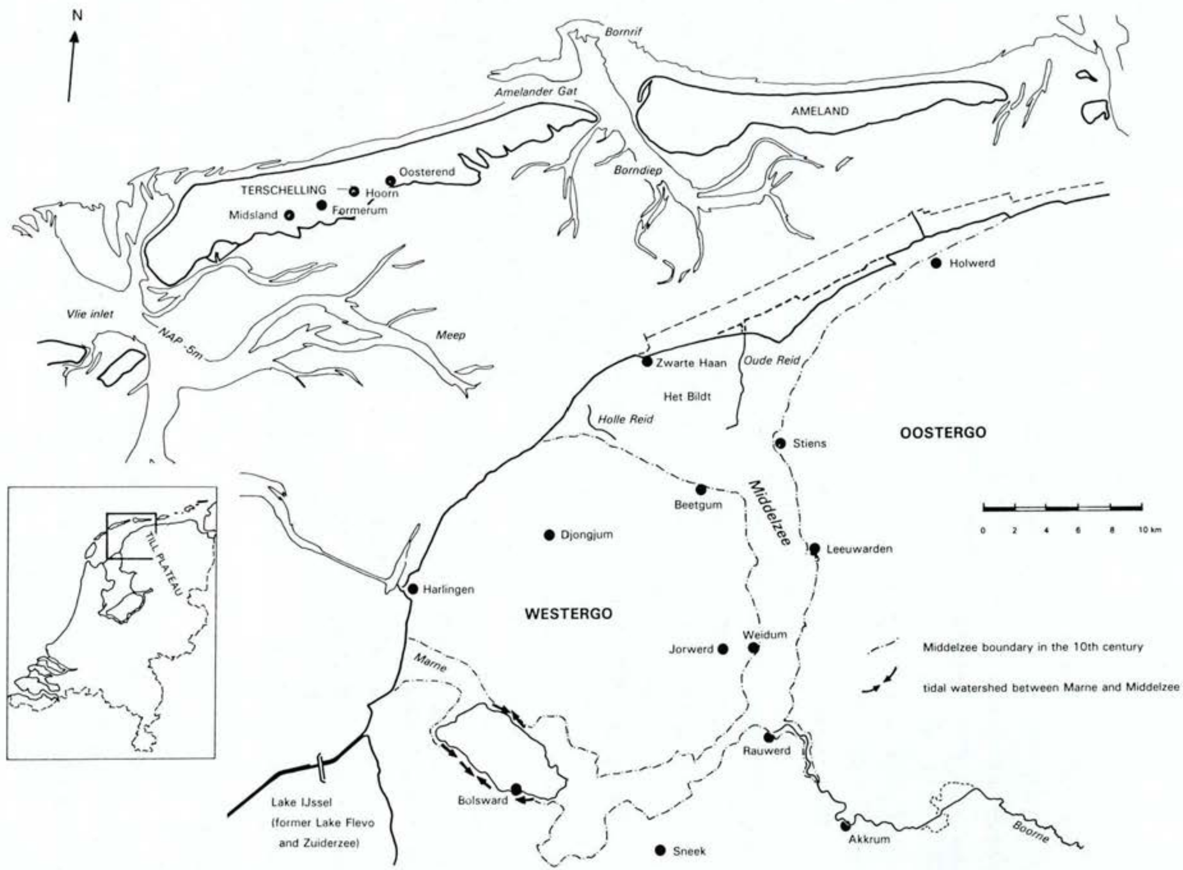

Figure 5.1 Location map of NW Friesland and the Middelzee in the Netherlands. The 5m-isobath is given relative to NAP, the Dutch Ordnance Datum, which is about present-day mean sea level.

The changes in paleo-morphology of a part of the former Wadden Sea in northwest Friesland during the medieval period are reconstructed in this paper. Marine erosion between 800 AD and 1000 AD created a tidal basin reaching 30 km inland. This basin is called Middelzee (Fig. 5.1). The expansion and the subsequent silting up and reclamation of this basin was described by contemporary authors (see e.g. Boeles, 1951, and Halbertsma, 1955, for overviews). The stepwise reclamation of the Middelzee in 600 years illustrates the rate of silting up of the embayment. Archaeological, geological (Cnossen, 1958; Ter Wee, 1976; De Groot et al., 1987), geomorphological and soil-compositional (Cnossen, 1971; Kuier, 1974, 1976a,b, 1981) publications and maps complement the historical descriptions.

Tidal inlets and channels are the most mobile elements in a tidal basin. Determination of their position and dimensions is essential for the analysis of tidal basin evolution. The position of the tidal inlet and channels of the Middelzee, however, are poorly known. Shoreface retreat and lateral inlet migration destroyed most of the evidence of former Holocene tidal inlets and barrier islands. Tidal channel and tidal flat deposits in the back-barrier area are bound to be reworked by lateral migration of younger channels. Only the major channels that scoured deep into the Pleistocene subsurface can still be traced. Reduction of the tidal prism caused by silting up of the tidal basin must have resulted in a decrease in width and/or depth of the channels in the basin and in the inlet, since the cross-sectional area and the tidal prism in channels and inlets are directly related (see below).

Channel and inlet reconstructions can be improved using the empirical relationships between the cross-sectional area of a channel and its tidal prism. This relationship was introduced for tidal inlets by Le Conte in 1905 (FitzGerald et al., 1984) and has been quantified by O'Brien (1931, 1969) and many others since. Gerritsen and De Jong (1985) established a relationship for the tidal inlets of the Netherlands Wadden Sea. A similar relationship between the cross-sectional areas of channels in the tidal basin and their tidal prisms has been quantified by Eysink (1979, 1991) and Gerritsen (1990). Using these relationships, the dimensions of tidal inlets or tidal channels can be estimated if the surface area of the tidal basin is known, since the tidal prism of a basin can be approximated by the product of the surface area of the basin times the tidal range. Thus, the decrease of the inlet and channel dimensions of the Middelzee caused by the silting up of the basin with time can be estimated using the reduction in surface area indicated by the reclamation.

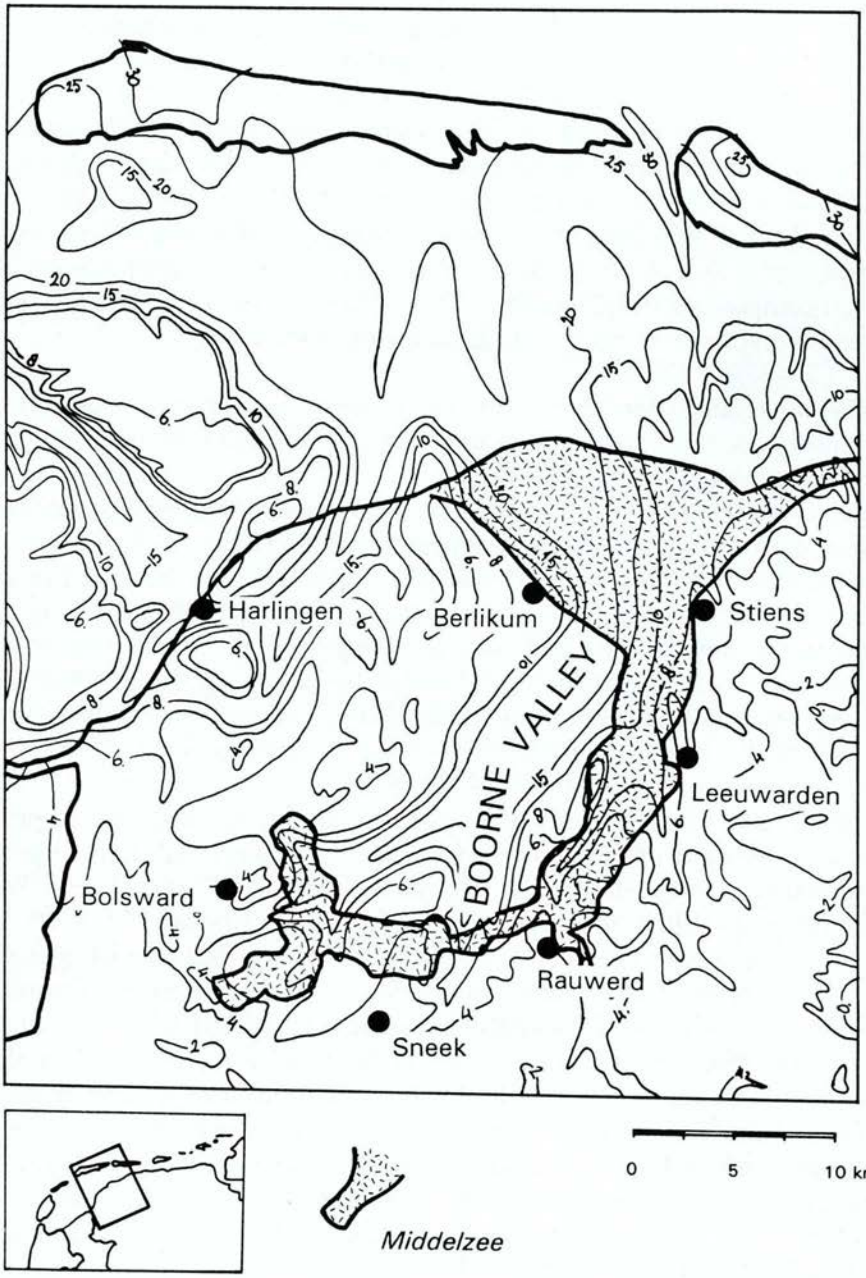

Figure 5.2 Base Holocene map of NW Friesland. Depth contours are in metres below NAP. See inset for location.

Formation and silting up of the Middelzee

The Boorne valley and the formation of the Middelzee

The Middelzee was the final stage of the Holocene transgression in the Boorne valley. The Boorne was a small river draining the Saalian glacial till plateau in Friesland, Groningen and Drente (Fig. 5.1) from the Late Saalian onwards. It originated as a glacial stream that ran to the south-west. Its course became blocked by aeolian sands during the Weichselian. The lower reach of the river shifted gradually towards a northwesterly direction (Cnossen and Zandstra, 1965). Finally, the Boorne ran from Akkrum to the northnorthwest (Fig. 5.1).

During the Holocene the sea penetrated into the Boorne valley from the north, changing it into an estuary. The oldest preserved estuarine deposits in the Boorne valley are found west of Jorwerd (Fig. 5.1) at 8.0 m to 10.5 m below present mean sea level (Ter Wee, 1975, 1976). They were formed in the Late Atlantic (6400 BP-5300 BP).

The sea level rose rapidly in the coastal plain of the Netherlands before 7000 BP, with rates up to 0.75 m per century. Between 7000 BP and 5500 BP the sea-level rise decelerated. After 5500 BP the average rate of sea-level rise was only 0.15 m per century. This allowed sediment supply in the western part of the Netherlands to fill in the tidal basins which had been created there. Eventually the tidal inlets closed between 5500 BP and 3300 BP (Beets et al., 1992; Chap. 4). The situation in the northern part of the Netherlands was different. The tidal basins were not completely filled in with sediment, and consequently the inlets remained open.

The slowly but continuously rising mean sea level caused the sea to penetrate further south in the Boorne valley until it reached into the area south of Westergo (Fig. 5.1) in the Late Subboreal. Initially, this caused expansion of the tidal basin and scouring of the tidal channels (Ter Wee, 1976). However, sediment transport into the basin resulted in infilling of the landward part of the basin with time. The levees along the channels were built up to high-lying, supratidal areas which became inhabited around 2600 BP (Ter Wee, 1976).

Further away from the channels predominantly clay was deposited, which got compacted with time, creating depressions in the landscape. The Boorne diverted its course to such a depression east of the former estuary (Fig. 5.2). With the continuing rise in sea level the tidal action gradually penetrated landward during the Post-Roman and Early-Medieval period (Cnossen, 1958). At the end of the 9th century the basin expanded rapidly and tidal channels scoured deep into the subsurface (Kuier, 1974, 1976a; Ter Wee, 1976; De

Groot et al., 1987). The expansion of the basin was most likely enhanced by human activities such as peat digging. In the 10th century the lower reach of the Boorne had changed into the Middelzee (Ter Wee, 1975, 1976). Sea water penetrated as far inland as Sneek (Fig. 5.1).

The Marne, a channel of the Vlie tidal inlet, penetrated Westergo from the west (Fig. 5.1) and made contact with the Middelzee near Bolsward, where a tidal watershed developed (Kuijer, 1974).

The inlet of the Middelzee was situated between the central part of the island of Terschelling and the present western coast of the island of Ameland (Fig. 5.1). Radiocarbon dating of peat layers indicated that the central part of Terschelling must have been present from at least 360 - 620 AD The pollen content of the peat suggests human occupation by then (De Jong, 1984). Information on the age of Ameland is restricted. The oldest peat layers from dune valleys on Ameland have been radiocarbon dated at 670 - 850 AD (De Jong, 1984).

Channels in the Middelzee and Het Bildt

The course and dimension of former channels and creeks in the Middelzee south of Weidum (Fig. 5.1) are known from geological mapping (Ter Wee, 1976; De Groot et al., 1987). North of Weidum and in the wider part of the Middelzee, later on known as Het Bildt (Fig. 5.1), and the adjacent Wadden Sea this information must be inferred from other sources.

Written sources, going back to early medieval times, give rough indications. Neither accurate maps nor charts are known from the period of full extent of the Middelzee. Isbary (1936) and Rienks and Walther (1954) suggest that the 2 major marsh creeks which are still recognizable in the landscape, the Holle Rijd and the Oude Rijd (Fig. 5.1), are the remnants of medieval tidal channels.

Siltation and reclamation of the Middelzee

Increased flooding and marine erosion with rising sea level resulted, according to Kuijer (1976 a,b), in the damming of channels and the construction of dikes along the high-lying reaches of land. Improved social organisation also contributed appreciably to these activities (Borger, 1985). The reconstruction of the reclamation of and dike construction along the Middelzee is mainly based on the historical study of Rienks and Walther (1954). Figure 5.3 gives an overview of the dikes along the Middelzee and their date of construction.

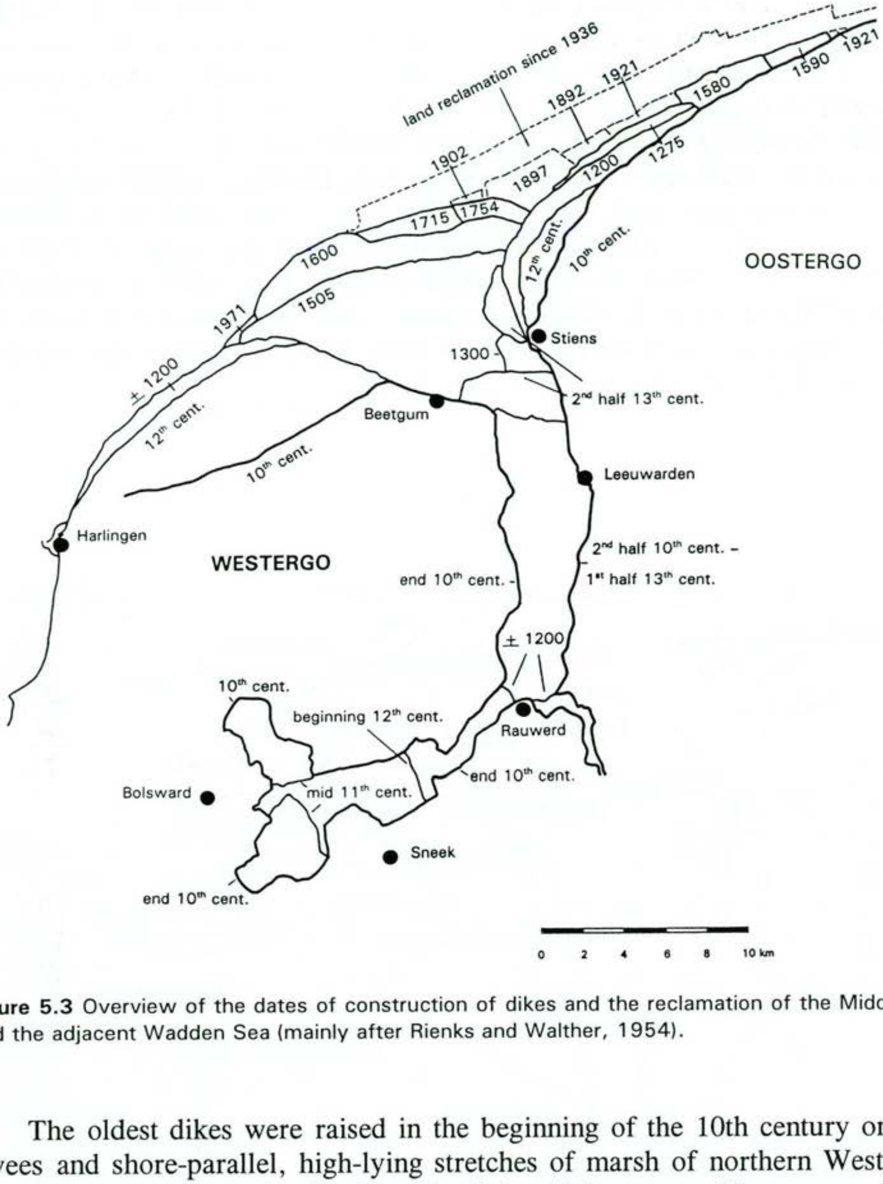

Figure 5.3 Overview of the dates of construction of dikes and the reclamation of the Middelzee and the adjacent Wadden Sea (mainly after Rienks and Walther, 1954).

The oldest dikes were raised in the beginning of the 10th century on the levees and shore-parallel, high-lying stretches of marsh of northern Westergo and Oostergo (Fig. 5.3). At the end of the 10th century Westergo and the branch of the Middelzee between Rauwerd and Bolsward were completely encircled by a system of dikes (Fig. 5.3). The western part of Oostergo was protected by a single, more or less north-south running dike. The silting up of the tidal watershed near Bolsward to a supratidal level, followed by the construction of a dike across it, had changed this branch of the Middelzee into a dead end. The now quiet conditions caused rapid accretion of the intertidal (mud)flats. The latter evolved into salt marshes which could be protected with dikes. Thus, the southwestern branch of the Middelzee was reclaimed stepwise from west to east (Fig. 5.3). By 1200 AD it was closed off from the estuary.

The remaining Middelzee silted up rapidly and by 1300 AD it was reclaimed up to Beetgum and Stiens (Fig. 5.3), leaving a coastal embayment, now known as Het Bildt. Het Bildt silted up to supratidal level within a century. In 1505 a dike was raised on the seaward marsh bar (Schotanus à Sterringa, 1664). With the construction of this dike, which connected the dikes of Oostergo and Westergo, an almost linear coastline was formed. Salt marshes that accreted at the toe of these dikes were reclaimed in the following centuries (Fig. 5.3).

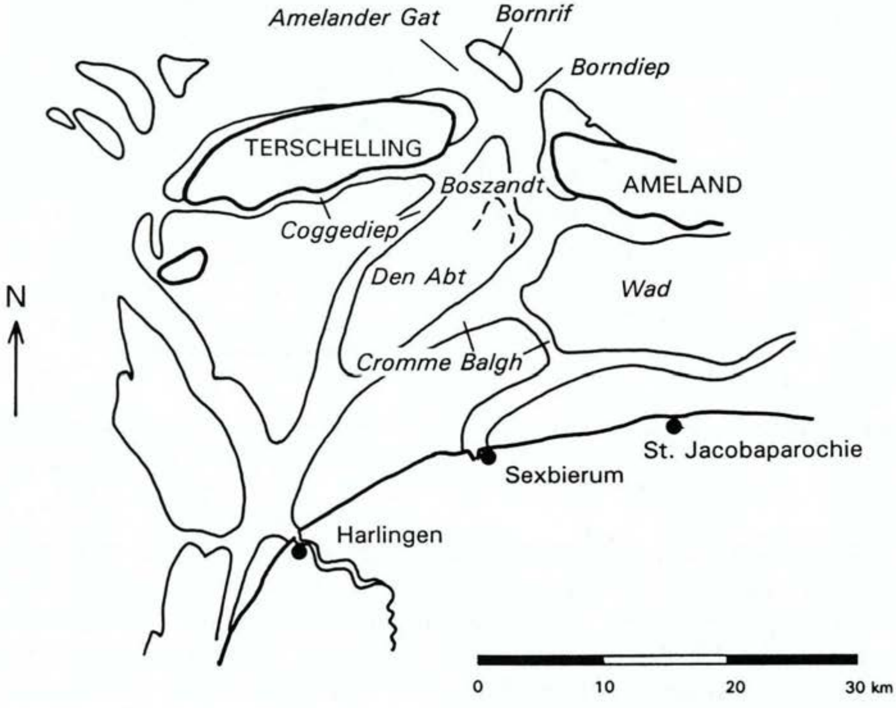

Figure 5.4 Simplified nautical chart of the Amelander Gat around 1585 after Waghenaer (" 'Tvlie ende 'Tmaersdiep", in Spieghel der Zeevaerdt, part 1, 1584).

The first known charts of the North Sea coasts and the Wadden Sea were published by Waghenaer (1584; Fig. 5.4) and Haeyen (1585; Fig. 5.5), when the Middelzee had already been silted up and reclaimed. In the 16th century the Amelander Gat, the inlet between Terschelling and Ameland, had two channels, the Coggediep in the west and the Borndiep in the east. A shoal that was called Bosch or Camper Zandt separated these channels. The Amelander Gat was the main channel in the ebb-tidal delta. It was bordered by shallow grounds to the north, called Bornrif.

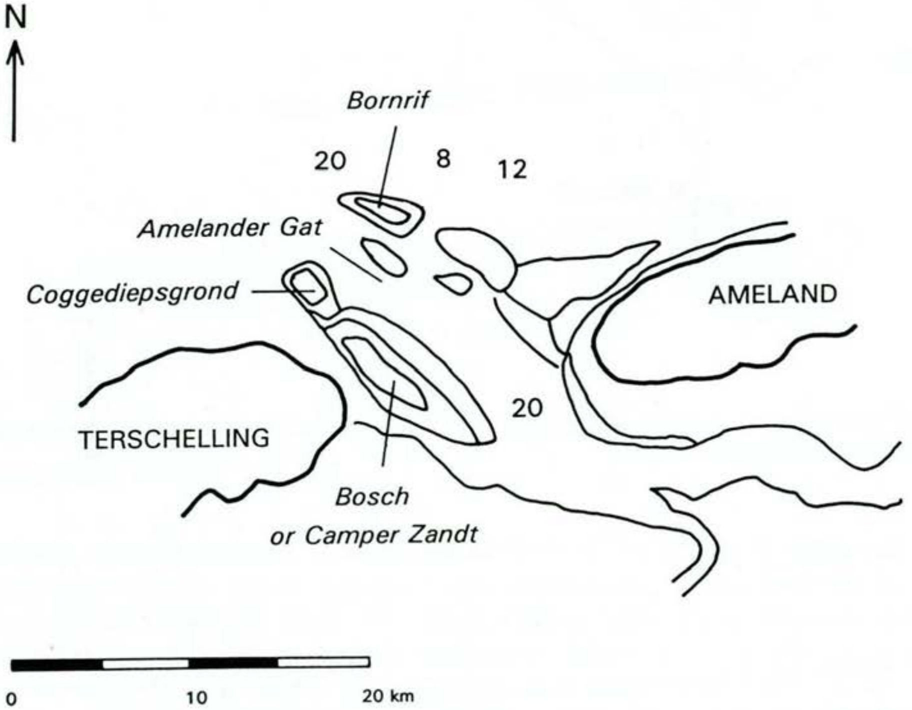

Figure 5.5 Simplified nautical chart of the Amelander Gat around 1585 after Haeyen (1585). Depths in metres.

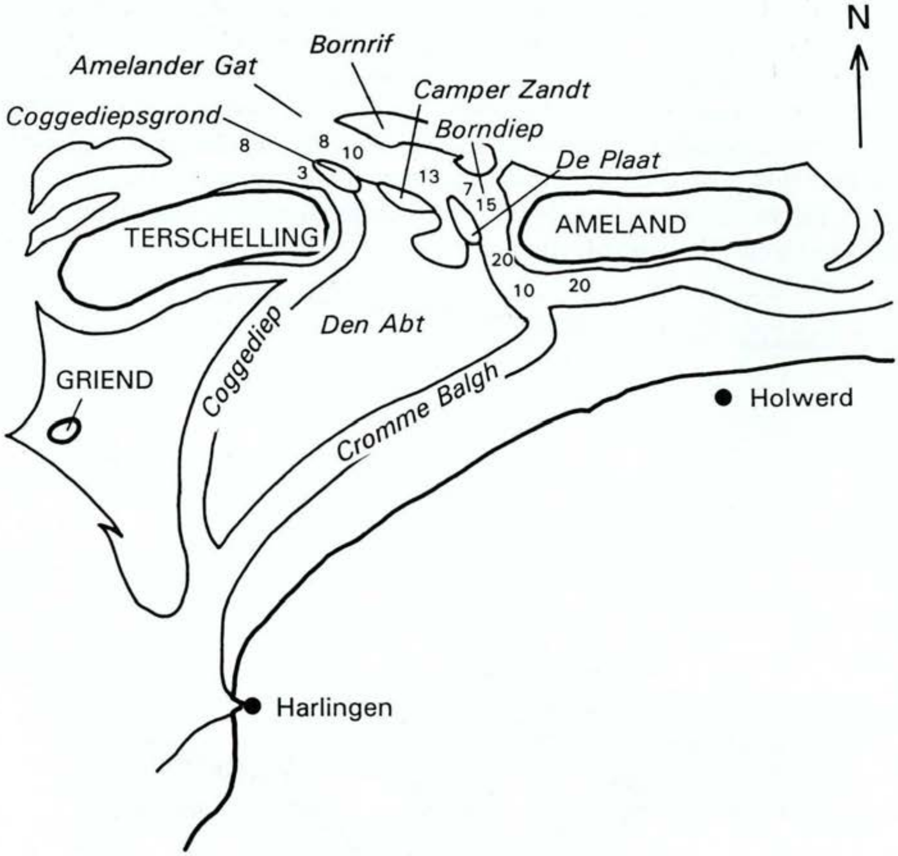

Figure 5.6 Simplified nautical chart of the Amelander Gat after Blaeu, 'Licht der Zeevaert' (1608). Depths are given in metres.

The channels and shoals in the tidal inlet show a distinct evolution. At the end of the 16th century Waghenaer and Haeyen pictured a wide tidal inlet with a relatively small shoal surface (Figs. 5.4, 5.5). In 1608 Blaeu's map showed a more extended shoal, with three distinct bars at its seaward side (Fig. 5.6). The chart which was published by Blaeu in 1623 shows an extensive shoal area in the inlet with the Camper Zandt having silted up to supratidal level (Fig. 5.7). From this sequence of maps it can be concluded that the inlet width was reduced over this period.

Haeyen (Fig. 5.5) indicated a depth of '12 vadem' (20.4 m) for the Borndiep. He did not give a depth for the Coggediep. Apparently it was not considered important for shipping. Blaeu's chart from 1608 gives identical depth information (Fig. 5.6). Winsemius (1622) reported that in 1610 the Coggediep had a depth of '9 vadem' (15.3 m).

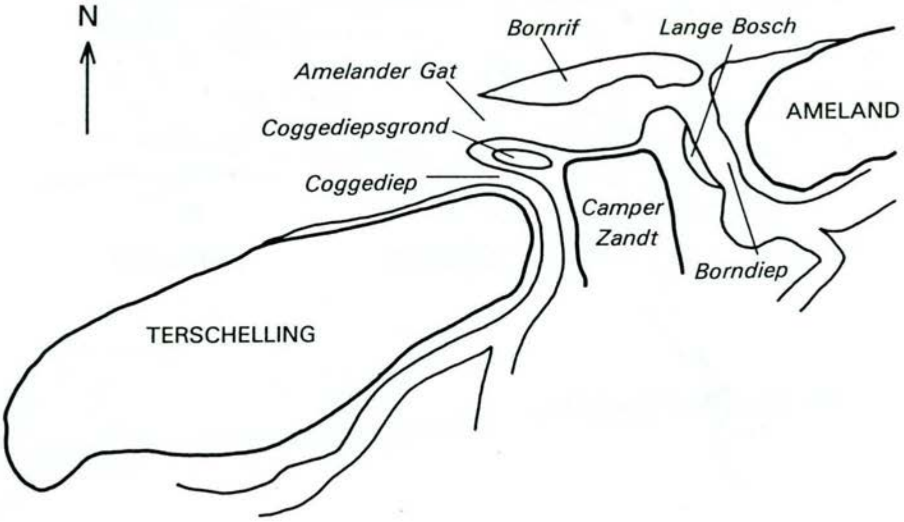

Figure 5.7 Simplified nautical chart of the Amelander Gat after Blaeu, 'Zeespieghel' (1623).

The Amelander Gat after the 17th century

In the beginning of the 18th century the Coggediep was still in existence, according to the charts of Witsen and Guitet dating from 1708 and 1710/1712 respectively. Guitet indicated a depth of '10 vadem' (16.8 m) in 1710 (Fig. 5.8). From his map it can be seen that the Coggediep at that time was a wide inlet channel. This suggests that the discharge must have been divided between the two channels. Reconstructions by Schoorl (pers. comm.), however, show that the Coggediep was very small in 1695. According to the hydrographical chart of the Amelander Gat by Buyskes, the Coggediep had disappeared completely in 1798 and the shoals Camper Zandt and Bosch were connected to the island of Terschelling. The Wadden Sea south of the eastern part of Terschelling had accreted to intertidal level, without being dissected by channels. Buyskes measured a depth of '15 vadem' (25.5 m) in the Borndiep.

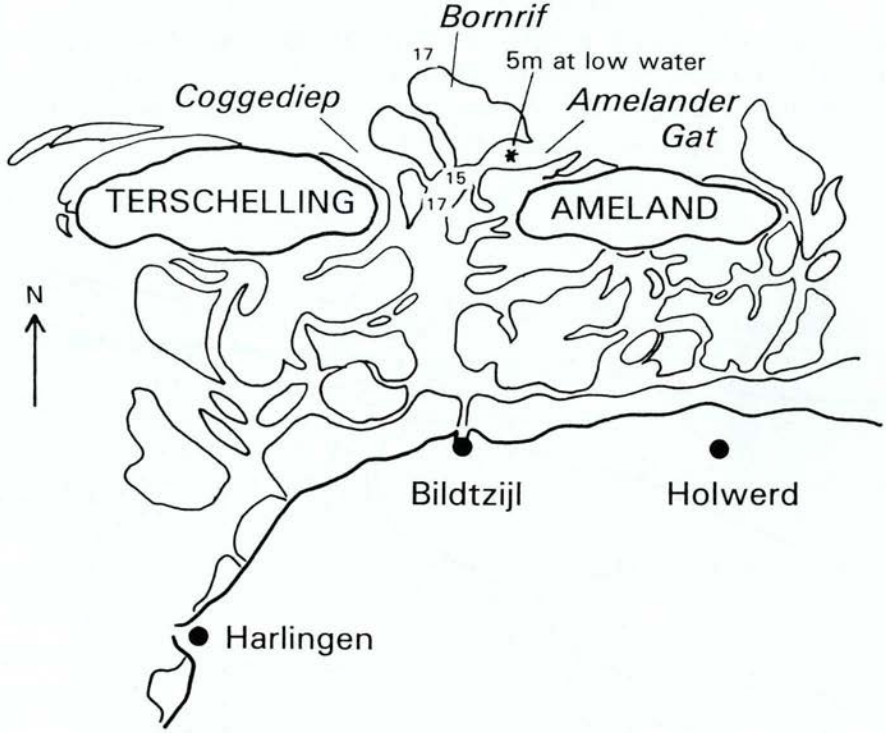

Figure 5.8 Detail of the map of the Wadden Sea by Guitet ("Wad en Buytenkaart", 1708/1710), after the original in the library of Leiden University. Depths in metres.

The silting up of the Coggediep cannot be a consequence of the reclamation of the Middelzee. The Coggediep remained in existence for 2 centuries after the reclamation of the Middelzee and Het Bildt as shown above. It is not plausible that the silting of a channel in a tidal inlet will lag 2 centuries behind such a major reduction of its tidal prism. The dimensions of the Coggediep would have followed this reduction in drainage area closely, since the wave-driven shoreward sediment flux that provides the sand for inlet sedimentation was not diminished. The Coggediep must have been (partly) connected to another tidal basin to gain sufficient discharge to remain open. Historical evidence suggests that the Coggediep was connected to the Zuiderzee (see Fig. 5.1 for location of the latter). The Coggegat silted up only after the establishment of a firm connection between the Vlie tidal inlet and the Zuiderzee.

The shallowing of the Coggegat delayed the arrival of the flood tide on the Terschelling tidal watershed via the Amelander Gat. The flood tide arrived earlier at the tidal watershed via the westerly tidal inlet since the tidal wave runs from southwest to northeast along the Dutch coast. Thus a water-level gradient was created on the watershed that resulted in a net eastward water and sediment displacement and, consequently, migration of the tidal watershed. This process would have been amplified by the prevailing westerly winds (FitzGerald and Penland, 1987). The tidal watershed south of Terschelling, although still dissected by channels, started to shift eastward in the first half of the 18th century (Isbary, 1936). This coincides very well with the final silting up of the Coggediep. Simultaneously, the tidal watershed accreted to an intertidal level, strengthening the separation between the Vlie and Borndiep tidal basins.

After the silting up of the Middelzee tidal currents started to penetrate further eastward between Ameland and Friesland. Southward running channels like the Cromme Balgh (Fig. 5.4) were abandoned while eastward running channels gained more discharge and consequently became deeper. This, as explained above, caused the tidal watershed south of Ameland to move to the east. This watershed migrated 4 km to the east between 1831 en 1950. The Borndiep reacted to this eastward shift by rotating its course from north-south to northwest-southeast and started to erode the island of Ameland. The erosion forced the southwestern shore of Ameland 1.4 km to the east before it was stopped by protection works.

Harle inlet, between the islands of Spiekeroog and Wangerooge in the German Wadden Sea, has a similar history of inlet narrowing caused by partial basin reclamation (FitzGerald et al., 1984). The tidal watershed south of Spiekeroog, the island west of the inlet, moved to the east concomitantly with the shallowing of the western inlet channel.

Basin reconstruction

From historical and geological data it is clear that since approximately 600 AD the inlet of the successor of the river Boorne must have been situated somewhere between the village of Formerum in the island of Terschelling and the present-day west coast of Ameland (Fig. 5.1). The maximum depth of Holocene channel erosion here is 25 to 28 m below present MSL (Fig. 5.9). The maximum depth can be up to 31 m below MSL if reworking of Eemian deposits by Holocene channels is considered.

Map reconstructions of the Middelzee have been made per century in order to assess the reduction in the basin surface area with time. After estimation of the tidal prism from the surface area, the dimensions of the tidal

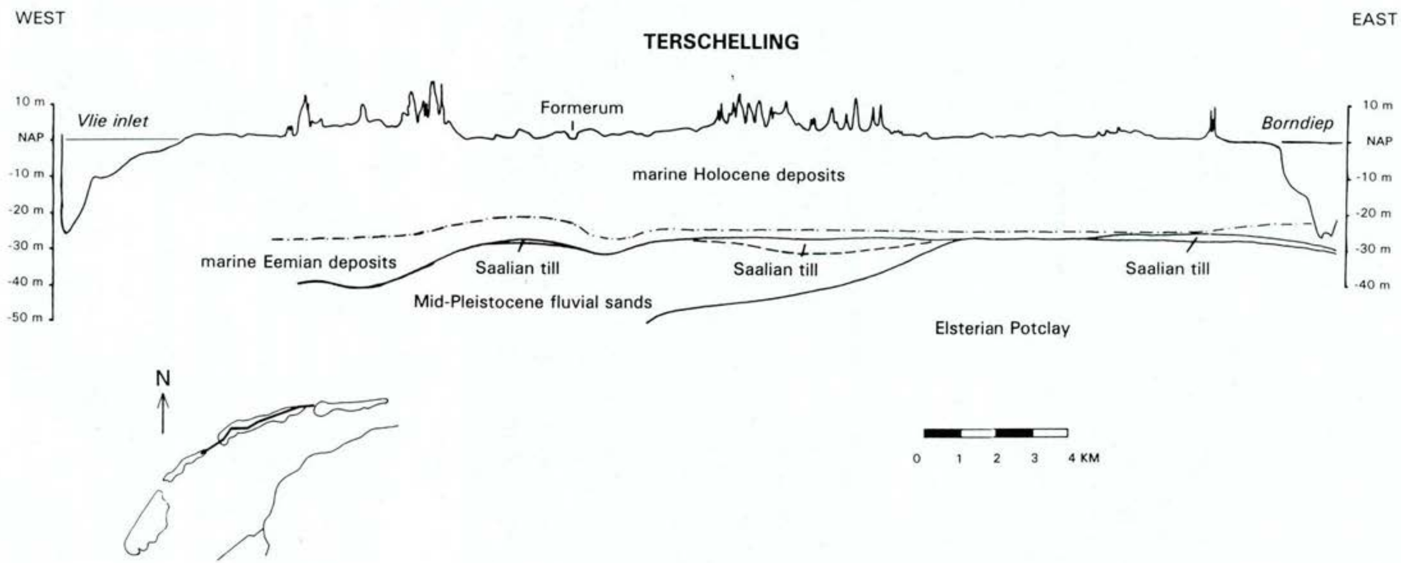

Figure 5.9 West-east cross section through the island of Terschelling, after Van Staalduinen (1977).

inlet can be derived from the relationships between tidal volume and cross-sectional profile of the inlet. Thus a reconstruction of the evolution of the inlet dimensions can be made.

The Middelzee basin

The maximum extension of the deposits associated with the Middelzee are based on the distribution of Duinkerke-III sediments on geological maps (Ter Wee, 1976; De Groot et al., 1987). The distribution in the area north of Weidum (Fig. 5.1) was inferred from soil-composition maps. The maximum distribution of these sediments, however, is related to storm floods and therefore will not be incorporated in the calculations, which are based on average tidal activity.

The landward boundaries of the Middelzee were formed by dikes from ca. 1000 AD onwards. These boundaries have been determined per century from 1000 AD to 1900 AD for reconstructional purposes (Fig. 5.10). The dating of the dike construction is mainly based on the study of Rienks and Walther (1954).

The tidal watersheds in the Wadden Sea are also considered to be basin boundaries, although the watershed south of Terschelling was initially dissected by channels that ran to the Zuiderzee. The position of this watershed moved towards the east with time. The position before 1300 AD is assumed to have been situated between Midsland and Dongjum (Figs. 5.1, 5.10), roughly along the western contour of MSL-20 m shown in Fig. 5.2. In 1300 AD, when the Middelzee was reduced to a funnel-shaped embayment, the divide was situated between Midsland and Minnertsga (Fig. 5.10), where it remained until 1600 AD (Isbary, 1936). By 1800 it had shifted to a position between Hoorn and Zwarte Haan. In 1900 the divide was at its present position between Oosterend and Zwarte Haan (Fig. 5.10). The tidal watershed south of Ameland did not shift eastward until 1831. Therefore, its position is assumed to have been fixed on the position of the dam between Holwerd and Ameland that was constructed in 1870 (and that was destroyed within a couple of years). The earlier stated migration of this divide from 1831 was neglected in the reconstruction for 1900.

The seaward boundary of the basin is assumed to be at the present southern shores of Terschelling and Ameland, and the shortest connection between the two islands through the tidal inlet.

The surface areas of the reconstructions shown in Fig. 5.10 were determined and the results are given in Table 5.1. A graph of the areal reduction of the Middelzee tidal basin with time is shown in Fig. 5.11. The surface area of the Middelzee decreased almost linearly from 737.5 km^2 in

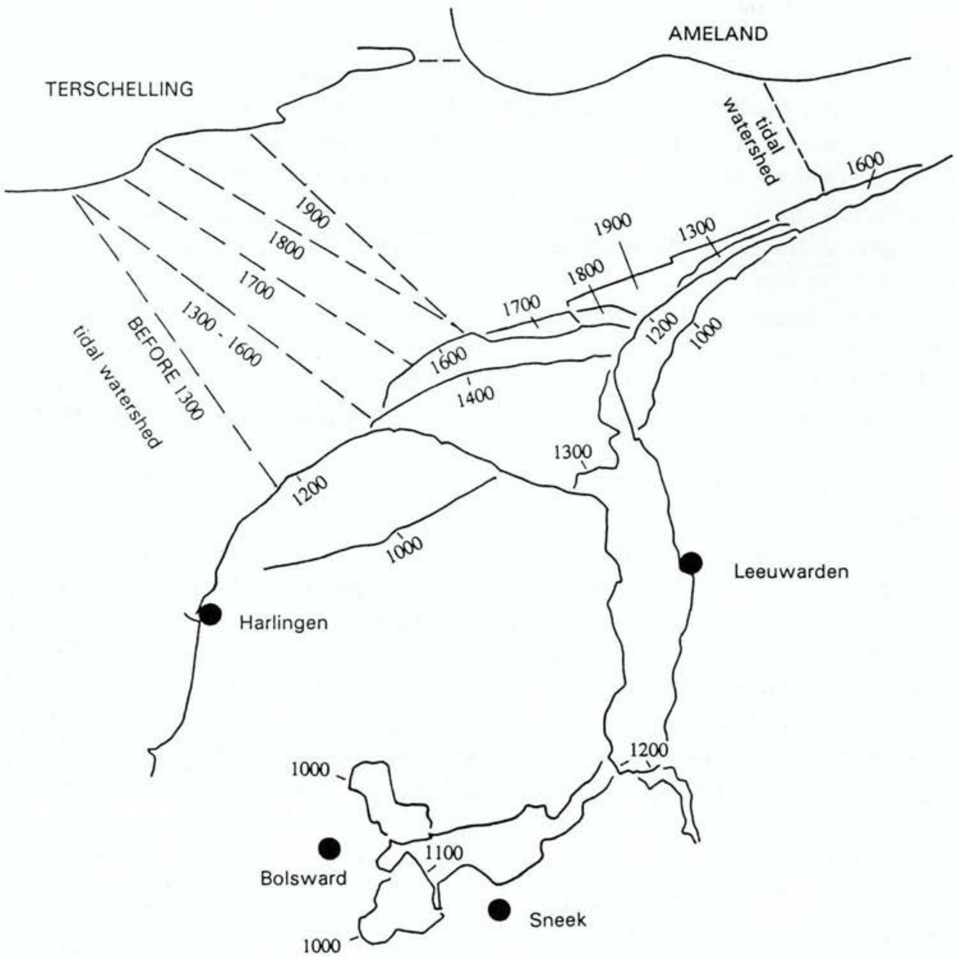

Figure 5.10 Reconstruction of the extension of the Middelzee and the position of the tidal watersheds behind the islands Terschelling and Ameland per century since 1000 AD. Dikes raised within 20 years after the reconstructed dates have been considered as present at the reconstructed dates, since the salt marsh they were built on must already have been accreted to a supratidal level at that particular time.

1000 AD to 275.5 km² in 1900 AD, a reduction of 63 per cent.

Table 5.1 Surface area in km² of the Middelzee tidal basin for the reconstructed situations since 1000 AD. The tidal prisms, cross-sectional areas and inlet depths have been derived using the relationships stated in the text.

reconstructed year AD	surface area (10^6 m²)	tidal prism (10^6 m³)	x-sectional area below MSL (10^3 m²)	max. inlet depth (m)
maximum	923.4			
1000	737.5	992	64	50
1100	716.3	964	62	49
1200	625.0	841	55	44
1300	495.1	667	44	38
1400	444.9	600	40	35
1600	421.5	569	38	34
1700	367.2	496	34	31
1800	316.7	428	30	29
1900	275.5	373	26	27
equation		(1)	(3)	(4)

Inlet dimensions

The tidal prism can be estimated based on the above stated reconstructions of the basin surface area, since tidal prisms are determined by the size and shape of the basin and the tidal range (Van Veen, 1950; O'Brien, 1969). If the tidal prism is known, the cross-sectional area of the tidal inlet can be calculated, using the empirical relationship between these two parameters. The maximum inlet depth can also be derived from the tidal prism.

In Fig. 5.12 the tidal prisms of recent tidal basins in the Netherlands Wadden Sea are plotted against the basin surface area at mean high-water level (data from De Glopper, 1967, Anonymous, 1974, and Endema, 1979). A linear regression function of the form:

$$P = 3.66 + (1.34 * SA) \tag{1}$$

(where P is tidal prism in 10^6 m³, SA is surface area at mean high water in 10^6 m²), can be calculated. This relationship is valid for surface areas from $50*10^6$ m² to $820*10^6$ m². The tidal prisms that were calculated for the reconstructions of the Middelzee range from $373*10^6$ m³ to $992*10^6$ m³ (Table 5.1).

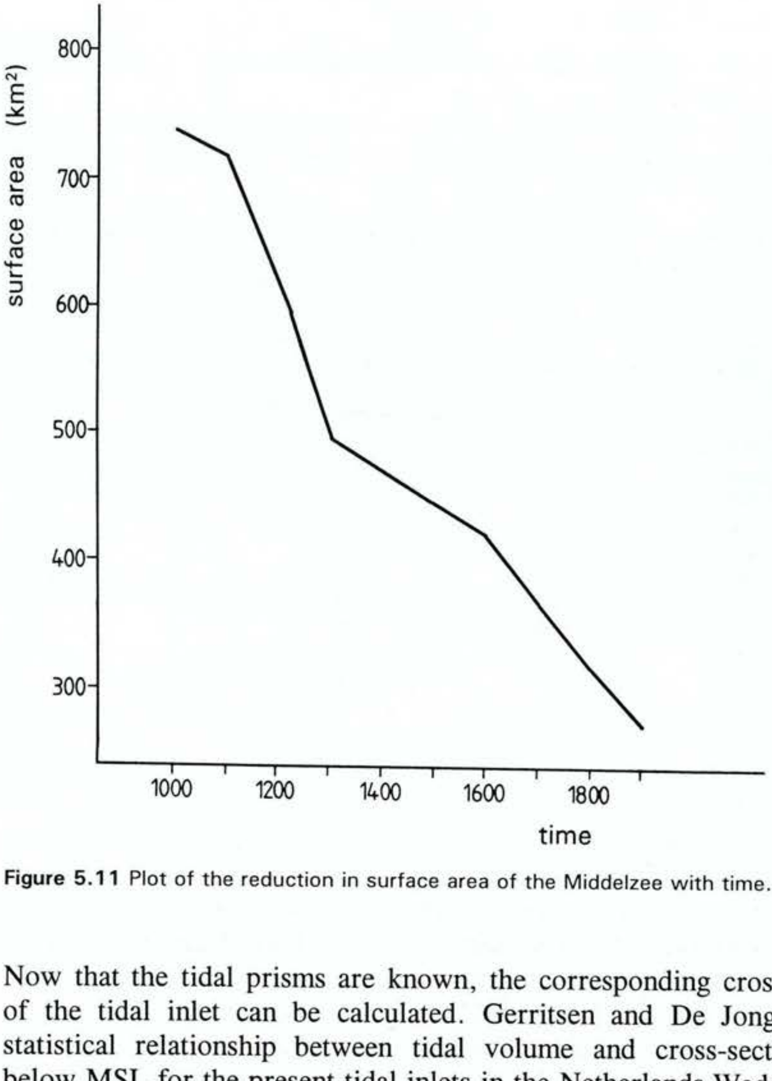

Figure 5.11 Plot of the reduction in surface area of the Middelzee with time.

Now that the tidal prisms are known, the corresponding cross-sectional areas of the tidal inlet can be calculated. Gerritsen and De Jong (1985) gave a statistical relationship between tidal volume and cross-sectional inlet area below MSL for the present tidal inlets in the Netherlands Wadden Sea:

$$TV = (33198 * A_{c,msl,inlet}) - 127.6 * 10^6 \text{ m}^3 \qquad (2)$$

(where TV is tidal volume in 10^6 m^3 and $A_{c,msl,inlet}$ is inlet cross-sectional area below mean sea level in m^2). From a hydraulic point of view the closest correlation is to be expected between the cross-sectional inlet area and the largest of the ebb or flood volumes, the so-called dominant volume. However, in this case the tidal prism, the mean value of the ebb and flood volumes, is used since the dominant volume cannot be estimated from the basin surface area.

Since the tidal prism is the half of the tidal volume (Gerritsen, 1990, 1992), equation (2) can be rewritten in the form:

$$A_{c,msl,inlet} = 60.2 * 10^{-6} * P + 3844 \tag{3}$$

The inlet cross-sectional areas calculated using this formula range from $26*10^3$ m^2 to $64*10^3$ m^2 (Table 5.1).

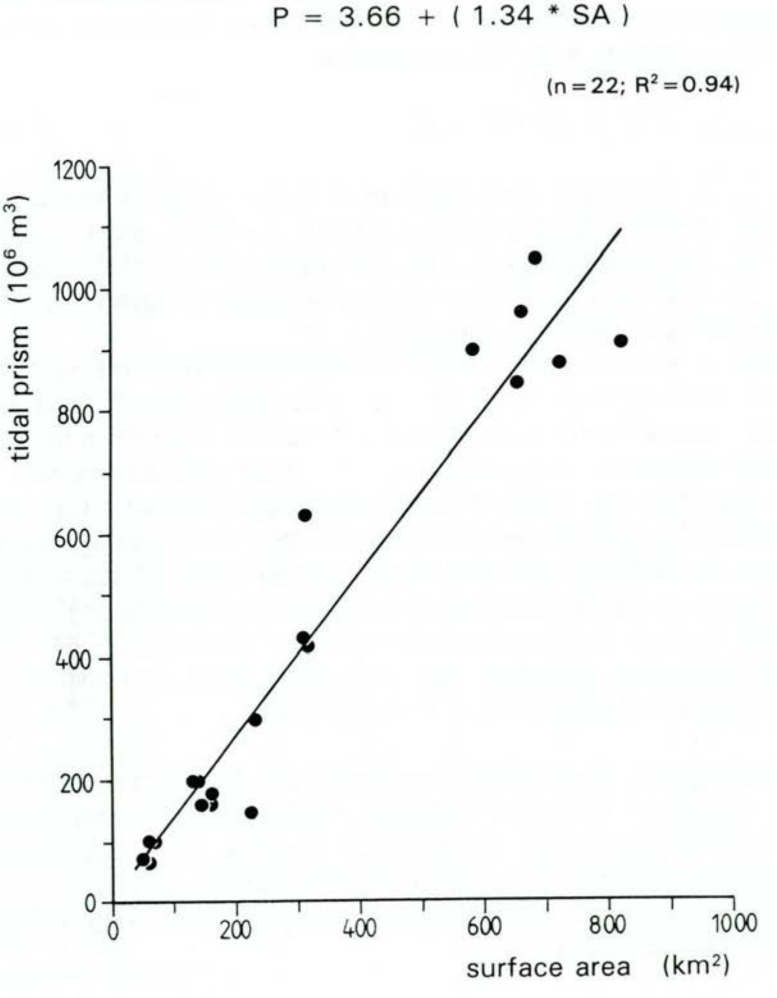

Figure 5.12 Plot of tidal prism versus basin surface area for the tidal basins in the present-day Dutch Wadden Sea. (Based on data from De Glopper, 1967; Anonymous, 1974; Endema, 1979).

However, cross-sectional areas are difficult to assess from geological information. Tidal inlets very often migrate laterally along the coast, leaving a sequence of point-bar deposits. This prevents a reliable determination of the inlet width. The thickness of channel-fill sequences, however, gives the maximum inlet depth. The relationship between tidal prism and maximum inlet depth will not be as strong as that between cross-sectional area and tidal prism, since inlet width and shape are not incorporated (De Glopper, 1967). Sha (1990, p. 38, his fig. 16) shows a graph of a linear relationship between tidal prisms of present tidal basins in the Wadden Sea and maximum inlet depths. This relationship was quantified using data from Anonymous (1974) and Endema (1979), see Fig. 5.13. This resulted in:

$$h_{NAP,max,inlet} = 37 * 10^{-9} * P + 13 \tag{4}$$

(where $h_{NAP,max,inlet}$ is maximum inlet depth in m below NAP (NAP=Dutch Ordnance Datum, which is about present-day mean sea level) and P is tidal prism in 10^6 m^3; the relationship is valid for prisms from $70*10^6$ m^3 to $1050*10^6$ m^3). The inlet depths calculated for the Middelzee decrease from 50 m in 1000 AD to 27 m in 1900 AD (Table 5.1).

From borings it is known that Holocene erosion has occurred up to a maximum depth of 31 m below NAP between Oosterend in Terschelling and the present west coast of Ameland, the location of the inlet since the formation of the Middelzee (Fig. 5.9). The calculated inlet depths indicate that before 1700 AD the inlet was too large to fit in one single channel. The tidal discharge must have been distributed over two channels. This is in agreement with the situation as shown by historical maps. Around 1700 AD the channel Coggediep got silted up and the Borndiep became the only main channel in the Amelander Gat. It also can be concluded that in 1000 AD, when the Middelzee had its widest extension, the inlet must have consisted of 2 channels, with maximum depths of about 30 m below MSL.

The historical nautical charts of the Amelander Gat do not give sufficient information to verify the calculated maximum inlet depths. In most cases depth values were only given for the Borndiep. Besides, it is questionable whether the maximum depths are among the few depths given. From a nautical point of view maximum depths are less important since navigators are interested in the minimum depths.

$$h_{NAP,max,inlet} = 37 * 10^{-9} * P + 13$$

$(n = 13;\ R^2 = 0.97)$

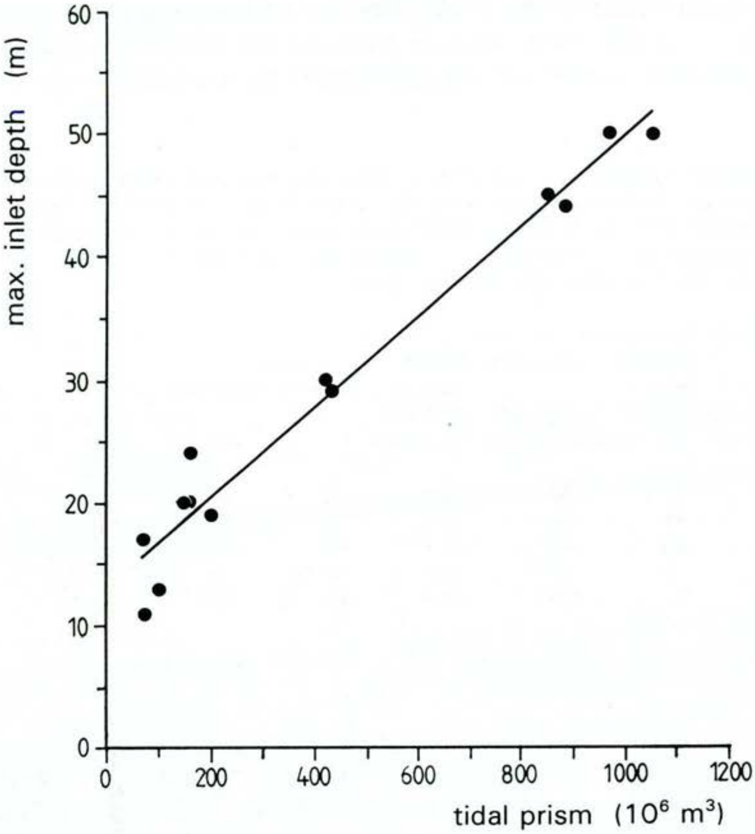

Figure 5.13 Plot of maximum inlet depth versus tidal prism for the tidal basins in the present-day Dutch Wadden Sea. (Based on data from Anonymous, 1974; Endema, 1979).

Channel dimensions

Relationships between tidal discharge and cross-sectional area were derived for channels within the Wadden-Sea tidal basins by Eysink (1979) and Gerritsen and De Jong (1985), see Table 5.2. However, since channel depth is the only meaningful variable in the study of fossil channel deposits (channel width cannot be established because of lateral channel migration), it is geologically more relevant to use a relationship between tidal discharge or prism and maximum channel depth. Figure 5.14 shows 69 combinations of maximum channel depth and observed discharge for the present Wadden Sea tidal basins (data from De Glopper (1967), Endema (1979) and Gerritsen and De Jong (1985)). The variation in channel depth given a certain discharge is large (see the scatter band in Fig. 5.14). This is a consequence of variations in channel depth to width ratios due to variation in sediment composition, branching of channels, scouring of channels caused by constructions etc.

Table 5.2 Calculated discharges, cross-sectional areas and maximum channel depths for 5 cross-sections through the Middelzee (see Fig. 5.16) for the situation in 1000 AD. These values have been calculated with the formulas stated in the text. The cross-sectional areas were calculated with the equation for channels in the Wadden Sea tidal basins: $A_c = 71.6*10^{-6}*P + 134.6$ (Gerritsen and De Jong, 1985)

cross section	surface area (km^2)	discharge (10^6 m^3)	x-sect. area (10^3 m^2)	max. channel depth (m)		
1	37	53	3.9	10	9	9
2	45	64	4.7	11	10	9
3	66	92	6.7	13	12	11
4	93	129	9.4	14	14	13
5	161	220	15.9	18	18	16
equation		(1)		(5)	(6)	(7)

Van Bendegom (1949) described channel width as a function of depth for an idealised Wadden-Sea channel with an approximately rectangular profile: $w = 5 * h^2$ (w is channel width in m, h is depth in m). From this it can be estimated that the cross-sectional area A_c of a channel is related to the cubic power of the channel depth: $A_c = h * w = 5 * h^3$. Since the tidal prism has a linear relationship with the cross-sectional area (see above), the prism will also be related to the cubic power of the depth. When the cube root of the prism (in 10^6 m^3) is related to the maximum channel depth, a linear relationship of the form:

$$h_{NAP,max,channel} = 3.49 * P^{1/3} - 3.09 \qquad (5)$$

can be calculated (Fig. 5.15). Direct correlation of both data sets yields:

$$h_{NAP,max,channel} = 1.48 * P^{0.46} \qquad (6)$$

(with P in 10^6 m^3), see Fig. 5.14. Geyl (1976) correlated maximum channel depth in a cross-section and the drained surface area behind the cross-section for the tidal basins of the Wadden Sea. This yields:

$$h_{NAP,max} = 1.98 * SA^{0.41}, \tag{7}$$

with SA in 10^6 m^2. Approximations of the maximum channel depth can be calculated with these equations if the discharge, or the surface area of a part of a basin, is known.

The above derived equations were applied to the Middelzee. The maximum channel depth was calculated from the surface area behind a number of cross-sections through the Middelzee (Fig. 5.16), using the equations (1), (5), and (6). The depths were calculated for the reconstruction of the basin in 1000 AD, when the basin had its greatest extension, and thus the deepest channels. Direct calculation of the maximum channel depth from the surface area with equation (7) gives almost identical results. The maximum channel depth below MSL ranges from 9 to 10 m north of Sneek to 16 to 18 m in the northern part of Het Bildt (Fig. 5.16; Table 5.2).

The base of the channel deposits in the cross-sections 2 and 3 (Fig. 5.16) was found in boreholes at 12.5 m and 10.7 m below NAP respectively. Channel depths of 9 m to 11 m below NAP (cross-section 2) and 11 m to 13 m below NAP (cross-section 3) were calculated (Table 5.2). The channel in cross-section 2 is confined in a narrow passage. This might have caused the channel to scour deeper than under normal conditions. The calculated depth for cross-section 1 (Fig. 5.16) seems to be in agreement with geological information from the southern part of the Middelzee given by Ter Wee (1976).

$$h_{NAP,max,channel} = 1.48 * P^{0.46}$$

$(n=69;\ R^2=0.77)$

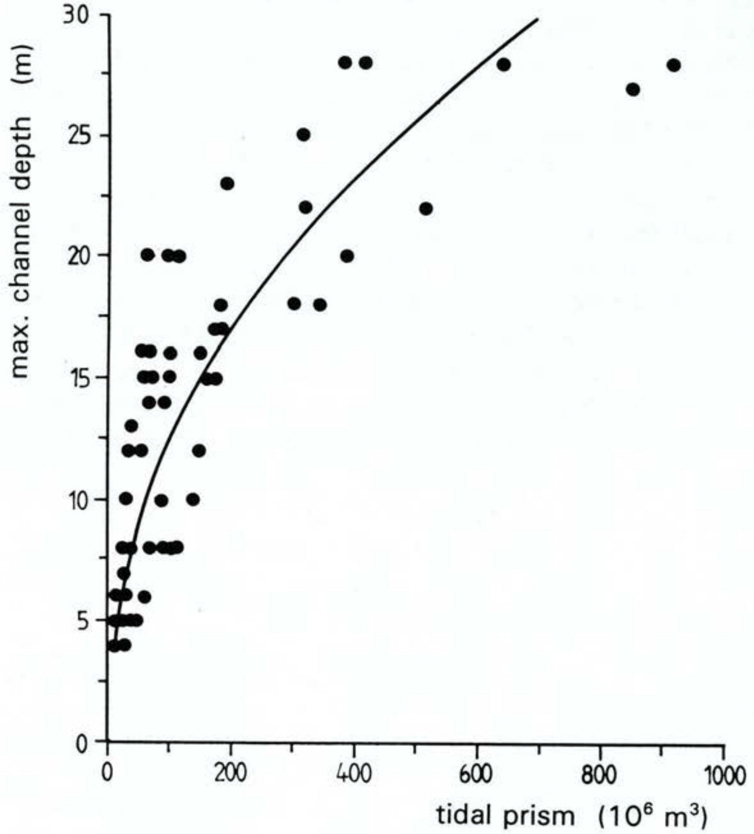

Figure 5.14 Plot of maximum channel depth versus tidal prism for the present-day Dutch Wadden Sea. (Based on data from De Glopper, 1967; Endema, 1979; Gerritsen and De Jong, 1985).

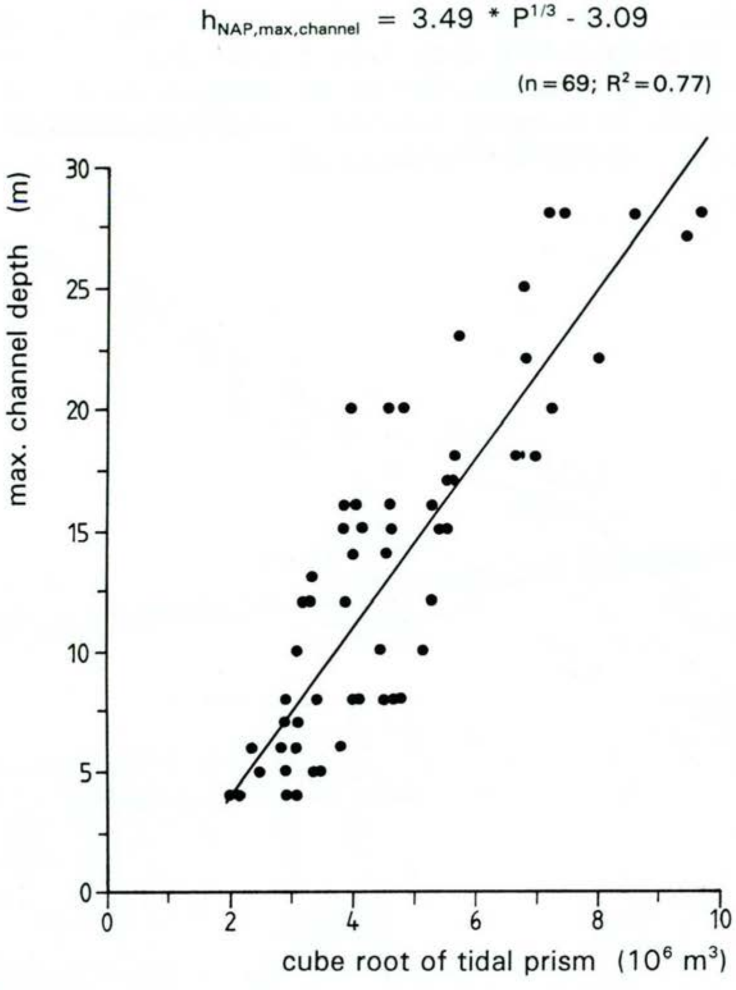

Figure 5.15 Plot of maximum channel depth versus the cube root of the tidal prism for the present-day Dutch Wadden Sea (based on the same data set as in Fig. 5.14).

According to the Base-Holocene map (Fig. 5.2) the calculated maximum channel depth of 14 m (Table 5.2) for cross-section 4 (Fig. 5.16) can only have been reached in the most western part of the Middelzee. The calculated maximum depth of erosion caused by a channel connected to the Middelzee for cross-section 5 (Fig. 5.16) is about 18 m. The maximum depth of channel erosion will have been less if the suggestion by Isbary (1936) and Rienks and Walther (1954) that two channels existed at this location during the greatest extent of the Middelzee (see above), is true. This suggests that the deepest erosion of over 20 m below NAP at the location of this cross-section (Fig. 5.2) was not caused by Middelzee channels but during an earlier marine transgression in the Boorne valley and that at least two different generations of channel deposits are found here on top of each other.

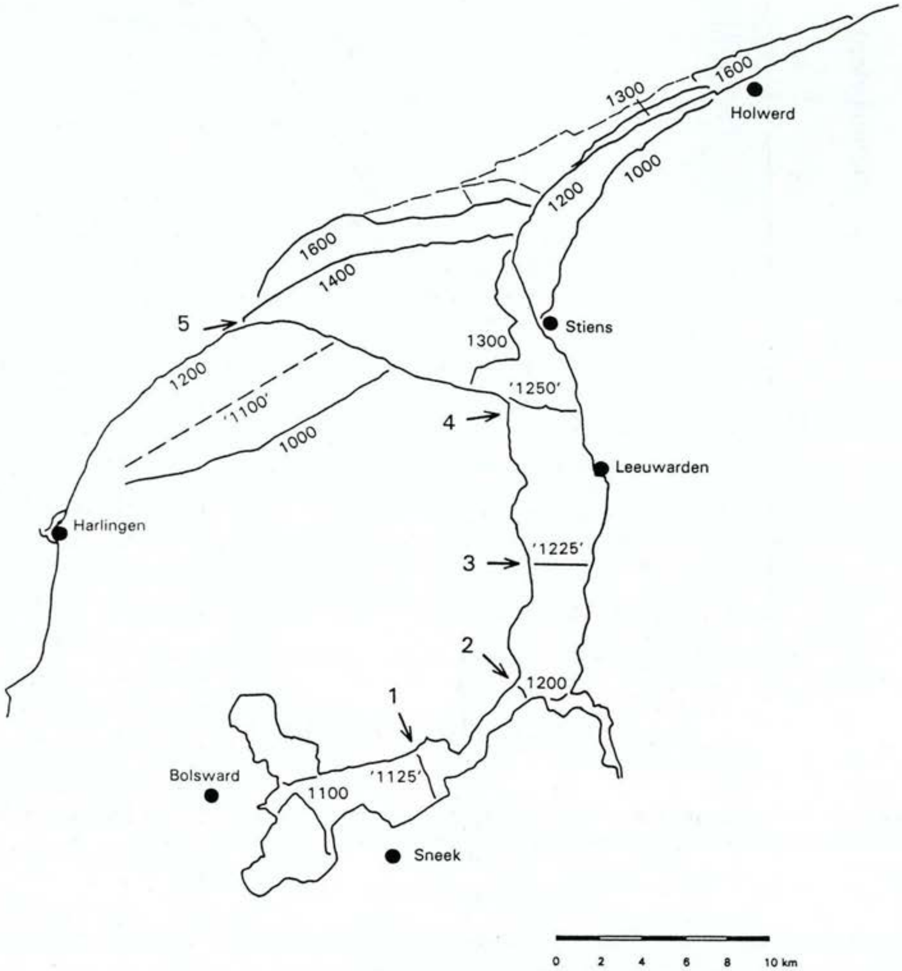

Figure 5.16 Position of a number of cross-sections through the Middelzee (1 to 5) for which maximum channel depths were calculated (see Table 5.2). The dates indicate the steps of sediment budget calculation. Dates in quotation marks are hypothesised.

Budget calculations

A sediment budget for the Middelzee was calculated using the decrease in surface area with time, as illustrated by the history of dike construction, and the thickness of the deposited sediments. For the southern part of the Middelzee the distribution and thickness of the deposits is known from the geological map. The deposits were subdivided into channel deposits and mudflat- and marsh deposits, based on sediment thickness and composition. The average thicknesses were estimated for both categories. The deposited sediment volumes were calculated for the intervals shown in Fig. 5.16, based on the ages of the dikes and a number of inferred stages in between.

The southern part of the Middelzee had been completely silted and reclaimed by ca. 1225 AD (Fig. 5.16). A volume of $224*10^6$ m^3 to $279*10^6$ m^3 of sediment had been deposited (Table 5.3).

The thickness of Middelzee deposits north of cross-section 3 (Fig. 5.16) that were formed in the period 1225 - 1600 AD were based on a few borings. This means that calculations for this period are only approximations. An amount of $292*10^6$ m^3 to $404*10^6$ m^3 of sediment accumulated in the Middelzee between 1225 AD and 1600 AD (Table 5.3).

In the period 1000 - 1600 AD the salt marshes north of Oostergo and Westergo accreted from intertidal to supratidal level and were secured by dikes (Figs. 5.3, 5.16). Figure 5.16 illustrates the step-wise history of this process. Based on Bakker (1954) and Bakker and Wensink (1955) the average thickness of these deposits is estimated to be 0.5 to 0.6 m. A sediment volume of $77*10^6$ m^3 to $108*10^6$ m^3 was deposited in the salt marshes before 1600 AD (Table 5.3).

The total sediment volume deposited in and along the Middelzee between 1000 AD and 1600 AD was $507*10^6$ m^3 to $668*10^6$ m^3. The average annual sedimentation was $0.9*10^6$ m^3 to $1.1*10^6$ m^3. This amount is about the same as the present-day annual import of sand into the Borndiep tidal basin of $0.9*10^6$ m^3, calculated by Stive et al. (1991). The sediment composition is estimated from borings at 75 per cent fine to very fine sand and 25 per cent clay for the channels and 50 per cent sand and 50 per cent clay for the other deposits, on the basis of information by De Groot et al. (1987). As the volume of the channel deposits is $267*10^6$ m^3 to $399*10^6$ m^3, this means that about 65 per cent of the sediment deposited in the Middelzee was sand. Figure 5.17 illustrates the total deposition in the considered period.

Table 5.3 Calculated ranges of sediment volumes deposited in the Middelzee basin and in the salt marshes along and north of it, up until 1600 AD.

interval	Middelzee (10^6 m^3)	salt marshes (10^6 m^3)	total (10^6 m^3)
> 1000	44 - 56	39 - 64	83 - 120
1000 - 1100	26 - 36	13 - 15	122 - 177
1100 -'1125'	25 - 42		147 - 213
'1125'- 1200	74 - 76	20 - 24	241 - 313
1200 -'1225'	55 - 69		296 - 382
'1225'-'1250'	91 - 115		387 - 497
'1250'- 1300	32 - 51	2	421 - 550
1300 - 1400	99 - 158		520 - 708
1400 - 1600	70 - 80	3	590 - 788

The budget calculated above relates to the Middelzee. The silting of this part of the basin also caused sedimentation in the adjacent Wadden Sea. The reduction of the tidal flow between the inlet and the Middelzee due to the silting of the latter will have caused sedimentation in the channels in the Wadden Sea. To make the sediment budget for the Borndiep tidal basin more complete, these amounts must be calculated as well. Eysink (1979, 1991) derived an equation relating the total channel volume below mean sea level to the tidal prism through the inlet:

$$I_{msl} = 65 * 10^{-6} * P^{3/2} \tag{8}$$

(where I_{msl} is channel volume below MSL in 10^3 m^3 and P is tidal prism in m^3). The sedimentation in the channels was calculated with this equation from the reduction of the tidal prism with time (Table 5.1). Between 1000 AD and 1900 AD, $1562*10^6$ m^3 of sediment were deposited in the channels of both the Middelzee tidal basin and the adjacent Wadden Sea (Table 5.4; Fig. 5.17). This is an annual sedimentation of $1.7*10^6$ m^3. For the period 1000 - 1600 AD the annual sedimentation in the channels in both Wadden Sea and Middelzee is $1.9*10^6$ m^3. The sedimentation in the channels in the Middelzee proper in this period was $267*10^6$ m^3 to $399*10^6$ m^3, which is only 17 to 26 per cent of the total sedimentation in the channels.

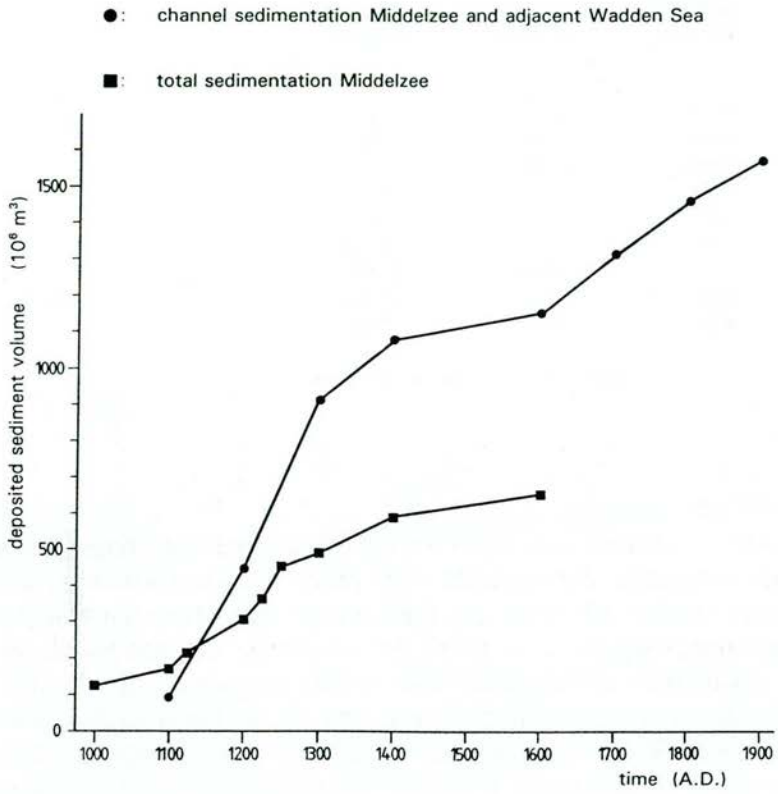

Figure 5.17 Plot of sediment volumes deposited in the Middelzee and the adjacent Wadden Sea since 1000 AD.

The calculated sedimentation rate of $1.9*10^6$ m^3 per year falls well within the range of yearly sand import into the present individual tidal basins in the Dutch Wadden Sea. The Vlie tidal basin, with a surface area of $668*10^6$ m^2 and a tidal prism of $1078*10^6$ m^3 (Kool et al., 1984) comparable with the Middelzee at its largest extension, has an annual sand import of $2.6*10^6$ m^3 (Stive et al., 1991). This means that the rapid silting up of the Middelzee can be explained without the exceptionally high rates of sediment import that were suggested in history papers (Halbertsma, 1955; Schoorl, 1980).

Table 5.4 Time history of the decline of the total channel volume of the Borndiep tidal basin and the sedimentation in the channels that can be concluded from this.

reconstruction AD	channel volume (10^6 m^3)	sedimentation (10^6 m^3)	total sedimentation (10^6 m^3)
1000	2030		
1100	1944	86	86
1200	1586	358	444
1300	1120	466	910
1400	955	165	1075
1600	881	74	1149
1700	717	164	1313
1800	576	141	1454
1900	468	108	1562

Discussion

The relationship between the basin surface area and the tidal prism (equation (1)) varies greatly. Although the tidal prism is approximated by the basin surface area multiplied with the tidal range, the three-dimensional geometry of the basin which determines, for example, the extent of the intertidal area, also plays an important role in the magnitude of the tidal prism. The intertidal area ranges from 20 per cent of the basin surface area for the large basins to 80 per cent for the small basins (De Glopper, 1967). The relationship given in this paper holds for the present-day tidal basins in the Netherlands Wadden Sea, although the mean tidal range increases from 1.4 m in Texel inlet in the west to 2.2 m in the mouth of the Eems estuary in the east.

The coast of Friesland had a more or less linear course after the silting up of the Middelzee and its final reclamation in 1600 AD The geometry of the Borndiep tidal basin had changed from elongate to square. The morphodynamics of the basin changed considerably with the new geometry. When the basin was dominantly north-south orientated the main channels were running parallel to this direction and the position of the inlet did not vary much. After 1600 AD the tidal flow penetrated more to the east, between the island of Ameland and the Frisian coast. This resulted in migration of the tidal watershed south of Ameland to the east. The inlet channel rotated to a more NW-SE orientation and eroded the western end of Ameland.

So far it is not clear why the tidal prism of $992*10^6$ m^3 in the Amelander Gat in 1000 AD was distributed over 2 channels with a maximum depth of 31 m, while in the present-day situation the tidal prisms in the Texel and Vlie inlets, amounting to $965*10^6$ m^3 and $848*10^6$ m^3 respectively, are contained in single channels, with maximum depths of 50 m and 45 m respectively. For the Texel inlet the extensive protection works on the southern shore inhibit lateral migration of Marsdiep channel and force it to scour deeply into the subsurface (Sha, 1990). This offers an explanation for the Texel inlet. For the Vlie inlet there is no such explanation. However, it is clear that the basin length relative to basin width is small for the present-day tidal basins in the Wadden Sea (with exception of the Marsdiep basin) when compared to the Middelzee. The estuaries in the southwestern Netherlands, with large basin length to width ratios, all have more than one tidal channel in the inlet. There seems to be a complicated interaction between the basin topography, including subsoil resistance, and the hydrodynamical forces that accounts for this difference.

Conclusion

The Middelzee, the latest stage of marine activity in the Pleistocene Boorne valley, was formed during the medieval period. The subsequent silting up of the basin is illustrated by the age of the reclamations. At least $1562*10^6$ m^3 sediment was deposited in the basin in the period from 1000 AD to 1900 AD This caused a decrease in the tidal prism from $992*10^6$ m^3 to $373*10^6$ m^3, a reduction of 62 per cent. The reduction of the tidal prism caused a decrease in the dimensions of the tidal channels in the inlet and the basin, as can be illustrated with a series of nautical charts. The calculated annual sediment import in the basin falls well within the range of the present-day values for the Netherlands Wadden Sea.

The empirical relationships established for the present tidal basins of the Wadden Sea proved to be a valuable tool in the analysis of the evolution of fossil tidal basins. Besides geological information, such as thickness of deposits and age, other aspects of channels can be assessed to elaborate and refine basin reconstructions. This is an important contribution to the understanding of tidal basin development and the behaviour of coastal systems. This paper gives examples using the surface area of (part of) the basin to estimate channel depths. Thus, two different generations of Holocene channel deposits could be distinguished in the sediment fill of the mouth of the Boorne valley. Conversely, if the depth of a channel is known from geological data, the dimension of the connected basin can be estimated. Both types of information complement each other.

Acknowledgements

This research was funded by the Netherlands Organisation for Scientific Research (NWO), grant CO_2-77.125, and the Ministry of Home Affairs, file number DUO 789612.

I would like to thank Dirk Beets, Janrik van den Berg, Poppe de Boer, Doeke Eisma, Kiek Jelgersma, Henk Schoorl and Marcel Stive for the valuable discussions and careful examination of earlier drafts of this paper. Furthermore, I would like to thank the Oosterwolde Department of the Geological Survey for making borings in the former Middelzee, Arent Vos for retrieving the map by Guitet from the library of Leiden University and James Baker for correcting the English. Finally, thanks to Burg Flemming for his patience.

6. Tidal asymmetry and long-term evolution of Holocene tidal-basins in the Netherlands: simulation of palaeo-tides in the Schelde estuary.

Abstract

This paper investigates the possibility to reconstruct the deformation of the tide in ancient tidal basins. The evolution of tidal basins strongly depends on the interaction of basin morphology and tidal wave deformation. Therefore, when studying tidal basin evolution, information on the behaviour of the tidal wave is an important factor. However, the tidal distortion inside tidal basins is complex and cannot be deduced directly from the basin morphology, especially in the case of large basins. Therefore, in the present analysis, the reliability of reconstruction of tide deformation in ancient basins with limited topographical information by using a one-dimensional numerical flow model, is tested. As a test case two former situations of the Schelde estuary were chosen, 1800 AD and 1650 AD For both situations only limited hydrographical information is available, especially concerning 1650. It is shown that for both situations known information of amplitude and propagation rate of the tidal wave is reproduced reasonably well by the model.

These simulations indicate that the counteracting effect of the tidal flats on sediment influx at the entrance of the basin has increased since 1650, despite a reduction in the size of the tidal-flat area in the basin. As a result of a dramatic increase in the celerity of the tidal wave in the basin, the remaining intertidal area in the basin is flooded or drained within a relatively short interval. Therefore, the retarding effect of intertidal areas on the ebb tide became more pronounced notwithstanding the fact that the total shoal area in the basin decreased.

Introduction

The balance between sediment accommodation space, created by a rise in sea level, and sediment supply determines the long-term evolution of estuaries and tidal basins such as those along the Dutch coast (Fig. 6.1). In this paper the terms estuary and tidal basin are used as equivalents, since the fluvial discharge into the systems discussed here is small to very small. The sea-level rise that started at the end of the last ice age created a series of tidal basins in the Early-Holocene landscape in the Netherlands (e.g., Pons et al., 1963; Van Straaten, 1965; Zagwijn, 1986; Beets et al., 1992). These basins shifted

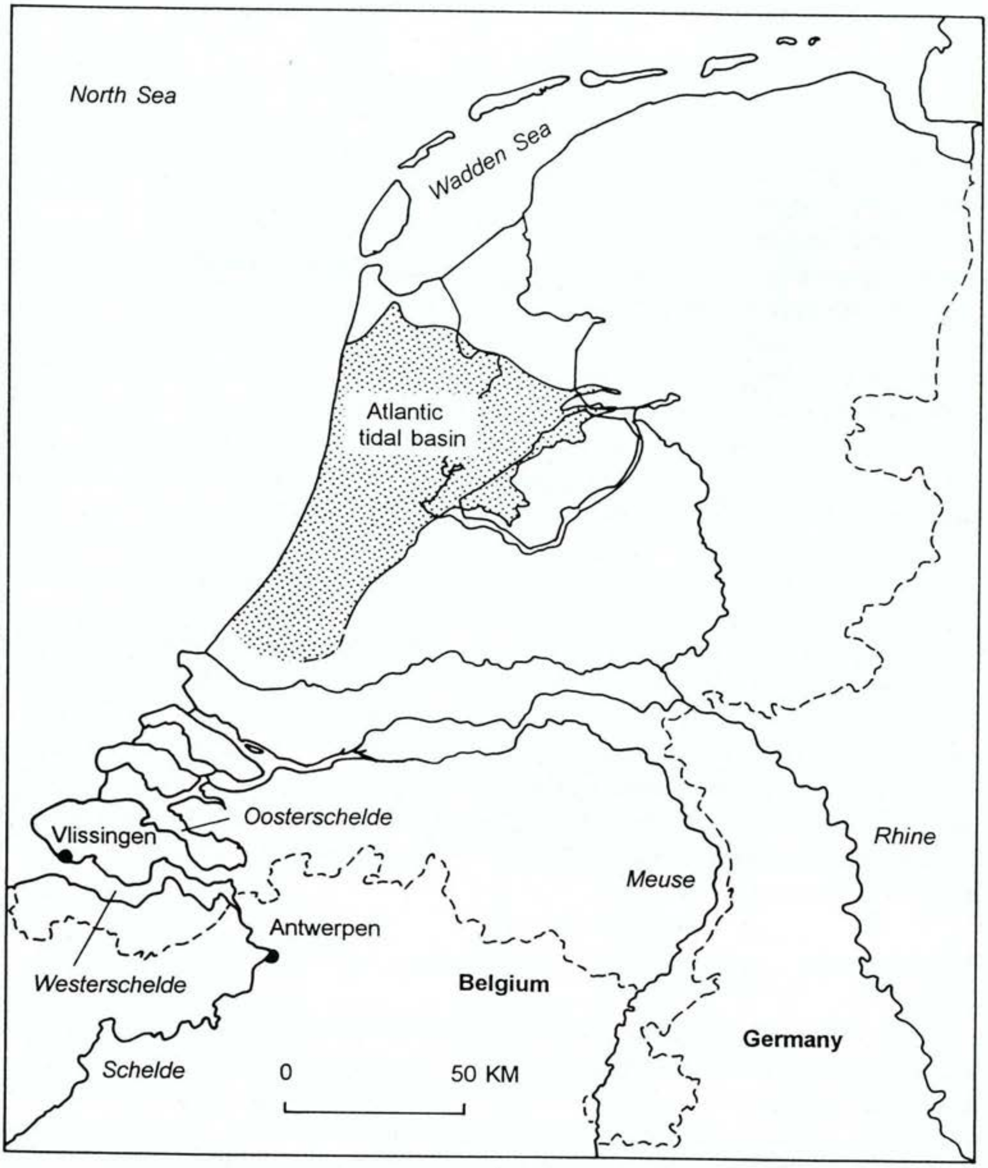

Figure 6.1 Position of the recent tidal basins in the Netherlands.

landward with the rising sea level. They trapped large volumes of marine sediment, part of which was eroded from the adjacent coast. This resulted in a rapid retreat of the coastline. The rivers Rhine and Meuse discharged directly into the North Sea and not into the flanking tidal basins (Beets et al., 1992; Chap. 4). Consequently, their sediments only reached the tidal basins via the North Sea and the coastal zone. When the rate of sea-level rise decelerated around 5500 BP the basins filled up with sand and mud, resulting in closure of the tidal inlets and, subsequently, stabilisation and progradation of the coastline (Beets et al., 1992). The new tidal basins which developed after 2000 BP initiated renewed erosion of the adjacent coastline.

Reconstruction of the morphology of the Atlantic tidal basins in the western part of the Netherlands (Fig. 6.1), which were formed during rapid sea-level rise, mainly on the basis of facies analysis of sediments suggests that these basins differed from the present tidal basins. Sandy tidal flats existed only along relatively straight tidal channels, while clay settled further away from the channels in a lagoonal setting (Westerhoff et al., 1987; Vos and De Wolf, 1994; Chap. 4). This situation is different from the present-day basins of the Dutch Wadden Sea and the SW Netherlands (Fig. 6.1), where intertidal shoals fill most of the area between the channels.

The evolution of tidal-basin morphology depends on supply, transport and deposition of sediment. In the basins sediment is largely transported by tidal flow. The interaction between basin morphology and tide deforms the tidal wave resulting in a net sediment transport. The direction and magnitude of the residual sediment transport determines the evolution of the basin and affects the sand balance of the adjacent coast. This net sediment transport is the very small residual sum of the quantities of sediment imported by the flood tide and exported by the ebb tide during a tidal cycle. Since net sediment transport involves such a small quantity, it is not possible to determine it by subtracting flood and ebb sediment transport fluxes obtained from detailed measurements at the inlet entrance. Of course, the same applies to a numerical flow model of a basin equipped with a sediment-transport module. However, simulation of the tidal flow during several stages in the evolution of a former basin with a flow model may provide an explanation for the apparent changes in sediment influx revealed in cores. This study is a first attempt to simulate the tidal motion in reconstructed former tidal basins in the Netherlands. The interaction of basin morphology and tide, and its evolution with time are the main subjects. This paper gives an overview of the physical concepts of tidal propagation and distortion and the consequences for sediment transport. In addition, a simple simulation procedure developed for the Schelde estuary in its present-day situation (Fig. 6.1) is described. This procedure uses the numerical water-flow model DUFLOW (Spaans et al., 1989). Since not all input parameters could be reconstructed adequately from geological information, the procedure had to determine if (1) A schematic representation of the basin geometry can be based on parameters derived from geological information, (2) Calculation of tidal ranges in the basin is possible within the order of decimetres and (3) The sensitivity of the model to inaccuracies in input data is limited. The procedure was developed on the basis of a detailed flow model for the present-day Schelde estuary (Dekker and Bollebakker, 1981). The model input was simplified, and subsequently the performance of the procedure was compared with field information. Then, the procedure was applied to a reconstruction of the Schelde estuary in 1800 AD, known from sounding charts, and the 1650 AD morphology of the estuary, which is only known approximately. The Schelde developed from a highly branched estuary with large tidal-flat and marsh areas in 1650 AD into the funnel-shaped estuary of today. Consequently, the tidal characteristics changed greatly. These changes are discussed at the end of this paper.

Tidal asymmetry and sediment transport

The interaction between oscillating tide and basin morphology causes distortion of the tidal wave during propagation (Boon and Byrne, 1981; Aubrey and Speer, 1985; Dronkers, 1986; Friedrichs and Aubrey, 1988). This results in differences in magnitude and duration of ebb and flood tidal currents, called tidal asymmetry. A decrease in duration causes an increase in maximum current velocity.

Tidal asymmetry results in residual sediment transport. Asymmetry of the maximum current velocities of ebb and flood determines non-cohesive sediment transport since settling and erosion of sand respond quickly to variations in current velocity. Moreover, sand transport is proportional to a third or higher power of the flow velocity. Consequently, the sand transport during the strongest current is not compensated by the transport during the subordinate current, which results in a net displacement of sediment.

Tidal asymmetry and long-term basin evolution

Distortion of the tide off the basin entrance

The offshore tidal wave, which drives the tidal motion in the Dutch tidal basins, becomes distorted during propagation in the shallow southern North Sea. The water depth varies over the tidal cycle and is greater at the wave crest than at the trough. Thus the wave crest tends to move more quickly than the trough. Consequently, the rising part of a tidal wave becomes increasingly steeper and the falling part steadily flatter. This is illustrated in Fig. 6.2, locations I to III: the tidal wave becomes progressively more asymmetric during propagation from south to north along the Dutch North Sea coast. The steeper water-level gradient during flood tide causes a short-lasting, strong flood current and a weaker, longer-lasting ebb current in the tidal inlets along the Dutch coast (Fig. 6.3).

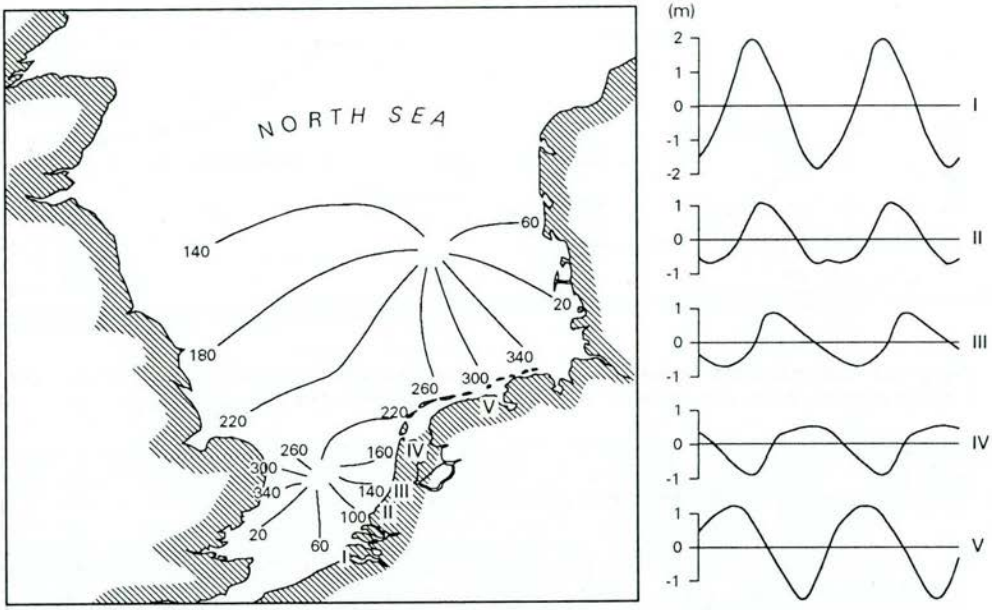

Figure 6.2 Distortion of the tidal wave travelling along the Dutch coast (after Dronkers, 1986).

Distortion of the tide in the basin

The tidal wave becomes further distorted during propagation within the basin. Tidal distortion in the inner part of the basin is controlled more by the geometry of the basin than by the asymmetry of the offshore tide (Friedrichs and Aubrey, 1988). Friction in shallow channels retards the propagation of the trough of the tidal wave (low water!) through the inner estuary. This increases the ebb period and reduces the flood period and thus favours flood dominance (Dronkers, 1986). This effect increases with decreasing relative depth, with increasing basin length and with increasing distance from the entrance

(Friedrichs and Aubrey, 1988). In addition, a shallow water depth over the tidal-flat areas will induce a strong, locally generated, flood dominance in the tide moving over the flats during high water (Friedrichs et al., 1992).

The lengths of tidal basins in the Netherlands range from 25 km to over 80 km. It is likely that the flood dominance which exists in the North Sea tide is enhanced during propagation through these basins.

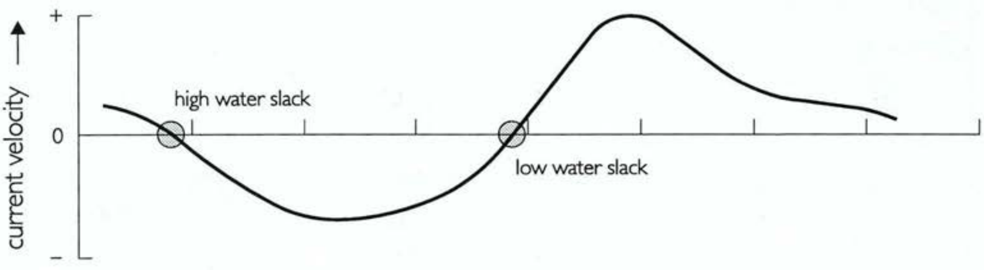

Figure 6.3 Changes in current velocity during the tidal cycle. Note that the maximum flood flow velocity exceeds the maximum ebb flow velocity. Example from the Wadden Sea.

Tidal asymmetry at the entrance of the basin

The flood-dominance of the North Sea tide at the basin entrance is counteracted by the effect of the presence of large areas of tidal flats in the basin on the tide. The maximum of the flood discharge will shift to a later stage in the flood period at a higher water level, during which the flats become flooded. This means that the flow cross-section of the main inlet channel(s) during maximum flood discharge is larger, resulting in a reduction in flow velocity. On the other hand, the drainage of the tidal flats during ebb tide lags behind the drop in water level in the channels and retards the maximum ebb discharge. Consequently, the maximum ebb discharge takes place later in the ebb period, at a lower water level, which enhances the maximum ebb flow velocity (Boon and Byrne, 1981; Speer and Aubrey, 1985). This results in a decrease in ratio of maximum flood to maximum ebb current at the entrance of the basin as the extent of the tidal flats increases (Friedrichs et al., 1990) and opposes the effect of the flood-dominated tidal distortion.

The outcome of the interaction of the induced flood-dominated distortion and the counteracting effect of the flooding and draining of tidal flats for a given tidal basin cannot be predicted. In theory, the counteracting effect of tidal flats on the tidal asymmetry at the entrance of the basin can grow to a point where the flood-dominance of the faster rising North Sea tide is neutralized, or ebb dominance is even reached. Simulation of the tidal motion for a certain basin geometry will give an indication of the resulting tidal distortion at the entrance of the basin. In the present-day tidal basins in the Netherlands the areal extent of the tidal flats is too small to overcome the flood dominance (Dronkers, 1986). In small, cooscillating tidal basins, as described by Friedrichs and Aubrey (1988) from the US Atlantic coast, ebb dominance can be reached when the volume of intertidally stored water is large compared with the volume of the channels.

Sediment transport and long-term basin evolution

An asymmetry in the tidal flow at the inlet of a tidal basin results in net landward or seaward of sand. This will lead to changes in basin geometry which, in turn, will affect the tidal distortion. Sediment accumulation in a flood-dominated tidal basin (if not compensated by basin subsidence and/or a rise in sea level) will eventually result in expansion of the tidal flats and shoaling of the channels. The expansion of the tidal-flat area leads to an increase in ebb flow velocity (see above) at the entrance of the basin and, consequently, to a decrease in sediment transport into the basin. This implies that infilling of the basin with sediment as a consequence of flood dominance at the entrance results in a decrease in the net basinward sand transport capacity.

Besides tide-induced residual transport, other factors such as sediment supply, wind waves and biological activity, affect net sediment transport into tidal basins. Landward near-bed sediment transport is enhanced by vertical, density-driven water circulation induced by the supply of fresh water from the hinterland. Wave action enhances both basinward transport, e.g. longshore drift and net cross-shore transport in ebb-tidal deltas, and the transport of coarse sediment in the estuary (e.g., Postma, 1961; Boon and Byrne, 1981). The extent of the wave impact on sediment transport depends on local wind and wave conditions. However, waves breaking on shallow areas in the basin during high tide counteract the accumulation of suspended sediment by resuspension or prevention of settling (Postma, 1961; Dronkers, 1986). Severe wave action combined with a higher water level in the basin during storms causes large-scale resuspension of sediment which will subsequently be displaced seaward during the ebb surge. The influence of waves, which counteracts the settling of fine-grained sediments on tidal flats and thus the landward sediment flux, increases with the expansion of the tidal-flat area. The interaction of these transport mechanisms determines the long-term sediment budget of a tidal basin. The balance between the sediment transport into the basin and the accommodation space created by basin subsidence or an absolute rise in sea level, determines the long-term evolution of a tidal basin.

In the present tidal basins in the Netherlands the landward transport of sand during the flood exceeds the ebb transport.

Development of a simple numerical flow model for tidal basins in the Netherlands

DUFLOW, a personal-computer package for simulating one-dimensional, unsteady flow in open channels, is the basis of the 'simple' flow model which was developed for the tidal basins in the Netherlands. It solves the equations for non-uniform flow which are based on the laws of conservation of mass and momentum, by discretization in time and space using a four-point finite-difference scheme (Spaans et al., 1989). The mass equation states that changes in water level at a certain location are the net result of local inflow minus outflow, whereas the momentum equation shows that the net change in momentum is the result of interior and exterior forces such as friction, wind and gravity. Spaans et al. (1989) give a detailed description of the mathematical and physical aspects of the package.

The basin geometry is subdivided in several sections. The width-of-flow profile must be defined at the start and the end of each section. The width-of-storage profile is specified for each section as a whole. Alternatively, the model can be run with descriptions of the channel cross-sectional area for the start and the end of each section and the section-averaged hydraulic radius and storage width (P. Bollebakker, Rijkswaterstaat-RIKZ, pers. comm., 1992). All parameters can be specified for several levels above the channel floor.

DUFLOW uses both Fourier components and time series of water levels as hydraulic input parameters. It calculates water levels and discharges at the start and the end of each section as well as the sectionally-averaged discharge and current velocity, in this case every 10 minutes.

A 'simple' modelling procedure was developed for the relatively well-known Schelde estuary in the present-day situation. The estuary, which has a total length of 167 km from Vlissingen to Gentbrugge, was divided into 12 sections, the lengths of which range between 9 km and 24 km (Fig. 6.4). The geometrical description of the sections is based on information from a detailed model of the morphology of the Schelde estuary in 1968, comprising almost

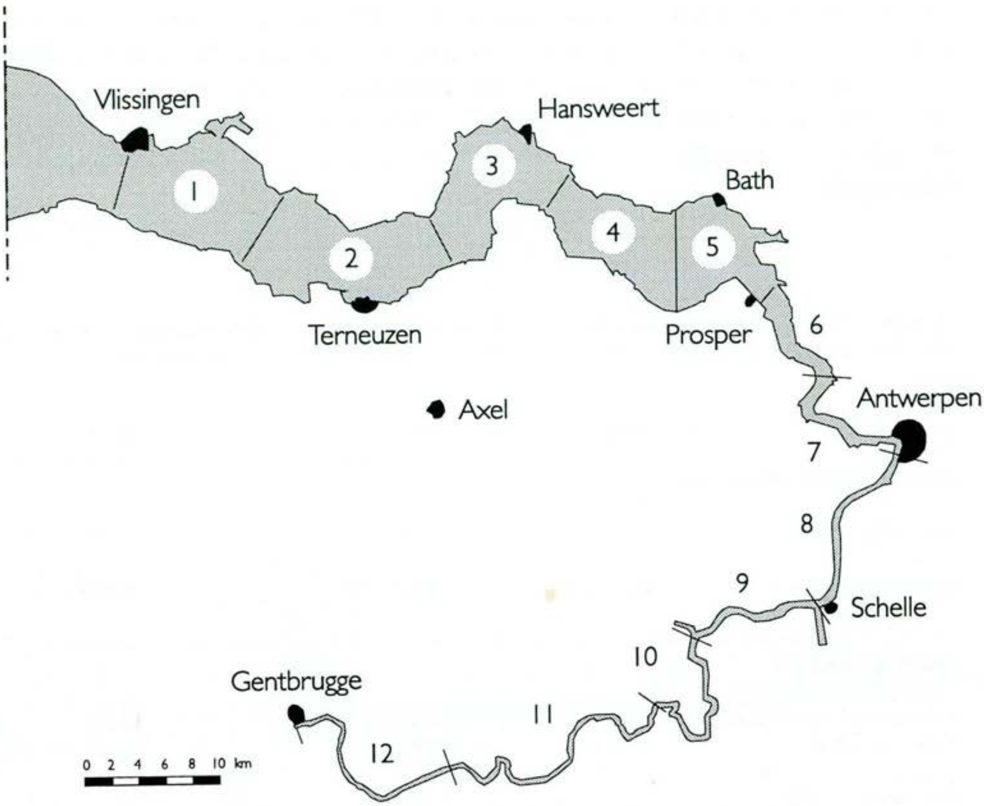

Figure 6.4 The Schelde estuary from Vlissingen to Gentbrugge. The estuary has been subdivided into 12 sections. See Fig. 6.1 for location.

200 sections (Hengst, 1980). A water-level time series, collected during moderate spring tide in May 1970 in the mouth of the estuary, is used as boundary condition for the simulations. Water-level and discharge registrations collected simultaneously in the estuary (Dekker and Bollebakker, 1981), were used to check the calculated results. The friction values for the ebb and flood direction of the model were manipulated until the calculated water levels at Antwerpen were in agreement with the observed ones. The maximum difference in tidal range at Antwerpen was 2 %, see Table 6.1 and Fig. 6.5. Tidal phases deviated maximally 10 min, which is about the resolution of the calculations. The calculated flood volume at the mouth of the estuary was 1140 million m^3 (Table 6.1), which is about 6 % too large. These calculated results are almost identical to those of the original, detailed model of Dekker

and Bollebakker (1981). The calculated tidal discharge near Hansweert, halfway up the estuary (Fig. 6.4), deviated 6 % at most from the observed one. Finally, the influence of river discharge on the water level near Antwerpen was found to be negligible. This was to be expected since the average river discharge of 100 m^3s^{-1} is less than 3 % of the tidal volume at Antwerpen.

Table 6.1 Results of tidal simulations for the Schelde for 1968 AD, 1800 AD and 1650 AD The indicated reference values are after Coen (1988). See Figs. 6.1 and 6.4 for locations.

	1650	1800	1968
input parameters Vlissingen			
tidal range (m)	3.43	3.58	3.80
mean sea level (m)	NAP-0.70	NAP-0.47	NAP-0.04
modelling results			
tidal range Antwerpen (m)	3.47	3.95	5.29
reference value	3.18	3.82	5.21
travel time Vlissingen - Antwerpen (min)	230	180	130
reference value	265	210	112
tidal characteristics calculated for Vlissingen:			
flood volume (10^6 m^3)	1190	1100	1140
flood period (min)	338	354	378
ebb period (min)	406	390	372
flood period/ebb period	0.83	0.91	1.02
$V_{max., flood}$ (ms^{-1})	1.69	1.50	1.15
$V_{max., ebb}$ (ms^{-1})	1.30	1.23	0.95
$V_{max., flood}/V_{max., ebb}$	1.30	1.22	1.21
water level H, relative to MSL			
$H_{Vmax, flood}$ (m)	+1.77	+1.85	+1.79
$H_{Vmax, ebb}$ (m)	-0.76	-0.65	-0.19

Uitnodiging

Voor het bijwonen
van de verdediging
van mijn proefschrift

op dinsdag
4 oktober 1994
om 10.30 uur precies

in het Academiegebouw
van de Universiteit
Utrecht
Domplein 29 te Utrecht

Receptie na afloop van
de promotie in het
Academiegebouw

Ad van der Spek
Dillenburglaan 23
2281 CZ Rijswijk
070-3193894

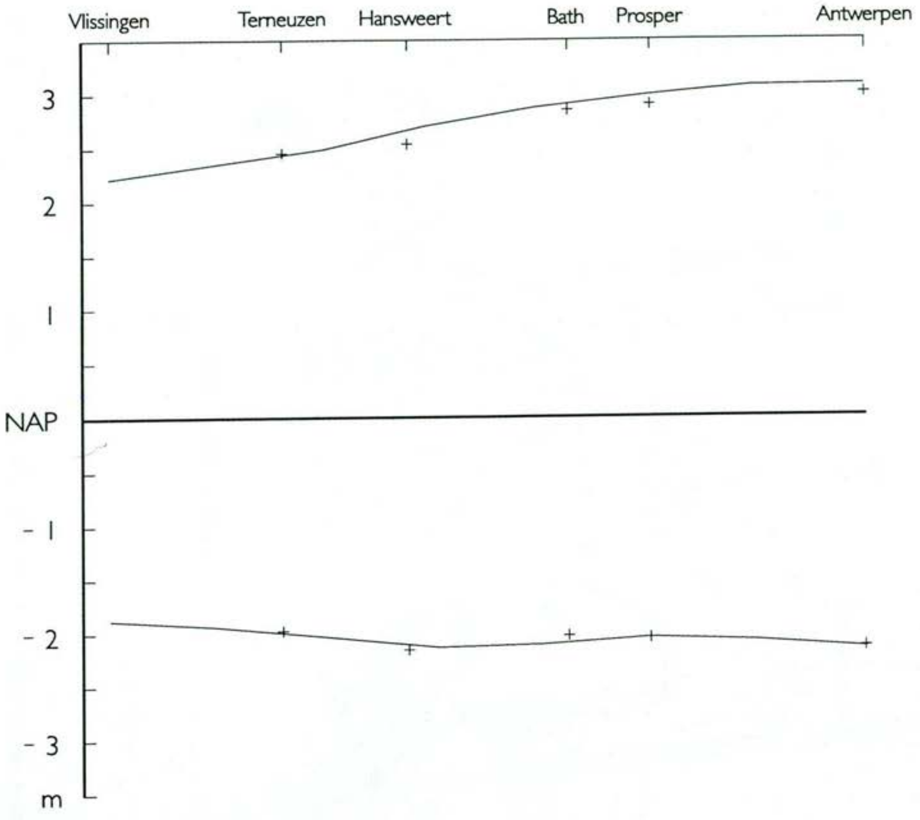

Figure 6.5 Calculated high and low water levels along the Schelde estuary for 1968. The crosses indicate observed water levels. Direct comparison of calculated and observed water levels is only possible for the locations Prosper and Antwerpen.

Evolution of the Schelde estuary

The Westerschelde, the seaward part of the Schelde estuary, evolved from the Honte, a tidal channel which has penetrated landward since the early Middle Ages. The Honte became connected to the Schelde river, north of Antwerpen, and became its new mouth: the Westerschelde. Subsequently, the Oosterschelde gradually lost its significance as mouth of the Schelde river. In the 14th century, the Westerschelde had become deep enough to become the new shipping route to the city of Antwerpen (Denucé, 1933). In the 17th century, the Westerschelde had become a large tidal basin. It was connected to the Oosterschelde by the shallow, tidal-watershed-like areas Sloe and Kreekrak (Figs. 6.6 and 6.7) and had several branches and extensive tidal flats and marshes with large water-storage capacities. In the following centuries the

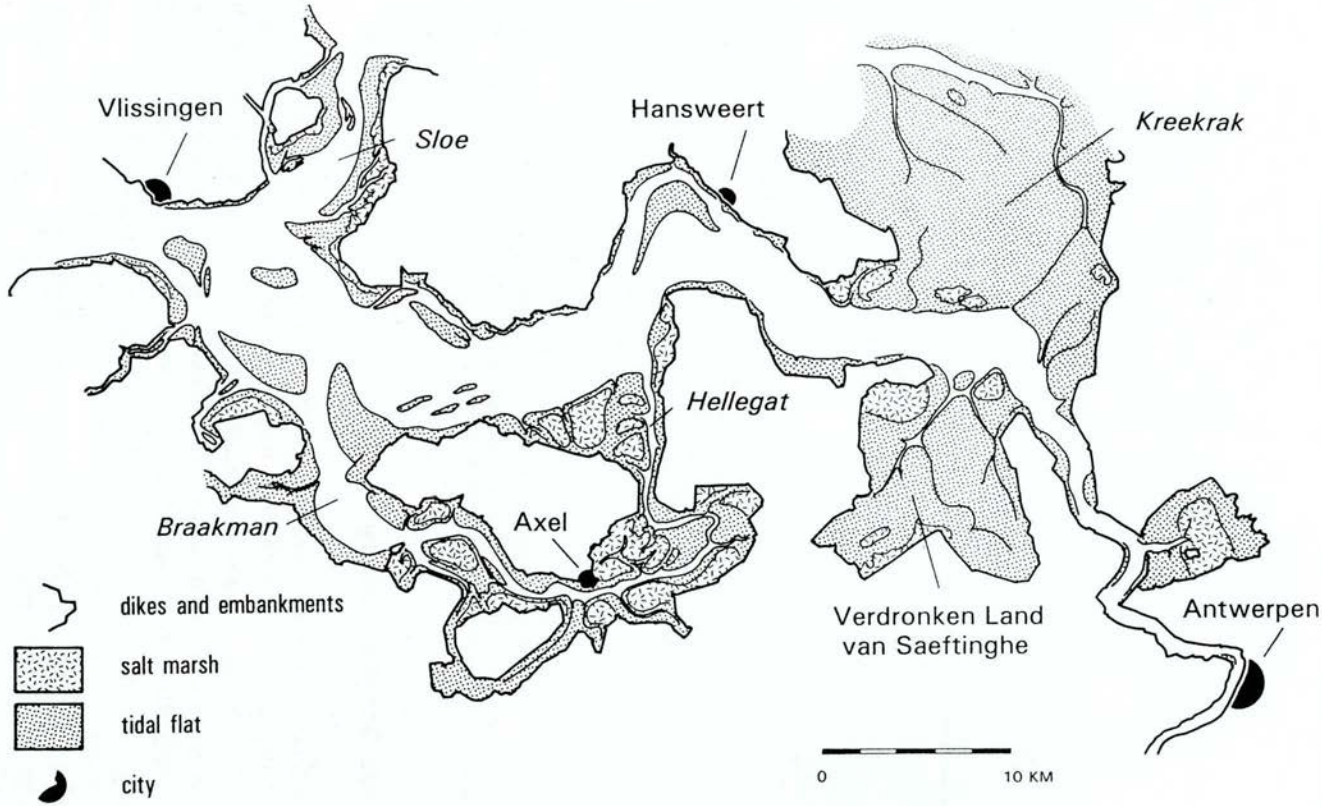

Figure 6.6 The Schelde estuary in 1650 AD. Reconstruction based predominantly on the map *"Zelandia Comitatus Novissima"* by Roman and Visscher (1655). After Van der Spek (1993.)

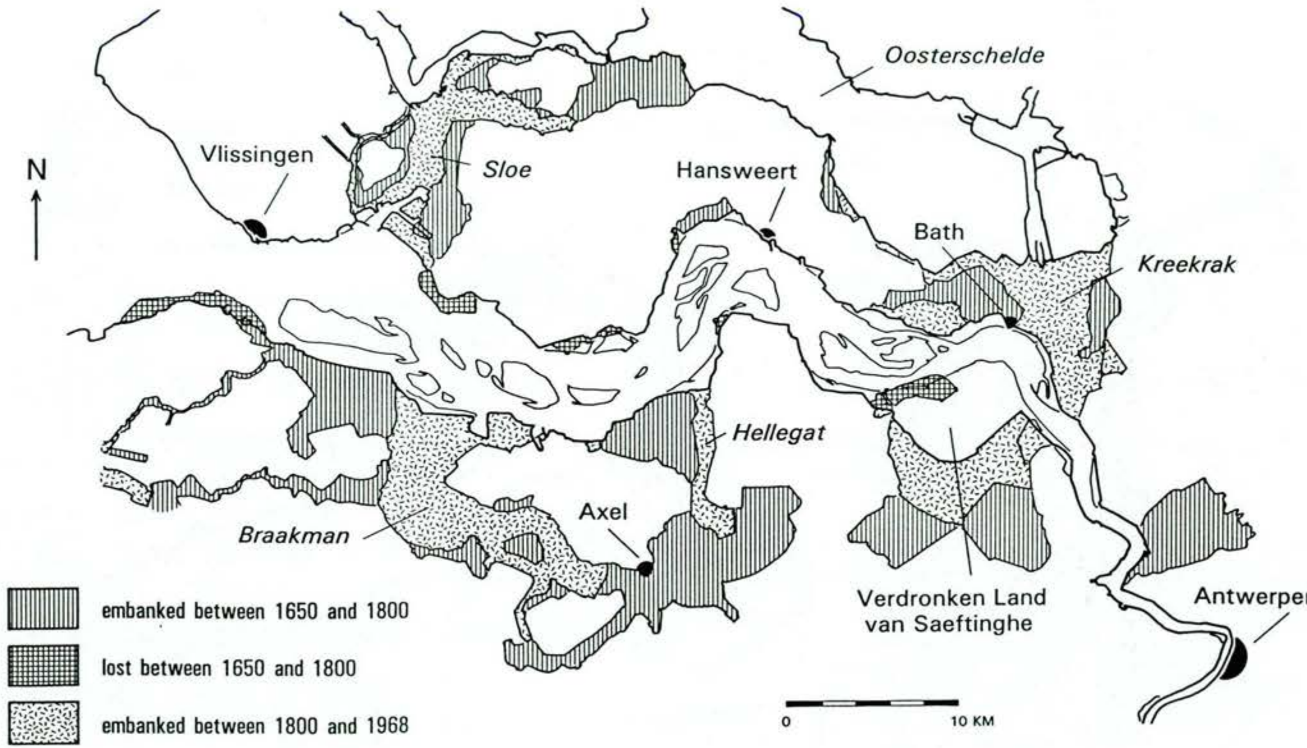

Figure 6.7 Map showing the accretion and subsequent embankment of the intertidal flats and marshes along the Schelde estuary between 1650 and 1968. The given intertidal morphology represents the situation in 1968.

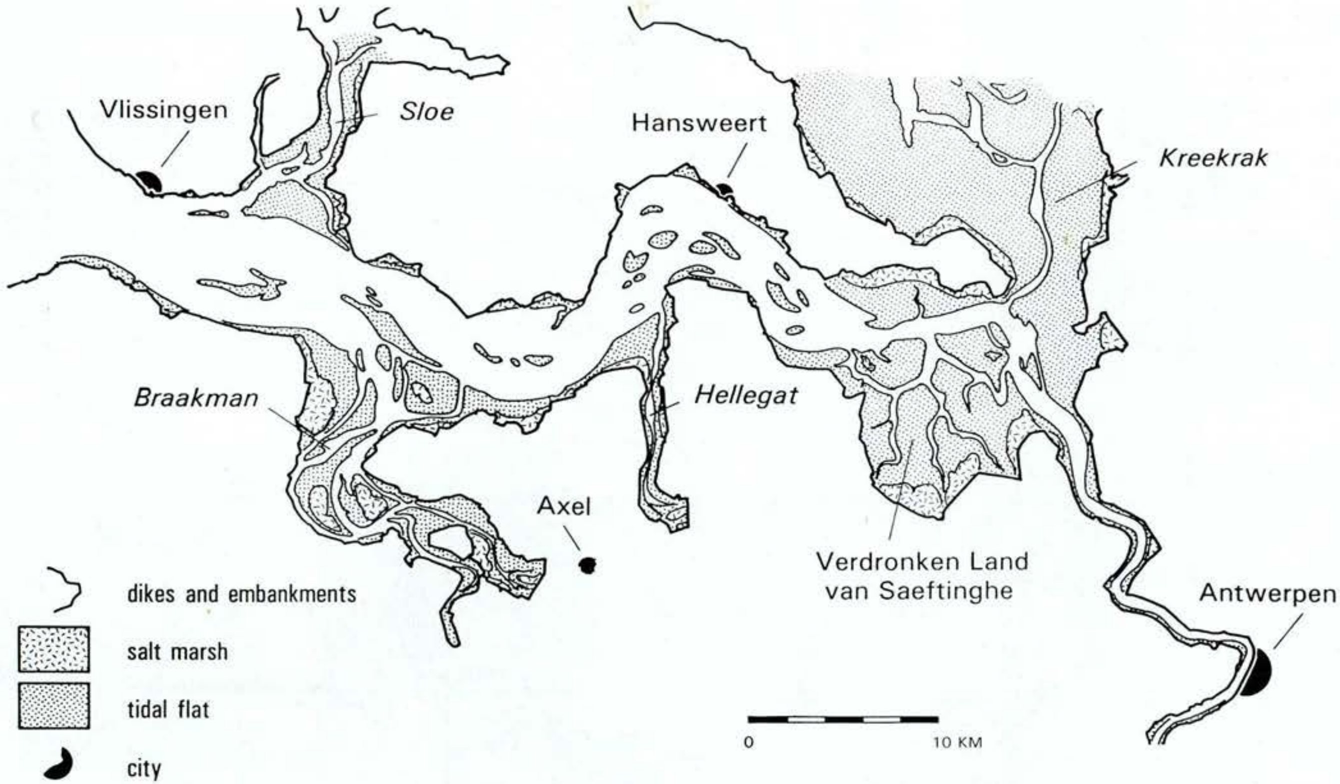

Figure 6.8 The Schelde estuary in 1799-1800 AD. Schematic representation of the hydrographical chart of Beautemps-Beaupré.

branches silted up. The tidal flats accreted to supratidal levels and were subsequently embanked. The intertidal storage area between NAP-2 m and NAP+2 m (NAP = Amsterdam Ordnance Datum, which is about present-day mean sea level) decreased from 350 km^2 in 1650 AD to 180 km^2 in 1800 AD and, finally, to 90 km^2 in the recent Westerschelde (Van der Spek, 1993; see also Fig. 6.7). The present-day Schelde resembles a classical, funnel-shaped estuary. The connections with the Oosterschelde and the large branches along the southern shore of the estuary silted up and were subsequently dammed in the 19th and 20th century (Figs. 6.7 and 6.8). Laterally migrating main channels in the estuary eroded the shores which sometimes resulted in the collapse of the embankments and loss of the polders they protected (Fig. 6.7). The 'Verdronken Land van Saeftinghe' is the only remaining substantial tidal marsh in the present-day Westerschelde (Fig. 6.7).

The tidal characteristics of the Schelde estuary changed with the decrease in its areal extent. Coen (1988) reconstructed the tidal ranges and the moments of high tide along the estuary and the river from nautical almanacs which go back as far as the 16th century. The tidal range along the Schelde increased with time (Fig. 6.9). Near Antwerpen it increased from about 3.2 m in 1650 to 5.2 m in the present-day situation (Coen, 1988). The celerity of the tidal wave in the estuary increased considerably. In 1650 the high tide travelled from Vlissingen to Antwerpen in about 4.5 hr (Coen, 1988). Filling and draining of the extensive storage areas in 1650 delayed the tidal wave considerably. At present this time lag is reduced to only two hours (Table 6.1). During the same period, mean sea level must have risen. The absolute amount of sea-level rise, however, is not known.

The tidal motion in the Schelde has been simulated in this numerical model for reconstructions of the estuary for 1650 AD and 1800 AD Van der Spek (1993) presents an extensive treatise on the reconstruction of the sea-/landscape of the estuary from historical maps and charts and the approximation of tidal ranges and mean sea levels for 1650 and 1800.

The Schelde estuary in 1800 AD

The French hydrographer C.F. Beautemps-Beaupré produced the earliest geometrically accurate sounding charts of the Westerschelde from 1799 onwards. He used the triangulation network that had been established by then by Kraayenhoff (Koeman, 1983). Around 1800, the Westerschelde was still connected to the Oosterschelde by the Sloe and Kreekrak channels (Fig. 6.8). The estuary also had three extensive tidal-flat and marsh areas along its southern shore (Fig. 6.8). These charts form the basis for simulating of the anno 1800 tides in the Schelde. Input parameters, in the form of water-level time histories are not available for 1800. Extrapolation of the time series of water-level observations at Vlissingen, which have been collected since 1862, to 1800 yields a tidal range of 3.58 m (Table 6.1). The time series for 1970 has been adapted for 1800 by reducing the tidal range at Vlissingen to this value. Mean sea level was assumed at 0.47 m below the present MSL, on the basis of initial model runs. NB The main reason for these calculations was to determine the effect of different estuarine geometries on propagation and distortion of the tidal wave, not to attempt an exact reconstruction of historical tides. River discharge and water exchange with the Oosterschelde were considered too small to be relevant and have therefore been neglected in the simulations.

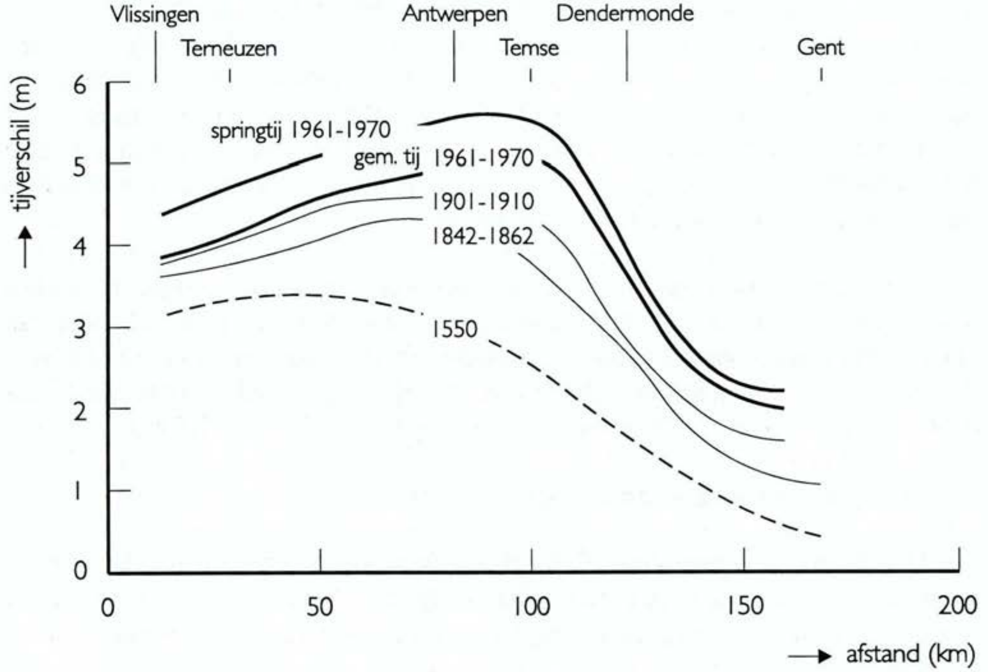

Figure 6.9 Reconstructions of the variation in tidal range along the Schelde estuary since 1550 AD (from Coen, 1988).

modelling results

The simulation for 1800 yields a tidal range of 3.95 m for Antwerpen, which is 3 % too large (Table 6.1). High water arrives 30 minutes earlier than in the reconstructions of Coen (1988), which is a deviation of about 15 % (Table 6.1). These deviations are probably caused by the friction values used in the calculations. These were determined for 1968 and have been applied straightforward in the calculations for 1800, for reasons of simplicity. In 1800, however, the estuary comprised several, strongly meandering main channels while the average depth was less than in 1968. These facts suggest that for 1800 a larger friction is appropriate. This would result in a smaller tidal range at Antwerpen and a larger time lag between high water at Vlissingen and at Antwerpen.

The Schelde estuary in 1650 AD

In the 17th century, the Westerschelde reached its widest extension. The oldest map of the islands along the estuary was published at the end of the 16th century. The map of the province of Zeeland (literally: sea land) compiled by Roman and published by Visscher in 1655 (Fig. 6.6) is the first map that gives a good impression of the distribution of dikes, tidal marshes, channels, creeks and tidal flats and other accretions (Donkersloot-De Vrij, 1975). Hydrographical charts of the estuary are not available for this period. The areal extent of the diked land is relatively small and large tidal marshes occurred (Fig. 6.6). The Westerschelde was connected to the Oosterschelde by the channels Sloe and Kreekrak. A large channel system with many branches existed along the southern shore (Braakman, Hellegat; Fig. 6.6). The schematization of the basin geometry for 1650 AD was based on this map. The channel dimensions were derived from the charts of 1800.

No other information on the hydraulic situation of the Westerschelde in 1650, apart from the reconstructions by Coen (1988), is available. Therefore, the water-level time history for Vlissingen which was used in the calculations for 1968, has been used again. It has been reduced to a tidal range of 3.43 m. The mean sea level was assumed at 0.7 m below the present-day one (Table 6.1), on the basis of initial simulations. The river discharge and the water exchange with the Oosterschelde were neglected since no information on these parameters is available. All other input parameters have been left unaltered.

The calculations for 1650 yield a tidal range of 3.47 m for Antwerpen, which is 9 % too large (Table 6.1). High water at Antwerpen occurs 35 minutes earlier than the reconstructions of Coen (1988) suggest, which is a deviation of 13 % (Table 6.1).

Evolution of the Schelde tides between 1650 AD and 1968 AD

The reconstructions by Coen (1988) show that the tidal range at Antwerpen increased from 3.2 m in 1650 to 5.2 m at present (Fig. 6.9). Simultaneously, the tidal celerity increased. This means that in the present-day situation high water reaches Antwerpen 2.5 hr earlier than in 1650.

The decrease in the surface area of tidal flats since 1650 has caused an increase in the average depth of the estuary and a higher celerity of the tidal wave. Consequently, the remaining flats are flooded almost simultaneously which led to a clear peak in flood discharge at the mouth of the estuary in 1968 (Fig. 6.10). The overall cross-sectional area of the estuary increases suddenly when the flats are flooded and the mean depth decreases, which results in a drop in velocity. This is reflected in the 'shoulder' in the discharge curve for 1968 (Fig. 6.10). In 1650, the inundation of the tidal flats was distributed more evenly over the flood period resulting in a smooth, symmetrical discharge curve for the flood. Apparently, in long tidal basins, where the delay in the tidal cycle from the mouth inwards is significant, the effect of the moment of flooding of the tidal flats on the tide at the basin entrance predominates over the effect of the total surface area of the tidal flats. The reduced surface area of tidal flats in 1968 is drained more quickly, which is reflected in a shorter duration of the ebb tide. Moreover, the maximum ebb discharge occurs sooner after high tide, at a higher water level (Table 6.1).

The flood volume diminished only slightly between 1650 and 1968 (13 %; Table 6.1), despite a reduction in intertidal surface area from 350 km^2 to 90 km^2. This is predominantly caused by the increase in tidal range. Moreover, a larger part of the intertidal storage capacity is filled during flood as a result of the higher tidal celerity, which will also have diminished the reduction in flood volume.

At the mouth of the estuary, near Vlissingen, the horizontal and vertical tide came to coincide more, since the moments of high and low water slack occur progressively sooner after the moments of high tide and low tide respectively (Fig. 6.11). This may be due to the increase in tidal celerity which causes a shorter period of landward flow after high tide has been reached in the mouth of the estuary.

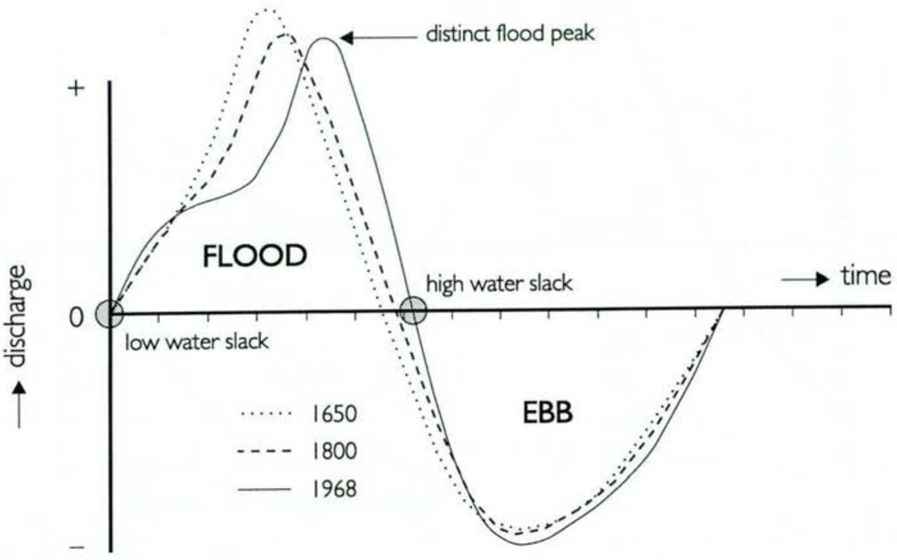

Figure 6.10 Calculated discharge curves for Vlissingen for 1650, 1800 and 1968. The curves show an increase in flood duration and the development of a distinct flood peak.

Tidal asymmetry and sediment transport

The asymmetry in maximum flood and ebb velocities at the mouth of the estuary has decreased since 1650. The flood period became 36 min longer (Table 6.1) and, consequently, the maximum flow velocity during flood tide decreased relative to the maximum ebb flow velocity (Table 6.1). The absolute maximum flow velocities also decreased (Table 6.1). The increase in flood duration and decrease in maximum flood flow velocity are probably the result of the increased average depth of the estuary, which permits a higher celerity of the tidal wave. Despite the almost identical durations of ebb and flood in the present-day situation, the maximum flood flow velocity is still higher than the corresponding maximum ebb flow velocity. This is caused by the faster rise of the North Sea tide.

The volume of the Westerschelde basin decreased by about $2*10^8$ m^3 between 1650 and 1968. This corresponds with an average net annual import of about $0.6*10^6$ m^3 (N.B. these figures are not corrected for sea-level rise).

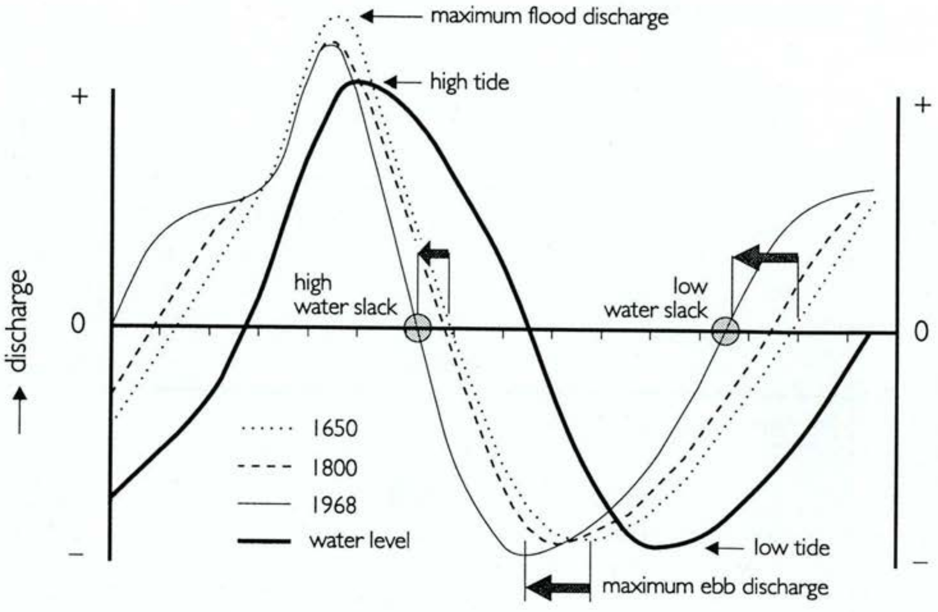

Figure 6.11 Calculated tidal discharges at Vlissingen relative to the water level, for 1650, 1800 and 1968. N.B. the discharges and water levels are not given in mutual correct proportions. The curves indicate that since 1650 the slack tides occur progressively sooner after high and low water. Moreover, the maximum ebb discharge occurs sooner after low water, at a higher water level. The moment of maximum flood discharge remains the same.

Conclusion

In conclusion it can be stated that the 'simple' modelling procedure described in this paper can produce workable results. The calculations for the Schelde for 1650 and 1800 show that valuable information on palaeo-hydraulic conditions can be generated, based on estimates of the input parameters.

The modelling shows that in long, elongate tidal basins the moment of flooding of the tidal flats is more important for the tidal distortion at the basin entrance than the total extent of the tidal flats in the basin.

The Westerschelde evolved from a relatively shallow, highly branched tidal basin comprising extensive tidal flats in 1650 AD into the present more linear and deeper, funnel-shaped estuary mouth. Most of the tidal flats and marshes accreted to supratidal levels and thus the total tidal-flat surface area decreased. The remaining tidal flats are flooded more simultaneously because of an increase in tidal celerity caused by the deepening of the basin. This affects tidal flow at the basin entrance in the same way as an increase in tidal-flat surface area. The maximum flood discharge occurs in a short interval at the end of the flood period, at a higher waterlevel and thus larger cross-sectional area of the inlet, resulting in reduced flood flow velocities. Draining of the tidal flats retards the maximum ebb discharge at the entrance, which consequently occurs at a lower water level. This reduction in cross-sectional area increases the ebb flow velocity. Consequently, the stronger flood currents at the entrance of the basin, caused by the faster rise than fall of the North Sea tide, are reduced and the tide at the basin entrance becomes more symmetric. Still, the tide is flood dominated near Vlissingen at the inlet in the current situation.

Acknowledgements

This investigation is a contribution to the multi-disciplinary Coastal Genesis project. It was supported by Rijkswaterstaat-National Institute for Coastal and Marine Management/RIKZ, contract DG-477, and the Ministry of Home Affairs, file number DUO 2002674. The research was carried out at the Geological Survey of The Netherlands (RGD) at Haarlem. Many thanks to Ruud Schüttenhelm of RGD for providing working space and a powerful PC.

I would like to thank Janrik van den Berg for all kinds of support during the project. Ad Langerak of RIKZ was my patient oracle on questions about numerical modelling and the Westerschelde. Many thanks for that. Thanks also to Peter Bollebakker and Teunis Louters of RIKZ for their pleasant cooperation. This paper benefitted from comments by Dirk Beets, Janrik van den Berg, Wilfried ten Brinke, Doeke Eisma and Ad Langerak on an earlier draft. Engelbert Vennix prepared the major part of the drawings.

7. Simulation of palaeo-tides as a tool in Reconstructing the long-term evolution of the Holocene North-Holland tidal basin.

Abstract

Geological data of ancient tidal basins generally do not provide all the detailed information that is necessary to reliably reconstruct the palaeogeographic evolution of the basin. Checking the hydraulic validity of a proposed reconstruction using a numerical water flow model may reduce inconsistencies. The calculated tidal-energy and transport gradients in the basin have to correspond with the reconstructed sedimentary facies. If not, the reconstruction has to be adjusted taking into account the geological constraints. In this paper, the preliminary results of the application of this method to three reconstructions of the Holocene North-Holland tidal basin in the Netherlands are discusses.

It is shown that around 7200 BP the basin was not predominantly lagoonal, as had been inferred from core data. The seaward part of the 7200 BP basin, located offshore, in the present-day North Sea, must have contained large tidal flats damping the tide and creating the protected facies found in the cores.

The cross-sectional area of the Bergen inlet, indicated by the size of the Bergen Clay that was deposited in it, is too large for the flood volume calculated for the maximum basin extension around 5500 BP. This means that the cross-sectional area suggested by the Bergen Clay does not represent the inlet dimensions at any particular moment and that part of the Bergen Clay was deposited while the inlet was still active.

While the inlet and the western part of the North-Holland tidal basin silted up, the landward part of the basin remained open water. The modelling results show a net basinward sediment transport capacity in and near the basin entrance and a net seaward transport capacity more landward. This probably restricted sedimentation to the western part of the basin. This might have enhanced silting up of the inlet.

Introduction

The long-term evolution of tidal basins and estuaries depends on the supply, transport and deposition of sand and mud. Net sand transport in the basins largely depends on tidal asymmetry, which results from tidal-wave deformation as a consequence of the interaction between basin morphology and tides. The direction and magnitude of the residual sand transport determines the evolution of a tidal basin. Reconstructions of Holocene tidal basins are mainly based on general morphology and on analysis of lateral and vertical facies successions in cores. However, the palaeogeography of tidal basins in the Netherlands (e.g., Pons et al., 1963; Zagwijn, 1986) usually is reconstructed from information scattered both in time and space. This may result in reconstructions bearing inconsistencies, despite their agreement with the geological data. Relatively simple simulations of the tidal motion, the most important transporting mechanism in the basin, may provide a check on the reliability of the geological reconstructions and may suggest improvements of the reconstructions. This paper describes the preliminary results of the application of this method to reconstructions of three stages in the development of the North-Holland tidal basin. This basin has been selected since it is the best-known Holocene tidal basin in the subsurface of the Netherlands (Chap. 4).

A relatively simple modelling procedure was developed for the Schelde estuary (Van der Spek, 1993a; Chap. 6). It uses input variables such as tidal range at sea, length and width of the channels and the total surface area of the tidal flats to calculate tidal ranges, discharges, flow velocities and deformation of the tide by the basin morphology. The basin is subdivided in a small number of sections for each of which the depth and width of the channels and the surface area of the tidal flats are estimated (see Chap. 6). Channel dimensions are estimated from the thickness and width of channel-sand bodies, whereas the surface area of tidal flats is estimated from the remaining basin surface area. Geological data frequently do not provide sufficient detail to derive these input variables with the required accuracy. Therefore, the hydraulic results that were calculated using initial estimates of the input variables were compared with basic information derived from geological variables such as for instance grain-size distribution. If necessary, the estimated input variables were adjusted within the geological constraints. Consequently, this simulation is a process of trial and error. The objective of these calculations is to test and improve the basin reconstructions. Moreover, it gives the geologist an impression of the propagation of a tidal wave in a basin, the consequences for sediment transport and the resulting basin morphology.

Evolution of the North-Holland tidal basin

At the start of the Holocene, an east-west trending valley system in the subsurface of the central part of the present-day province of North Holland, was occupied by the rivers Overijsselse Vecht and Eem (Fig. 7.1). Around 7500 BP, the expanding North Sea inundated this valley system and reached the present-day mainland of the Netherlands. During the Atlantic, the valley system evolved into a major tidal basin which extended as far as 60 km inland when it started to silt up in the Subboreal. Only small rivers with no or very little sediment load debouched into this tidal basin, so that all sediment was transported by tidal currents and entered the basin via the tidal inlets.

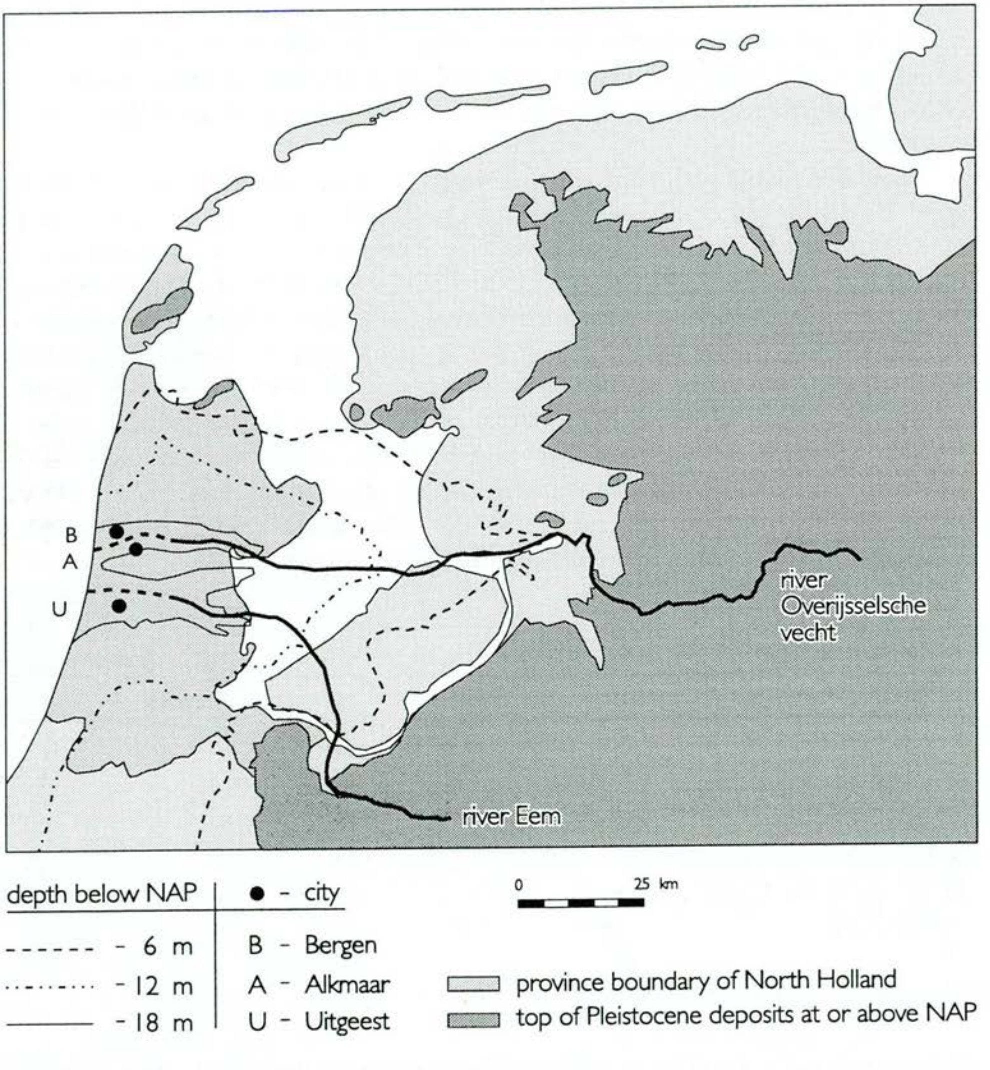

Figure 7.1 Top of the Pleistocene deposits in the northern part of the Netherlands.

The oldest deposit is a thin basal peat layer which formed as a result of the rise in ground-water level caused by the rapid rise in sea level. In a large number of cores, this peat is conformably overlain by an up to 2-m-thick, dark-coloured, organic-rich clay, the Velsen or Hydrobia Clay, which is considered to be of lagoonal origin, mainly on the basis of its lithology and diatom content (Van Straaten, 1957; Vos and De Wolf, 1994). This clay dates from the period between 7500 BP and 7000 BP, when the rate of sea-level rise was still in the order of 0.75 - 1.00 m/century. At 7200 BP, sea level stood at about 15 m - NAP (NAP is Amsterdam Ordnance Datum, which is about the present-day mean sea level; Fig. 7.2). The exact location of the coastline of the basin is unknown as it was situated offshore in the present-day North Sea. Because of the high rate of sea-level rise the basin shifted rapidly eastward.

The bulk of the sediments in the North-Holland tidal basin was deposited after 7000 BP, and consists of sands and muds deposited in sub- and intertidal environments. As the rate of sea-level rise decelerated to a mean value of 0.35 m/century between 7000 BP and 5500 BP, and to 0.15 m/century between 5500 BP and 3500 BP, the balance between sediment supply and creation of accommodation space by the rising sea level changed in favour of the first. The eastward migration of the basin caused by the rise in sea level stopped between 5500 and 5000 BP. The retreat of the coastal barrier on both sides of the inlets stopped between 4500 BP and 4000 BP. After that, the inlet and the western part of the North-Holland tidal basin quickly filled in. The last inlet of the system closed around 3300 BP (De Mulder and Bosch, 1982; Westerhoff et al., 1987; Roep and Van Regteren Altena, 1988).

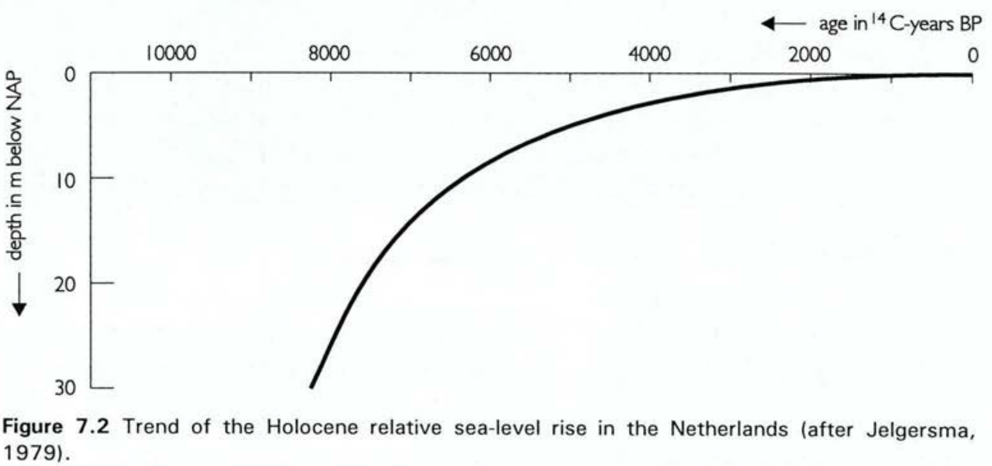

Figure 7.2 Trend of the Holocene relative sea-level rise in the Netherlands (after Jelgersma, 1979).

Facies analysis indicates that prior to about 5000 BP, the tidal basin was drained by two major channel systems, which up to then more or less followed the original courses of the former rivers Overijsselse Vecht and Eem in the subsurface (Fig. 7.3; Beets et al., 1992; Chap. 4). Sand-rich flood-tidal deltas developed behind the inlets, which were situated south of the village of Bergen and near the village of Uitgeest (Fig. 7.3). Basinward, sandy tidal flats developed along the tidal channels. They were separated by subtidal interchannel areas in which large quantities of mud accumulated. The landward fringe of the basin consisted of a brackish lagoon grading into a fresh-water tidal area and swamps with peat accumulation (Wiggers, 1955; Deckers et al., 1980).

Between 5000 and 4500 BP, the Uitgeest inlet closed (De Mulder and Bosch, 1982; Westerhoff et al., 1987). The deep inlet of the Bergen channel was partly filled with mud, the Bergen Clay, between 4700 and 4200 BP (De Mulder and Bosch, 1982; Westerhoff et al., 1987; De Groot and Westerhoff, 1993; Beets et al., in press). From about 4500 BP onward, the surface area of the North-Holland tidal basin decreased as it gradually filled up with sediment and changed into a fresh-water swamp (De Mulder and Bosch, 1982; Westerhoff et al., 1987). By 3700 BP, the large basin had shrunk to less than 40 % of its original size (Fig. 7.3). At that time, the basin was split up in a western part which was filled by clastic deposits up to supratidal level, and an eastern part which received little sediment and changed into a lake.

Aim of research

Major questions, brought up by this reconstruction of the evolution of the North-Holland tidal basin, which we hope to clarify by simulating palaeotidal conditions, are:

1 The nature of the tidal basin in the early Atlantic. The sediments older than 7000 BP in the cores in North-Holland are predominantly lagoonal. Did lagoonal conditions prevail in the entire tidal basin in the early Atlantic, because of a rapid rate of sea-level rise, or are the lagoonal deposits the innermost facies of a tidal basin which consisted of channels and tidal flats near its inlets?

2 What was the behaviour of the tidal wave in the North-Holland basin when it attained its maximum size around 5500 BP? What tidal ranges and current velocities occurred in the most landward part of the basin? Are the latter in agreement with the geological data?

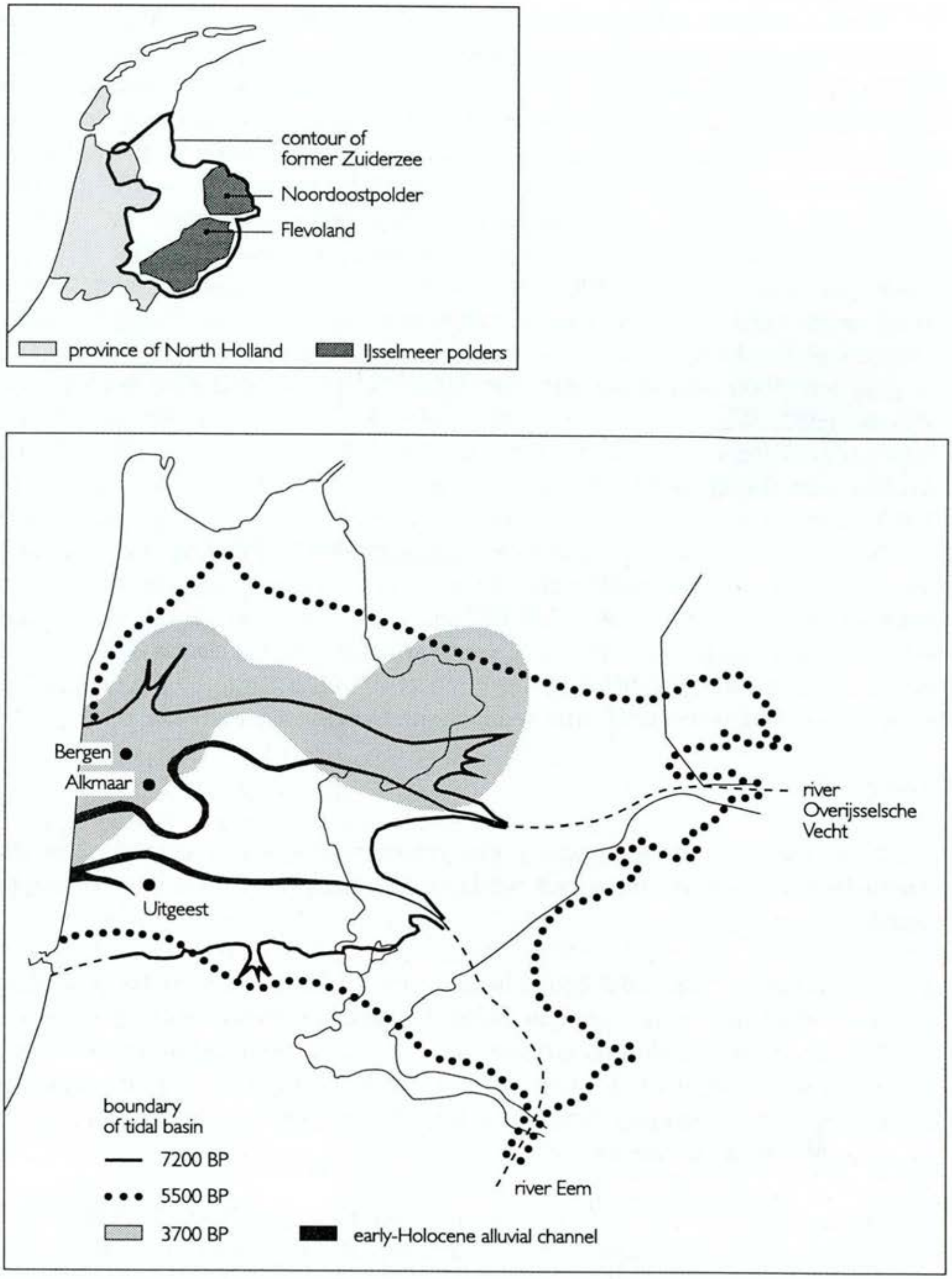

Figure 7.3 Extent of the North-Holland tidal basin in 7200 BP, 5500 BP and 3700 BP. During its maximum extent the basin included the area of the present-day IJsselmeerpolders in the east.

3 The size of the late-Atlantic/early-Subboreal Bergen Inlet. The clay plug which was deposited in the deepest part of the inlet suggests that the cross-section of the channel prior to mud deposition was in equilibrium with the flood volume, and that mud deposition started when the flood volume decreased as a result of silting of the basin. However, it is not clear if this is correct.

4 Why did the tidal basin split up into a tidally influenced western part and a lake in the east around 3700?

To answer these questions, the tides in the North-Holland basin have been simulated for three periods: around 7200 BP, around 5500 BP and around 3700 BP.

Evolution of the North Sea tide

Franken (1987) simulated the tidal motion in the North Sea basin using a two-dimensional flow model, for sea levels which are respectively 5 m, 10 m, 15 m and 20 m below present-day mean sea level. These levels correspond with the mean sea levels along the dutch coast in 5000 bp, 6500 bp, 7200 bp and 7800 bp respectively (jelgersma, 1979; fig. 7.2). The simulations by franken indicate the following. Around 7800 bp (mean sea level -20 m) the tidal range along the dutch coast varied between 0.8 m and 1.0 m. The nearshore tidal currents had a distinct two-dimensional character since their direction rotated with the tidal cycle. The maximum current velocities reached about 0.5 ms^{-1}, which is about 40 % below the present-day values. With the rise in mean sea level, the tidal dissipation in the north sea basin decreased whereas the amplitudes of the different tidal constituents and the tidal celerity increased. Consequently, the tidal ranges and tidal currents along the dutch coast increased. Moreover, the tidal currents became strongly bidirectional, with distinct slack water periods between flood and ebb tides. High-water levels and tidal ranges along the dutch coast have increased ever since, except along the north-holland coast (fig. 7.4). Here, the tidal ranges have decreased since 6500 bp (sea level at -10 m, see fig. 7.4: locations 4 and 5) because of an eastward shift of the centre of the amphidromic system of the southern North sea (franken, 1987).

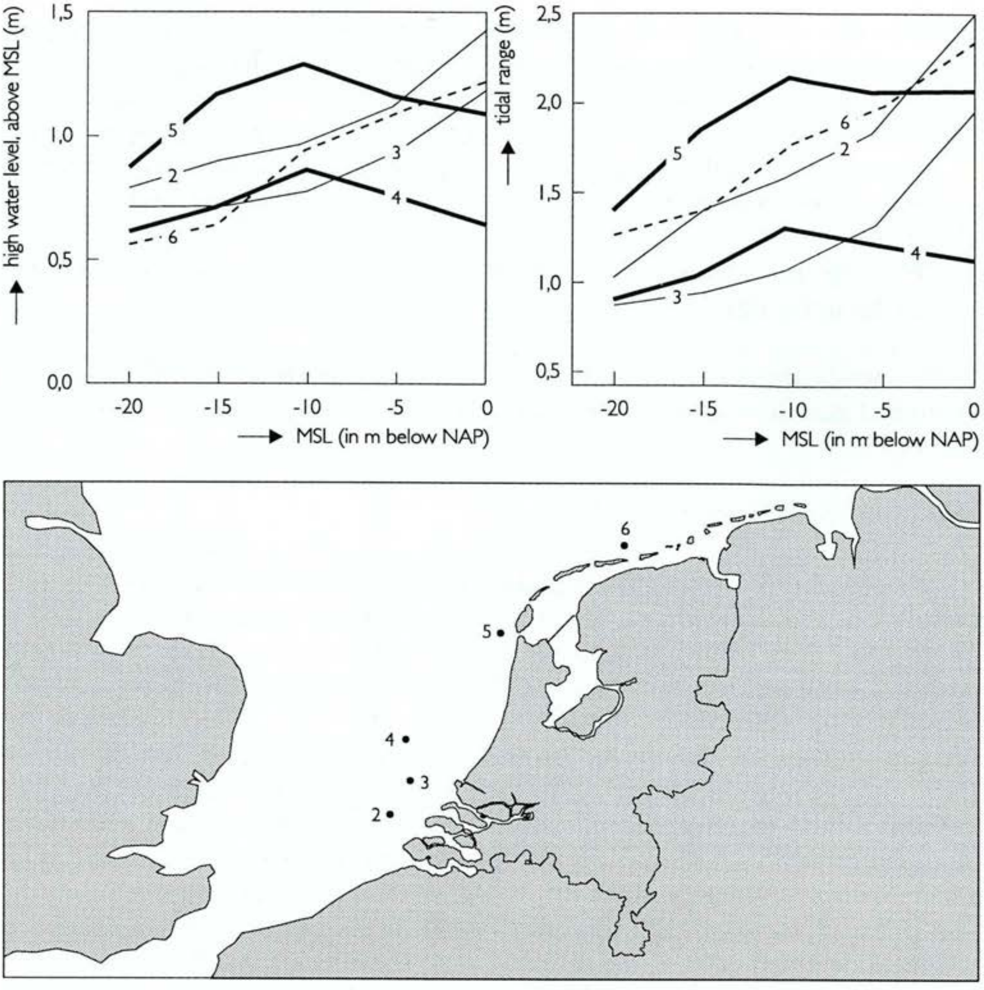

Figure 7.4 Changes in high water level and tidal range along the Dutch coast during the Holocene rise in sea level. Mean sea level stood at NAP-20 m in 7800 BP, at -15 m in 7200 BP, at -10 m in 6500 BP and at -5 m in 5000 BP. (After Franken, 1987.)

Simulation of the tides in the north-holland tidal basin

A schematization procedure, described in Chapter 6, and the one-dimensional flow model DUFLOW (Spaans et al., 1989) are the tools used in the model simulations. Values for bottom-roughness derived for the Westerschelde estuary were applied in these simulations. Van der Spek (1993b) describes the development of the basin schematizations and the underlying ideas, the input parameters and the model calculations. The simulations were executed using a water-level time series for Vlissingen, which was reduced to the tidal ranges calculated by Franken (1987), since no time series was available yet for the North-Holland coast. However, the tidal curve for Vlissingen is more or less symmetric, whereas the tidal curve for the North-Holland coast is and has been strongly asymmetric, both in the past and at present, with a relatively short and fast flood rise (Fig. 7.5: Egmond aan Zee). This deviation from the used time series bears some important repercussions on the calculations of residual sand import into the basin, which will be discussed later.

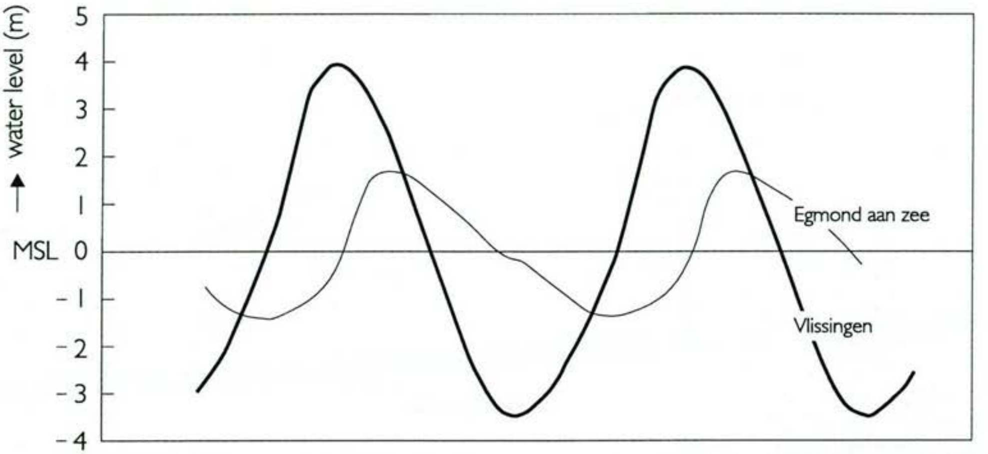

Figure 7.5 Tidal curves for Vlissingen in the Westerschelde mouth (in the SW part of the Netherlands) and Egmond aan Zee, west of Alkmaar.

1 The North-Holland tidal basin in 7200 BP

Basin reconstruction and model schematization

The main purpose of the simulations for 7200 BP is to study the tidal propagation in a lagoonal system and to determine if the simulated tidal conditions are in agreement with the reconstructed sedimentary facies. Cored boreholes from the North-Holland tidal basin predominantly show lagoonal sediments. However, it is not clear whether lagoonal conditions prevailed throughout the basin or appeared only locally, along the inner margin of the basin. In the simulations, the basin is considered to be one, extensive lagoon. On the basis of the information of cored boreholes it is assumed that a clay layer of 1 to 2 metre thickness has been deposited prior to 7200 BP (Fig. 7.6).

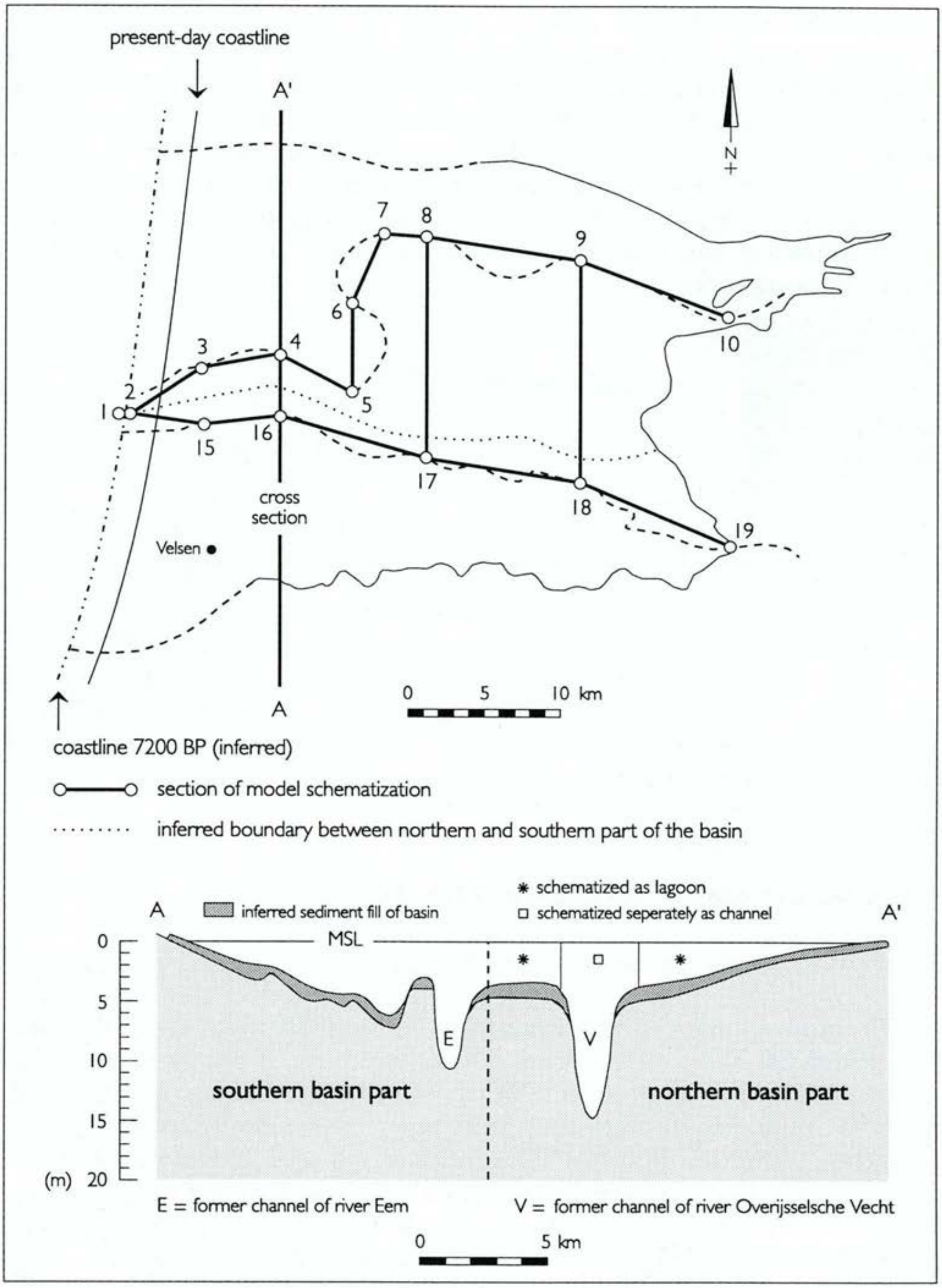

Figure 7.6 Reconstruction of the North-Holland tidal basin for 7200 BP. The thick lines and numbered dots represent the network of model sections.

In 7200 BP, mean sea level was 15 m lower than the present-day level. This means that the -15 m contour of the top of the uneroded Pleistocene deposits (Westerhoff et al., 1987; De Gans and Van Gijssel, 1994) defines the extent of the basin for 7200 BP (Fig. 7.6). The two tidal channels follow the original courses of the rivers Overijsselse Vecht and Eem. Borehole information shows that these channels reached depths of 18 m below palaeo-mean sea level. Maximum water depth outside the channels amounts to 5 m (Fig. 7.6). The coastline is assumed to have been situated 2 km west of the present-day coastline (see Fig. 7.6), based on the occurrence of pollen-dated lagoonal clays offshore North Holland.

For the model, the basin is subdivided in a northern and a southern part. The northern part consists of one main channel and a relatively shallow, flat-bottomed lagoon area along that channel (see cross-section AA', Fig. 7.6). The water flow is concentrated predominantly in the channel. The total length of the channel exceeds the length of the basin because the channel meanders (Fig. 7.6). Therefore, the channel and the shallow lagoon are treated as separate flow areas in the model schematization. For each section in the northern part of the basin (Fig. 7.6), the length and width of both the deep channel and the shallow lagoon were defined. Such a subdivision is not used for the southern part of the basin. The shallow lagoon area of this part is modelled as a water storage area, which was instantly flooded and drained by the successor of the Eem channel (Fig. 7.6). The northern and southern parts of the basin are connected, since a free exchange of water across the boundary between the two must be assumed.

Calculations by Franken (1987) indicate a mean tidal range of 1.2 m along the North-Holland coast around 7200 BP.

Results

The results of the simulations for the schematized lagoon show relatively strong currents of 0.4 to 0.7 ms^{-1} at the landward basin limit. The reduction in the tidal range during propagation of the tide from the basin entrance (Fig. 7.6: location 1) to the inner part of the basin is very small: 0.05 to 0.10 m. The water-level gradient between the northern and southern part of the basin is small: the maximum current velocities in the connecting channels do not exceed 0.15 ms^{-1}.

The maximum current velocities at the landward side of the basin are not in agreement with the fine-grained texture of the Velzen Clay. They are much too high. Apparently, the damping of the tidal wave in the basin around 7200 BP must have been stronger than simulated by the model.

The position of the North-Sea coastline in 7200 BP is not known exactly.

This position determines the length of the basin and thus the tidal dissipation. However, extension of the basin length would hardly reduce the tidal range at the landward boundary. If the coastline was located 10 km more seaward, a 0.05 to 0.10 m reduction in tidal range results, whereas a 40 km more seaward position would result in a reduction of about 25 % to 0.9 m (Fig. 7.7). This illustrates that under the given lagoonal conditions, the position of the coastline hardly affects the tidal conditions in the basin.

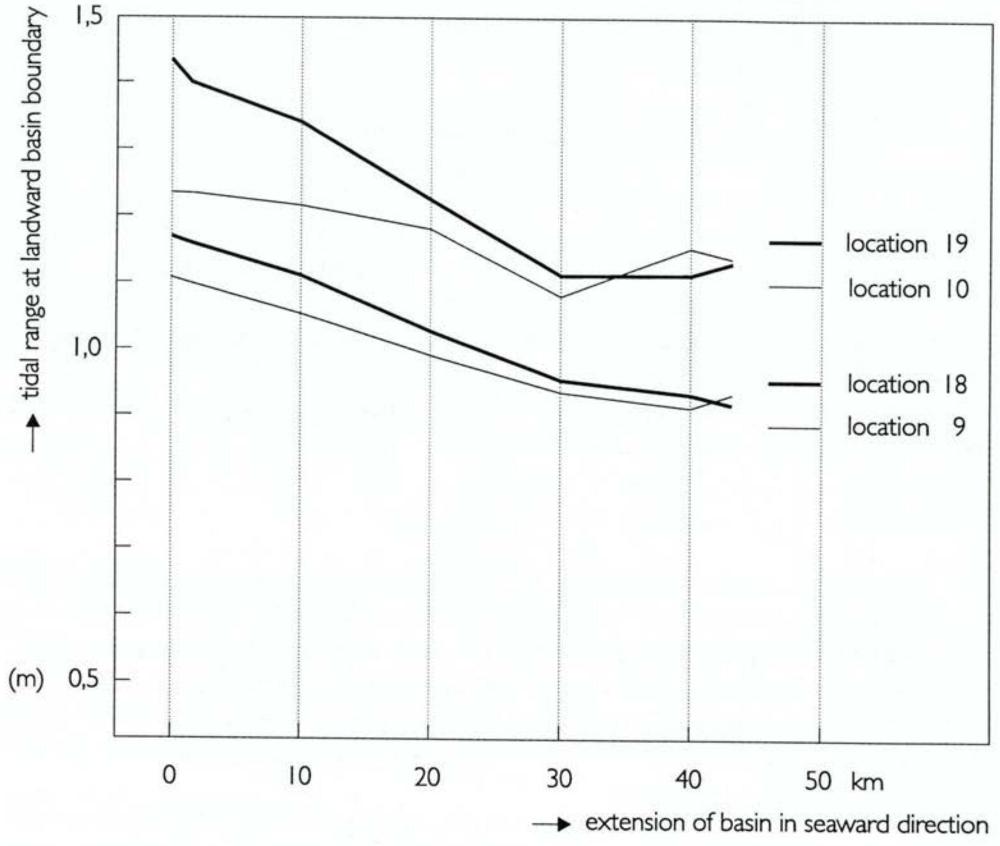

Figure 7.7 Changes in the tidal range at the landward boundary of the North-Holland tidal basin in 7200 BP, caused by an increase in basin length. See Fig. 7.6 for locations. From Van der Spek, 1993b.

Since the calculated tidal conditions do not correspond with the geological information it must be concluded that the 'lagoon' model does not represent the 7200 BP basin morphology. The environmental conditions necessary for deposition of the Velzen clay (Van Straaten, 1957; Vos and De Wolf, 1994), which must have existed along the landward limit of the basin, cannot be reproduced by the model. Consequently, the tidal motion must have been damped more efficiently in the seaward part of the basin. An increase in storage surface area combined with a decrease in overall flow cross-section in the seaward part will strongly reduce the tidal range and tidal currents in the landward part of the basin. This makes it very likely that tidal flats, dissected by tidal channels, existed in the seaward part of the basin. These tidal flats must have been situated offshore, in the present-day North Sea. Consequently, the 7200 BP coastline was situated further offshore than the 2 km assumed here. The branching channels gave access to more or less enclosed, poorly interconnected lagoons at the back of the basin. High water levels during the prevailing westerly storms transported marine clay and organisms into remote areas of the basin.

2 The North-Holland tidal basin in 5500 BP

Basin reconstruction

By 5500 BP, mean sea level had risen 8.5 m since 7200 BP and stood at 6.5 m below the present-day mean sea level (Fig. 7.2). The basin had shifted eastward and extended as far as the present-day IJsselmeer polders (Figs. 7.3 and 7.8). The coastline was situated about 4 km east of its present-day position, with tidal inlets near Uitgeest and Bergen (Fig. 7.8). Flood-tidal deltas existed landward of the inlets and continued basinward in tidal-flat areas along the relatively straight channels (Fig. 7.8). Clay settled further away from the channels in subtidal interchannel areas (Westerhoff et al., 1987; Chap. 4).

In the easternmost part of the basin, in the present-day IJsselmeer polders (Fig. 7.8), a fresh-water tidal area existed, consisting of a dense network of tidal creeks, embanked by clayey levees (Wiggers, 1955; Ente, 1964, 1971, 1976; Ente et al., 1986). The creeks were no more than a few metres deep and the tidal range was about 0.2 m (Ente, 1976). Fossils found in the clay indicate that the environment must have been completely fresh (Deckers et al., 1980). Apparently, the discharge of the Overijsselse Vecht, which debouched into the basin at this location, was sufficiently large to prevent salt water from penetrating this far eastward. The levees were regularly inhabited by Neolithic hunters around this period (Deckers et al., 1980).

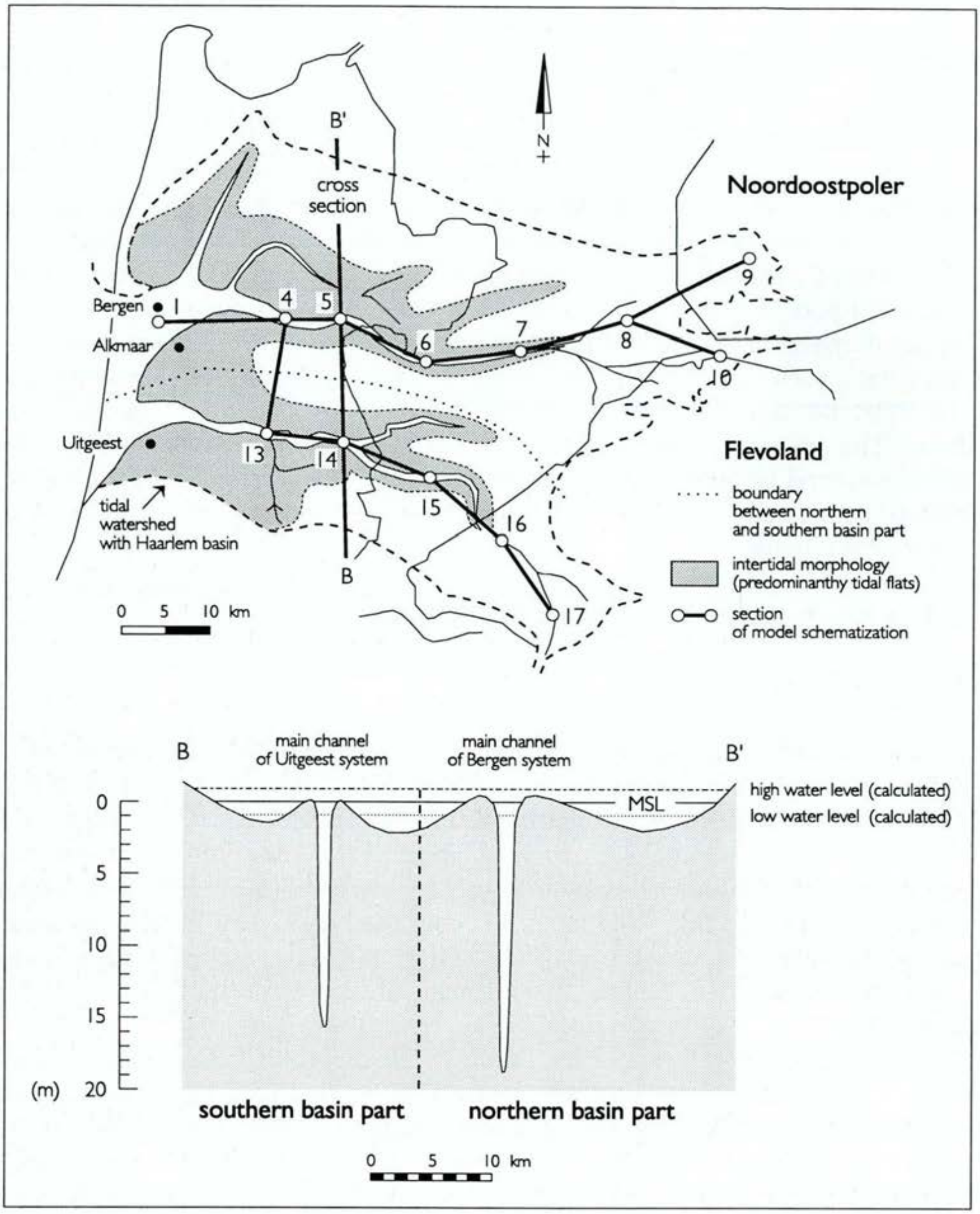

Figure 7.8 Reconstruction of the North-Holland tidal basin for 5500 BP. The thick lines and numbered dots represent the section network used in the model of the maximum extent of the basin, corresponding with the maximum cross-sectional area of the inlet (see text for further explanation).

The transition from the marine part of the North-Holland tidal basin to the fresh-water tidal area, which was situated in the present-day Lake IJssel, is poorly known.

The main objective of the simulation for 5500 BP is to get an impression of the tidal characteristics in the eastern part of the tidal basin. Moreover, calculation of the flood volume enables reconstruction of the size of the tidal inlet.

Model schematization

The extent of the North-Holland tidal basin around 5500 BP is well known. The distribution of Atlantic-age marine deposits in North Holland and the IJsselmeer polders is given by Wiggers (1955), Ente (1964, 1971, 1976) and De Mulder and Bosch (1982). The tidal watershed with the Haarlem tidal basin (Van der Valk, 1992) formed the southern basin boundary. Core data and cone-penetration tests provided estimates of the depths of tidal inlets (the inlets of Bergen and Uitgeest were as deep as 25 m and 17 m respectively below palaeo-mean sea level) and tidal channels in North Holland. We used the cross-sectional area of the Bergen Clay, deposited in the inlet after 4700 BP, as cross-sectional area for the Bergen inlet, in the initial model schematization for 5500 BP.

The creek dimensions in the easternmost part of the basin are derived from Ente (1976) and Ente et al. (1986). Channel depths in the transition zone were interpolated. A tidal watershed is assumed to divide both inlet/basin systems. Figure 7.8 shows a rough reconstruction of the basin morphology. This reconstruction comprises two channels with their main tributaries. The geological information is insufficient to obtain a good estimate of the total channel surface area, since smaller tributaries have not been mapped.

The tidal flats along the channels must have restricted the exchange of water with the interchannel lagoons. Therefore, tidal channels have been schematized as flow areas whereas the tidal flats and interchannel lagoons have been considered as storage area only. The interchannel basins were between 1 to 3 m deep.

Franken's calculations (1987) suggest an average tidal range of 1.5 m along the coast of North Holland. All other model parameters were left unchanged for reasons of simplicity.

Results

The initial calculations showed low current velocities in the tidal inlets. This indicates that the assumed dimensions of the tidal inlets were too large.

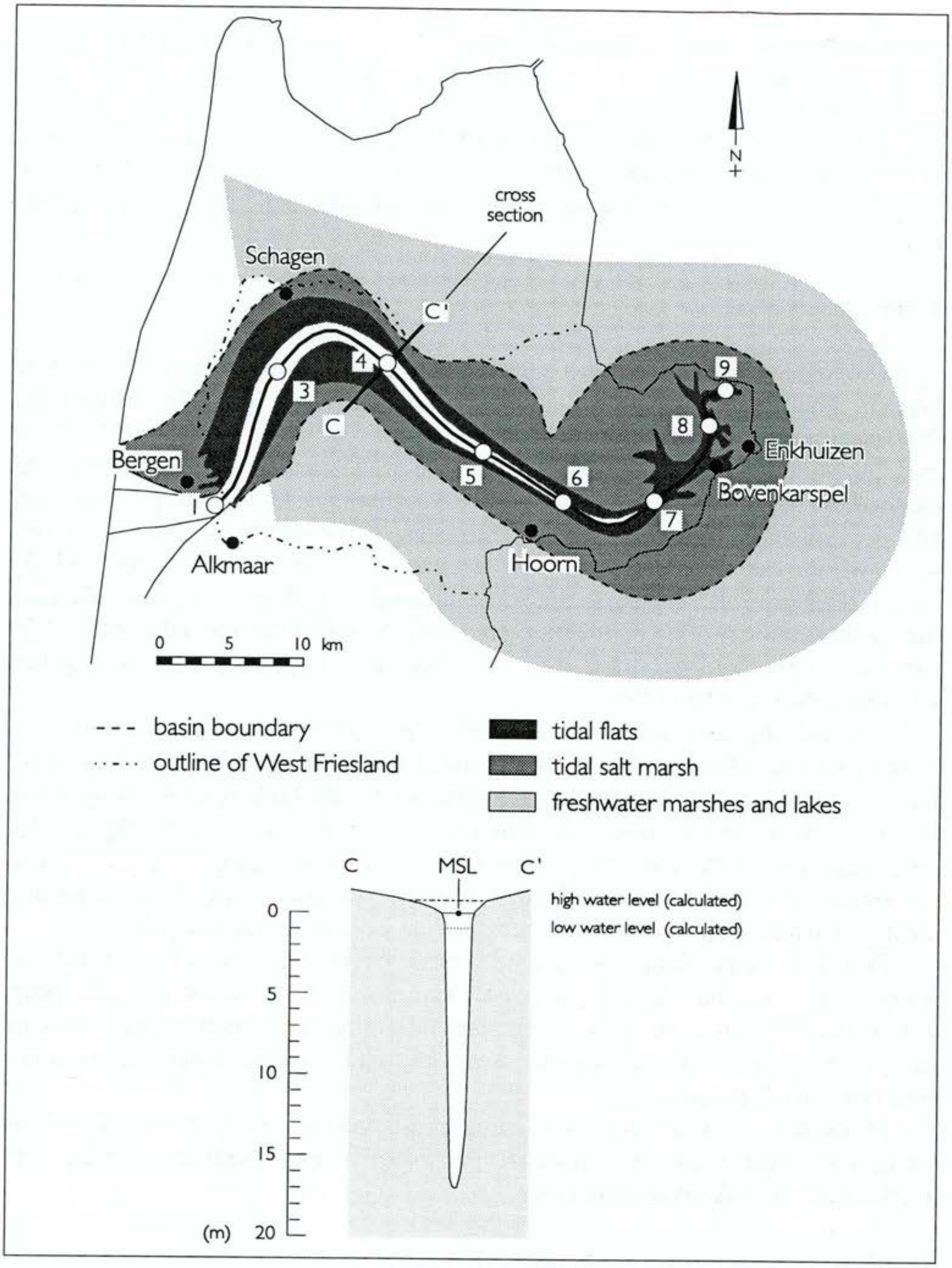

Figure 7.9 Reconstruction of the North-Holland tidal basin for 3700 BP. The thick lines and numbered dots represent the network of model sections. Distribution of tidal flats and salt marshes is used for the initial schematization.

The cross-sectional area of tidal inlets along sandy coasts usually is in equilibrium with the tidal prism, resulting in maximum current velocities in the inlet of about 1 m per second (Bruun, 1966; Van de Kreeke and Haring, 1979). The tidal range varies between 1.7 m at the inlet to 1.9 m in the basin and 0.3 m at the landward boundary. There, the mean water level rises to 0.3 m above palaeo-mean sea level and the tidal curve becomes strongly distorted. A short, vigorous ebb tide (V_{max} = 0.7 ms^{-1}) follows a long slow flood (V_{max} = 0.5 ms^{-1}). The water level stands above mean water level for more than 60 % of the tidal cycle. These calculated tidal characteristics are assumed to hold for the inner part of the North-Holland tidal basin in 5500 BP, although the inlet dimensions are too large.

3 The North-Holland tidal basin in 3700 BP

Basin reconstruction

After 5500 BP, the Uitgeest tidal inlet had silted up and the tidal inlet at Bergen shifted to the north. Meanwhile, the basin expanded to the north and large channel systems developed north of the former main channel (De Mulder and Bosch, 1982). One of the larger channels supplied a vast amount of sediment to present-day West Friesland (Fig. 7.9). This area still has a higher elevation than the surrounding areas.

Around 3700 BP, this large channel was in its final stage and it was filled up completely within 400 years (De Mulder and Bosch, 1982; Roep en Van Regteren Altena, 1988). The new tidal inlet was now situated north of the city of Alkmaar (Fig. 7.9) and had decreased in size (Westerhoff et al., 1987; Beets et al., in press). The basin was largely filled with sediment to above high-water level and its morphology was similar to the present-day tidal basins in the Netherlands. Sandy tidal flats flanked the channel. The sand flats merged into mud flats and finally into tidal salt marshes. The individual extent of these environments relative to the total basin surface area is not known. Around this time, the connection between the tidal channel and its adjacent tidal flats and salt marshes in West Friesland, and the fresh-water lake and marsh area east of it, which had not been filled up with sediment, deteriorated and was finally blocked. The moment of this decoupling is not known. In this reconstruction it is assumed that the two parts of the basin were no longer connected by 3700 BP.

Ente (1963) and Roep and Van Regteren Altena (1988) studied the eastward part of the basin, between Hoorn and Enkhuizen (Fig. 7.9). Beets et al. (in press) present a revision of the evolution of the tidal inlet and the coastline south of it. The basin area between the inlet and the eastern part of

West Friesland is described in general by De Mulder and Bosch (1982) and Westerhoff et al. (1987).

Model schematization

The general basin outline for 3800 BP to 3500 BP of De Mulder and Bosch (1982) was followed in the reconstruction for 3700 BP. Width and depth of channels in the eastern part of West Friesland were estimated from data given by Ente (1963), Westerhoff et al. (1987) and Roep and Van Regteren Altena (1988). The channel dimensions north of Bovenkarspel (location 8, Fig. 7.9) were derived directly from Roep and Van Regteren Altena (1988: fig. 3). The tidal inlet dimension was estimated from data given by Beets et al. (in press). Channel width and depth between the inlet and eastern West Friesland were interpolated.

The tidal flats adjacent to the channels were considered to have predominantly been storage areas and were not incorporated in the stream cross-section until the moment they were covered by one metre of water. The salt marshes are assumed to be situated above mean high water level and to cover the major part of the basin area.

The mean tidal range at sea was 1.4 m (Franken, 1987). Mean sea level stood at NAP-2.4 m (Jelgersma, 1979; Fig. 7.2). The boundary tide was forced on the tidal inlet (location 1, Fig. 7.9). All other model parameters were, again, as before.

Results

The model schematization described above leads to the following results. The maximum values of the calculated current velocities in the inlet and channels are 0.6 ms^{-1} during flood tide and 0.8 ms^{-1} during ebb tide. The relatively slow currents indicate that the channel was too large for the discharge conveyed through it, since maximum current velocities should reach values of about 1 ms^{-1} in inlets and channels that are in dynamic equilibrium (Bruun, 1966; Van der Kreeke and Haring, 1979). The tidal range increases strongly with distance from the inlet. North of Bovenkarspel (location 8, Fig. 7.9) the calculated tidal range is 2.6 m, whereas Roep and Van Regteren Altena (1988) concluded a tidal range of about 1.4 m on the basis of sedimentological criteria. Apparently, the calculated tidal ranges at the landward side of the basin are much too large.

Maximum current velocities, calculated after the widths of the channels were reduced by a third, increase to 0.9 ms^{-1}. The tidal ranges at the back of the basin, however, would still be too large. Doubling of the storage width at

1 m above mean sea level, which represents expansion of the tidal flat area at the cost of the salt marsh area of Fig. 7.9, would reduce the tidal range at location 8 (Fig. 7.9) to about the tidal range at sea or less. At the same time, the average water level at this location would increase from MSL+0.2 m to MSL+0.4 m.

The cross-section of the tidal channel near Bovenkarspel (Fig. 7.9, location 8; from Roep and Van Regteren Altena, 1988: fig. 3) shows stacking of channel bodies of varying widths, which were all filled around 3700 BP. In the above simulations, the dimensions of one of the intermediate channels were used. Around 3700 BP the width of the smallest channel at this location at mean sea level was 180 m and its depth 4 m below mean sea level (Roep and Van Regteren Altena, 1988, p. 220: channel system C2). The channel dimensions at Bovenkarspel have been reduced to these. For the other model sections, the initial channel widths, derived from Fig. 7.9, have been maintained. Moreover, in this simulation we have assumed that the entire area adjacent to the channels consisted of tidal flats.

Simulation of the tide using this adjusted basin schematization shows maximum current velocities at the inlet of 0.9 ms^{-1} during flood tide and 0.7 ms^{-1} during ebb tide. Apparently, the postulated cross-sectional area of the inlet is still too large, since the current velocities are below the equilibrium values of 1 ms^{-1} (see above). The flood volume at the inlet amounts to 0.23 $*10^9$ m^3. The corresponding cross-sectional area of the inlet would be $17*10^3$ m^2 ($A_c=62.1*10^{-6}$ * FV +3008; Gerritsen and De Jong, 1985). The cross-sectional inlet area derived from Beets et al. (in press) is a maximum value and amounts to $27*10^3$ m^2. This discrepancy suggests that the surface area of the reconstructed basin for 3700 BP, and thus the flood volume at the inlet, may be too small.

At Bovenkarspel (location 8, Fig. 7.9) the current velocity would have reached a maximum of 0.8 ms^{-1} during flood tide and 0.9 ms^{-1} during ebb tide. The local flood volume is 8.2 $*10^6$ m^3. The tidal range amounts to 1.1 m, with a mean water level of 0.3 m above mean sea level.

Long-term evolution of the tide in the North-Holland tidal basin

For 7200 BP, the North-Holland tidal basin was schematized as a lagoon. Although the lagoon reconstruction was rejected, the characteristics calculated for the basin tides are given here as a contrast to the reconstructions for 5500 BP and 3700 BP. The calculations show that the tidal range decreased only slightly in the basin, whereas the mean water level rose (Fig. 7.10a). The tidal wave was distorted only slightly (Fig. 7.11).

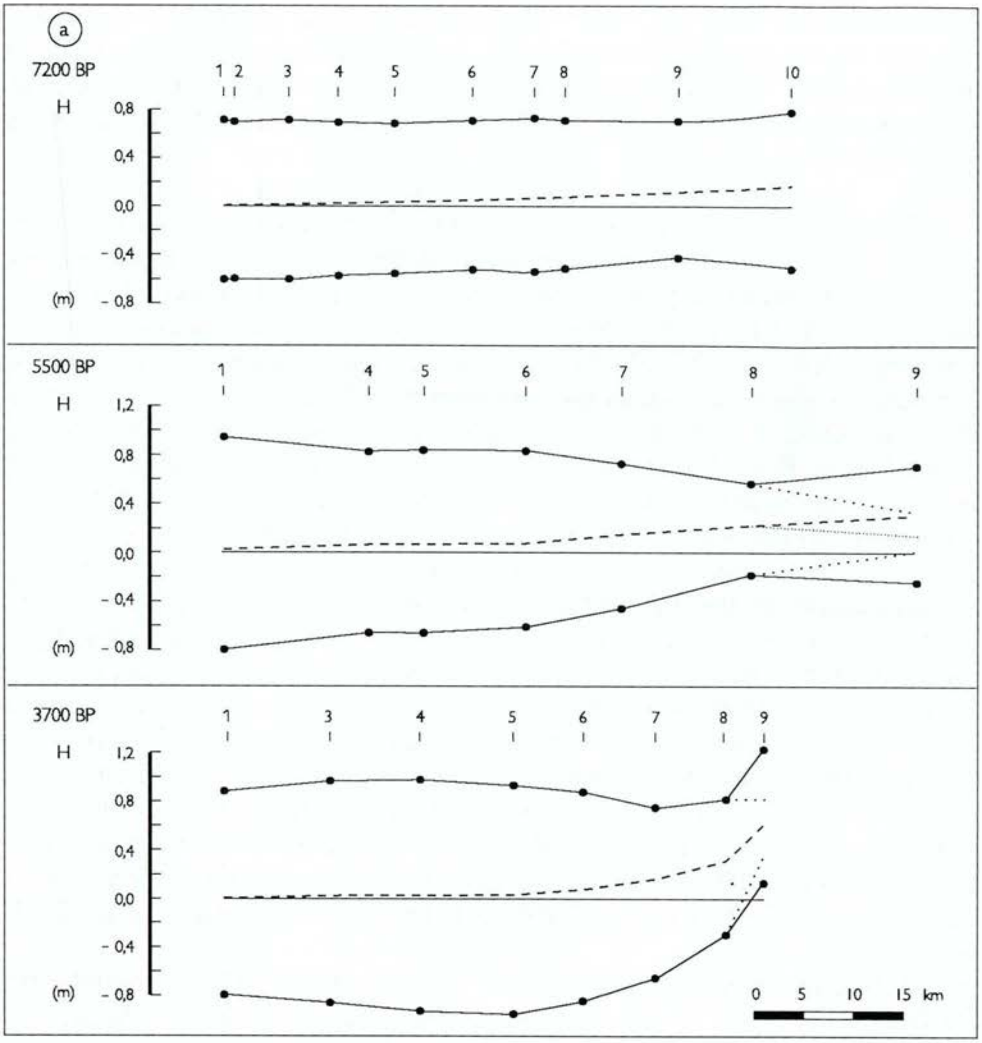

Figure 7.10a Variation in calculated tidal ranges for 7200 BP, 5500 BP and 3700 BP in the northern part of the basin. Location numbers correspond with the basin schematizations of Figs 7.6, 7.8 and 7.9. The hatched lines indicate the tidal ranges at the most distal locations after lengthening of the model schematization with an extra section in order to eliminate boundary effects.

In 5500 BP, the basin contained tidal flats along the channels, separating shallow lagoons. The basin surface area and total basin length had increased (Table 7.1). The calculated tidal range would have decreased with distance from the inlet, whereas the mean water level would have increased (Fig.

7.10a). At location 8 (Fig. 7.8), 52.5 km from the inlet, the tidal range would have fallen from 1.72 m to 0.73 m. and the local mean water level would have stood at MSL+0.21 m. However, the tidal range calculated for location 9 was too large because the tidal wave reflected against the closed model boundary. Lengthening of the model schematization with an extra section yielded a more realistic tidal range for this location (Fig. 7.10a, hatched lines). The flood period shortens progressively with distance from the inlet. The ratio of the maximum flood- to ebb-current velocity is more or less constant (Fig. 7.10b). The tidal wave maintained a flood-dominant distortion (Fig. 7.11).

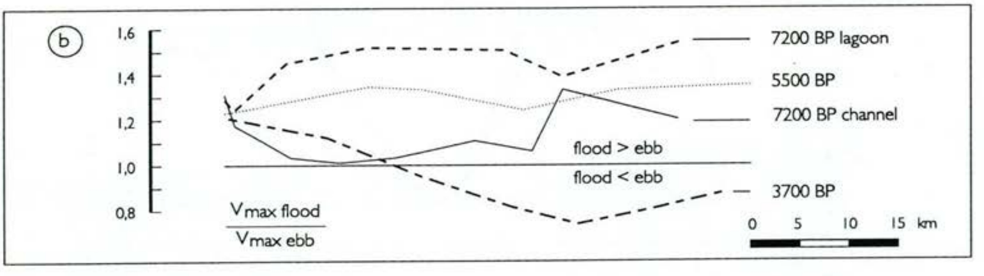

Figure 7.10b Tidal asymmetry, expressed as the ratio of maximum flood flow velocity to maximum ebb flow velocity in the northern part of the basin.

In 3700 BP, the surface area of the North-Holland tidal basin was reduced to 15 % of its 5500 BP value (Table 7.1). The basin consisted of one main channel bordered by tidal flats and salt marshes. Figure 7.10a shows the landward decrease in tidal range and the strong rise in mean water level. At location 8 (Fig. 7.9) the tidal range had fallen to 1.09 m (Fig. 7.11). The mean water level stood 0.3 m above palaeo-mean sea level. Landward of location 3, the tidal asymmetry had changed from flood-dominant to ebb-dominant (Figs. 7.9 and 7.10b).

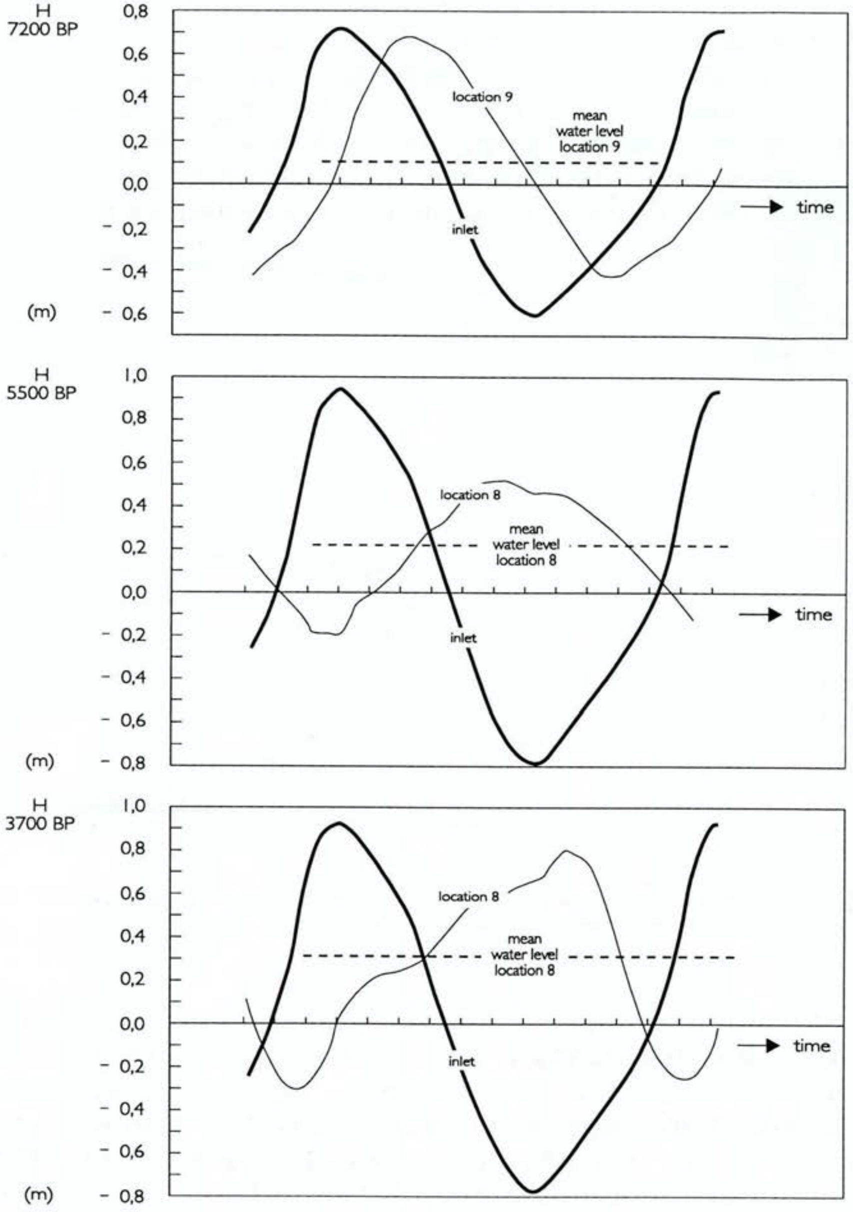

Figure 7.11 Time series of the boundary tide and the calculated tide at the reference locations in the northern part of the basin. Location numbers correspond with the basin schematizations of Figs 7.6, 7.8 and 7.9. Note the elevation of the mean water level at the reference locations.

Table 7.1 Results of the tidal simulations for the entrance of the North-Holland tidal basin for 7200 BP, 5500 BP and 3700 BP. N.B. the tidal ranges given in this table are tidal ranges during moderate spring tide; they are therefore larger than the mean tidal values given in the text.

	7200 BP	5500 BP	3700 BP
input parameters			
tidal range (m)	1.31	1.72	1.69
mean sea level (m)	NAP-15	NAP-6.5	NAP-2.4
basin characteristics			
surface area (10^6 m^2)	1145	1230	178
average length (km)	50	70	54
mean depth (m)	4.43	1.73	0.98
modelling results			
flood volume (10^9 m^3)	1.12	1.44	0.23
tidal celerity (ms^{-1})	6.3	3.1	1.9
flood period (min)	360	345	390
ebb period (min)	390	390	350
flood period/ebb period	0.92	0.88	1.08
tidal asymmetry: $V_{max., flood}/V_{max., ebb}$	1.28	1.23	1.20

Tidal asymmetry at the entrance of the basin

The simulated results underestimate the flood dominance in the tidal flow at the entrance of the basin, as a consequence of the almost symmetric boundary tide. The tides along the North-Holland coast show a short, fast rising flood tide and a long ebbing tide. A faster rising than falling tide implies that the flood currents along the coast and in the tidal basins of North Holland will have strongly exceeded the ebb currents, and that the residual sand transport into the basins was stronger than indicated by the simulations.

Comparison of the simulated tides at the basin entrance yields the following conclusions. The strong flood-dominant asymmetry of the tide at the basin entrance, calculated for 7200 BP (ratio of the maximum flood to ebb velocity is 1.28, against 1.23 in 5500 BP; Table 7.1), would have resulted in a large influx of sand and infilling of the basin. This shows once more that the lagoon reconstruction for 7200 BP is not probable, since it would have caused a large influx of sediment which would have resulted in the accretion of an intertidal morphology.

Once the basin started to silt up between 5500 BP and 3700 BP, the flood period was gradually extended (Table 7.1) and eventually was 45 min longer than the ebb period (Fig. 7.12). The maximum current velocity occurred later during the flood period (Fig. 7.12). The reduction in tidal-flat surface area caused a shorter ebb period, while the maximum ebb discharge occurred shorter after high tide (Fig. 7.13). The phase difference between the horizontal and vertical tide was reduced.

The tide at the basin entrance became less asymmetric as a result of infilling of the basin between 5500 BP and 3700 BP. The tidal asymmetry at the basin entrance, expressed by the ratio of the maximum flood- to ebb-current velocities, dropped from 1.23 to 1.20 (Table 7.1). This means that the interaction of the tide with the changing basin morphology progressively opposed the basinward sediment transport caused by the asymmetric North Sea tide. In the basin, the flood-dominant asymmetry gradually changed into an ebb-dominant asymmetry. The counteracting effect of tidal flats (these cause a delay because of the time involved in flooding and draining of the flats) was discussed by Friedrichs et al. (1990) and in Chapter 6. The accretion of part of the tidal-flat area to high water level between 5500 BP and 3700 BP did not reduce the counteracting effect of the flooding and draining of the flats on the tidal asymmetry. The opposition of the flood asymmetry forced by the North Sea tide increased instead.

The dimension of the bergen tidal inlet

The North-Holland tidal basin reached its maximum eastward extent around 5500 BP. Consequently, the maximum tidal prism and thus the maximum cross-sectional area of the inlet near Bergen were expected for 5500 BP. However, the Bergen Clay, which filled this inlet after it attained its maximum dimensions, was deposited after 4700 BP (Westerhoff et al., 1987; De Groot and Westerhoff, 1993; Beets et al., in press), which suggests that the maximum inlet dimensions were reached around 4700 BP.

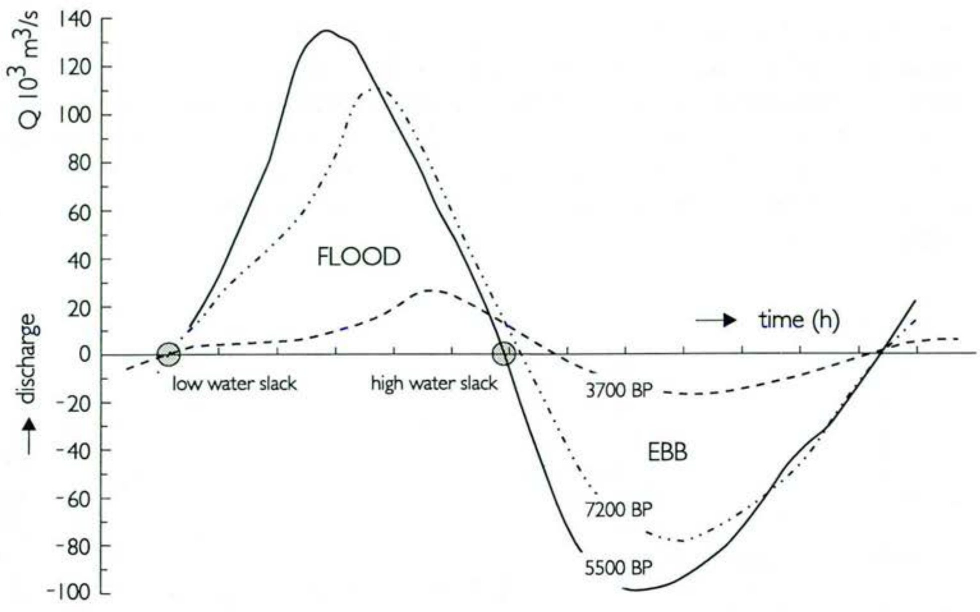

Figure 7.12 Calculated discharge curves for the inlet of the North-Holland tidal basin for 7200 BP, 5500 BP and 3700 BP. Between 5500 BP and 3700 BP the flood period became considerably longer.

Although the Bergen basin expanded to the north between 5000 BP and 4800 BP (De Mulder and Bosch, 1982) and the tidal flow penetrated further to the east (witnessed by deposition of a second brackish clay layer in the Noordoostpolder between 4900 BP and 4700 BP; Ente, 1971, 1976; Ente et al., 1986), the basin surface area around 4700 BP was only slightly larger than around 5500 BP. Shortly afterwards, large-scale peat formation started in the southern part of the Bergen basin. This must have neutralized the increase in flood volume caused by the basin expansion. Consequently, it is not likely that the flood volume and thus the dimension of the Bergen inlet was much larger around 4700 BP than around 5500 BP.

The southern inlet of the North-Holland tidal basin near Uitgeest silted up shortly after 4800 BP (De Mulder and Bosch, 1982; Westerhoff et al., 1987). The Bergen channel may have taken over the role of main flooding inlet to the southern part of the North-Holland tidal basin from the Uitgeest inlet. This would have resulted in an increase in the flood volume in the Bergen inlet and a decrease in the Uitgeest inlet. Consequently, the former would have scoured out, whereas the latter would have silted up. However, it is doubtful whether closing of the Uitgeest inlet was due to expansion of the Bergen basin. The tide travels along the Dutch coast from south to north and would have reached the Uitgeest inlet earlier than the Bergen inlet further north. Therefore, the distance to the southern part of the North-Holland tidal basin via the Uitgeest inlet is considerably shorter than via the Alkmaar-Bergen inlet. Unless some kind of barrier prohibited tidal propagation from the Uitgeest inlet further east, silting up of this inlet, which forms the shortest route to the storage area in the basin seems very unlikely. Evidence of such a barrier has not been found.

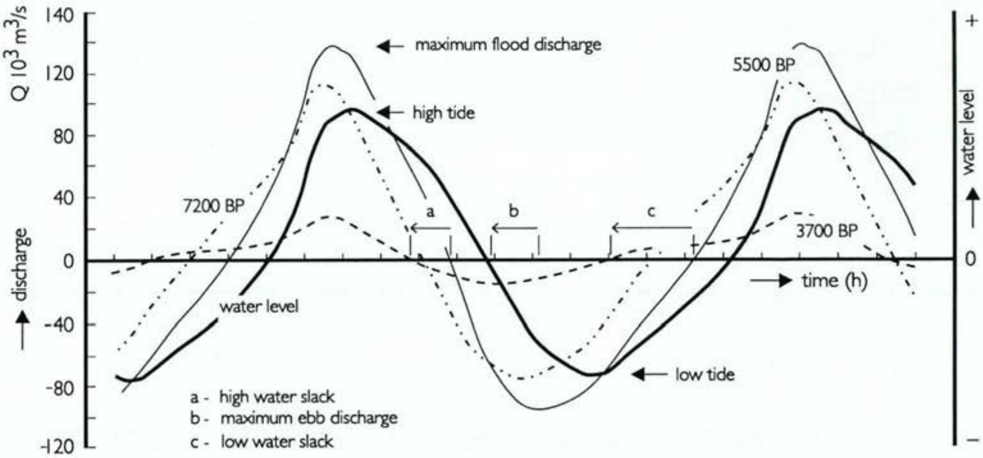

Figure 7.13 Calculated discharges at the inlet relative to water level, for 7200 BP, 5500 BP and 3700 BP. N.B. the water-level curve is not representative for all simulations.

The model calculates a flood volume of 726 * 10^6 m^3 in the inlet for 5500 BP. The cross-sectional area for a tidal inlet in dynamic equilibrium can also be calculated from the flood volume using an empirical relationship between both parameters (e.g., O'Brien, 1969; Jarret, 1976; see also Chap. 5). Gerritsen and De Jong (1985) derived the following relationship for the western part of the present-day Dutch Wadden Sea, about 40 km north of the former Bergen inlet: cross-sectional inlet area A_c = 62,1*10^{-6} * flood volume FV + 3008. If we use this formula, the cross-sectional area of the inlet corresponding with the simulated flood volume must have been 48 * 10^3 m^2, which is only 41 % of the cross-sectional area of 117 * 10^3 m^2 now filled with Bergen Clay. This shows that the cross-sectional area of the Bergen inlet derived from the cross-sectional area of the Bergen Clay is too large.

This empirical relationship, in combination with the known cross-sectional area of the inlet of 117 * 10^3 m^2 derived from the Bergen Clay, suggests a flood volume of about 1,8 * 10^9 m^3. Flooding of the entire North-Holland tidal basin via the Bergen inlet would produce a flood volume of only 854 * 10^6 m^3. An increase in channel volume or even a total elimination of intertidal morphology from the model schematization would not result in a calculated flood volume of a magnitude of 1,8 * 10^9 m^3. An increase in channel surface area of 300 % would result in a flood volume of only 1,3 * 10^9 m^3. This confirms once more that the reconstructed cross-sectional area of the inlet cannot be correct; it is too large. This implies that deposition of part of the Bergen Clay already took place while part of the inlet was still active. Deposition of clay in tidal-inlet channels is therefore expected after a sudden decrease abandonment of flow, e.g., caused by a shift of the active channels to another part of the inlet.

Water levels at Bovenkarspel

Roep and Van Regteren Altena (1988) concluded that the mean high-water level near Bovenkarspel in 3700 BP must have been at NAP-1.6 m, on the basis of the lowest level of appearance of salt-marsh vegetation and the upper presence of tidal deposits. The simulated mean high-water level at location 8 corresponds well with this information. Determination of the mean low-water level is much more complicated. On the basis of the level of the top of the subtidally-deposited clays and the level of appearance of sub- and intertidal sedimentary structures, Roep and Van Regteren Altena (1988) place the 3700 BP low-water level, after correction for compaction, at 0.6 m below palaeo-mean sea level. The simulations suggest that the mean low-water level is 0.1 to 0.3 m below 3700 MSL. Moreover, the simulated mean water level near Bovenkarspel stood at 0.3 to 0.4 m above 3700 BP mean sea level, instead of 0.1 m as Roep and Van Regteren Altena inferred from field data.

The conclusion that mean water level in the distal part of the basin stood at 0.3 to 0.4 m above palaeo-mean sea level in the Bovenkarspel area is supported by the occurrence of subtidally deposited clays. These clays date from 4150 BP (Roep and Van Regteren Altena, 1988) and occur below a depth of NAP-2.75 m. In 4150 BP, the mean sea level stood at roughly the same level (Roep and Beets, 1988), so that low-water level in the inner part of the basin corresponded roughly with mean sea level. Around 3275 BP, when the basin had silted up and the inlet had closed, the mean water level near Bovenkarspel, which corresponded roughly with the groundwater level by that time, had dropped and was close to mean sea level (Roep and Van Regteren Altena, 1988). Thus, the difference between local mean water level and mean sea level decreased and finally disappeared between 4150 BP and 3275 BP near Bovenkarspel. During this period the tidal basin silted up and the tidal influence disappeared from the area. This implies that the silting of the basin and the closure of the inlet probably caused a relative lowering of the groundwater level. Conclusions concerning mean sea level, on the basis of information from locations inside a tidal basin must be treated with great caution, since the mean water level in a tidal basin depends on the tidal motion and increases with distance from the inlet. Consequently, mean sea levels deduced from water levels in tidal basins will be above the real mean sea levels.

Discussion

Basin evolution

The occurrence of fresh-water tidal deposits in the eastern part of the basin indicates that the flux of fresh water from the hinterland cannot be ignored. This implies that a vertical, density-driven circulation probably existed in the basin. This circulation would have reinforced landward sediment transport along the bottom. Moreover, the flood-dominant asymmetry of the boundary tide used in the calculations is too small. Hence, the landward sediment transport at the tidal inlet and probably also in the basin itself must have been underestimated.

The change in tidal asymmetry in the basin from flood- to ebb-dominant between the locations 3 and 4 in 3700 BP (Fig. 7.10b) probably resulted in sediment being deposited mainly in this part of the basin. This may have accelerated the silting up of the seaward part of the basin and the tidal inlet while the tidal basin did not fill up completely with sediment as yet. The Alkmaar-Bergen inlet closed around 3300 BP (Roep and Van Regteren Altena, 1988). The celerity of the tidal wave of 1.9 ms^{-1}, which was calculated for the 3700 BP reconstruction (Table 7.1), suggests that if West Friesland had been connected to the lake east of it, the tidal wave would have reached the Noordoostpolder (Fig. 7.3) only after 10 hours. This means that the tidal motion in the IJsselmeer polders would have run behind that in the inlet by almost a complete tidal cycle. Consequently, the contribution of tidal flow in this area to the tidal prism in the inlet would have been negligible. Moreover, transport of any sediment this far east other than very fine-grained suspended matter is very unlikely. This situation is comparable with the tidal motion in the Zuiderzee which developed after 1600 AD.

In general, it can be stated that the shallowing of long, elongate tidal basins led to a decrease in tidal celerity. Consequently, the contribution of the discharges caused by tidal motion in the innermost part of the basin to the tidal prism in the inlet declines. This means that the evolution of the basin entrance came to be determined by a smaller part of the basin. In the North-Holland tidal basin this resulted in silting up of the seaward part of the basin and the inlet, whereas the innermost part of the basin was not filled up with sediment.

Method

The simulations presented in this paper are a first attempt to model the tidal motion in fossil tidal basins. Both the basin reconstructions and input parameters are estimates used to develop the method and to produce the first results. Therefore, the results of the simulations must be considered preliminary. in spite of this, the simulations resulted in considerable improvement of the basin reconstructions.

Some of the input parameters used in the simulations (e.g., bottom roughness) were derived from the Westerschelde model (Chap. 6), since no data for the North-Holland tidal basin was available. An analysis of the consequences of this has not been made. The tidal asymmetry in the forcing tide at the entrance of the North-Holland tidal basin has been underestimated (see above). Consequently, the results presented in this paper must be considered preliminary. New boundary tides for the North-Holland tidal basin during the Holocene sea-level rise will be available in short time. Definite simulations must be made using these more asymmetric tides.

The following improvements of the simulations are recommended here:

- A sensitivity analysis of the North-Holland tidal basin for the bottom roughness as applied in the model;
- New simulations using the boundary tides for the North-Holland coast. New boundary tides are being produced at this moment;
- A further refinement of the geological basin reconstructions; and
- Calculation of the sand transport at the basin entrance, which thereafter can be compared with geological data on sediment influxes.

Long-term evolution of the North-Holland tidal basin: concluding remarks

The preliminary results of tidal simulations led to adjustment of the ideas on the long-term evolution of the North-Holland tidal basin. The calculations for 7200 BP showed that around that time the landward part of the basin probably comprised small, more or less enclosed, un- or only poorly connected lagoons, whereas the seaward part of the basin most likely consisted of tidal flats, dissected by channels. These lagoons were the result of poor drainage, which in itself is an argument for the absence of tidal motion. An extensive lagoon, as was assumed in the calculations proved to be improbable. Sediment transport to the landward part of the basin must have been small because of the long distance from the source, the North Sea coast. Most sediment would have been deposited closer to the tidal inlet. The basin morphology in 7200 BP would have been roughly similar to that in 5500 BP.

The sediment transported basinward by waves and the North Sea tide was transported further into the basin by the flood-dominant tide. Deposition of the sediment resulted in shallowing of the basin and the formation of tidal flats. The changing morphology of the basin, in turn, caused a change in tidal distortion inside the basin, which weakened the flood dominance. Continued expansion of the shoal area finally resulted in a net transport capacity in the ebb direction in the main channel in 3700 BP. Sediment deposited on the tidal flats by the flood tide and on the salt marshes during storm will not have been affected by this, so eventually the basin was filled up with sediment.

The flood volume calculated from the maximum cross-sectional area of the Bergen inlet is too large considering the maximum basin extension. Reduction of this inlet area in order to adjust the ratio of flood volume and basin extent, implies that the cross-sectional area of the Bergen Clay does not represent the dimensions of one single inlet and that part of the Bergen Clay was deposited while the inlet was still active.

Acknowledgements

This investigation is a contribution to the multi-disciplinary Coastal Genesis project. It was supported by Rijkswaterstaat-National Institute for Coastal and Marine Management/RIKZ, contract DG-477, and the Ministry of Home Affairs, file number DUO 2002674. The research reported here was carried out at the Geological Survey of The Netherlands (RGD) in Haarlem. Thanks to Ruud Schüttenhelm of RGD for providing working space and aa adequate PC.

I would like to thank Dirk Beets and Janrik van den Berg for all kinds of support during the project. Dirk Beets made the basin reconstructions. Ad Langerak of RIKZ advised on modelling problems. Many thanks for that. Engelbert Vennix prepared the drawings. Also thanks to Piet Cleveringa and Peter Vos for the sometimes heated discussions on the palaeo-ecology of the North-Holland tidal basin. Finally, I highly appreciated the critical though constructive remarks of Dirk Beets on an earlier draft of this paper.

References

Anonymus, 1974. Rapport van de Waddenzeecommissie; advies inzake de principiele mogelijkheden en de voor- en nadelen van inpolderingen in de Waddenzee. The Hague, 326 pp.

Aubrey, D.G. and Speer, P.E., 1985. A study of non-linear tidal propagation in shallow inlet/estuarine systems. Part I: Observations. Estuar. coast. Shelf Sci., 21: 185-205.

Bakker, J.P., 1954. Relative sea-level changes in Northwest Friesland (Netherlands) since prehistoric times. Geol. Mijnbouw, 16: 323-346.

Bakker, J.P. and Wensink, J.J., 1955. Overzicht van de Holocene reliefgeneraties en sedimentopvolging in Barradeel. In: Anonymus, Barradeel, Rapport Betreffende het Onderzoek van het Landskip-Genetysk Wurkforbân fan de Fryske Akademy. Laverman, Drachten, pp. 16-42.

Beets, D.J., Van der Valk, L. and Stive, M.J.F., 1992. Holocene evolution of the coast of Holland. Mar. Geol., 103: 423-443.

Beets, D.J., Roep, Th.B. and Westerhoff, W.E., in press. The Alkmaar-Bergen inlet: closing history and related barrier progradation. Meded. Rijks Geol. Dienst, 53.

Beukema, J.J. and De Vlas, J., 1979. Population parameters of the Lugworm, Arenicola marina, living on tidal flats in the Dutch Wadden Sea. Neth. J. Sea Res., 13: 331-353.

Blaeu, W.J., 1608. Licht der Zeevaert, Amsterdam.

Blaeu, W.J., 1623. Zeespiegel, Amsterdam.

Boeles, P.C.J.A., 1951. Friesland tot de 11e eeuw. 2nd edit. M. Nijhoff, The Hague, 598 pp.

Boon, J.D. and Byrne, R.J., 1981. On basin hypsometry and the morphodynamic response of coastal inlet systems. Mar. Geol., 40: 27-48.

Borger, G.J., 1985. De ouderdom van onze dijken. Hist. Geogr. Tijdschrift, 3 (3): 76-80.

Bosch, J.H.A., 1990. Toelichtingen bij de Geologische Kaart van Nederland 1: 50.000, Blad Assen West (12W) en Blad Assen Oost (12O). Geological Survey of The Netherlands, Haarlem, 188 pp. (with English summary).

Bruun, P., 1966. Tidal Inlets and Littoral Drift Stability of Coastal Inlets. Vol. 2, Universitetsforlaget, 193 pp.

Coen, I., 1988. Ontstaan en ontwikkeling van de Westerschelde. Water, 43: 156-162.

Cnossen, J., 1958. Enige opmerkingen omtrent het ontstaan van het Beneden-Boornegebied en de Middelzee in verband met de subatlantische transgressie. Boor en Spade, 9: 24-38. (With English summary.)

Cnossen, J., 1971. De Bodem van Friesland. Toelichting bij Blad 2 van de Bodemkaart van Nederland, Schaal 1:200.000. Stichting voor Bodemkartering, Wageningen, 132 pp.

Cnossen, J. and Zandstra, J.G., 1965. De oudste Boorneloop in Friesland en veen uit de Paudorftijd nabij Heerenveen. Boor en Spade, 14: 62-87. (With English summary.)

Deckers, P.H., De Roever, J.P. and Van der Waals, J.D., 1980. Jagers, vissers en boeren in een prehistorisch getijdengebied bij Swifterbant. ZWO Jaarboek, ZWO, The Hague, pp. 111-114.

Dekker, L. and Bollebakker, G.P., 1981. Getijdeberekeningen in Verband met het Onderzoek naar de Verdieping van de Westerschelde. Deel Ia: Matig Springtij. Report WWKZ-81.V008, Rijkswaterstaat, Vlissingen, 31 pp.

Dekker, R., 1989. The macrozoobenthos of the subtidal western Dutch Wadden Sea. I; Biomass and species richness. Neth. J. Sea Res., 23: 57-68.

De Gans, W. and Van Gijssel, K., in press. The Late Weichselian morphology of the Netherlands and its influence on the Holocene coastal development. Meded. Rijks Geol. Dienst, 53.

De Glopper, R.J., 1967. Over de bodemgesteldheid van het Waddengebied. Van Zee tot Land, 43. Tjeenk Willink, Zwolle, 67 pp. (with English summary).

De Groot, T.A.M. and Westerhoff, W.E., 1993. Storm Depositional Sequences Underneath a Subboreal Barrier in The Western Netherlands. Report RGD 40.007, Geological Survey of The Netherlands, Haarlem, 7 pp.

De Groot, T.A.M., Van Adrichem Boogaert, H.A., Fischer, M.M., Klijnstra, B., Van Montfrans, H.M., Uil, H., Ter Wee, M.W., Van Weeperen M.J. and Zandstra, J.G., 1987. Toelichtingen bij de Geologische Kaart van Nederland 1: 50.000, Blad Heerenveen West (11W) en Blad Heerenveen Oost (11O). Geological Survey of The Netherlands, Haarlem, 251 pp. (with English summary).

De Jong, J., 1984. Age and vegetation of the coastal dunes in the Frisian Islands, the Netherlands. Geol. Mijnbouw, 63: 269-275.

De Mulder, E.F.J. and Bosch, J.H.A., 1982. Holocene stratigraphy, radiocarbon datings and paleogeography of central and northern North-Holland (the Netherlands). Meded. Rijks Geol. Dienst, 36-3: 111-160.

Denucé, J., 1933. De Loop van de Schelde van de Zee tot Rupelmonde in de XVe Eeuw. Veritas, Antwerpen, 24 pp.

De Ronde, J.G. and Vogel, J.A., 1988. Zeespiegelrijzing, Hydro Meteo scenario's. Report GWAO-88.015, Rijkswaterstaat, The Hague, 58 pp.

Dijkema, K.S., Bossinade, J.H., Bouwsema, P. and De Glopper, R.J., 1990. Salt marshes in the Netherlands Wadden Sea: rising high-tide levels and accretion enhancement. In: J.J. Beukema, W.J. Wolff and J.J.W.M. Brouns (Editors), Expected Effects of Climatic Change on Marine Coastal Ecosystems. Developments in Hydrology 57. Kluwer, Dordrecht, pp. 173-188.

Donkersloot-De Vrij, Y.M., 1975. De heruitgave van een 17de eeuwse wandkaart: de Roman-Visscherkaart van Zeeland. Kartogr. Tijdschr., 1 (3): 21-24.

Dörjes, J., Gadow, S., Reineck, H.E. and Singh, I.B., 1970. Sedimentologie und Makrobenthos der Nordergrunde und Aussenjade (Nordsee). Senckenbergiana Mar., 2: 31-59.

Dronkers, J., 1986. Tidal asymmetry and estuarine morphology. Neth. J. Sea Res., 20: 117-131.

Eisma, D., Berger, G.W., Chen Wei-Yue and Shen Jian, 1989. Pb-210 as a tracer for sediment transport and deposition in the Dutch-German Waddensea. In: W.J.M. van der Linden, S.A.P.L. Cloetingh, J.P.K. Kaasschieter, W.J.E. van de Graaff, J. Vandenberghe and J.A.M. van der Gun (Editors), Proceedings KNGMG Symposium Coastal Lowlands, Geology and Geotechnology, 1987, The Hague. Kluwer, Dordrecht, pp. 237-253.

Endema, D., 1979. Grootheden / Gegevens Waddenzee, Waddeneilanden en Noordzeekust. Report WWKZ-79.H003, Rijkswaterstaat, Hoorn, 20 pp.

Ente, P.J., 1963. Een Bodemkartering van het Tuinbouwcentrum "de Streek". Thesis, Wageningen. Also in Verslagen Landbouwkundige Onderzoekingen, 68.16. Pudoc, Wageningen, 193 pp. (with English summary).

Ente, P.J., 1964. Thickness variations of the sandy Almere deposits (Holocene) in the former Zuiderzee area (The Netherlands). In: L.M.J.U. van Straaten (Editor), Deltaic and Shallow Marine Deposits. Developments in Sedimentology, 1, Elsevier, Amsterdam, pp. 123-128.

Ente, P.J., 1971. Sedimentary geology of the Holocene in Lake IJssel region. Geol. Mijnbouw, 50: 373-382.

Ente, P.J., 1976. The geology of the northern part of Flevoland in relation to the human occupation in the Atlantic time. Helinium, 16: 15-35.

Ente, P.J., 1977. Geologische opbouw van het Holoceen. In: C.J. van Staalduinen (Editor), Geologisch Onderzoek van het Nederlandse Waddengebied, Geological Survey of The Netherlands, Haarlem, pp. 58-63.

Ente, P.J., Koning, J. and Koopstra, R., 1986. De bodem van oostelijk Flevoland. Flevobericht, 258. Rijksdienst voor de IJsselmeerpolders, Lelystad, 174 pp. (with English summary).

Ente, P.J., Zagwijn, W.H. and Mook, W.G., 1975. The Calais deposits in the vicinity of Wieringen and the geogenesis of northern North-Holland. Geol. Mijnbouw, 54: 1-14.

Eysink, W.D., 1979. Morfologie van de Waddenzee; Gevolgen van Zand en Schelpwinning. Report R1336, Delft Hydraulics Laboratory, Delft, 92 pp.

Eysink, W.D., 1991. Morphologic response of tidal basins to changes. The Dutch coast: Paper no. 8. Proc. 22nd Coast. Eng. Conf., Delft 1990, ASCE, New York, pp. 1948-1961.

FitzGerald, D.M. and Penland, S., 1987. Backbarrier dynamics of the East Friesian islands. J. Sed. Petr., 57: 746-754.

FitzGerald, D.M., Penland, S. and Nummedal, D., 1984. Changes in tidal inlet geometry due to backbarrier filling: East Friesian Islands, West Germany. Shore and Beach, 52: 2-8.

Franken, A.F., 1987. Rekonstruktie van het Paleo-Getijklimaat in de Noordzee. Report X0029-00, Delft Hydraulics Laboratory, Delft, 74 pp.

Friedrichs, C.T. and Aubrey, D.G., 1988. Non-linear tidal distortion in shallow well-mixed estuaries: a synthesis. Estuar. coast. Shelf Sci., 27: 521-545.

Friedrichs, C.T., Aubrey, D.G. and Speer, P.E., 1990. Impacts of relative sea-level rise on evolution of shallow estuaries. In: R.T. Cheng (Editor), Residual Currents and Long-term Transport. Coastal and Estuarine Studies, 38, Springer-Verlag, New York, pp. 105-122.

Friedrichs, C.T., Lynch, D.R. and Aubrey, D.G., 1992. Velocity asymmetries in frictionally-dominated tidal embayments: longitudinal and lateral variability. In: D. Prandle (Editor), Dynamics and Exchange in Estuaries and the Coastal Zone. Coastal and Estuarine Studies, 40, American Geophys. Union, Washington D.C., pp. 277-312.

Gerritsen, F., 1990. Morphological Stability of Inlets and Channels of the Western Wadden Sea. Report GWAO-90.019, Rijkswaterstaat, The Hague, 86 pp.

Gerritsen, F., 1992. Morphological stability of inlets and tidal channels of the Western Wadden Sea. In: N. Dankers, C.J. Smit and M. Scholl (Editors), Proc. of the 7th Int. Wadden Sea Symp., Ameland, 1990. Neth. Inst Sea Res., Publ. Ser., 20-1992, pp. 151-160.

Gerritsen, F. and De Jong, H., 1985. Stabiliteit van Doorstroomprofielen in het Waddengebied. Report WWKZ-84.V016, Rijkswaterstaat, Vlissingen, 53 pp.

Geyl, W.F., 1976. Tidal neomorphs. Z. Geomorph. N. F., 20: 308-330.

Griede, J.W., 1978. Het Ontstaan van Frieslands Noordhoek. Thesis, Free University, Amsterdam, 186 pp. (with English summary).

Griede, J.W. and Roeleveld, W., 1982. De geologische en paleogeografische ontwikkeling van het noordelijk zeekleigebied. Geogr. Tijdschr. K. Ned. Aardr. Genoot., 16: 439-455.

Haeyen, A., 1585. Amstelredamsche Zee-caerten. Christoffel Plantyn, Leiden.

Hageman, B.P., 1969. Development of the western part of the Netherlands during the Holocene. Geol. Mijnbouw, 48: 373-388.

Halbertsma, H., 1955. Enkele oudheidkundige aantekeningen over het ontstaan en de toeslijking van de Middelzee. Tijdschr. Kon. Ned. Aardr. Gen., 72: 93-105. (With English summary.)

Hengst, P., 1980. Inhoudsberekeningen Scheldebekken Traject Vlissingen - Antwerpen, Opneming 1968-1969. Report WWKZ-79.V018, Rijkswaterstaat, Vlissingen, 11 pp.

Hydrografische Dienst, 1987. Stroomatlas Waddenzee, Westelijk Deel. The Netherlands Hydrographer, The Hague, 13 charts with introduction (also in English).

Isbary, G., 1936. Das Inselgebiet von Ameland bis Rottumeroog. Morphologische und Hydrographische Beitrage zur Entwicklungsgeschichte der Friesischen Inseln. Aus dem Archiv der Deutschen Seewarte, 56 (3), Hamburg, 55 pp.

Jarret, J.T., 1976. Tidal Prism-Inlet Area Relationships, General Investigations of Tidal Inlets. Report 3, Coastal Engineering Research Centre, Ft. Belvoir, Virginia, 32 pp.

Jelgersma, S., 1961. Holocene Sea-Level Changes in The Netherlands. Thesis, Leiden, 100 pp. Also in: Meded. Geol. Stichting, ser. C-IV, 7.

Jelgersma, S., 1977. Zeespiegelbeweging en bodemdaling. In: C.J. van Staalduinen (Editor), Geologisch Onderzoek van het Nederlandse Waddengebied, Geological Survey of The

Netherlands, Haarlem, pp. 72-74.

Jelgersma, S., 1979. Sea-level changes in the North Sea basin. In: E. Oele, R.T.E. Schüttenhelm and A.J. Wiggers (Editors), The Quaternary History of the North Sea. Acta Univ. Ups. Symp. Univ. Ups. Annum Quingentesimum Celebrantis, 2, pp. 233-248.

Jelgersma, S. and Ente, P.J., 1977. Genese van het Holoceen. In: C.J. van Staalduinen (Editor), Geologisch Onderzoek van het Nederlandse Waddengebied. Geological Survey of The Netherlands, Haarlem, pp. 23-33.

Koeman, C., 1983. Geschiedenis van de Kartografie in Nederland. Zes Eeuwen Land- en Zeekaarten en Stadsplattegronden. Canaletto, Alphen aan de Rijn, 275 pp.

Koning, J.C.F.M. and Kreuk, J.J.N., 1974. De Golfbeweging nabij het Amelander Wantij. Report 74.8, Rijkswaterstaat, Hoorn, 18 pp.

Kool, G., Peereboom, P., Lieshout, M.F. and De Boer, M., 1984. Verloop Natte en Droge Oppervlakten en Kombergingen. Report WWKZ-84.H009, Rijkswaterstaat, Hoorn.

Kuijer, P.C., 1974. Bodemkaart van Nederland Schaal 1:50.000, Toelichting bij de Kaartbladen 10 W Sneek en 10 O Sneek. Stichting voor Bodemkartering, Wageningen, 126 pp.

Kuijer, P.C., 1976a. Bodemkaart van Nederland Schaal 1:50.000, Toelichting bij de Kaartbladen 5 W Harlingen en 5 O Harlingen. Stichting voor Bodemkartering, Wageningen, 95 pp.

Kuijer, P.C., 1976b. Bodemkaart van Nederland Schaal 1:50.000, Toelichting bij het Kaartblad 11 W Heerenveen. Stichting voor Bodemkartering, Wageningen, 140 pp.

Kuijer, P.C., 1981. Bodemkaart van Nederland Schaal 1:50.000, Toelichting bij de Kaartbladen 6 W Leeuwarden, 6 O Leeuwarden en het Vaste Land van de Kaartbladen 2 W Schiermonnikoog en 2 E Schiermonnikoog. Stichting voor Bodemkartering, Wageningen, 181 pp.

Kumar, N. and Sanders, J.E., 1974. Inlet sequence: a vertical succession of sedimentary structures and textures created by the lateral migration of tidal inlets. Sedimentology, 21: 491-532.

Lüders, K., 1934. Über das Wandern der Priele. Abh. naturwiss. Verein Bremen, 29: 19-32.

Misdorp, R., Steyaert, F., Hallie, F. and De Ronde, J., 1990. Climate change, sea level rise and morphological developments in the Dutch Wadden Sea, a marine wetland. In: J.J. Beukema, W.J. Wolff and J.J.W.M. Brouns (Editors), Expected Effects of Climatic Change on Marine Coastal Ecosystems. Developments in Hydrology 57. Kluwer, Dordrecht, pp. 123-131.

Nio, S.D., Van den Berg, J.H., Goesten, M. and Smulders, F., 1980. Dynamics and sequential analysis of a mesotidal shoal and intershoal channel complex in the Eastern Scheldt (Southwestern Netherlands). Sediment. Geol., 26: 263-279.

O'Brien, M.P., 1931. Estuary tidal prisms related to entrance areas. Civil Eng., 1: 738-739.

O'Brien, M.P., 1969. Equilibrium flow areas in inlets on sandy coasts. ASCE, J. Waterw. Harbors Div., 95, (WW1): 43-51.

Pons, L.J. and Wiggers, A.J., 1959. De Holocene wordingsgeschiedenis van Noord-Holland en het Zuiderzeegebied, Part 1. Tijdschr. K. Ned. Aardrijksk. Genoot. 76: 104-152 (with English summary).

Pons, L.J. and Wiggers, A.J., 1960. De Holocene wordingsgeschiedenis van Noord-Holland en het Zuiderzeegebied, Part 2. Tijdschr. K. Ned. Aardrijksk. Genoot., 77: 3-57 (with English summary).

Pons, L.J., Jelgersma, S., Wiggers, A.J. and De Jong, J.D., 1963. Evolution of the Netherlands coastal area during the Holocene. Verh. Kon. Ned. Geol. Mijnb. Gen., Geol. serie 21 (2): 197-208.

Postma, H., 1954. Hydrography of the Dutch Wadden Sea. Arch. Néerl. Zool., 10: 405-511.

Postma, H., 1961. Transport and accumulation of suspended matter in the Dutch Wadden Sea. Neth. J. Sea Res., 1: 148-190.

Postma, H., 1981. Exchange of materials between the North Sea and the Wadden Sea. Mar. Geol., 40: 199-213.

Reineck, H.E., 1958. Longitudinale Schrägschicht im Watt. Geol. Rdsch., 47: 73-82.

Reineck, H.E., 1972. Tidal flats. In: J.K. Rigby and W.K. Hamblin (Editors), Recognition of Ancient Sedimentary Environments. Soc. Econ. Paleontologists and Mineralogists, Spec. Publ. 16: 146-152.

Reineck, H.E. (Editor), 1978. Das Watt; Ablagerungs- und Lebensraum. 2nd edition. Waldemar Kramer, Frankfurt a. Main, 185 pp.

Reineck, H.E. and Singh, I.B., 1980. Depositional Sedimentary Environments, 2nd edition. Springer-Verlag, Berlin, 549 pp.

Rienks, K.A. and Walther, G.L., 1954. Binnendiken en Slieperdiken yn Fryslan. A.J. Osinga, Bolsward, 555 pp. (with English summary). Charts are published in a separate atlas.

Roeleveld, W., 1974. The Holocene Evolution of the Groningen Marine-Clay District. Thesis, Free University, Amsterdam, 132 pp.

Roep, Th.B. and Beets, D.J., 1988. Sea-level rise and paleotidal levels from sedimentary structures in the coastal barriers in the western Netherlands since 5600 BP. Geol. Mijnbouw, 67: 53-60.

Roep, Th.B. and Van Regteren Altena, J.F., 1988. Paleotidal levels in tidal sediments (3800-3635 BP); compaction, sea-level rise and human occupation (3275-2620 BP) at Bovenkarspel, NW Netherlands. In: P.L. de Boer, A. van Gelder and S.D. Nio (Editors), Tide-influenced Sedimentary Environments and Facies. Reidel, Dordrecht, pp. 215-231.

Roy, P.S., Thom, B.G. and Wright, L.D., 1980. Holocene sequences on an embayed high energy coast: an evolutionary model. In: A.H. Bouma, D.S. Gorsline, C. Monty and G.P. Allen (Editors), Shallow Marine Processes and Products. Sediment. Geol., 26: 1-19.

Ruegg, G.H.J., 1975. Sedimentary structures and depositional environments of Middle- and Upper-Pleistocene glacial time deposits from an excavation at Peelo, near Assen, the

Netherlands. Meded. Rijks Geol. Dienst, 26: 17-23.

Schotanus a Sterringa, C., 1664. Beschrijvinge van de Heerlyckheydt van Frieslandt. (Facsimile issue, 1978)

Schoorl, H., 1980. The significance of the Pleistocene landscape of the Texel-Wieringen region for the historical development of the Netherland coast between Alkmaar and East Terschelling. In: A. Verhulst and M.K.E. Gottschalk (Editors), Transgressions and the History of Settlement in the Coastal Areas of Holland and Belgium. Proceedings Colloquium 5-7 sep. 1978, Gent. Belgisch Centrum voor Landelijke Geschiedenis, publ. 66: 115-153.

Sha, L.P., 1989a. Sand transport in the ebb-tidal delta off Texel Inlet, the Wadden Sea, The Netherlands. Mar. Geol., 86: 137-154.

Sha, L.P., 1989b. Cyclic morphologic changes of the ebb-tidal delta, Texel Inlet. Geol. Mijnbouw, 68: 35-48.

Sha, L.P., 1989c. Variation in ebb-delta morphologies along the West and East Frisian Islands, The Netherlands and Germany. Mar. Geol., 89: 11-28.

Sha, L.P., 1989d. Holocene-Pleistocene interface and three-dimensional geometry of the ebb-delta complex, Texel Inlet, The Netherlands. Mar. Geol., 89: 207-228.

Sha, L.P., 1990. Sedimentological Studies of the Ebb-Tidal Deltas along the West Frisian Islands, The Netherlands. Geologica Ultraiectina, 64, 160 pp.

Sha, L.P. and De Boer, P.L., 1991. Ebb-tidal delta deposits along the west Frisian Islands (The Netherlands): processes, facies architecture and preservation. In: D.G. Smith, G.E. Reinson, B.A. Zaitlin and R.A. Rahmani (Editors), Clastic Tidal Sedimentation. Canadian Soc. Petrol. Geol. Mem., 16: 199-218.

Sha, L.P and Van den Berg, J.H., 1993. Variation in ebb-tidal delta geometry along the coast of The Netherlands and the German Bight. J. Coast. Res., 9: 730-746.

Spaans, W., Booij, N., Praagman, N., Noorman, R. and Lander, J., 1989. DUFLOW, a Micro-Computer Package for the Simulation of One-Dimensional Unsteady Flow in Open Channel Systems. SAMWAT, The Hague, 92 pp.

Speer, P.E. and Aubrey, D.G., 1985. A study of non-linear tidal propagation in shallow inlet/estuarine systems. Part II: Theory. Estuar. coast. Shelf Sci., 21: 207-224.

Stive, M.J.F., Roelvink, J.A. and De Vriend, H.J., 1991. Large-scale coastal evolution concept. The Dutch coast: paper no. 9. Proc. 22nd Coast. Eng. Conf., Delft 1990. ASCE, New York, pp. 1962-1974.

Terwindt, J.H.J., 1971. Lithofacies of inshore estuarine and tidal inlet deposits. Geol. Mijnbouw, 50: 515-526.

Terwindt, J.H.J., 1981. Origin and sequences of sedimentary structures in inshore mesotidal deposits of the North Sea. In: S.D. Nio, R.T.E. Schüttenhelm and Tj.C.E. van Weering (Editors), Holocene Marine Sedimentation in the North Sea Basin. Spec. Publs. int. Ass. Sediment., 5, Blackwell, Oxford, pp. 4-26.

Ter Wee, M.W., 1962. The Saalian glaciation in The Netherlands. Meded. Geol. St., 15: 57-76.

Ter Wee, M.W., 1975. Enkele momentopnamen uit de geologische geschiedenis van de Boorne. It Beaken, 37: 334-340.

Ter Wee, M.W., 1976. Toelichtingen bij de Geologische Kaart van Nederland 1: 50.000, Blad Sneek (10W, 10O). Geological Survey of The Netherlands, Haarlem, 131 pp. (with English summary).

Trusheim, F., 1929. Zur Bildungsgeschwindigkeit geschichteter Sedimente im Wattenmeer, besonders solcher mit schräger Parallelschichtung. Senckenbergiana, 11: 47-55.

Van Bendegom, L., 1949. Beschouwingen over de Grondslagen van Kustverdediging. Report Rijkswaterstaat, Hoorn, 84 pp.

Van de Plassche, O., 1982. Sea-Level Change and Water-Level Movements in the Netherlands during the Holocene. Thesis, Free University Amsterdam. Also in Meded. Rijks Geol. Dienst, 36: 1-93.

Van de Plassche, O. and Roep, Th.B., 1989. Sea-level changes in the Netherlands during the last 6500 years: basal peat vs. coastal barrier data. In: D.B. Scott, P.A. Pirazzoli and C.A. Honig (Editors), Late Quaternary Sea-Level Correlation and Applications, Kluwer, Dordrecht, pp. 41-56.

Van den Berg, J.H., 1981. Rhythmic seasonal layering in a mesotidal fill sequence, Oosterschelde mouth, the Netherlands. In: S.D. Nio, R.T.E. Schüttenhelm and Tj.C.E. Van Weering (Editors), Holocene Marine Sedimentation in the North Sea Basin. Spec. Publs. int. Ass. Sediment., 5, Blackwell, Oxford, pp. 147-159.

Van den Berg, J.H., 1982. Migration of large-scale bedforms and preservation of cross-bedded sets in highly accretional parts of tidal channels in the Oosterschelde, SW Netherlands. Geol. Mijnbouw, 61: 253-263.

Van den Berg, J.H., 1986. Aspects of sediment- and morphodynamics of subtidal deposits of the Oosterschelde (the Netherlands). Thesis, Utrecht. Also in Rijkswaterstaat Communications, 43. Rijkswaterstaat, The Hague, 123 pp.

Van den Berg, M.W. and Beets, D.J., 1987. Saalian glacial deposits and morphology in the Netherlands. In: J.J.M. van der Meer (Editor), Tills and Glaciotectonics, Balkema, Rotterdam, pp. 235-251.

Van der Borg, K. , Alderliesten, C., Houston, C.M., De Jong, A.F.M. and Van Zwol, N.A., 1987. Accelerator mass spectrometry with ^{14}C and ^{10}Be in Utrecht. Nucl. Instr. and Methods in Physics Research, B29: 143-145.

Van de Kreeke, J. and Haring, J., 1979. Equilibrium flow areas in the Rhine-Meuse delta. Coast. Eng., 3: 97-11.

Van der Spek, A.J.F., 1993a. Getij-Simulatie Voormalige Getijdebekkens, Deel 1: de Westerschelde in 1650 en 1800. Report 93-10, Institute for Marine and Atmospheric Research Utrecht, Utrecht University, 47 pp.

Van der Spek, A.J.F., 1993b. Getij-Simulatie Voormalige Getijdebekkens, Deel 2: het Zeegat van Bergen in 7200 BP, 5500 BP en 3700 BP. Report 93-15, Institute for Marine and Atmospheric Research Utrecht, Utrecht University, 36 pp.

Van der Valk, L., Westerhoff, W.E. and De Jong, J., 1985. Mid-Holocene wave dominated clastic tidal deposits at Rijswijk in the western part of the Netherlands. Abstr. symp. on modern and ancient clastic tidal deposits, Utrecht: 145-148.

Van der Valk, L., 1992. Mid- and Late-Holocene Coastal Evolution in the Beach-Barrier Area of the Western Netherlands. Thesis, Free University Amsterdam, 235 pp.

Van Staalduinen, C.J. (Editor), 1977. Geologisch Onderzoek van het Nederlandse Waddengebied. Geological Survey of The Netherlands, Haarlem, 77 pp.

Van Straaten, L.M.J.U., 1950. Environment of formation and facies of the Wadden Sea sediments. Tijdschr. K. Ned. Aardrijkskd. Genoot., 67: 354-368.

Van Straaten, L.M.J.U., 1951. Texture and genesis of Dutch Wadden Sea sediments. Proc. 3rd Int. Congr. Sed., Netherlands, Nijhoff, The Hague, pp. 225-244.

Van Straaten, L.M.J.U., 1954. Composition and structure of recent marine sediments in The Netherlands. Leidse Geol. Meded., 19, 110 pp.

Van Straaten, L.M.J.U., 1957. The Holocene deposits. In: L.M.J.U. van Straaten and J.D. de Jong (Editors), The Excavation at Velsen; a Detailed Study of Upper-Pleistocene and Holocene Stratigraphy. Verh. Kon. Nederl. Geol. Mijnb. Gen., Geol. Ser., 17: 158-183.

Van Straaten, L.M.J.U., 1961. Sedimentation in tidal flat areas. J. Alberta Soc. Petrol. Geologists, 9: 203-226.

Van Straaten, L.M.J.U., 1963. Aspects of Holocene sedimentation in The Netherlands. Verh. K. Ned. Geol. Mijnbouwkd. Genoot., 21: 149-172.

Van Straaten, L.M.J.U., 1965. Coastal barrier deposits in South- and North-Holland in particular in the areas around Scheveningen and IJmuiden. Med. Geol. Sticht., 17: 41-75.

Van Straaten, L.M.J.U., 1975. De sedimenthuishouding in de Waddenzee. In: Werkgroep Waddengebied, Report 1, pp. 5-20 (with English summary).

Van Straaten, L.M.J.U. and Kuenen, Ph.H., 1957. Accumulation of fine grained sediments in the Dutch Wadden Sea. Geol. Mijnbouw, 19: 329-354.

Van Straaten, L.M.J.U. and Kuenen, Ph.H., 1958. Tidal action as a cause of clay accumulation. J. Sed. Petr., 28: 406-413.

Van Veen, J., 1950. Eb- en vloedschaar systemen in de Nederlandse getijdewateren. Tijdschr. Kon. Ned. Aardr. Gen., 67: 303-325. (With English summary).

Vos, P.C. and De Wolf, H., 1988. Paleo-Ecologisch Onderzoek in de Noordzee en Provincie Noord Holland in het Kader van het Kustgenese Project, Taakgroep 5000. Geological Survey of the Netherlands, Haarlem, 144 pp.

Vos, P.C., and De Wolf, H., 1994. Palaeoenvironmental research on diatoms in Early and Middle Holocene deposits in central North Holland (the Netherlands). Neth. J. Aquat. Ecol., 28: 97-115.

Vos, P.C. and Van Heeringen, R.M., 1993. The Impact of Environmental Changes on the Occupation History in the South-Western Coastal Area of the Netherlands (Province of Zeeland). Report 1459, Geological Survey of The Netherlands, Haarlem, 72 pp.

Waghenaer, L.J., 1584. Spieghel der Zeevaerdt, Leiden.

Warrick, R.A. and Oerlemans, J., 1990. Sea-level rise. In: J.T. Houghton, G.J. Jenkins and J.J. Ephraums (Editors), Climate change, the IPCC scientific assessment. Cambridge University Press, Cambridge, pp. 257-281.

Wemelsfelder, P.J., 1957-1962. Golfaanval Afsluitdijk Lauwerszee. Memoranda I-VII, Rijkswaterstaat, Hydrometric Department, The Hague.

Wensink, J.J., 1958. De jongpleistocene en holocene ontwikkeling van een deel van Westergoo. Geol. Mijnbouw, 20: 73-87.

Wensink, J.J. and Bakker, J.P., 1951. Five types of fine tidal flat sands from the subsoil of Barradeel. Proc. 3rd International Congres of Sedimentology, Groningen-Wageningen, pp. 273-279.

Westerhoff, W.E. and Cleveringa, P., 1990. Sea-level rise and coastal sedimentation in central Noord Holland (The Netherlands) around 5500 BP: a case study of changes in sedimentation dynamics and sediment distribution patterns. In: J.J. Beukema, W.J. Wolff and J.J.W.M. Brouns (Editors), Expected Effects of Climatic Change on Marine Coastal Ecosystems. Developments in Hydrology 57. Kluwer, Dordrecht, pp. 133-138.

Westerhoff, W.E., De Mulder, E.F.J. and De Gans, W., 1987. Toelichtingen bij de Geologische Kaart van Nederland 1:50.000, Blad Alkmaar West (19W) en Blad Alkmaar Oost (19O). Geological Survey of the Netherlands, Haarlem, 227 pp. (with English summary).

Wiggers, A.J., 1955. De Wording van het Noordoostpoldergebied. Thesis, Amsterdam. Tjeenk-Willink, Zwolle, 214 pp.

Winsemius, P., 1622. Chronique ofte historische geschiedenisse van Vriesland etc., Franeker.

Wunderlich, F., 1978. Schichtbänke. In: H.E. Reineck (Editor), Das Watt; Ablagerungs- und Lebensraum. 2nd edition, Waldemar Kramer, Frankfurt a. Main, pp 81-88.

Zagwijn, W.H., 1973. Pollenanalytic studies of Holsteinian and Saalian beds in the northern Netherlands. Meded. Rijks Geol. Dienst, 24: 139-156.

Zagwijn, W.H., 1986. Nederland in het Holoceen. Geologie van Nederland, 1. Geological Survey of The Netherlands, Haarlem, 46 pp.

Zagwijn, W.H. and Van Staalduinen, C.J. (Editors), 1975. Toelichting bij de Geologische Overzichtskaarten van Nederland. Geological Survey of The Netherlands, Haarlem, 134 pp.

Curriculum Vitae

De schrijver van dit proefschrift werd geboren op 19 januari 1961 te 's Gravenhage. In 1979 behaalde hij cum laude het diploma Athenaem B aan het Edith Stein College aldaar, waarna hij in Leiden begon aan een Biologie studie. In 1982 werd het kandidaatsexamen Biologie en Geologie (B5) afgelegd.

Na zich aanvankelijk verdiept te hebben in de functionele anatomie van Cichliden uit de Oost-Afrikaanse Slenk-meren bleek de aantrekkingskracht van de Geologie groter. Hij volgde een groot bijvak Sedimentologie aan het Instituut voor Aardwetenschappen te Utrecht, een bijvak geautomatiseerde Dataverwerking aan het Geologisch Instituut van de Universiteit van Amsterdam en legde in 1986 het doctoraal examen Mariene Geologie af aan de Vrije Universiteit te Amsterdam. In 1985 nam hij deel aan de Snellius-II expeditie in Indonesië.

Na zijn afstuderen vertrok de auteur spoorslags naar Middelburg om zich bij de Dienst Getijdewateren van Rijkswaterstaat bezig te houden met de veranderingen op de buitendelta's in Zeeland en Zuid-Holland na afdamming van de zeegaten. Van 1988 tot 1991 was de auteur in dienst van NWO en deed bij de Rijks Geologische Dienst in Haarlem onderzoek naar de effecten van een mogelijke toekomstige versnelde zeespiegelrijzing op de Nederlandse Waddenzee. In 1991 werd de bruikbaarheid van satellietfoto's bij de analyse van geomorfologische ontwikkelingen in de Waddenzee onderzocht in samenwerking met het Nationaal Lucht- en Ruimtevaartlaboratorium. In 1992 en 1993 werkte de auteur, in opdracht van Rijkswaterstaat (project Kustgenese) aan de ontwikkeling van een methode voor het berekenen van de getijdebeweging in fossiele getijdebekkens. Daarna stond een bijdrage aan het rapport 'Lange-termijn kustgedrag bij versnelde zeespiegelrijzing', één van de achtergrondrapporten van de in 1995 te verschijnen Kustnota van het RijksInstituut voor Kust en Zee/RIKZ van Rijkswaterstaat op het werkprogramma. Een groot deel van de resultaten van het onderzoek uit de periode 1988-1993 is vastgelegd in dit proefschrift.

Vanaf 1 october 1994 werkt de auteur bij de Rijks Geologische Dienst aan de kwantificering van de Holocene kustontwikkeling in Nederland, in opdracht van het Environmental Program On Climatic Hazards, III van de EG.

Overigens, de Oost-Afrikaanse Cichliden zijn inmiddels vrijwel uitgeroeid.

Helaas.